Developing OpenSees Software Framework for Modelling Structures in Fire

Jian Zhang

Submitted for the degree of Doctor of Philosophy

Heriot-Watt University

School of the Built Environment

February 2014

ABSTRACT

Fire following an earthquake (FFE) is a hazard that is not usually accounted for in either earthquake or fire resistant design of structures. There have however been many instances in the past of FFE events causing even greater damage and even loss of life than the original earthquake. The potential damage associate with this hazard is increasing considerably with increasing urbanisation in seismically vulnerable regions. It is reasonable for users to expect that structures should maintain their integrity for a long enough period in an FFE event allowing emergency crews to assist the most vulnerable occupants to evacuate the building safely. Because of the lack of regulatory requirements there is naturally very little research on the response of structural frames under FFE events so far, but given the reasons discussed earlier, it is clearly a matter of increasing importance that engineers should develop a better understanding of the behaviour of seismically damaged structural frames in fire. This thesis project was fortunate to have occurred at a time when a set of full-scale fire tests were taking place at IIT Roorkee in India, in collaboration with the University of Edinburgh to address exactly this topic. This thesis research was undertaken to model these experiments (to determine the fire resistance of a reinforced concrete frame first subjected to simulated seismic damage). The open source software framework OpenSees was chosen for the modelling work as it was considered to be the best software tool for modelling structures under earthquake loading.

The first part of this thesis reports the development work done on OpenSees for adding thermomechanical analysis modules to enable the modelling of FFE events using this software framework. The code developed for OpenSees has been allowed the introduction of features not available in commercial software such as ABAQUS. Many new classes were developed, such as ThermalAction, ThermalElement, ThermalSeciton, TheramalMaterial, etc. The newly developed code was tested using a number of benchmark problems and modelling of real fire experiments on steel and composite framed structures. The results from these tests showed that the new developments were successful.

The second part of the thesis describes the modelling of the reinforced concrete (RC) frame tested at IIT Roorkee, which was first subjected to cyclic displacement loading (to introduce damage in the frame similar to that of a seismic event) and then to a one hour kerosene fire. The modelling was first used to provide predictions of the performance of the test frame under the proposed loading, to fine tune the design of the experiment. The modelling subsequent to the tests was gradually improved to achieve better comparisons with the test results and to develop a detailed understanding of the behaviour of seismically damaged RC frames in fire, which was also compared to the behaviour in fire of undamaged frames.

ACKNOWLEDGEMENTS

A special thank you to my supervisors Prof. A. Usmani, Prof. O. Laghrouche, Prof. I. May and Dr. P. Pankaj for their support and expert advice.

Thank you to my family, friends and Edinburgh University Fire Group for the support throughout the past several years.

The financial support of ERP JRI and the UKIRI is gratefully acknowledged.

ACADEMIC REGISTRY
Research Thesis Submission

Name*:*	Jian Zhang		
School/PGI:	School of the Built Environment		
Version: *(i.e. First, Resubmission, Final)*	Final	Degree Sought (Award **and** Subject area)	PhD (Civil Engineering)

Declaration

In accordance with the appropriate regulations I hereby submit my thesis and I declare that:

1) the thesis embodies the results of my own work and has been composed by myself
2) where appropriate, I have made acknowledgement of the work of others and have made reference to work carried out in collaboration with other persons
3) the thesis is the correct version of the thesis for submission and is the same version as any electronic versions submitted*.
4) my thesis for the award referred to, deposited in the Heriot-Watt University Library, should be made available for loan or photocopying and be available via the Institutional Repository, subject to such conditions as the Librarian may require
5) I understand that as a student of the University I am required to abide by the Regulations of the University and to conform to its discipline.

* *Please note that it is the responsibility of the candidate to ensure that the correct version of the thesis is submitted.*

Signature of Candidate*:*		Date:	

Submission

Submitted By *(name in capitals):*	
Signature of Individual Submitting:	
Date Submitted:	

For Completion in the Student Service Centre (SSC)

Received in the SSC by *(name in capitals):*			
■ *Method of Submission* *(Handed in to SSC; posted through internal/external mail):*			
■ *E-thesis Submitted* *(**mandatory for final theses)***			
Signature:		Date:	

TABLE OF CONTENTS

LIST OF FIGURES

LIST OF TABLES

LIST OF PUBLICATIONS BY THE CANDIDATE

Journal Papers:

A.Usmani, J. Zhang, J. Jiang, Y. Jiang, I. May. Using OpenSees for Structures in Fire. *Journal of Structural Fire Engineering*, Volume 3, Number 1 / March 2012, pages 56-70

U. K. Sharma, P. Bhargava, B. B. Singh, Y. Y Singh, V. Kumar, P. Kamath, A.Usmani, J. Torero, M. Gillie, P. Pankaj, I. May, J. Zhang. Full Scale Testing of A Damaged RC Frame in Fire. *Proceedings of the ICE - Structures and Buildings*, Volume 165, Issue 7, 01 July 2012, pages 335 –346

Jiang, J., Jiang, L., Kotsovinos, P., Zhang, J., Usmani, A., McKenna, F., and Li, G. OpenSees Software Architecture for the Analysis of Structures in Fire. *Journal of Computing in Civil Engineering*, 10.1061/(ASCE)CP.1943-5487.0000305 (Apr. 1, 2013)

Conference Papers:

Usmani AS, Zhang J, Jiang J, Jiang YQ, Kotsovinos P (2010) Using OpenSees for structures in fire. Proceedings of 6th International Conference on Structures in Fire, Michigan, pages 1089-1094

Zhang J, Usmani AS, Jiang J, Jiang YQ, Kotsovinos P, May I (2011) Using OpenSees for an RC frame in fire. Proceedings of International Conference on Applications of Structural Fire Engineering, Prague, pages 122-126.

Jiang J, Usmani AS, Zhang J, Kotsovinos P (2011) Numerical analysis of structures in fire using OpenSees. Proceedings of International Conference on Applications of Structural Fire Engineering, Prague, pages 319-323.

Zhang J, Usmani AS, Jiang J, Jiang YQ, Kotsovinos P, May I (2011) Development and application of OpenSees for a RC frame in fire. Proceedings of the 19th UK Conference of the Association for Computational Mechanics in Engineering, Edinburgh, 233-236.

Mariyana A. AbKadir, Jian Zhang, Jian Jiang, Asif S. Usmani, Martin Gillie, mesh K. Sharma and Pradeep Bhargava(2012) Modelling of an Earthquake

Damaged RC Frame Subjected to Fire – Seventh International Conference Structure in Fire (SIF 12), Zurich, pages 479-488

Mariyana A. Ab-Kadir, J. Zhang, Asif S. Usmani; Experimental and Numerical Study on softening and Pinching Effects of Reinforced Concrete; 8th Asia Pacific Structural Eningeeirng and Construction Conference (APSEC) and 1st International Conference on Civil Engineering Research (ICCER), Surabaya, Indonesia, October 2012

Chapter 1 - Introduction

1.1 Background

Structural engineers must design structures to safely and economically sustain all predictable loads imposed upon them during their lifetime. To achieve this, structural engineers analyse a model of the structure under a number of load combinations which usually are prescribed by regulatory authorities. The model can be physical or analytical for only the simplest of structures but for larger or more complex structures it is increasingly computational (or numerical).

Contemporary consciousness and new opportunities made available through development in technologies are adding to the basic requirements (of safety and economy), such as: sustainability; expectation of meeting pre-set performance levels; minimising life-cycle cost ; structural health monitoring for critical infrastructure (e.g. bridges) for maintenance/avoidance of disasters etc.

Furthermore the definition of design is continuing to evolve. 20th century engineers moved from “working stress design” to “limit state design” (or LRFD in USA). 21st century engineers are moving towards “performance-based” engineering PBE that requires much greater knowledge and understanding of the loading and the material and structural response, requiring the construction of ever more comprehensive and complex computational models and their analysis.

The decades since the 60s saw explosive growth in computing power. Structural Engineers were one of the earliest exploiters of the opportunity offered by digital computers driven very much by the need of solving larger and larger systems of linear equations to analyse structures. This led to a great deal of legacy code being written, primarily developed in Fortran. This activity however peaked in the 80s and much of the development founds its way into the many currently available commercial codes such as SAP, ANSYS, ABAQUS etc. Much of the millions of lines of special purpose research codes written in this period (representing thousands of man-years of effort) are now very likely to be unusable because of the dramatic changes in operating systems, interface software, storage media etc.

OpenSees is an open source object oriented software. It has so far been focussed on providing an advanced computational tool for analysing the non-linear response of structural frames subjected to seismic excitations. Given that OpenSees is open source and has been available for best part of this decade, it has spawned a rapidly growing community of users as well as developers who have added to its capabilities over this period.

OpenSees takes a different route to software development from the traditional research codes that routinely die and commercial packages which are by definition restricted access (both in terms of affordability and more importantly in terms of adding functionality for problems that cannot be adequately dealt with by the package as it stands). The OpenSees route is not in itself new and the most ubiquitous and successful expression of it is the linux movement, i.e. an open source "community" code offering free access to all developers wishing to add new functionality to the core framework.

OpenSees has an excellent track record in analysing structures subjected to earthquake and other dynamic loading. It could however not be used in the field of structural fire engineering before this PhD project started, due to the lack of a thermo-mechanical analysis module and limited wider application of OpenSees in problems such as the analysis of structures subjected to fire following an earthquake (FFE), which was required for the research of this project.

The risk of fires in the aftermath of earthquakes is well known. The fires following the 1906 San Francisco and the 1923 Tokyo earthquakes led to major conflagrations and widespread devastation resulting in far greater damage than caused by the original shaking. Fortunately the scale of those events have not been repeated, however there have been many major earthquakes which have been followed by fires.

Another fact that comes out rather starkly from the study of FFE events is that the risk of FFE is very non-uniform. Many recent earthquakes were not followed by widespread fire events. The level of urbanization and industrialization is an obvious factor which possibly explains this anomaly (most certainly for the relatively remote and backward mountainous regions of Kashmir – even here, however, the main market in the town of Uri suffered a major fire following the earthquake which caused extensive damage). If urbanization (and concomitant density of gas, fuel and electrical supply networks) is indeed one of the key reasons, the risk of fire after earthquakes must then be considered as a rapidly increasing risk to life, livelihoods and to the sustainability of growth and

development in some of the world's most densely populated regions. With an increasing integration of the world economy, major disasters of the future could have repercussions far beyond the local region. FFE events have the potential to create such disasters and should certainly be considered in the overall disaster mitigation strategies by governments and agencies with such a remit. Considerable new research effort is required to which this thesis makes a small contribution.

1.2 Aims of this research

The aims of this research are twofold.

The first and primary aim is to develop a thermo-mechanical module for OpenSees so that it can be used to analyse structures at elevated temperature. The fully developed version of the software will include: the facility of applying a good selection of fire loads, such as standard curves code based analytical fires; modelling of heat transfer into the structural members; and simulating the structural response as a result of elevated temperatures. In this thesis only the capability of performing structural analysis using beam-column elements under thermal action is provided. Further work has been completed or will be completed by other team members in Edinburgh. To do so, thermal load classes, temperature-dependent material classes, thermal section class, thermal beam-column element classes, etc. have been developed. The thermal load classes are used to provide an adequate temperature distribution to the structural section. Temperature-dependent material classes provide information on the variation of material properties at elevated temperatures according Eurocode and other standards. Benchmark problems and real fire tests have been modelled, to verify the developed code.

The secondary aim of this research is to model an earthquake damaged reinforced concrete frame subjected to a subsequent fire (one of a series experiments carried out as part of a UKIERI funded project between University of Edinburgh and Indian Institute of Technology, Roorkee). The modelling started by carrying out a pushover analysis of the frame at the planning stage of the test in order to establish the dimensions, reinforcement and the loading required to sufficiently damage the frame. Further cyclic loading analyses were performed before the test as this was the mechanism by which seismic damage was to be simulated in the test frame. Following the test, further analyses were performed to compare the model and test results. Mechanical strains at certain test points were compared with the test data, as well as the residual displacement

of the frame after applying cyclic loading. Thereafter, the damaged frame was subjected to fire loading based on the temperature loading which was used to analyse the "damaged" frame model in the newly developed version of OpenSees. Finally the pushover capacity of the original frame after fire and damaged frame after fire was compared against the analysis results from the OpenSees model.

1.3 Outline of remaining thesis chapters

"Chapter two – Literature review" A review chapter, including concrete and concrete structures in fire, nonlinear analysis of frame structures and software tools for analysing structures in fire.

"Chapter Three – Factors Affecting Frame structures at Elevated Temperatures" A discussion of the important factors governing structural behaviour at high temperatures. These include the material behaviour and structural behaviour of steel and concrete.

"Chapter Four – OpenSees Architecture for the Analysis of Structures in Fire" A description of the class and sequence diagrams and the interaction of thermomechanical analysis related classes with the existing classes in the OpenSees framework.

"Chapter Five – Developing OpenSees" Description of the development of the thermomechanical modules of the program, the analysis of benchmark problems and modelling of structural fire experiments to validate newly developed code.

"Chapter Six - Modelling of a RC Frame Subjected to Post Earthquake Fire" A description of the modelling of an RC frame subjected to cyclic loading and subsequent thermal loading after it was damaged carried out at IIT Roorkee in India.

"Chapter Seven – Conclusion and Further work" The final Chapter summarizes the main conclusions from the research conducted and discusses the scope and recommendations for further work.

Chapter 2 - Literature Review

2.1 Introduction

This chapter is a literature review of the research that is relevant to this thesis. The review is divided into three sections, which are listed as follows:

- Reinforced concrete structures subjected to fire.
- Nonlinear analysis of framed structures.
- Software tools for analysing structures in fire.

2.2 Concrete Structures Subjected to Fire

Reinforced concrete is not uniform as a construction material, on the contrary, it is a highly non-homogeneous material, consisting of cement, aggregate, and steel rebars. All of these components may affect how reinforced concrete behaves when subjected to elevated temperature. Modelling concrete is also much more difficult than homogeneous materials, such as steel. The behaviour of concrete in fire involves not only instantaneous physical changes, such as thermal expansion, but also various chemical changes. This response is complex due to the non-uniformity of the material. [1, 2]. Most of its mechanical properties are changeable due to chemical and physical changes that may occur due to high temperatures, such as compressive strength, splitting tensile strength, modulus of elasticity and ultimate strain etc. Generally, concrete will maintain its compressive strength until a critical temperature (around 300°C) is reached, and after that point it will rapidly drop off.

2.2.1 Spalling of Concrete

Spalling can be described as the breaking of layers or pieces of concrete from the surface of a structural element when it is exposed to the high and rapidly rising temperatures experienced in fires (as defined in CIRIA Technical Note 118). The damage from spalling can vary depending on the material properties, the length of heating and the loading conditions, as shown in Figure 2.1. Indeed, under certain circumstances, a whole cross-section can be deteriorated by spalling, see e.g. Figure 2.2.

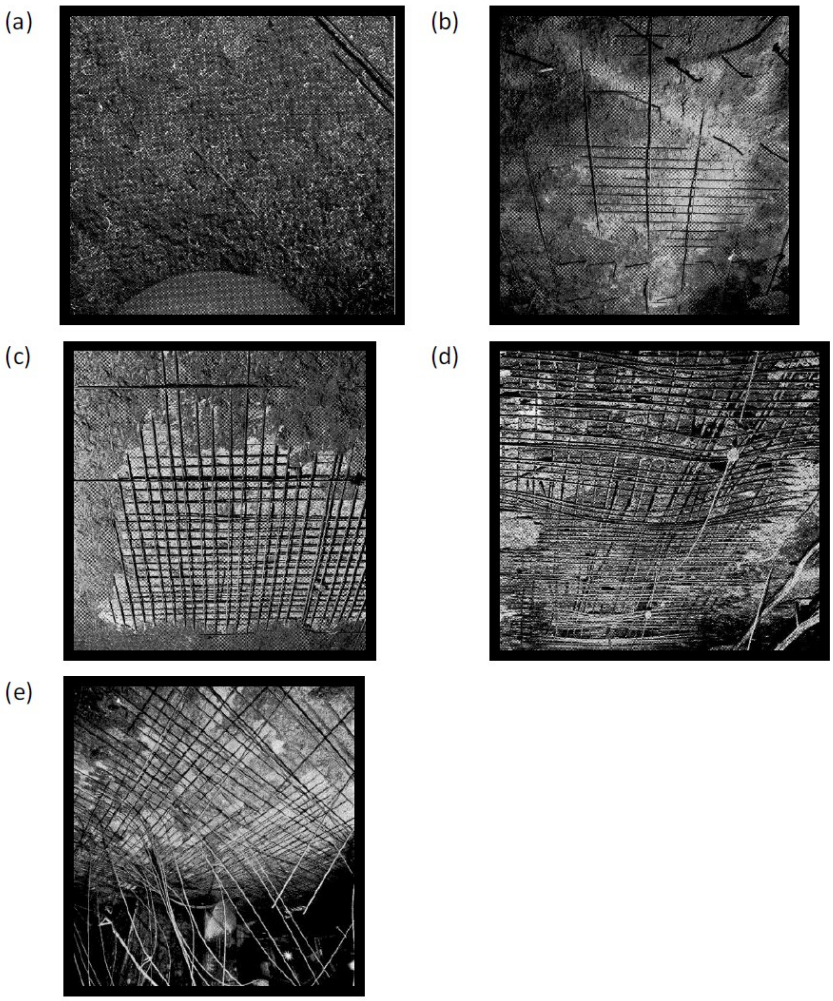

Figure 2.1: Photos showing the different levels of severity of spalling according to the investigation by Lindblad et al.: (a) first level, (b) second level, (c) third level, (d) fourth level, (e) fifth level. [3]

Figure 2.2: Severe fire spalling during fire testing of a high strength concrete floor slab exposed to unilateral fire. [4]

There are three main types of concrete spalling: surface spalling, corner break-off or sloughing off and explosive spalling. Explosive spalling is one of the most poorly understood processes in the reaction between concrete and high temperature [5]. Explosive spalling is thought to be caused by the build-up of water vapour pressure in concrete during a fire. The phenomenon is generally assumed to occur at high temperatures, yet it has also been observed in the early stages of a fire and at temperatures as low as 200°C[6].

It is generally believed that the rapid heating of concrete under fire is a more significant cause of spalling than the exposure of concrete to high temperatures over time. Some research suggests that thermal stresses and gas pressure may be of greater significance as causal factors of spalling than previously thought. Professor Khoury of Imperial College proposed that aggregate expansion caused by thermal stresses was an important cause of spalling, alongside the conventional 'moisture movement' theory at the 9 November 2004 meeting of the Concrete Fire Forum.

2.2.2 Cracking

In reinforced concrete and masonry structures, cracking and crushing of cover concrete could result in penetration of the flame and increasing the rate of heat transfer within the element. The processes leading to cracking are believed to be essentially the same as those leading to spalling. Thermal expansion and dehydration of the concrete due to heating may lead to the formation of fissures in the concrete rather than, or in addition to, explosive spalling. These fissures may provide pathways for direct heating of the reinforcement bars, possibly resulting in greater thermal stress and further cracking [7].

Geogali & Tsakiridis [8] studied the cracking in a concrete building subjected to fire, with particular emphasis on the depths to which cracking penetrates the concrete. Microscopically-petrographic examination, loading tests, and the macroscopic observation were used in order to determine the thermal history of fire-damaged concrete and to provide information regarding the maximum temperature at the surface exposed to fire. It was found that major damage was confined to the surface near to the fire origin, but the nature of cracking and discolouration of the concrete suggested that temperature exposure exceeded 700°C.

2.2.3 Effects of Reinforcement Bars

In reinforced concrete structures, steel enhances the concrete strength by carrying the tensile forces. It is also commonly used to reinforce timber constructions. In spite of its advantages, steel on its own is vulnerable in fire. Structural steel loses strength and stiffness at high temperatures which eventually leads to failure due to excessive deformations. This is crucial in steel as compared with concrete or timber members as steel conducts heat very well and often comes in thin or slender sections. Although steel is a non-combustible material, it has a high thermal conductivity, which adversely affects the structural performance during fire exposure. The structural strength of steel decreases by as much as half at a temperature of 600 degrees Celsius.

A great deal of research has been conducted to study the effects of using new types of reinforcement such as glass or carbon fibres, rather than steel, in concrete [9-12]. It has been found from most of the testing that with sufficient cover to the reinforcement, fibre reinforced polymer (FRP) reinforcement could have perfectly adequate fire endurance.

2.2.4 Deterioration in Material Properties

Deterioration in mechanical properties of concrete upon heating may be attributed to physicochemical changes in the cement paste and aggregate and their thermal incompatibility. It is also influenced by the temperature level, heating rate, applied loading, and so on. On a macro level, it can be observed that the compressive and tensile strength drop significantly at elevated temperatures, as well as the initial elastic modulus [2, 13]. Further details about the decrease of the strength of concrete are described in the Chapter 3.

2.2.5 Building Damage Caused by Fire

There are significant numbers of building fires every year worldwide. It is believed that steel structures are more vulnerable in fire than concrete structures, however some research and real fire incidents show that concrete structures may be equally vulnerable to collapse and damage. Results from a study, by the National Institute of Standards and Technology of the United States, indicate that 22 multi-story buildings have collapsed totally or partially due to fire worldwide since 1970 [14]. Fifteen of these incidents occurred in the USA, two in Canada, and 5 in Europe, Russia and South America. Out of the 22 building collapses, 7 buildings were reinforced concrete structures, 6 were steel frames, 5 were masonry systems, 2 timber structures and 2 unknown materials. A

study of these building collapses could reveal the fact that most of these collapses were mainly due to, not only strength degradation of the materials exposed to elevated temperature, but often due to the considerable effects of thermally induced deformation on the entire structural performance and thermal stresses and strains on the individual elements [15].

Figure 2.3: Collapse of CESP Building 2 due to fire in Sao Paulo, Brazil [14]

One of the largest building fire incidents, in Brazil, occurred on May 21, 1987 in Sao Paulo. The Sao Paulo Power Company (CESP) Building 2, a 21-story office reinforced concrete building partially collapsed two hours after the beginning of a fire. Studies show that the core of the building collapsed, throughout the building height, due to thermal expansion of the concrete T-beam, exposed to fire, leading to fracture of the vertical framing elements and their connections and resulting in a progressive collapse of the core structure. Fig. 2.3 shows the collapsed core area of the CESP building 2 after the incident [15].

Figure 2.4: Collapsed Textile Factory in Alexandria, Egypt [14]

In July 2000, a fire occurred in a 6-story reinforced concrete building, a textile factory in Alexandria Egypt, resulting in the mysterious collapse of the building. One thing that was ambiguous about this incident was the time of the collapse, which happened 9 hours after the start of the fire, when the blaze seemingly was under control and subsiding. Fig. 2.4 illustrates the building debris after the fire-induced collapse. In this case, again, thermal expansion could have been the main cause of the structural collapse [15].

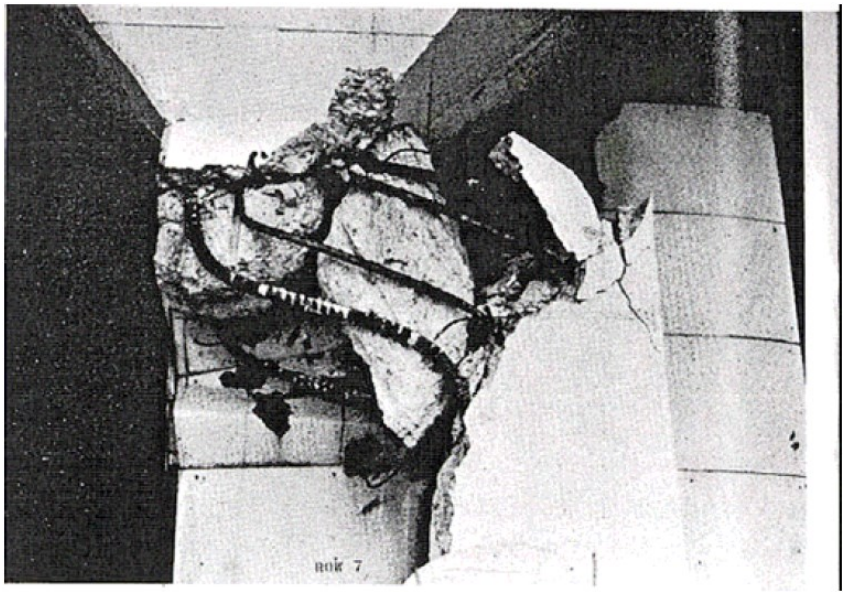

Figure 2.5: Large Lateral Deformations and Failure of Columns at Sixth Floor of Military Personnel Records Center

A partial roof and column collapse occurred in the Military Personal Record Center building due to a large fire in Overland in the USA on July 12, 1973. The building had a

large 86 m by 222 m 6-story reinforced concrete structure. The fire started on the 6th floor but due to the large amount of fuel, 21.7 million record files stored on the floor, it burned out of control for 20 hours. Collapse of the roof started approximately 12 hours after the fire started followed by collapse of the columns on the same floor. Fire damage on the lower floors was not significant. Results from the study on the structural damage indicated that the collapse of the building 6th floor was mainly due to the floor thermal expansion. The slab on the 6th floor was an 18 cm thick conventional concrete roof slab, supported by 41 cm reinforced square-tied columns and with no expansion joints in the floors or roof. Thermal expansion of the floor exposed to fire induced displacements of almost 60 cm in one corner. Fig. 3 shows shear failure of the column located at the floor corner, which is similar to the brittle column failures that have often occurred during earthquakes [15].

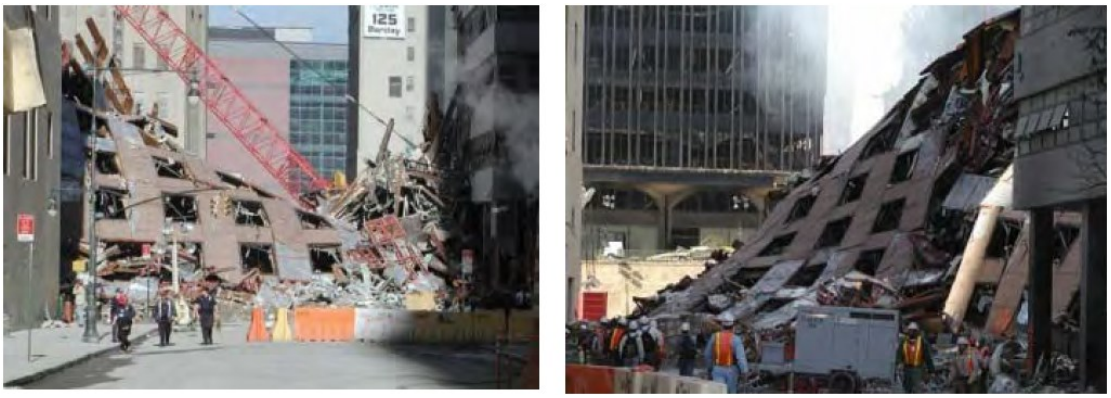

Figure 2.6: The World Trade Center Building 7 after the collapse due to fire [16]

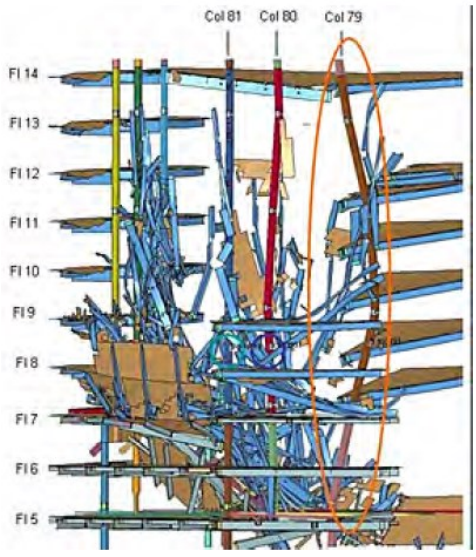

Figure 2.7: Collapse simulation of WTC Building 7 [17]

Fig. 2.6 illustrates the WTC Building 7 after the collapse. Result from modelling and collapse simulation of the building indicates that the progressive collapse of the building initiated by buckling of a column, as shown in Fig 2.7, as a result of the floor thermal expansion. As principal findings of this investigation, factors contributing to the building failures were identified as: “thermal expansion occurring at temperatures hundreds of degrees below those typically considered in design practise for establishing structural fire resistance ratings; significant magnification of thermal expansion effects due to the long-span floors, which are common in office buildings in widespread use; connections that were designed to resist gravity loads, but not thermally induced lateral loads; and a structural system that was not designed to prevent fire-induced progressive collapse” [15, 17].

Figure 2.8: Collapse of Pentagon building due to fire induced by crash of an aircraft September 11, 2001 [14]

Figure 2.9: World Trade Center twin towers collapse due to fire induced by crash of two aircrafts, September 11, 2001 [14]

Figure 2.10: World Trade Center Building 5 collapse due to fire, September 11, 2001 [14]

Figure 2.11: Collapse of a 9 story reinforced concrete building in St. Petersburg, Russia, on June 3, 2002, collapsed after a one hour fire [14]

Figure 2.12: Katrantzos Department Building, an 8 story reinforced concrete structure, in Athens after the 1980 Fire [14]

Figure 2.13: Collapse of the historic Vendome Hotel, a 5 story masonry and cast iron building, on June 17, 1972 in Boston, MA [14]

Figs. 2.8 to 2.13 illustrate further collapses of buildings on fire. A complete list of building collapses due to fire since 1970 is provided by the NIST [14]. A study of most of these past collapses suggest that most of these structural failures seem to share a similar pattern of collapse with considerable effects of systemic structural interactions,

especially thermal expansion effects, on the structural performance. Further investigation needs to be conducted to simulate and understand the collapse sequence and structural performance of these buildings due to the fire. Analytical models for consideration of the structural interactions, and especially effects of thermal expansion of floors, columns, beams and connections, are vital for fire safety and improvement of new and existing structures [15].

2.2.6 Performance-based Fire Design

Current building fire engineering practice is largely based on the application of prescriptive codes whereby the engineer designs in accordance with the furnace test [2]. The fact that buildings resist fire in a far more complex manner than furnace fire tests could make prescriptive design methods inappropriate for fire resistant design. Thermal expansion of structural members and the resultant forces to adjacent subassembly due to restraints on the heated members by cool parts were considered to be a significantly important reason which caused collapse of buildings in fire illustrated in the last section. Unfortunately this factor usually is not considered by prescriptive design because of testing isolated structural elements in furnaces. Furthermore, prescriptive design based on standard tests can also be too conservative since there no alternative load paths in members tested in furnaces, therefore once the material properties degrade beyond a certain point, the tested element collapses, but alternative load paths are likely to be available under real fire conditions in a building structure. Conservative design methods cause unnecessary expense, up to 30% of the total material cost of a multi-storey steel frame could end up being spent on fire protection [18]. Therefore considering behaviours of whole structures is a more appropriate approach.

Performance-based structural fire engineering/design can be defined simply as a design approach to simulate and evaluate performance of structures under realistic loads, which includes fire, to determine and design the level of protection against structural failure [15]. Khoury also provided a description as follows: Performance-based methods are based on fire engineering calculations, and provide a cost-effective and flexible method of assessment superior to prescriptive methods. A given problem can be studied for different fire scenarios, geometries, material properties, loading or support conditions. This can be performed in a relatively short period of time, thus allowing a better understanding of the behaviour of the structure subjected to fire until collapse. Moreover, computer programs can even simulate structural conditions that are very

difficult to study in a fire test [2]. Anderberg mentioned that the structure may not be allowed to collapse during the complete fire process in a performance-based design, including the cooling phase [19].

Recent advances in the area of structural fire engineering have enhanced the understanding of structural performance in fire, with particular consideration for the thermo-mechanical behaviours that arise in isolated members as well as interconnected structural components. Despite recent advances, performance-based structural fire design continues to be highly uncommon in practice due to existing limitations in standards, design guidelines, analytical methodologies, and/or educational practices [20]. In the USA and Canada, performance-based fire design and engineering is still only an emerging design option [21]. It has been applied for only notable projects in which fire safety has been a major concern and detailed investigations were required to assess and determine a reliable level of performance [15]. In the UK, performance-based fire design is also one of the options as a complement of prescriptive according Eurocode and British Standard [22-26]. Researches and studies still need to be carried out to develop the required analytical tools and information for the application of such performance-based fire design approaches in practice.

2.2.7 Fire Testing

Recent tests of structures in fire are performed based on either standard fire tests, which usually include one single structural member tested in furnaces, or infrequent full-scale fire tests, which are not so frequent considering the high cost. The standard fire tests are more acceptable and practical compared with full-scale tests for the reason of low cost. The shortcomings of furnace tests are: 1) in the most of cases the effects of loads and boundary conditions are not considered; 2) the tested element is regarded as an isolated member and not a part of the structure as in the practice; 3) the applied fire loads are derived from standard fire time-temperature curves such as ISO 834, which has little relevance to the real fire condition. Although standard tests are useful benchmarks for the sake of structural performance comparison of individual elements in fire, they hardly simulate performance of the structural elements in a realistic fire, sometimes less severe heating environments[27]. Full-scale tests provide more reasonable simulations of structures under realistic fire scenarios but for the reason of high cost very few large scale tests have been carried out. Furthermore, most of these tests have been on steel or composite structures. Full scale tests of reinforce concrete structures in fire are

especially rare. One of the most well-known experimental programs on a reinforced concrete frame in fire was the full-scale test conducted by the Building Research Establishment (BRE) in Cardington [28]. Unfortunately key data was lost during this test, which makes it of limited use for numerical modelling, however, the available results and observations provided valuable insight into the holistic behaviour of reinforced concrete building frames when subjected to fire.

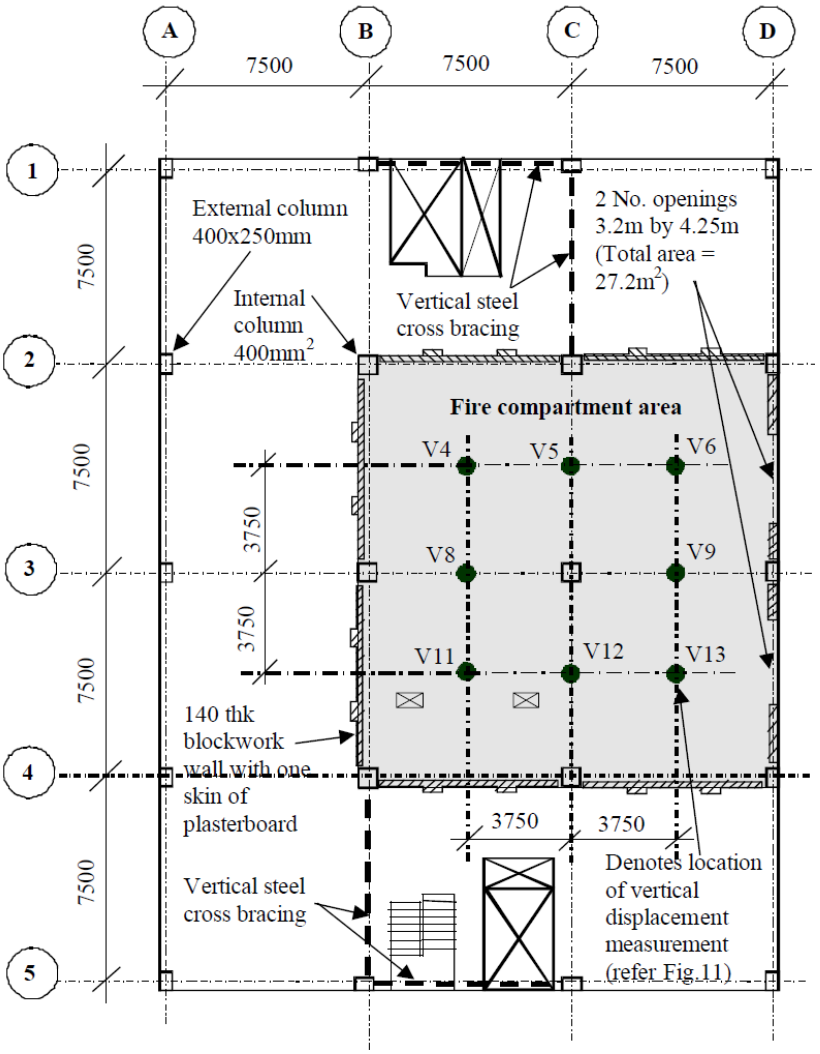

Figure 2.14: Plan of building showing location of fire compartment [28]

The full-scale seven-storey reinforced concrete building constructed in situ at the BRE Laboratories in Cardington, was designed to represent a commercial office building situated in the centre of Bedford. It was constructed in 1998. The completed building comprised 3 bays by 4 bays each 7.5m, with two core areas (Figure 2.14), which included steel cross-bracing to resist lateral loads. Each floor slab is nominally 250mm

thick, grade C37 normal weight concrete and designed as a flat slab supported by internal columns 400mm square and external columns 400mm by 250mm.

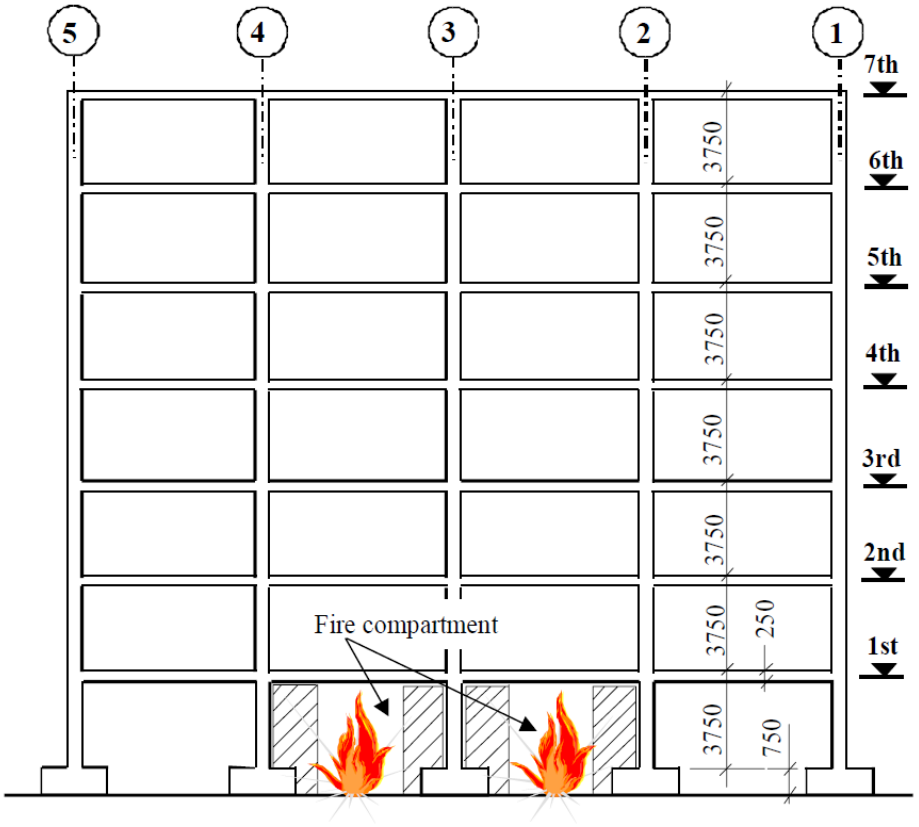

Figure 2.15: Cross-section through the building showing location of fire test [28]

A fire compartment, with a floor area of 225m^2, was constructed between the ground and first floors (Figures 2.14 and 2.15). Due to the height of the footings, the overall height of the compartment from the laboratory floor to the underside of the first floor was 4.25m (Figure 2.15). The compartment walls were constructed using 140mm thick Topcrete blocks and lined, inside the compartment, with one skin of plasterboard. The laboratory floor was also lined with plasterboard. The design of the fire was based on the parametric approach from Annex A of the fire part of the Eurocode 1 for Actions.

The test was conducted on the 26th September 2001. Unfortunately, all the instruments malfunctioned approximately 18 minutes after ignition. When the concrete to the soffit began to spall, the fixings to the blanket failed. The fire escaped the compartment and burnt through the cables.

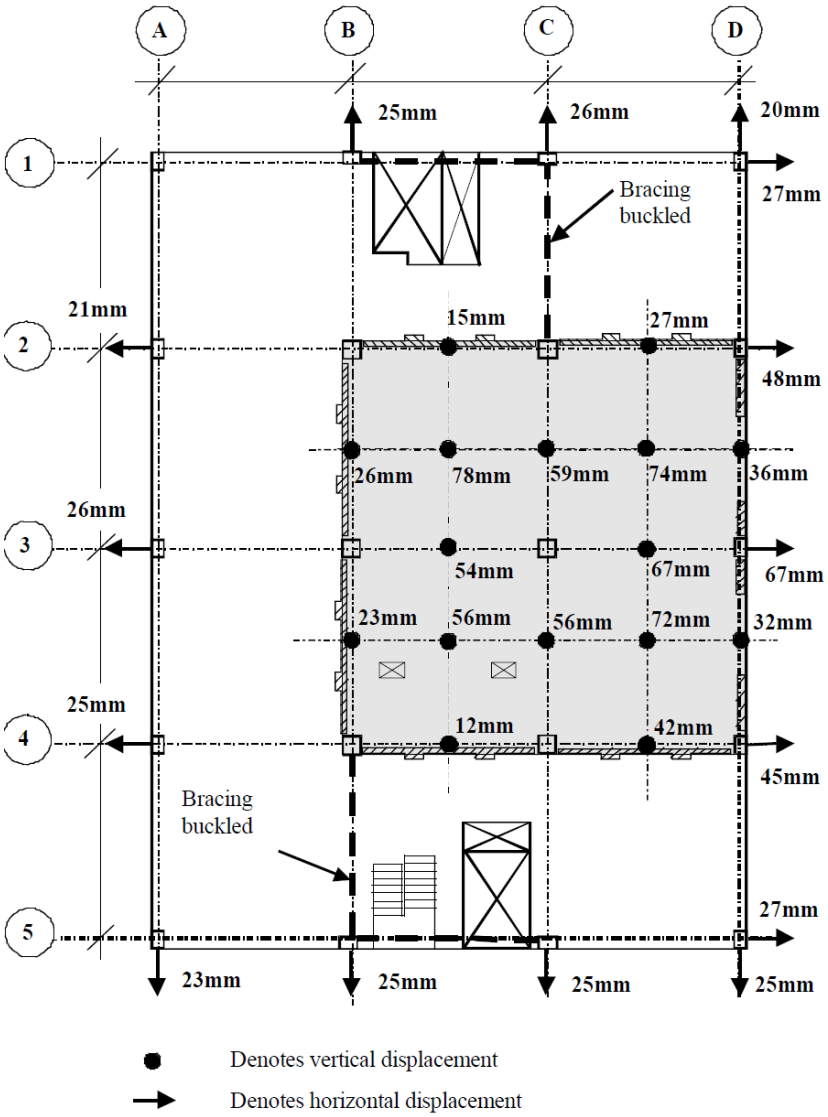

Figure 2.16: Residual horizontal and vertical displacements [28]

Figure 2.17: Buckling of bracing between columns B4 and B5 (similar buckling of bracing between columns C2 and C1 was also observed) [28]

The structure showed no signs of collapse during or after the fire. The residual vertical and horizontal displacements at first floor level are shown in Figure 2.16. The horizontal movement of the floor slab also caused buckling of the steel cross-bracing positioned on gridline B and C (refer Figure 2.16), as shown in Figure 2.18.

Although the Cardington fire test for the reinforced concrete frame building was not perfect, it was a very important experiment. This test showed clearly the effects of heated structural members to the adjacent cool parts of structure, which are not considered in the traditional prescriptive design thereby supporting the performance based design approach for designing fire resistance of structures.

2.2.8 Structural Performance and Modelling

Khoury et al presented a general brief outline of the effect of fire on both concrete material and concrete structures and reviewed the following subject areas that were receiving most attention before 2001 [2]. Usmani et al presented some of the most important and fundamental principles that govern the behaviour of composite frame structures in fire in a simple and comprehensible manner, in order to provide a means of estimating forces and displacements in real structures with appropriate idealisations [29]. They recognised that contrary to popular belief, composite steel framed structures

possess a much larger inherent fire resistance than that apparent from testing single steel members in fire furnaces. This is based upon the analysis of the response of single structural elements under a combination of thermal actions and end restraints representing the surrounding structure [29].

It's very clear that heated members in a structure show very different behaviours compared to individual elements in a furnace, which is confirmed by the Cardington test of the reinforced concrete building. Modelling of single concrete beam or column in fire has been performed by many people, such as [30-34], there is also some literature conducting the modelling of whole concrete structures in fire, a selection of which is discussed as follows.

Huang etc.[35] performed numerical modelling of a commercial office building with a concrete frame subjected to a large scale standard fire. The building was on a 7.5m grid with a 250mm slab and downstand beams between columns and typical office loads and was designed to have 2h fire resistance. The modelling did not allow for any spalling so reinforcement temperatures could be regarded as conservative.

After 120min fire exposure, the maximum floor deflection was calculated to be 250mm, and significant tensile membrane action was shown to have developed at the mid-span of the slab. This was accompanied by three-fold increases in the tensile forces in the downstand beams. Columns showed an initial upward expansion of up to 25mm, followed by a downward movement due to loss of strength and stiffness, and the analysis was stopped when column buckling occurred. Overall horizontal movements of the slab were not reported.

Again, given the considerable reliance of the structure on tensile membrane action for slab support, a mechanism which is dependent on the tensile strength of the bottom reinforcement, it is probable that spalling could have a very detrimental effect on this beneficial membrane action. It was unclear whether column buckling was caused by horizontal expansion of the slab or simply by loss of vertical load carrying capacity [36].

Plank [37] later refined this study using the same structural configuration but allowing for the effects of spalling by using a reduced cover to reinforcement. Where no spalling was modelled, the slabs achieved the required 2h fire resistance with deflections limited to around 250mm. However, if spalling was included to the same depth as the cover, runaway deflection occurred at around 45min. This behaviour was more marked for a

flat slab configuration with failure occurring at only 19min where spalling of 23mm was modelled [36].

Cvetkovska [38] noted large horizontal slab displacements in modelling of a three bay, two storey flat slab structure exposed to various fires. Beneficial compressive membrane action occurred in the central restrained bay but not in the perimeter bays. Outward movements of the perimeter columns of up to 27mm occurred due to the lack of restraint, generating significant additional moments in these perimeter columns. This corresponds well with the effects seen at Cardington [36].

The performance of the Cardington building was also modelled numerically [39]. The scenario chosen was one in which a single internal column failed. In this scenario there was an initial outward thrust which reached a maximum lateral displacement of 24mm. After that, the catenary effect arising in the slabs from the loss of the column led to the compressive outward thrust being replaced by tensile membrane action. On the assumptions made, the whole frame above and around the failed column was able to redistribute loads to prevent collapse. These assumptions included continuity in reinforcement that enabled it to sustain the induced tensions and excluded consideration of spalling that could have jeopardised the strength of the reinforcement. The behaviour of the frame actually observed in the full-scale test is very different from this as there was extensive spalling, and significantly larger outward lateral thrusts because there was no internal column failure in the real fire that occurred. Also, it would appear from the report that the modelling of the concrete behaviour did not include transient strain. This omission means that the results of the modelling are almost certainly unconservative and therefore, by implication, may well be unsafe [40, 36].

Wu and Tang summarized the state-of-the-art of fire-resistance study on concrete structures including retrofitted structures and re-used structures in 2010. The authors suggested that Random fire resistance of structures, cooperative action of structural members at high temperature and fire behaviour of the whole structure are main problems for concrete structures in fire and need to be studied in the future [41].

2.3 Nonlinear Finite Element Analysis of Frame Structures

Much research has been carried out on nonlinear structural analysis at many different research centres around the world. More specifically, there are several studies on the nonlinear behaviour of frames, which have been conducted since the 1960s. As the

number of these studies is large, only a few of the relevant works are discussed herein. Both material and geometrical nonlinearity are included. The proposed elements are based on the displacement formulation, which include lumped model, and distributed nonlinearity model. Force based elements are not discussed in this chapter.

2.3.1 Material and Geometrical Nonlinearity

Nonlinearities in framed structures usually refer to material nonlinearity (inelasticity of the materials) and geometrical nonlinearity (changes in the geometry of the structure). For a reinforced concrete structure, the material nonlinearity is connected to properties of concrete and steel, both of which show inelasticity when subjected to large strain. Concrete is a mixed material and one of its notable features is that it responsds differently to tension and compression. Although its tensile stiffness is as large as compressive stiffness, the tensile strength of concrete is very low, so that it is often neglected in design codes (the tensile stiffness can not be used without the tensile strength). When subjected to compression, concrete shows an elastic behaviour at the beginning, which can be observed from the stress-strain curve. Thereafter concrete stiffness decreases significantly for stresses larger than about $0.5f_c$, where f_c is the concrete strength in uniaxial compression. For that reason, the initial stiffness of concrete is derived from the equation $E_0 = \frac{2f_c}{\varepsilon_0}$ in some design codes, where E_0 is initial stiffness, ε_0 is corresponding strain to f_c. After reaching its compressive strength, concrete softens at a rate which decreases sharply and then increases gradually. Compressive and tensile stress-strain curves of steel are almost symmetrical, and both of them exhibit elastoplastic behaviour. Furthermore, steel reinforcement may contain residual stresses due to the fabrication or erection processes. Connections between steel and concrete components contribute to the nonlinearity of a composite system due to bond slip.

Geometric nonlinearities are generally classified into global and local nonlinearities. Global geometric nonlinearities, often referred to as *P-δ* and *P-Δ* effects, may be incorporated in global models following basic procedures used in nonlinear frame analysis [42]. Typically, in a global geometry nonlinear solution, (1) deflections of the structure are large compared with the original dimensions of the structure, and (2) changes in stiffness and loads occur as the structure deforms. Local geometric nonlinearities are usually neglected in reinforcement concrete frame analysis, and

considered only in steel or composite frame analysis, such as local buckling of steel components. There are three numerical approaches for geometrically non-linear frame analysis problems, total Lagrangian, updated Lagrangian and co-rotational formulations. These kinematic formulations are similar for finite deformation problems in continuum mechanics, with the only difference being the reference configuration system adopted to describe the motion of the body. However, for structural elements based on approximate geometrically nonlinear theories, the results of the different formulations may not be the same.

2.3.2 Displacement-based Beam-column Elements

The development of elements for elastic nonlinear analysis of frames started in the 1960s [43-46]. From then on, generally two models have been developed to describe the nonlinear beam-column element, lumped model, and distributed nonlinearity model.

For lumped elements, all of the inelasticity is assumed to occur at the two ends of the member, and the rest of the member remains elastic. Inelastic material behaviour can be dealt with in an approximate but computationally efficient manner in this case. Although lumped plasticity models imply behaviour that is a physical impossibility, they have the advantage of being conceptually simple in addition to the computational convenience of having a stiffness matrix in a concise form. Hajjar and Gourley [47] presented a lumped plasticity model for concrete filled tube members.

Distributed plasticity models, on the other hand, provide a more accurate description of the inelastic behaviour of reinforced concrete members. In distributed nonlinearity models, material nonlinearity can take place at any element section and the element behaviour is derived by weighted integration of the section. Thus distributed models are more expensive in terms of computational cost. In practice, since the element integrals are evaluated numerically, only the behaviour of selected sections at the integration points is monitored.

In the classical two-node, Euler- Bernoulli displacement-based frame element, the beam displacements are expressed as functions of the nodal displacements using shape functions [42]. Displacement method was developed earlier than other methods. This method is quite simple and easy to implement. However, it is not very accurate, due to the assumption of cubic displacements (and thus linear curvatures). This assumption is based on the assumption that the Euler-Bernoulli beam is in the linear elastic range, and

the cross sections of the element are unchanged. If the cross section changes (due to plasticity) and the material response is nonlinear, some errors will occur, and only approximate results can be derived by the displacement method. These are common phenomena in finite element analyses. The solution to these problems is dividing a single structure member into several elements to increase the number of global degrees of freedom.

In the two-node, Euler-Bernoulli force-based frame element, the beam section forces are expressed as functions of the nodal forces through force shape functions [48-51]. The force-based element is rather attractive because it is exact within the small-deformation Euler-Bernoulli beam theory. Spacone *et al.* [48, 49] propose an iterative method for the force-based element state determination. The iterative procedure is very robust for both strain-hardening and strain-softening section responses. However, the iterative procedure is so involved that it may cost twice as much as the displacement method in terms of processing time.

More points at which nonlinear behaviour is monitored, more accurate the solutions of a distributed model are. However, more computer memory is also required since the additional points being monitored require additional storage space for the variables involved. Inelastic analyses by Sfakianakis and Fardis [52] indicates that the use of five Gauss points along the element length results in sufficient accuracy for most practical purposes while maintaining a reasonable demand on computer memory requirements. It should also be noted that the use of a large number of Gauss points along the member may cause lack of objectivity in the response of softening elements. As soon as a section starts softening the inelastic response of the member tends to localize in this section, and different post peak results are obtained if the number of Gauss points is changed. Regularization techniques are available from the finite element literature, while a specific study on localization issues in force-based beam elements is presented by Coleman and Spacone [53].

2.3.3 Fibre Section Models

For the nonlinear analysis of reinforced concrete members, the most promising models are presently fibre elements. The definition of the fibre section model is not complex. The section of the element is subdivided into many areas, each small area represents a single fibre. There is only a uniaxial force along the fibre. And the total stresses are integrated over the cross-sectional area to obtain stress resultants such as axial force or

moment. Basically a number of assumptions are used in the fibre section model as follows.

(1) Plane sections remain plane and normal to the longitudinal axis during the element deformation history. It is generally believed that this is accurate even if the element is in the non-elastic range.

(2) Shear and torsion stresses are neglected. For this reason the Euler-Bernoulli beam theory can be reasonably applied on the fibre section element.

(3) Although constitutive relations are typically defined as uniaxial, multiaxial stress states can be included by increasing the concrete strength and by modifying the concrete post peak response.

(4) Concrete cracking is included. The effect of cracking can be included in the model by an appropriate modification of the stress-strain relation of reinforced steel or concrete according to the smeared crack approach.

Each fibre in the section can have its own material property, which means that concrete and rebar material properties can be assigned to fibres. According to the ‘‘plane sections remain plane’’ assumption and from relevant constitutive models of concrete and steel, fibre stresses can be derived from the fibre strains. There are different approaches to finding the fibre strains as the load history on the section progresses. The first way is that, (1) find the reference line of the cross section, which is fixed from the beginning and calculated by the area and coordinate of every single fibre; (2) assign the section axial strain and curvatures according the reference line. In this way there is no need to trace the position of the neutral axis in every incremental step [48, 49]. More generally, El-Tawil and Deierlein [50, 51] follow the changing progress of the section neutral axis during the load history.

To compute the fibre stresses and moduli of elasticity, uniaxial constitutive models for concrete and steel are needed. For the concrete models, the Kent and Park [54] model, later enhanced by Scott et al. [55] to include the confinement effects, has been extensively used for the analysis of reinforced concrete and composite sections.

The assumption that concrete has no strength or stiffness when the cracking occurs has been frequently used in fibre analysis. There have been attempts to account for the tension stiffening effect in composite sections, mostly based on models developed for reinforced concrete [56, 57]. Another approach is possible whereby the strength and stiffness characteristics of the reinforcing bars are modified instead of the concrete properties. Tension stiffening mostly affects the section response up to and immediately after cracking, and does not affect the section response at failure.

Most steel models used for fibre section analysis are uniaxial stress-strain relationships. Several studies have analyzed composite structures using a simple bilinear relationship with or without strain hardening after yielding and have obtained satisfactory correlation between experimental and analytical responses [58, 59]. Alternatively, more accurate models such as the Ramberg-Osgood [60] Or Menegotto-Pinto [61] model have also found wide application. For their study on concrete-filled tubes, Hajjar et al. [62] derived the uniaxial steel constitutive model from a multiaxial constitutive law proposed by Shen et al. [63].

2.4 Software Tools for Analysing Structures in Fire

The existing computer programs used in structures in fire (SiF) modelling can be distinguished into two groups [64]:

Many programs that have been specifically developed for structural analysis under fire conditions. Most of these programs belong to individual researchers or research groups, and most of them have seen their development stalled after a while. Only some of them are still being developed and probably used by other researchers.

Commercial software that have been adapted for structural fire analysis. These software have not been developed with the objective of modelling structures in fire, but they offer numerous possibilities, have great pre- and post-processing capabilities and have normally received extensive attention for their validation.

A review of the capabilities of fire dedicated thermal and structural analysis programs should be mentioned here, which was provided by Sullivan et al. [65]. Although it was completed almost 20 years ago, most of the programs being used currently by people can be found in this review. In the work described in this review, no less than seven different thermal analysis programs and fourteen structural analysis models had been identified, including FIRES-T3 [66], TASEF [67], SUPER-TEMPCALC [68], STABA-

F [69], CEFICOSS [70] (Franssen then developed another software named SAFIR), ADAPTIC (Imperial College), FASBUS-II [71], FIRES-RCII, CONFIRE [72], ISFED [73], BFIRE [74], FIRESTRUCT, INSTAF (which became VULCAN) and FEAST.

Most of the specialist codes mentioned above have ceased to develop any further [75] with the notable exceptions of SAFIR, VULCAN and ADAPTIC. In this chapter, some of the codes currently being used for SiF analysis are reviewed in detail, in the following sub-section.

The commercial software that can be used to perform thermal and following mechanical analysis includes ABAQUS, ANSYS, DIANA.

2.4.1 FIRES series

The first attempt to model the behaviour of structures in fire numerically was the work completed at Berkeley, where the team of Bresler developed the software FIRES-T [76] and FIRES-RC [77] for the analysis of reinforced concrete elements [64]. These programs have been developed later by Iding, and received a wider field of application. Subsequent versions were named FIRES-T3 and FIRES-RC.

FIRES-T3 (the **Fi**re **Re**sponse of **S**tructures – **T**hermal –**Three**-Dimensional version) is a computer program for evaluating the temperature distribution history of structures subjected to fires [66]. There are options for fully three-dimensional solids, two-dimensional cross-sections, and structures in which heat flow is one-dimensional. This program also permits the use of one, two, and three-dimensional elements together in the same structure. Structures may consist of one material or may be composites such as reinforced concrete. The temperature distributions generated by FIRES-T3 can be used in conjunction with any stress analysis program (FIRES-RC II for example), together providing an overall capability of predicting the response of structures subjected to fires.

The computer program FIRES-RC II, **Fi**re **Re**sponse of **S**tructures – **R**einforced **C**oncrete Frames, **Second** (revised) version, is used to evaluate the structural response of reinforced concrete framed structures in fire environments [78]. The structural response analysis accounts for: (1) dimensional changes caused by temperature differentials, (2) changes in mechanical properties of materials with changes in temperature, (3) degradation of sections by cracking and/or crushing, and (4) acceleration of shrinkage and creep with an increase in temperatures. The solution method chosen for use in FIRES-RC II is a nonlinear direct stiffness procedure coupled

with time step integration. That is to say, within a given time step, an iterative approach is used to find a deformed shape resulting in equilibrium between forces associated with external loads and internal stresses. Degradation of strength and stiffness can be caused by concrete crack/crash and steel reinforcement yield in the program, but spalling of concrete is not accounted due to calculation of temperature distribution histories in FIRES-T is based on the assumption that across-sections remain intact. The analysis is concerned with structural response history prior to development of large deformations and failure in FIRES-RC II, so that neither geometric nonlinearities are considered.

For unknown reasons, the interest for SiF modelling decreased progressively in the U.S.A. and most of the activity in the field since the 1980s has occurred in Europe [64].

2.4.2 FEAST

Finite Element Analysis of Structures at Temperatures (FEAST) has been developed at the University of Manchester by T. C. H. Liu. This program was originally developed focusing on structural behaviour of steel portal frames at ambient temperatures [79].

The computer program was then developed to simulate the response of steel structures in the event of a fire [80]. It was further developed to model the behaviour of steel/concrete composite connection at elevated temperatures [81].

The program's library of finite elements includes shell elements, solid elements, bolt, gap and contact elements. A particular useful feature of this program is modelling bolts [82]. In a bolt connection, when the bolt expands under an increasing temperature, it may become slack, so that this is no axial force in the bolt. Under these circumstances, any form of conventional 1D finite element (bar or beam type) connection two components, such as a column flange and end-plate, would normally result in an axial compression force being induced inside the bolt with local compressive reactions at the two ends. In order to solve this problem, a special type of element has been developed.

The frontal-solver technique has been employed in this program. With the technique, it does not have to terminate when a structure encounters a local failure which causes the diagonal element of the stiffness matrix to become non-positive. Therefore, FEAST can be used to find solutions for post-failure analysis.

The FEAST program is capable of accurately predicting the detailed behaviour of steel members and steel and composite connections under fire conditions. Buckling in a steel member can also be simulated. However, it is not practical to analyse the non-linear behaviour of large-scale steel fames with many members since the beam element formulation is linear elastic. The concrete constitutive model is not robust and not suitable to simulate composite structural behaviours [75].

2.4.3 SAFIR

The subject of SiF modelling was first investigated at the University of Liege by Dotreppe, based on a previous program published in France [64]. Some principles of the program were used when Franseen wrote the software CEFICOSS for the steel producer ARBED [70]. As ARBED had no interest in further development of CEFICOSS, a new SiF modelling software has been developed by Franssen and his co-workers.

The software SAFIR can be used for both the thermal and the mechanical analysis at elevated temperature, and has an automatic transmission of information form one analysis to the other. Like most specific SiF software, thermal and mechanical analyses are carried out separately and subsequently, not fully coupled.

SAFIR has a finite element library of 2D and 3D solid elements, 1D beam elements, shell and truss elements [75]. Various temperatures-dependent materials are included, and user defined materials are permitted.

If beam finite elements (2D or 3D) are used in a mechanical analysis, 2D thermal analysis will be performed to derive the temperature distribution on the cross section of the beam. That is to say, assuming the temperature is constant along the length of one single element.

While shell elements are used in the mechanical analysis, the assumption is that the temperature varies only in the thickness. Both concrete and steel structures can be simulated using shell elements, as well as local buckling. Recently, the possibility has been introduced for the user to define a temperature distribution in the shell element which varies both along the thickness and along directions orthogonal to the thickness [83]. This is done by a Dynamic Link Library procedure that the user has to write and compile separately.

The arc-length method is also included in the program to analyse post –buckling behaviour. However the arc-length method is implemented in such a way that at present, only simple structures can be analysed [75].

If a truss finite element is used in the mechanical analysis, this is mainly to represent slender steel elements in tension. It is then assumed that the temperature is uniform on the section of the element and this temperature can be determined by simple calculation models based on the hypothesis of uniform temperature and on the massivity factor.

2.4.4 VULCAN

VULCAN has been developed by successive researchers since 1985 in the Department of Civil and Structural Engineering at the University of Sheffield [75].

The predecessor of VULCAN is INSTAF [84-86], which was used to analyse the behaviour of 2D steel frames at ambient temperature in Canada. This program was modified to incorporate the stress-strain relationships of steel at elevated temperatures firstly by Saab at Sheffield University [87, 88]. Deterioration in material strength with increasing temperature is represented by a set of nonlinear stress-strain-temperature relationships using a Ramberg-Osgood equation in which creep effects are implicitly included. Structures subjected to increasing loads or temperatures are analysed using an incremental Newton-Raphson iterative procedure. It includes the effects of geometric nonlinearity, temperature dependent nonlinear material behaviour and variations in temperature distributions both along and across each member.

INSTAF was extended by Najjar [89, 90] later, so that the program can be used to perform 3D analysis. This extension enables simulation of warping and lateral-torsional buckling.

Further development of this program was carried out by Bailey [91, 92]. Shell finite elements were introduced in the program, which can be used to simulate the floor slabs. Bailey's treatment of concrete slabs was essentially linear and high temperatures were not considered, while simulating the Cardington tests[93]. Other extensions performed by Bailey included the modelling of semi-rigid connections, lateral torsional buckling, continuous floor slabs and strain reversal, and so on.

In 1998, the name of the program was changed from INSTAF to VULCAN. The next stage of development of the program was by Huang et al. [94, 95], who introduced a

layered approach to model the reinforced concrete floor slabs. In this approach, a concrete slab is divided into a number of layers in the thickness direction and the reinforcement is treated as a smeared layer. The layered approach allows temperature variation in the concrete slab to be included. The objective of the current phase of the research has been to extend the layered procedures previously developed by the authors intended for modelling in fire conditions of solid and ribbed reinforced concrete slabs, to include geometric nonlinearity [96-100]. A total Lagrangian approach is adopted throughout, in which displacements are referred to the original configuration. The influence of thermal expansion, tensile membrane action and different temperature distributions across the thickness of slabs, the connection, as well as concrete spalling have been accounted for [101, 102].

It is worth noting that VULCAN is primarily a structural analysis software, and temperature distributions are treated as input data.

2.4.5 ABAQUS

Abaqus FEA (formerly ABAQUS), a suite of software applications for finite element analysis and computer-aided engineering, was originally developed and marketed by Hibbitt, Karlsson & Sorensen, Inc., (HKS). HKS was founded in 1978 by Dr. David Hibbitt, Dr. Bengt Karlsson and Dr. Paul Sorensen and were acquired by Dassault Systèmes in 2005 [103].

Both thermal and mechanical analysis can be performed using ABAQUS. An early attempt on temperature analysis of concrete structures exposed to fire was carried out using ABAQUS by Palm in Sweden [104]. Various structural members were studied, such as rectangular beams, slabs with circular enclosures, and steel-concrete composite slabs. Influences of phase changes and other nonlinearities were taken into account. The results were compared with results from the relatively “mature” computer codes TASEF and SUPER-TASEF. It was observed from the results that (1) the temperature histories derived from the three programs agreed with a high accuracy for the beams and composite slabs; (2) they also agreed for slabs with circular enclosures hollow core modelled as perfectly insulated; (3) however, the ABAQUS results did not match with results from other two program if the circular enclosures were modelled with internal radiation heat transfer. Since then, ABAQUS has been used to perform heat transfer analysis and mechanical analysis of structures by more and more people at many different research centres.

The program was used to study the behaviour of steel and composite framed structures in fire by Edinburgh University [29, 105-108] and Corus Research in the United Kingdom [109, 110] with reference to the Cardington tests. Beam and shell elements were used in these models. To avoid convergence problems while using standard ABAQUS shell elements, Gillie [111] developed a user subroutine to use the stress resultant approach to deal with concrete slabs to model composite slab behaviour in fire.

Since then ABAQUS has been used to model other structural components. To understand the behaviour of cold-formed thin-walled steel panel systems if fire, a series of tests have been performed as well as numerical analysis by ABAQUS at the University of Manchester [112, 113]. Concrete-filled steel tubular columns were also tested and modelled numerically by the same group[114]. Local buckling of the steel tube was modelled in this study.

The program has been also used to model the bolted end-plate connections [115-118]. In contrast with VULCAN, where the connection is modelled as a special component based element, the bolt and end plate are usually modelled using 3D solid elements in ABAQUS. Contact between all connected parts is modelled using the surface interaction command in ABAQUS allowing small relative sliding at the interface of the contact surfaces.

ABAQUS has been also used to model the behaviour of reinforcement concrete structures in fire over the past decade (Usmani and Cameron 2004; Ellobody and Bailey 2009; Law and Gillie 2010). Some of the phenomena associated with concrete at high temperature are not modelled easily, eg. spalling, not in the case of ABAQUS, but also other software like ANSYS, SAFIR and Vulcan [119].

Chapter 3 - Factors Affecting the Frame Structure at Elevated Temperatures

In this chapter important relevant aspects of material and structural behaviour under elevated temperatures are discussed. As the modelling concerns a reinforced concrete frame, the discussion is limited to steel and concrete. Structural behaviour will be discussed in the context of a beams subjected to uniform temperature increments and thermal gradients in order to illustrate the key features of response.

3.1 Material Behaviour under Fire

The two most commonly used materials in reinforced concrete frame structures are concrete and steel which are often combined to form reinforced concrete. The effects of temperature on material behaviour can be broadly divided into 1) changes of the mechanical properties. Both steel and concrete become weaker and more flexible at high temperatures; and 2) thermal expansion. The behaviour of these materials at elevated temperatures is more complex than at ambient temperature. To understand these complex behaviours, it is necessary to avail the basic information on material properties. This information is usually presented in the form of stress-strain relationships of steel and concrete under different temperatures, changes of initial Young's modulus and ultimate strength with temperature, temperature induced strains (including thermal expansion and creep), Poisson's ratio and thermal properties, such as thermal conductivity and specific heat, all of which can and do vary with temperature.

3.1.1 Steel

Steel at ambient temperature is generally considered to have a relatively simple material behaviour, because it can be assumed that it has the same stress-strain curve in tension and compression. The important mechanical properties of most structural steels under static load are indicated in the idealised tensile stress-strain diagram shown in Figure 3.1 [120]. Initially the steel has a linear stress-strain curve ($\boldsymbol{E}$), and after reaching the yield stress $\boldsymbol{f_y}$, the steel flows plastically without any increase in stress until the strain-hardening strain $\boldsymbol{\varepsilon_{st}}$ is reached. Beyond this point, the stress increases until the ultimate tensile stress $\boldsymbol{f_u}$. After this, reductions occur, and the load capacity decreases until fracture takes place.

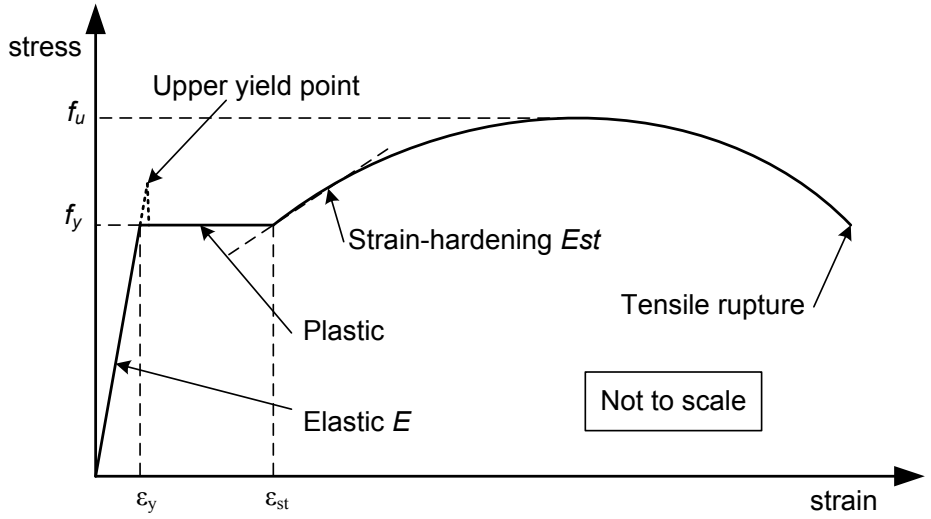

Figure 3.1: Idealised tensile stress-strain diagram of mild steel at room temperature

The material properties of steel at high temperatures are very different to those at room temperature. For example, the yield point is no longer clear while the temperature is above 200ºC, and the stress-strain curve becomes increasingly non-linear other than bi-liner before mechanical strain reaches ε_{st}. Figure 3.2 shows this trend of steel S690 [121]. To obtain an alternative of the yield stress, the nomination of a stress corresponding to the plastic strain 0.2% is often adopted [122].

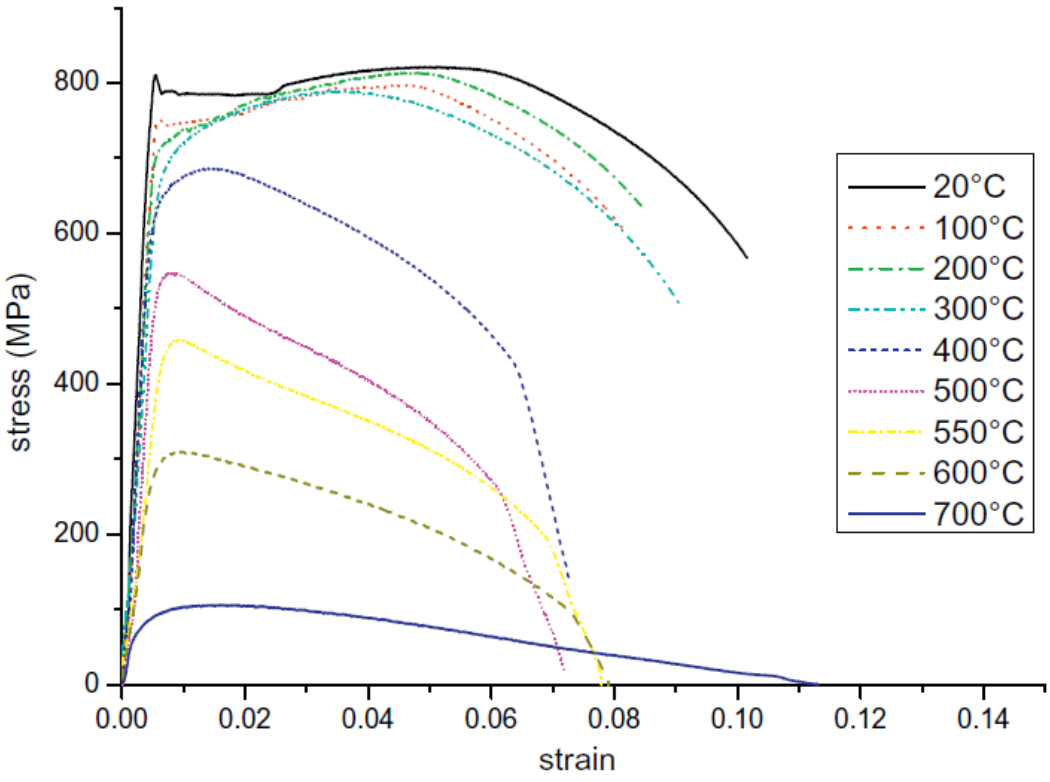

Figure 3.2: Stress – strain curves at various temperatures from tested steel S690 [211]

Numerical Representation

The test results of steel at elevated temperature vary according to the testing methods and materials. However, for the purposes of modelling and design a reasonable description of the stress, strain and temperature relationship needs to be determined, some of the most commonly used descriptions are introduced here. The modelling for steel at elevated temperatures in this chapter is based on Eurocode specifications for structural steels representing material properties of both structural and reinforcing steel.

1)Bilinear Representation

There are three parameters for this model, yield strength f_y, initial elastic tangent E_0, and strain-hardening ratio b (Figure 3.3). Strain hardening ratio is the ratio between post-yield tangent E_{sh} and initial tangent

$$b = \frac{E_0}{E_{sh}} \tag{3.1}$$

b can be defined a constant, indepedent of temperature. If b is set to 0, the material would become elastic-perfectly plastic. b could also be allowed to vary with temperature (Fig 3.4). Whilst suitable for design at ambient temperatures it is recognised that a bilinear model for steel at high temperatures is over simplified.

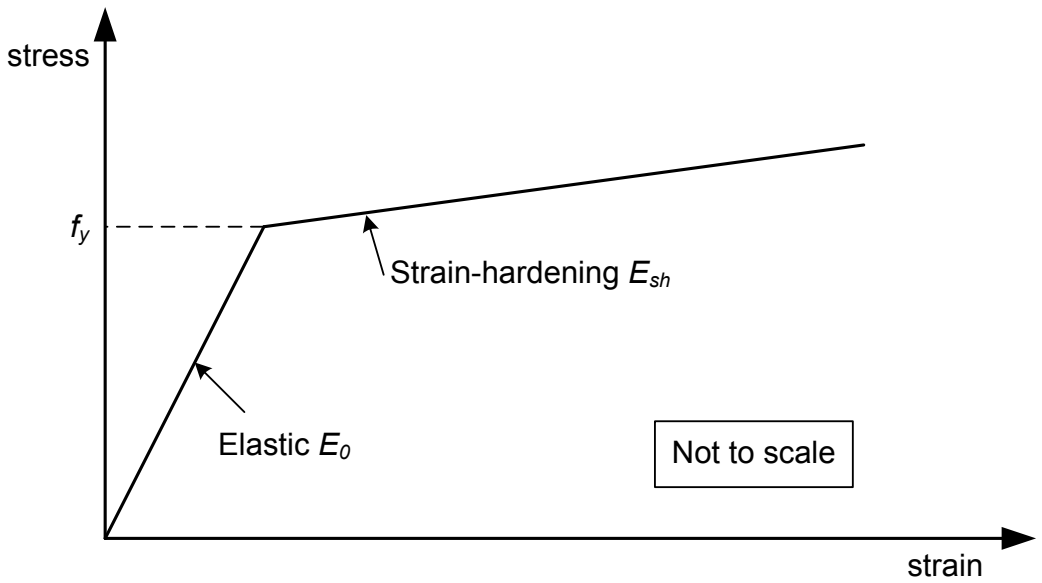

Figure 3.3: Bilinear stress-strain curve at ambient

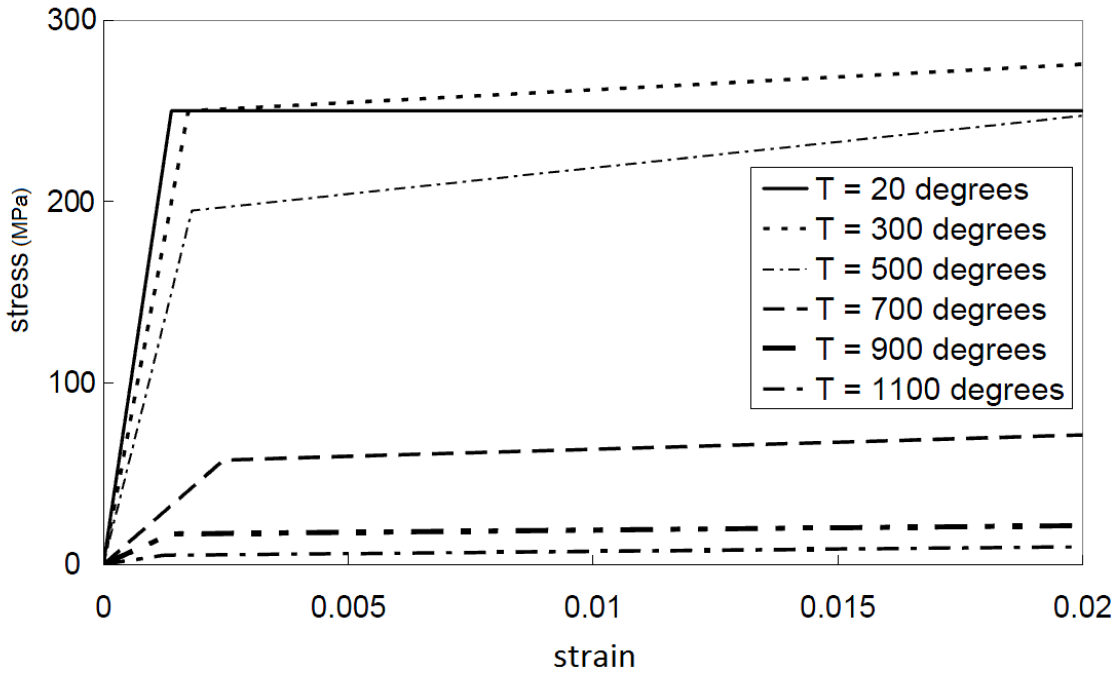

Figure 3.4: Bilinear model for steel under various temperatures

2) Multi-linear Representation

Similar to the bilinear model, a series of straight lines are used to fit the experimental curves based on fire tests. For example, Zhao proposed a simplified trilinear model based on the ECCS recommendations, where the creep strain is assumed to be implicitly included [123].

3) Eurocode Representation

In the European steel structures design code for fire resistance, Eurocode 3 [22], the stress-strain curves at elevated temperature are described by a linear-elliptic-linear equation. Strain-hardening is allowed in this model at temperatures below 400ºC. Figure 3.5 and 3.7 show the stress-strain relationship for steel at elevated temperatures above and below 400ºC respectively.

For temperatures above 400ºC, strain hardening is ignored, and the curves are defined as follows:

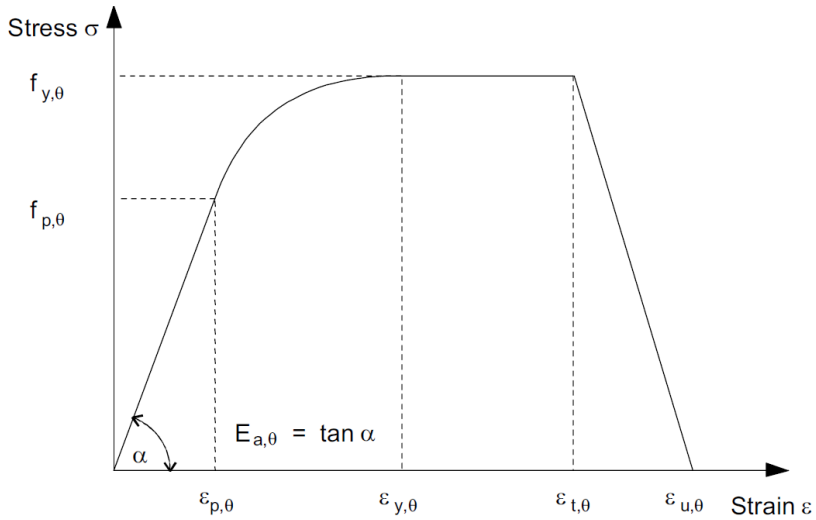

Figure 3.5: Stress-strain relationship for steel at elevated temperatures over 400ºC in Eurocode 3.

For the stain range $\varepsilon \le \varepsilon_{p,\theta}$: (figure 3.5)

$$\sigma = \varepsilon E_{a,\theta} \tag{3.2}$$

$$E = E_{a,\theta} \tag{3.3}$$

For the strain range $\varepsilon_{p,\theta} < \varepsilon < \varepsilon_{y,\theta}$:

$$\sigma = f_{p,\theta} - c + (b/c)\left[a^2 - (\varepsilon_{y,\theta} - \varepsilon)^2\right]^{0.5} \tag{3.4}$$

$$E = \frac{b(\varepsilon_{y,\theta} - \varepsilon)}{a\left[a^2 - (\varepsilon_{y,\theta} - \varepsilon)^2\right]^{0.5}} \tag{3.5}$$

For $\varepsilon_{y,\theta} \le \varepsilon \le \varepsilon_{t,\theta}$:

$$\sigma = f_{y,\theta} \tag{3.6}$$

$$E = 0 \tag{3.7}$$

For $\varepsilon_{t,\theta} < \varepsilon < \varepsilon_{u,\theta}$:

$$\sigma = f_{y,\theta}\left[1 - (\varepsilon - \varepsilon_{t,\theta})/(\varepsilon_{u,\theta} - \varepsilon_{t,\theta})\right] \tag{3.8}$$

For $\varepsilon = \varepsilon_{u,\theta}$:

$$\sigma = 0 \tag{3.9}$$

in which: $\varepsilon_{p,\theta} = f_{p,\theta} / E_{a,\theta}$,

$\varepsilon_{y,\theta} = 0.02$,

$\varepsilon_{t,\theta} = 0.15$,

$\varepsilon_{u,\theta} = 0.2$

$$a^2 = (\varepsilon_{y,\theta} - \varepsilon_{p,\theta})(\varepsilon_{y,\theta} - \varepsilon_{p,\theta} + c / E_{a,\theta})$$

$$b^2 = c(\varepsilon_{y,\theta} - \varepsilon_{p,\theta})E_{a,\theta} + c^2$$

$$c = \frac{(f_{y,\theta} - f_{p,\theta})^2}{(\varepsilon_{y,\theta} - \varepsilon_{p,\theta})E_{a,\theta} - 2(f_{y,\theta} - f_{p,\theta})}$$

Key:

$f_{y,\theta}$	effective yield strength;
$f_{p,\theta}$	proportional limit;
$E_{a,\theta}$	slope of the linear elastic range;
$\varepsilon_{p,\theta}$	strain at proportional limit;
$\varepsilon_{y,\theta}$	yield strain;
$\varepsilon_{t,\theta}$	limiting strain for yield strength;
$\varepsilon_{u,\theta}$	ultimate strain;

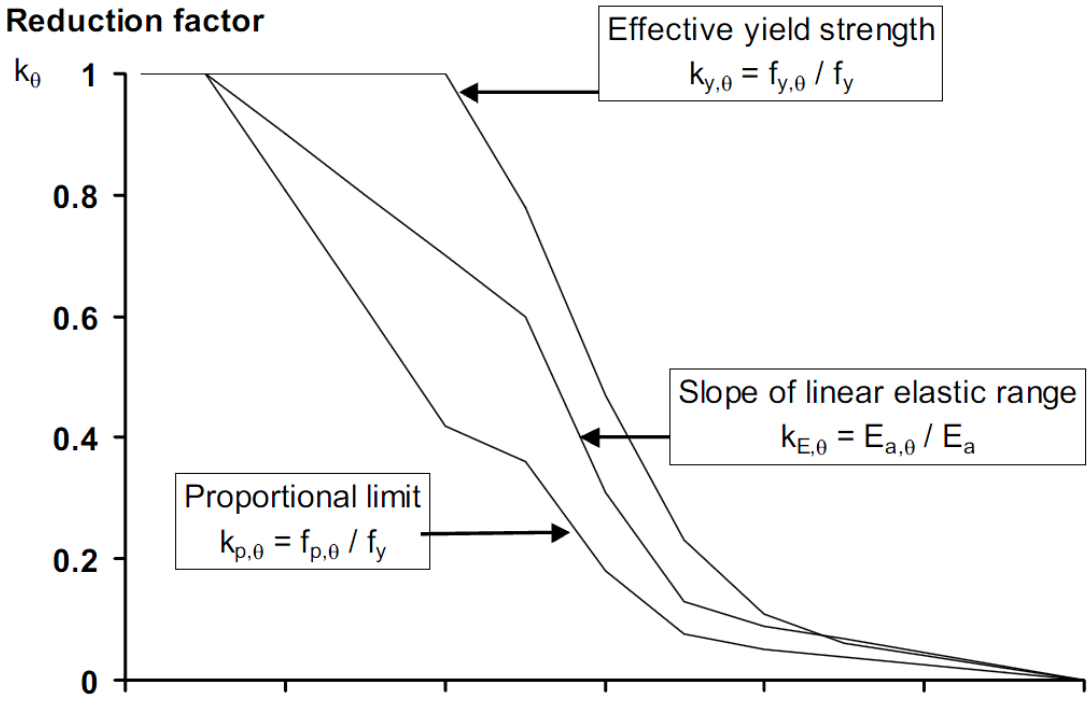

Figure 3.6: Reduction factors for the stress-strain relationship of carbon steel at elevated temperatures

The values of $\boldsymbol{E_{a,\theta}}$, $\boldsymbol{f_{y,\theta}}$, $\boldsymbol{f_{p,\theta}}$, can be derived by multiplying $\boldsymbol{E_a}$, $\boldsymbol{f_y}$, $\boldsymbol{f_p}$ by reduction factors $\boldsymbol{k_\theta}$. The factors are shown graphically in Figure 3.6.

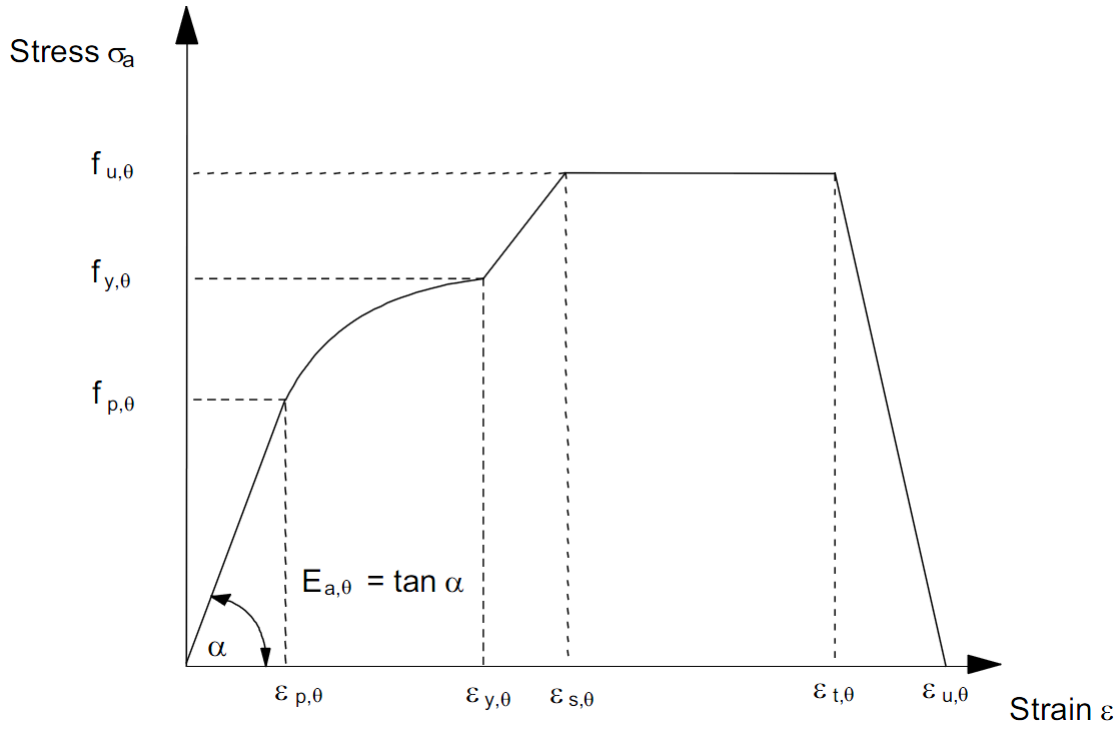

Figure 3.7 Alternative stress-strain relationship for steel allowing for strain hardening

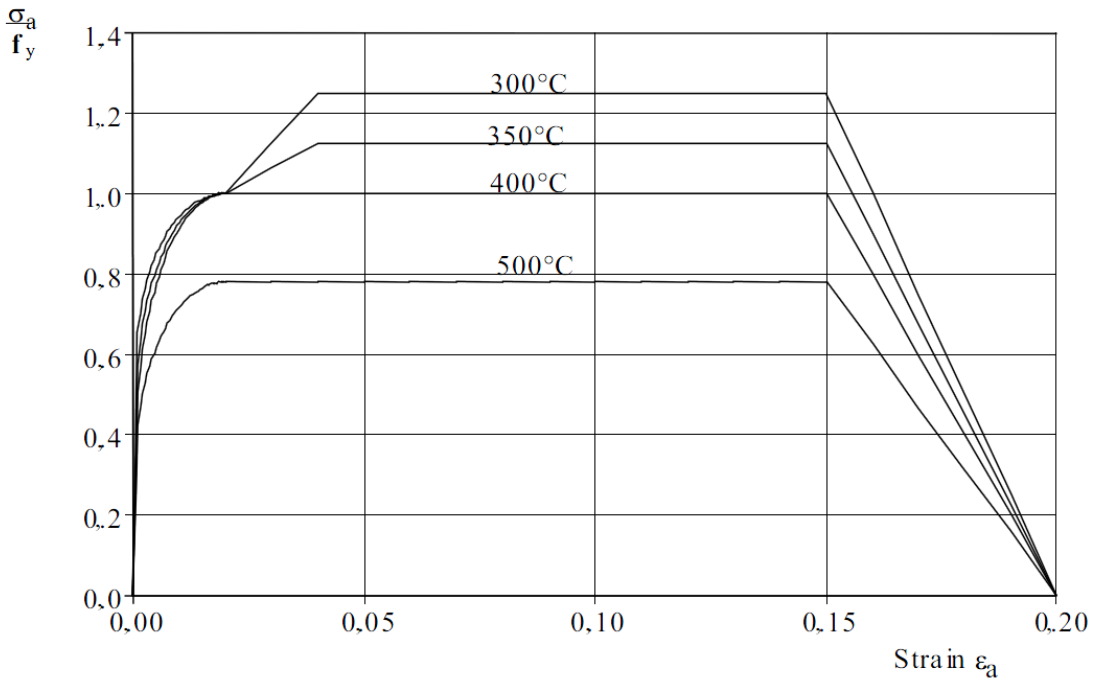

Figure 3.8: stress-strain relationships for steel at elevated temperatures, allowing for strain hardening

For temperatures below 400ºC, an alternative stress-strain relationship can be used which includes strain-hardening and is calculated as follows:

for $0.02 < \varepsilon < 0.04$:

$$\sigma = 50(f_{u,\theta} - f_{y,\theta})\varepsilon + 2f_{y,\theta} - f_{u,\theta} \tag{3.10}$$

for $0.04 \le \varepsilon \le 0.15$:

$$\sigma = f_{u,\theta} \tag{3.11}$$

for $0.15 < \varepsilon < 0.20$:

$$\sigma = f_{u,\theta}\left[1 - 20(\varepsilon - 0.15)\right] \tag{3.12}$$

for $\varepsilon \ge 0.20$:

$$\sigma = 0.00 \tag{3.13}$$

The ultimate strength at elevated temperature, allowing for strain hardening, should be determined as follows:

for $\theta_a < 300$ºC:

$f_{u,\theta} = 1.25 f_{y,\theta}$

for 300ºC $\le \theta_a \le$ 400ºC:

$f_{u,\theta} = f_{y,\theta}(2 - 0.0025\theta_a)$

for $\theta a \ge 400$ºC:

$f_{u,\theta} = f_{y,\theta}$

Thermal Expansion

A heated material usually expands, and the degree of this expansion can be measured by the material's coefficient of thermal expansion,

$$\alpha = \frac{\varepsilon_{th}}{\Delta T} \tag{3.14}$$

where $\boldsymbol{\varepsilon_{th}}$ is thermal stain, and $\boldsymbol{\Delta T}$ is the change of temperature.

To simplify calculations in simple models, the coefficient of thermal expansion of steel is often assumed to be a constant value such as, 1.2×10^{-5}. However, a more rigorous approach is provided in Eurocode 3 (Fig. 3.9), where the thermally induced strain of steel is defined in three ranges from 20ºC to 1200ºC as follows:

for 20ºC $\le \theta_a <$ 750ºC:

$$\Delta l / l = 1.2\times10^{-5}\theta_a + 0.4\times10^{-8}\theta_a^{\,2} - 2.416\times10^{-4} \tag{3.15}$$

for 750ºC $\leq \theta_a \leq$ 860ºC:

$$\Delta l / l = 1.1 \times 10^{-2} \tag{3.16}$$

for 860ºC $< \theta_a \leq$ 1200ºC:

$$\Delta l / l = 2 \times 10^{-5} \theta_a - 6.2 \times 10^{-3} \tag{3.17}$$

where: ***l*** is the length at 20ºC, and ***Δl*** is the temperature induced elongation.

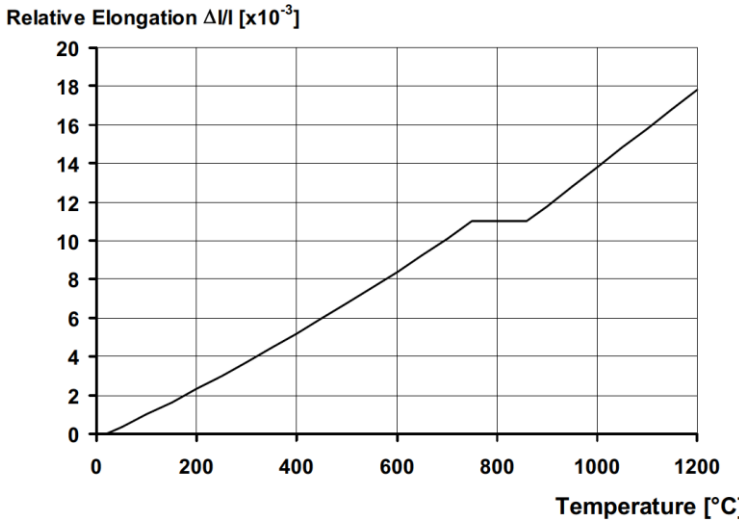

Figure 3.9: Thermal strain of steel as a function of the temperature

Creep

Steel creep can be observed even at ambient temperatures if stressed, but it becomes more apparent at elevated temperatures. There are some reported values of steel creep at high temperatures. According to the data from Anderberg [124], the value is around 0.0002 after one hour at 600ºC. It is a really small value relative to the thermal expansion (especially when the material temperatures are high).

3.1.2 Concrete

As concrete is incombustible in fire and has a very low thermal conductivity compared to steel it is considered to have very good fire resistance. This does not however mean that concrete is unaffected by fire, the main effects of heating on concrete are: deterioration in mechanical properties as the temperature rises, caused by physicochemical changes in the material during heating; and spalling, which results in loss of material, reduction in section size and exposure of the reinforcing steel to

excessive temperatures [2]. In this chapter, the discussion of concrete is focused on the change in its mechanical properties at elevated temperatures.

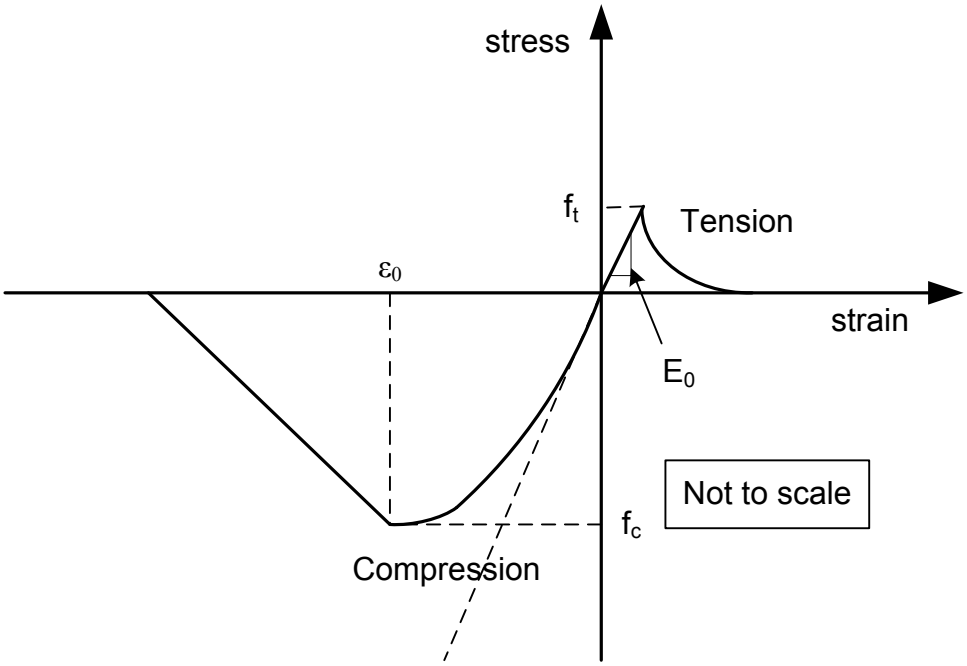

Figure 3.10: Stress-strain diagram for concrete.

Stress-strain Relationships

The stress-stain behaviour of concrete is much more complex than that of steel. Most importantly, when compared to steel, its very different behaviour under compression and tension (see figure 3.10). Furthermore, concrete is not ductile and will crush under high compressive stresses and crack under tensile stresses. The concrete failure in both, tension (cracking) and compression (crushing) causes discontinuities in the displacement fields, which are in basic disagreement with the assumptions of continuum mechanics [125]. To mitigate this problem and to account for the high degree of variability in concrete samples (even in the same batch), in practice the stress-stain curves are "idealised" in order to simplify computations.

For the stress-strain curve at ambient temperature, there is no linear elastic region in compression side. It shows a nonlinearity from the beginning, and the nonlinearity becomes greater and greater with the increase of stress, until it reaches the peak point, where it has a compressive strength $\boldsymbol{f_c}$ and strain $\boldsymbol{\varepsilon_0}$ corresponding to $\boldsymbol{f_c}$. After the peak, the curve is difficult to define, however an idealised softening curve is commonly used. The stress-strain curve in tension is assumed to be linear elastic until the stress reaches

the tensile strength f_t, followed by an idealised softening curve. The tensile strength f_t is much smaller than the compressive strength f_c, usually approximated as 10% of it. The tensile elastic modulus E_0 is assumed to be equal to the initial modulus in compression. Therefore, E_0 can be calculated by the formulation

$$E_0 = \frac{b_c f_c}{\varepsilon_0} \tag{3.18}$$

where b_c is a factor, which is defined as 1.5 in Eurocode 2.

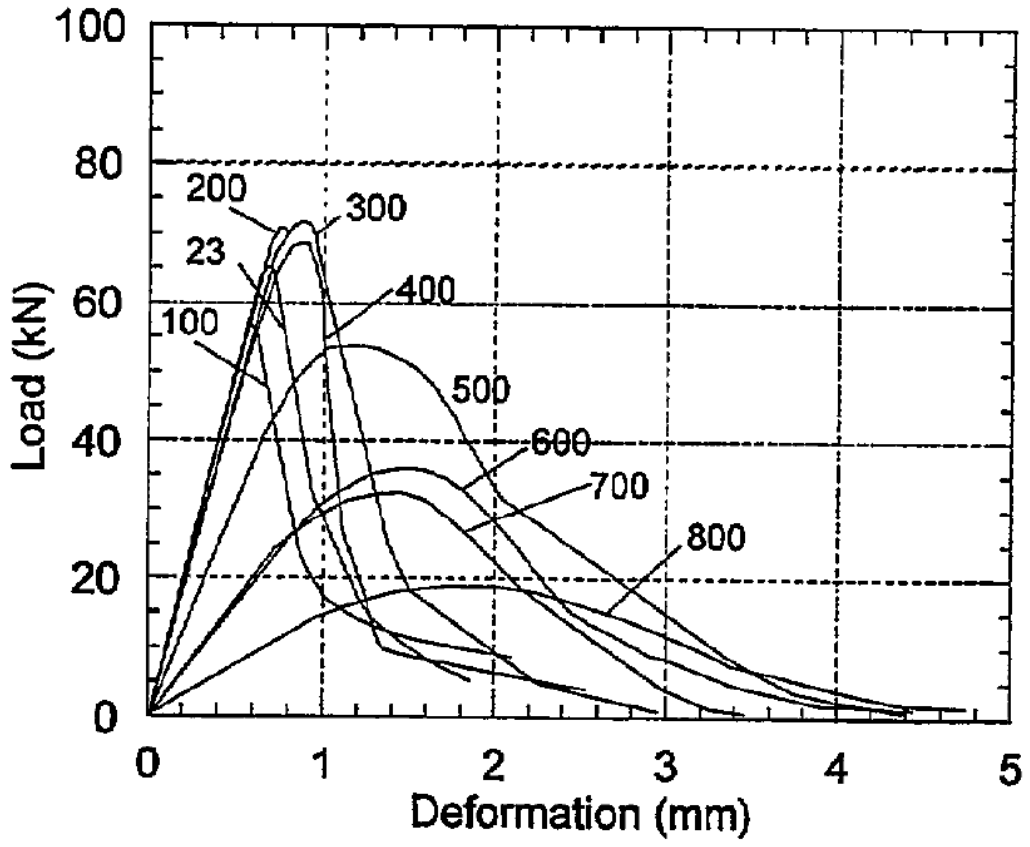

Figure 3.11: Load-Deformation behaviour of NSC at high temperatures [126]

Figure 3.11 shows the stress-strain curves of normal strength concrete in compression at elevated temperatures tested by Castillo and Durani [126]. As concrete is heated, the ultimate compressive strength decreases and ultimate strain increases as can be observed in the figure. As there is less data on the tensile behaviour of concrete at high temperatures the reduction of tensile capacity can be estimated from the reduction of the modulus of compressive capacity (see figure 3.12)

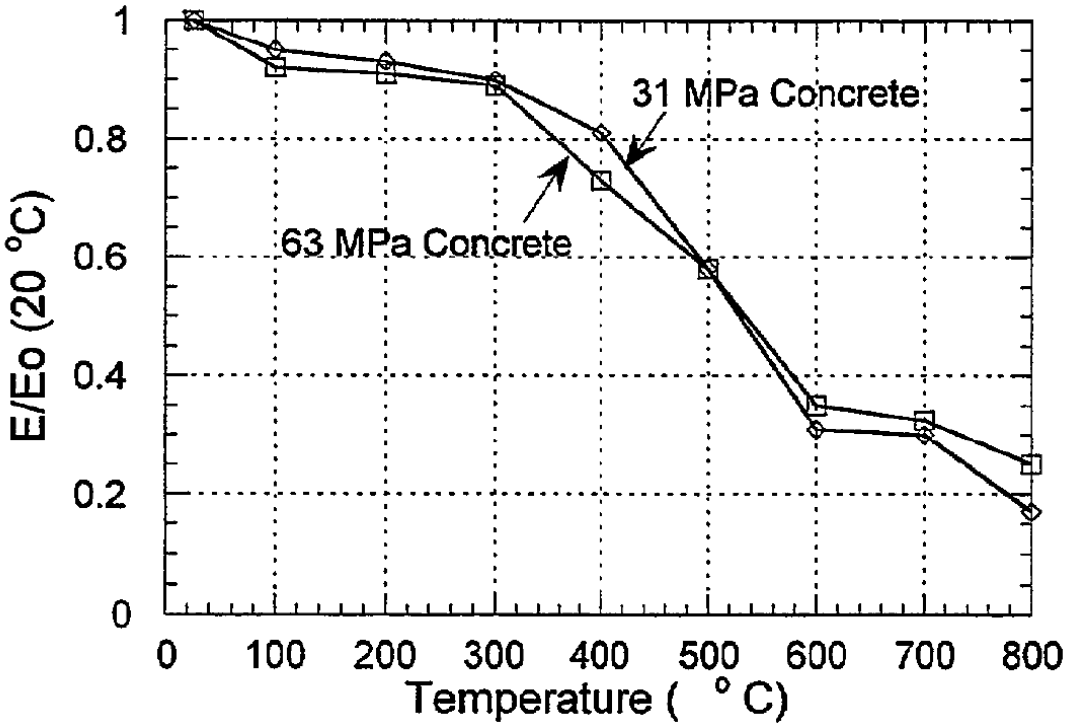

Figure 3.12: Modulus of elasticity at high temperatures [126]

Numerical Model of Stress-strain Relationships

Due to the complexities of the stress-strain behaviour of concrete at ambient and elevated temperatures, significant approximations are often made in computational models. For example, to simplify the representation, the tensile strength may be neglected. In this thesis, Eurocode representation of the stress-stain behaviour of concrete is mostly followed, and is introduced below.

Figure 3.13 shows the Eurocode 2 model for the stress-strain relationship in compression of concrete and definition of various parameters. The stress-strain relationship is divided in two parts: the ascending part and the descending part. The equation for the ascending part is :

$$\sigma(\theta) = \frac{3\varepsilon f_{c,\theta}}{\varepsilon_{c1,\theta}\left(2 + \left(\frac{\varepsilon}{\varepsilon_{c1,\theta}}\right)^3\right)} \tag{3.19}$$

where: $\sigma(\theta)$ = stress

$f_{c,\theta}$ = peak stress for concrete at elevated temperatures

$\varepsilon_{c1,\theta}$ = strain at peak stress for concrete at elevated temperatures

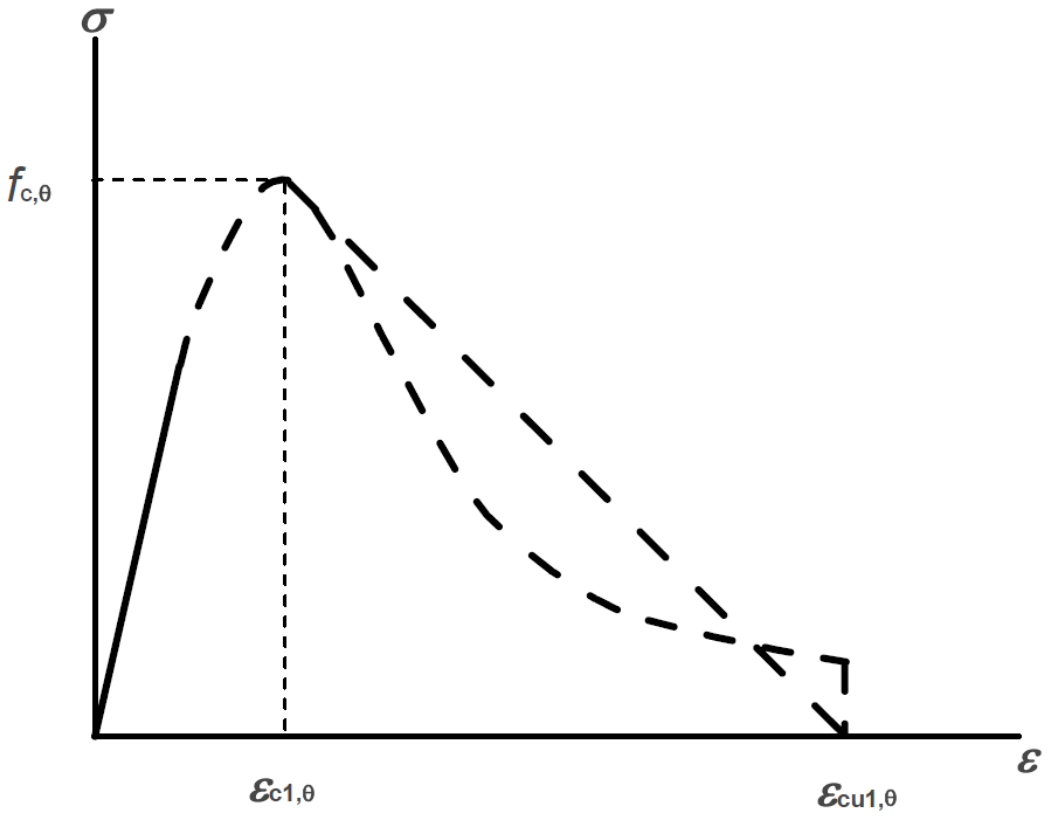

Figure 3.13: Mathematical model for stress-strain relationships of concrete under compression at elevated temperatures

Concrete temp. θ	Siliceous aggregates			Calcareous aggregates		
	$f_{c,\theta} / f_{ck}$	$\varepsilon_{c1,\theta}$	$\varepsilon_{cu1,\theta}$	$f_{c,\theta} / f_{ck}$	$\varepsilon_{c1,\theta}$	$\varepsilon_{cu1,\theta}$
[°C]	[-]	[-]	[-]	[-]	[-]	[-]
1	2	3	4	5	6	7
20	1,00	0,0025	0,0200	1,00	0,0025	0,0200
100	1,00	0,0040	0,0225	1,00	0,0040	0,0225
200	0,95	0,0055	0,0250	0,97	0,0055	0,0250
300	0,85	0,0070	0,0275	0,91	0,0070	0,0275
400	0,75	0,0100	0,0300	0,85	0,0100	0,0300
500	0,60	0,0150	0,0325	0,74	0,0150	0,0325
600	0,45	0,0250	0,0350	0,60	0,0250	0,0350
700	0,30	0,0250	0,0375	0,43	0,0250	0,0375
800	0,15	0,0250	0,0400	0,27	0,0250	0,0400
900	0,08	0,0250	0,0425	0,15	0,0250	0,0425
1000	0,04	0,0250	0,0450	0,06	0,0250	0,0450
1100	0,01	0,0250	0,0475	0,02	0,0250	0,0475
1200	0,00	-	-	0,00	-	-

Table 3.1: Values for the main parameters of the stress-strain relationships of normal weight concrete with siliceous or calcareous aggregates concrete at elevated temperatures

The descending part is less clearly defined by the code. Ultimate strain $\varepsilon_{cu1,\theta}$ is recommended as shown in Table 3.1. Both linear and non-linear descending branches are accepted.

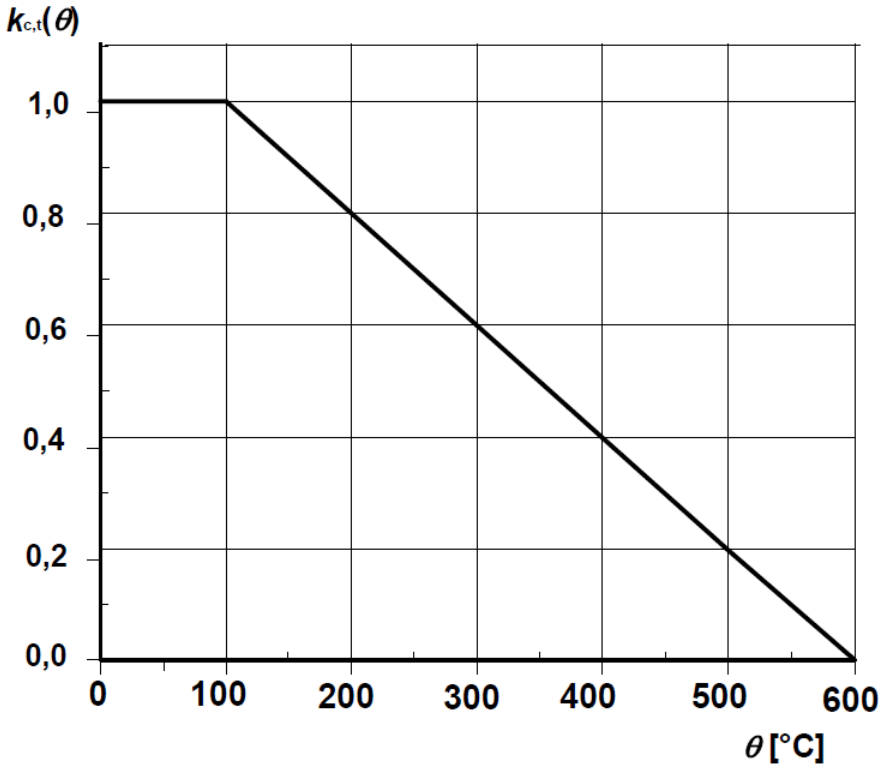

Figure 3.14: Coefficient $k_{c,t}(\theta)$ allowing for decrease of tensile strength ($f_{ck,t}$) of concrete at elevated temperatures

For the sake of conservatism, the tensile strength is allowed to be ignored in Eurocode. However, allowance may be made for it if desired. The reduction of the characteristic tensile strength of concrete is allowed for by the coefficient *k*c,t(θ) as given in Expression (3.20).

$$f_{ck,t}(\theta) = k_{c,t}(\theta) f_{ck,t} \qquad (3.20)$$

In absence of more accurate information the following $k_{c,t}(\theta)$ values should be used (see Figure 3.14):

for 20ºC $\leq \theta \leq$ 100ºC

$$k_{c,t}(\theta) = 1.0$$

for 100ºC $< \theta \leq$ 600ºC

$$k_{c,t}(\theta) = 1.0 - 1.0(\theta - 100)/500$$

Thermal Strain

The thermal strain of concrete is complex and is influenced by a number of factors such as stress level, the type of aggregate, the ratio of aggregate to cement and the rate of heating [2, 127]. The thermal strain may be divided into thermal expansion strain, creep strain and stress induced transient thermal strain. Eurocode 2 takes a simple approach and gives the thermal strain of concrete as follows:

Siliceous aggregates:

for 20ºC $\leq \theta \leq$ 700ºC

$$\varepsilon_c(\theta) = -1.8\times10^{-4} + 9\times10^{-6}\theta + 2.3\times10^{-11}\theta^3$$

for 700ºC $< \theta \leq$ 1200ºC

$$\varepsilon_c(\theta) = 14\times10^{-3}$$

Calcareous aggregates:

for 20ºC $\leq \theta \leq$ 805ºC

$$\varepsilon_c(\theta) = -1.2\times10^{-4} + 6\times10^{-6}\theta + 1.4\times10^{-11}\theta^3$$

for 805ºC $< \theta \leq$ 1200ºC

$$\varepsilon_c(\theta) = 12\times10^{-3}$$

Where θ is the concrete temperature (ºC).

The variation of the thermal elongation with temperatures is illustrated in Figure 3.15.

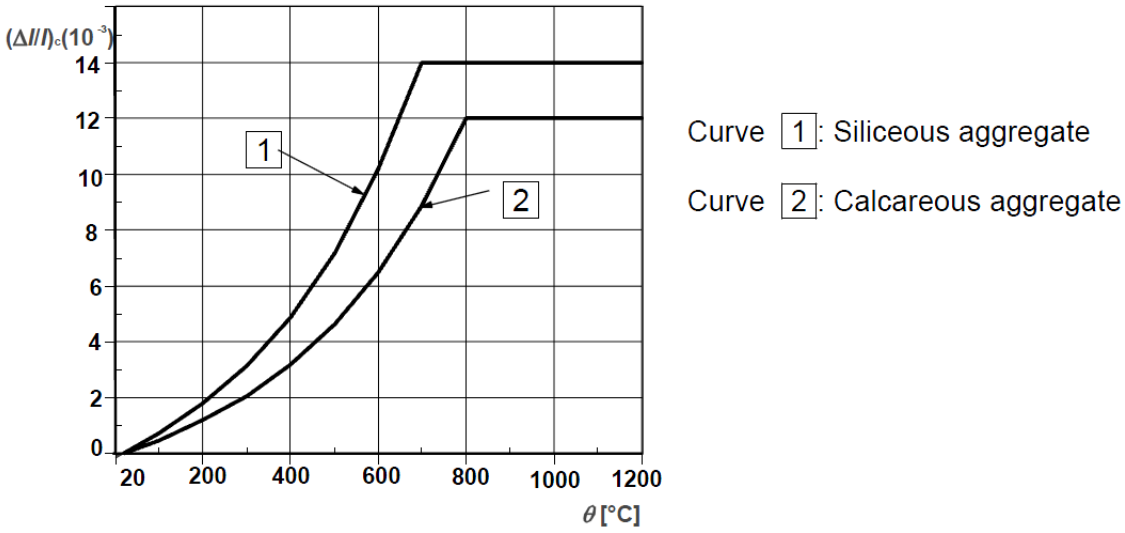

Figure 3.15: Total thermal elongation of concrete

3.2 Structural Behaviour under Fire

The expansion of most construction materials under heating naturally affects the behaviour of structural members made out of them. There are two main effects of heating on structural members, thermal expansion and thermal bowing. Thermal expansion is caused by an even increase of temperature, and thermal bowing is caused by a non-uniform distribution of temperature over the depth of the member. In a real fire these two phenomena act together, and both of them result in thermal strains and deformations. The most fundamental relationship governing the behaviour of structures when subjected to thermal effects is:

$$\varepsilon_t = \varepsilon_{th} + \varepsilon_m \tag{3.21}$$

where ε_t is total strain, ε_{th} is thermal strain, and ε_m is mechanical strain. The deformation of the structural members is determined by the total strain however stress state in the structure depends only on the mechanical strain. If the thermal strains are not restrained in a structural memebr without any external loads, equation 3.21 would become,

$$\varepsilon_t = \varepsilon_{th} \tag{3.22}$$

However, if the structural member is fully restrained without any external loads, the total strains would be zero and equation 3.21 would become,

$$0 = \varepsilon_{th} + \varepsilon_m \tag{3.23}$$

These equations show clearly that the effect of the level restraint present in structural members subjected to heating would have a significant effect on the member's mechanical response. In this section, a heated beam is analysed to show the effects of thermal expansion and thermal bowing in beams.

3.2.1 Thermal Expansion

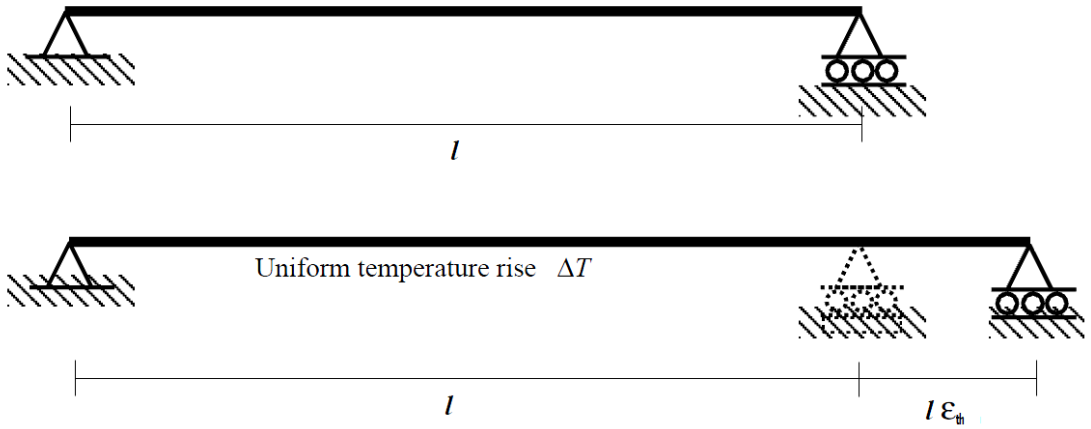

Figure 3.16: Uniform heating of a simply supported beam [29]

Axially free beam under uniform heating

As mentioned in section 3.1, thermal expansion strain in construction materials can be illustrated by the equation $\varepsilon_{th} = \alpha \Delta T$. Figure 3.16 shows that a simply supported beam subjected to uniform temperature rise ΔT, without any thermal gradient across the depth. Clearly, the beam will simply expand and the elongation can be calculated by the equation

$$\Delta l = l\varepsilon_t = l\varepsilon_{th} = l\alpha\Delta T \qquad (3.24)$$

Here, total strain $\boldsymbol{\varepsilon_t}$ is equal to thermal strain $\boldsymbol{\varepsilon_{th}}$, and there are no mechanical strains. No matter whether the Young's Modulus $\boldsymbol{E}$ changes with the rise of temperatures or not, the elongation always can be calculated by equation (3.24).

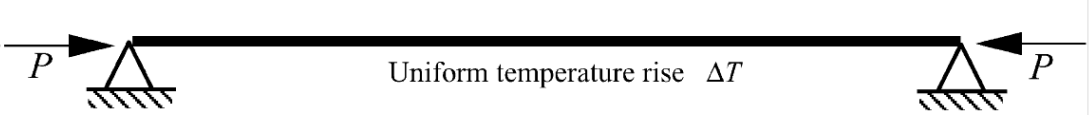

Figure 3.17: Axially restrained beam subjected to uniform heating

Axially Restrained Beam under Uniform Heating

The situation of a rigidly axially restrained beam subjected to a uniform temperature increase is very different from the beam without restraint. Obviously, the total strain is zero if buckling does not occur and the mechanical strain is equal and opposite to the induced thermal strain.

$$\varepsilon_t = \varepsilon_{th} + \varepsilon_m = 0$$
$$\varepsilon_m = -\varepsilon_{th} \tag{3.25}$$

The supports restrain the expansion of the beam, and a compressive force, ***P***, is built up, which equates to:

$$P = \sigma A = EA\varepsilon_m = -EA\varepsilon_{th} = -EA\alpha\Delta T \tag{3.26}$$

in which,

E The Young's Modulus

A Cross section area

The effect of restraints manifests itself even at relatively low temperatures because of the high stresses induced in the member, leading to local or global buckling. If the beam is stocky and the temperature continues to rise, the axial stress sooner or later will reach the yield stress σ_y. The yield temperature increment $\boldsymbol{\Delta T_y}$ is

$$\Delta T_y = \frac{\sigma_y}{E\alpha} \tag{3.27}$$

If the temperature carries on increasing beyond yield and the material has an elastic-perfectly plastic stress-strain relationship, the thermal strain keeps increasing with the increase of temperature beyond the yielding, but the stress in the beam is not increasing anymore and the compressive force in the beam stops increasing as well. Therefore, equation (3.26) must be redefined.

3.2.2 Thermal bowing

In real fires, the temperature distributions are usually not uniform. Thermal gradients exist through the cross-section structural members due to the heat transfer rate of materials and that the members might be heated from only one side. Steel has a very high thermal conductivity so steel structural members can attain uniform temperatures quickly and therefore are usually subjected to low thermal gradients. By contrast, concrete has a much lower thermal conductivity so concrete members heated on one side for instance, achieve very high gradients. This causes the outer exposed surfaces to expand much more than the inner surfaces inducing bending in the members. This effect is called thermal bowing. Similarly, a composite steel beam and concrete slab may have

high thermal bowing because of the large difference between the temperatures of the steel and concrete.

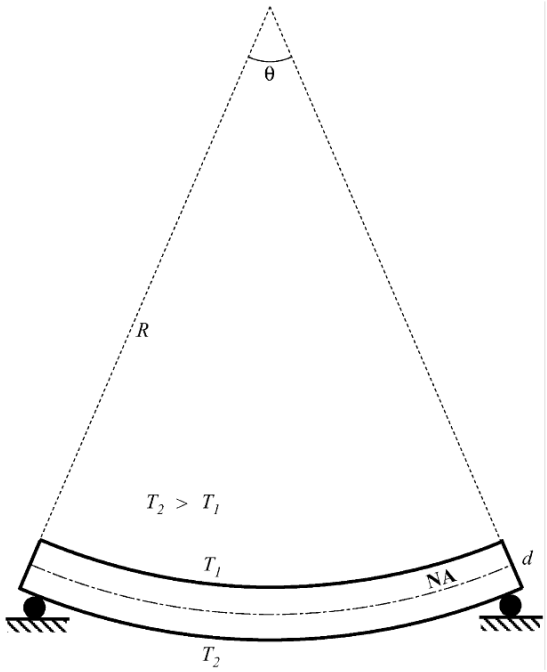

Figure 3.18: Simply supported beam subjected to uniform thermal gradient [29]

Figure 3.18 shows a simply supported beam subjected to a uniform temperature gradient through its depth (d) along its length (l). The thermal gradient over the depth can be represented by

$$T_{,y} = \frac{T_2 - T_1}{d} \tag{3.28}$$

A uniform curvature, φ, is induced along the length as a result of the thermal gradient,

$$\varphi = \alpha T_{,y} \tag{3.29}$$

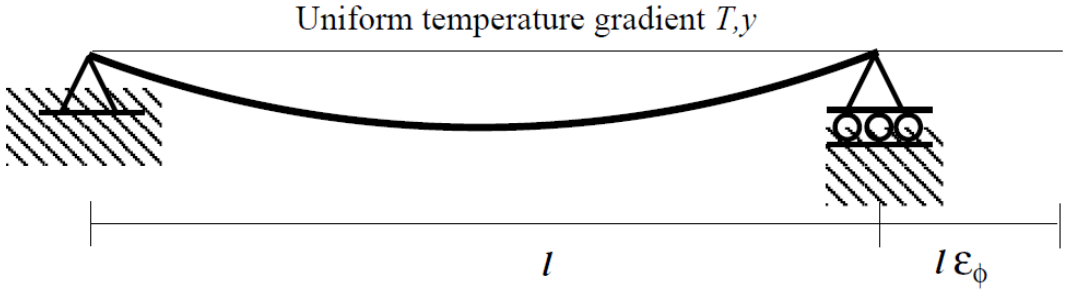

Figure 3.19: Laterally unrestrained beam subjected to a uniform thermal gradient

Assuming no mean temperature rise, the beam in Figure 3.19 has no thermal expansion strain. Due to the curvature of the beam, the horizontal distance between the ends of the beam will reduce (Fig. 3.19). The reduction can be interpreted as contraction strain, which is calculated by

$$\varepsilon_{\varphi} = 1 - \frac{\sin(l\varphi/2)}{l\varphi/2} \tag{3.30}$$

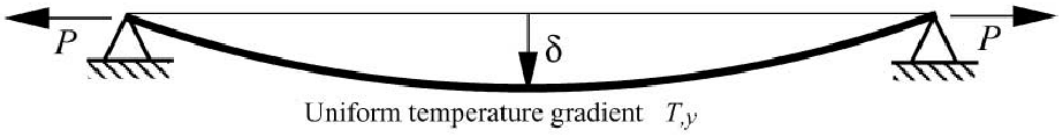

Figure 3.20: Laterally restrained beam subjected to a uniform thermal gradient

When the ends are pinned, the result is a thermally induced tension in the beam and corresponding reactions at the support (Fig. 3.20). This is clearly caused by the restraint to end translation against the contraction strain induced by the thermal gradient.

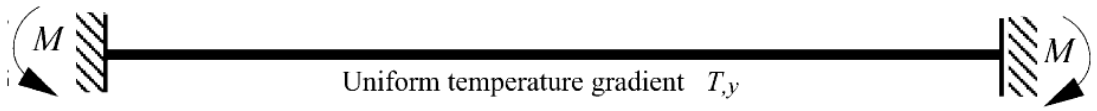

Figure 3.21: Fixed end beam subjected to a uniform thermal gradient

A fully fixed-ended beam is shown in Fig. 3.21, which is also subjected to a uniform temperature gradient. Compared with the pinned beam, the fixed ended beam is rotationally restrained by support moments M along the length. The thermal curvature, $\varphi = \alpha T_{,y}$, is cancelled out by the equal and opposite curvature induced by the support moments. Therefore the support moment can be calculated by

$$M = EI\varphi = EI\alpha T_{,y} \tag{3.31}$$

3.2.3 Combinations of thermal expansion and thermal bowing

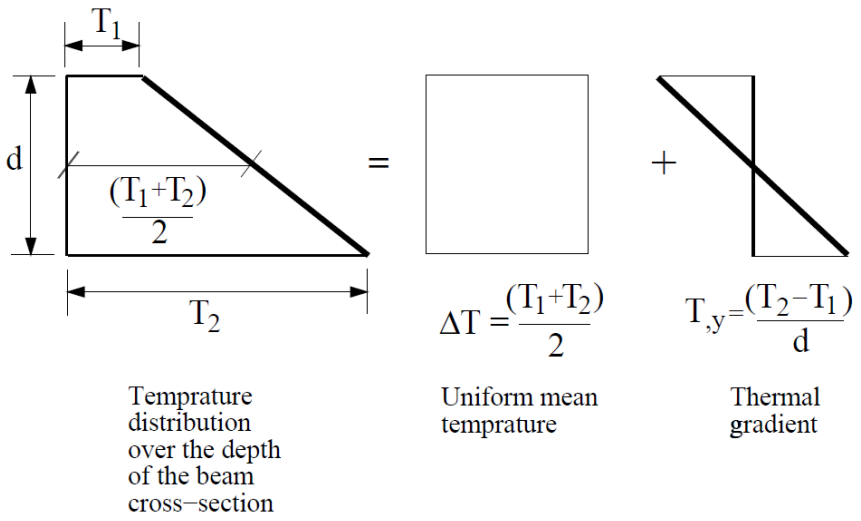

Figure 3.22: Uniform temperature and through depth thermal gradient over the cross-section of a beam

Pure thermal expansion and pure thermal bowing are non-existent at real fires and must act together (Fig. 3.22). In order to study the combined response, a case of a fully fixed beam is considered as shown in Fig. 3.23. The beam is subjected to a mean temperature increase and a uniform thermal gradient (this simply means that the gradient does not change across the section, which would often be the case in reality), therefore it experiences compressive forces and moments. These two thermal actions combine together causing stresses in the cross-section of the beam. Obviously, in this case, the bottom fibre is in high compression while the top fibre maybe in compression or tension. In the absence of gravity loading, such as a UDL or point load, this fixed-ended beam will not deflect at all because the end-restraints to rotation completely suppress all curvature leading to a uniform moment (as a result of uniform thermal gradient) along the beam.

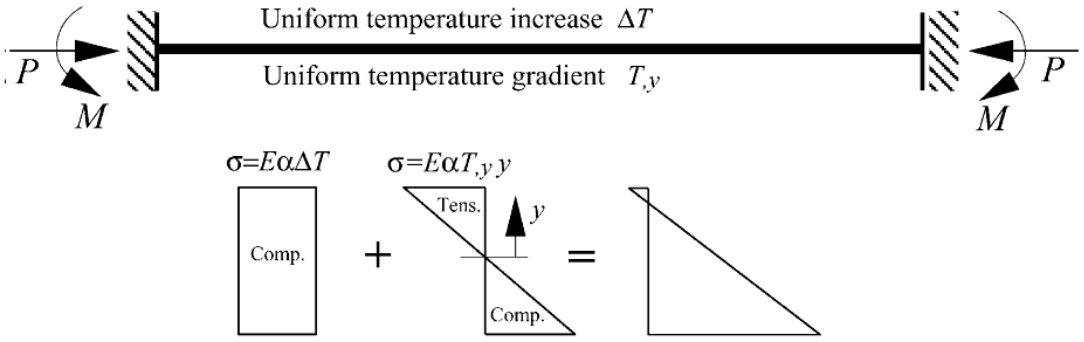

Figure 3.23: Combined thermal expansion and bowing in a fixed ended beam

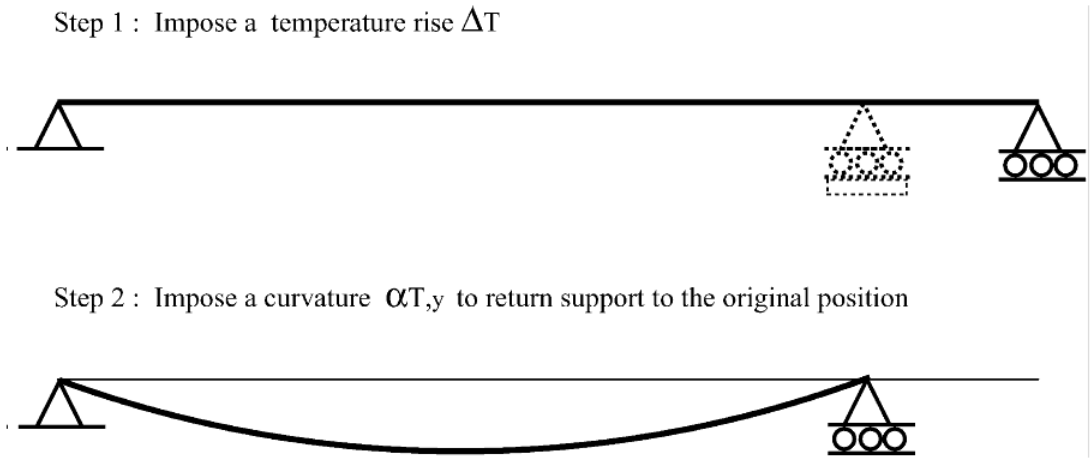

Figure 3.24: Axially unrestrained beam subjected to uniform temperature rise and thermal gradient

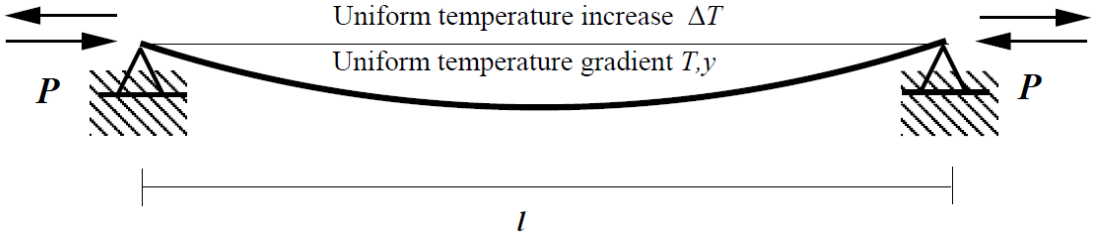

Figure 3.25: Pinned beam subjected to uniform temperature rise and thermal gradient [29]

The concept of effective strain described by Equation 3.34 allows the combined effects of thermal expansion and thermal bowing to be analysed.

$$\varepsilon_{eff} = \varepsilon_{th} + \varepsilon_{\varphi} \tag{3.32}$$

The effects of combined thermal expansion and thermal bowing on a beam have different results depending on the restraint.

When the beam is axially unrestrained (Fig. 3.24), the thermal expansion causes a longitudinal extension which is partially or totally absorbed by thermal curvature pulling the beam ends back. The deflection of the beam is caused by thermal bowing and is not affected by the thermal expansion. The total force of the section is zero, although there will be self-equilibrating stresses in the fibres over the section if the thermal gradient is non-uniform.

For a pinned beam (Fig. 3.25), axial tension or compression may exist depending on the relative magnitudes of the gradient and mean temperature. If the expansion strain and contraction strain cancel each other out a zero stress state could exist. Both thermal expansion and thermal bowing will affect deflection of the beam.

In a fixed ended member the mean temperature rise leads to compression and the uniform gradient causes a uniform moment over the length of the beam. Curvature caused by thermal gradient is restrained by the supports, so the thermal gradient has no effect on the shape of the beam.

Chapter 4 - OpenSees Architecture for the Analysis of Structures in Fire

Computational modelling of structures subjected to extreme static and dynamic loads (such as snow, wind, impact, and earthquake etc.) using finite element software are part of mainstream structural engineering curricula at universities (at least at graduate level) and many experts can be found in industry who routinely undertake such analyses. However, only a handful of institutions around the world teach structural response to fire (at any level) and only a few of the top consulting engineers in the world truly specialise in this niche area. Among the reasons for this are the lack of cheap and easily accessible software to carry out such analyses and the highly tedious nature of modelling the full (often coupled) sequence of a realistic fire scenario, heat transfer to structure and structural response (currently impossible using a single software). This chapter describes how the open source finite element software OpenSees can be extended to include the modelling of structures under fire load. The added advantage of extending OpenSees (which was developed for modelling structures subjected to earthquakes), as opposed to creating fire specific applications, is to enable multi-hazard type analyses, e.g. fire following an earthquake. The OpenSees software framework is used for this purpose due to its open source nature and object-oriented design. The OpenSees framework is extended by the adding new "concrete classes" (as opposed to "abstract classes") for thermal loads, temperature distributions across element cross-sections and material laws based on Eurocodes. This Chapter shows through class and sequence diagrams the interaction of these classes with the existing classes in the OpenSees framework [209].

4.1 Introduction

The traditional approach of evaluating the fire resistance of structures (based on prescriptive building codes) is by testing an individual structural member under a standard fire (such as [128] and [129]), where member capacity is associated with a limiting temperature. This approach does not consider natural fire scenarios and the enormous associated uncertainties, and furthermore the behaviour of structural members in isolation entirely ignores the structural interactions a member would experience as part of the whole structure. The unscientific nature of prescriptive approaches has led to gradual and accelerating adoption of so-called "performance-based design" or more

accurately "performance-based structural engineering" (PBSE) approaches, characterised by much greater reliance on scientific understanding and numerical modelling technologies. Admirable research advances have been made towards applying these methodologies in the field of earthquake engineering, most notably the PEER-PBEE methodology [130]. However to enable the application of an equivalent PBSE methodology for engineering structural fire resistance considerable further development of modelling technologies is required. This is because modelling tools for simulating fire, heat transfer to structural components and structural response are typically separate and unconnected due to the significantly different physics and length & time scales, making it impossibly tedious to simulate realistic hazard scenarios and unfit to meet the challenging demand for future computational tools in this branch of science and engineering. Considerable effort has gone into the development of software for individual components of modelling structural fire resistance, e.g. computational fluid dynamics (CFD) software such as FDS (Fire Dynamics Simulator) ([131], [132]), ANSYS Fluent [133], KFX (Kameleon FireEX) [134] and CFAST [135]. Software such as ANSYS, ABAQUS and FAGTS[136] can be used to conduct the heat transfer analysis. Many finite element simulations of structural analysis have been published and agree well with experiments, such as the Cardington tests [137-140]. These have mainly used specialist programs such as VULCAN [141, 142], ADAPTIC [143, 144], SAFIR [145, 146], and commercial packages such as ABAQUS [147, 148] and ANSYS [149, 150]. The computer program Vulcan has recently been extended to include a two-dimensional non-linear finite element procedure to predict the temperature distributions within the cross-sections of structural members subject to given fire time-temperature regimes [151, 152]. SAFIR implements an uncoupled two-phase analysis to model fire-exposed structures [153].

As mentioned earlier, the norm is to use separate software for fire, heat transfer and structural response, typically without considering coupling effects [154-156]. Even where the same software is used, for example in the case of a 3D thermomechanical analysis in ABAQUS, things are not easy. A heat ransfer analysis is first carried out (based on "available" heat flux boundary conditions from a separate fire model or from experimental data) on a mesh of continuum solid elements to establish the temperature evolution on sufficient points in the structure. The same solid element mesh can be used for simulating the subsequent mechanical response. This however is orders of magnitude more expensive computationally because of the much higher mesh resolution

required for the same accuracy compared to using much more efficient beam-column or frame elements. This would require the modeller to "manually" assign the highly variable temperature field (based on the heat transfer output) to the structural frame model. In addition to the extraordinarily tediousness and time-consuming nature of this task, an accurate heat transfer analysis is rendered meaningless as the temperature resolution obtained is not usable in the structural frame model (currently ABAQUS only allows five temperature points over the cross-section of a 3D beam-column element).

The need for a more automated software framework is also being voiced in other quarters. The National Construction Safety Team (NCST) recommended that, based on the investigation of the collapse of the World Trade Center Towers [157], efforts should be made to enhance the capabilities of computational methods to study the effect of realistic fire on buildings, all the way from the outbreak of fire to collapse. The FireGrid concept proposed by researchers from the University of Edinburgh [158] aimed to improve the information available under emergency in a timely manner to fire-fighters. This required a platform on which the data collection and interpretation was run super-real time. The enormous disparities in spatial and temporal length scales, numerical techniques and complexity of the computer programs make the development of an efficient coupled fire-structure analysis a challenging task.

Various methodologies and tools have been developed to study the interaction between fire, thermal and structural models. Ghojel [159] proposed a simple heat transfer model to simulate temperature profiles of steel structures under real fire condition accounting for the convective and radiative properties of the main products of combustion. It did not consider the geometrical shape of the enclosure and assumed uniform temperature distribution across or along the elements. A gap radiation model was proposed by Ali et al. [160] to simulate radiative heat transfer between the gas and the structure surface. It assumed the exposed portions of the structure were totally enveloped by the hot gas. Three-dimensional heat transfer analysis and subsequent two-dimensional structural analysis were performed using the ABAQUS software. Prasad and Baum [161] proposed a FDS-interface-ANSYS analysis procedure. The interface employed a "zone model" to manage the data generated by FDS. The zone model divided the compartment into a hot upper and cool lower layer. The properties of the two layers are taken from suitably chosen temporal and spatial average of output generated by FDS. A concept of Adiabatic Surface Temperature (AST) [162] was introduced as an efficient interface between the fire model and structural model. The AST was calculated from the heat flux

and gas temperature obtained from the fire mode and then translated back to a net heat flux in the structural model. The advantage was that only one quantity (AST) was transferred instead of heat flux and gas temperature from fire model which was computationally convenient and cost-effective. The method was tested by and FDS-AST-ANSYS simulation of series of compartment fire experiments.

Liew et al. [163] performed a transient heat transfer analysis using FAHTS [136]which forms a link between fire simulation model KFX and the structural analysis program USFOS. The gas temperature at each time step was prescribed in space grids that envelop the structures. The temperature distribution across the element section was calculated by subdividing line beam-column element into four node quadrilateral element which can be retrieved by structural analysis program. Shi et al. [164] developed an integrated simulation system BFireSAS to simulate the overall fire safety performance of large buildings supported by several software tools such as AutoCAD, FDS and ANSYS. Additional model transformers were created to transfer the gas temperature from FDS to structural analysis solved by ANSYS. AutoCAD was used to construct the geometry of the structural model, FDS to simulate a fire field and ANSYS for structural analysis. A core database was developed to support the data store and exchange of integrated system and bridge the connection between the different modules. Duthinh et al. [165] presented two interfaces in fire-thermal-structural analysis. A macroscopic finite element model was developed by Kodur et al. [166] for predicting the entire fire response of reinforced concrete structures from fire analysis to structural collapse analysis. Lee et al. [167] proposed a FDS-Interface-ABAQUS analysis. A matlab subroutine was created as a tool for transferring the FDS temperatures to ABAQUS input. The transfer was conducted by tracing the same coordinate of heat transfer model with the FDS model. A novel fiber element approach was developed by Jeffers and Sotelino [168] to evaluate the thermo-structural response of non-uniformly heated structural frames. The same fiber discretization in the structural model was used as in the heat transfer model.

Previous studies focused on the development of interfaces between specialist software or commercial packages. Although specialist programs are cost-effective to purchase and easy to use they lack generality and versatility. In addition, more tellingly continuous development, quality, robustness and long term sustainability of such research group based software must remain in perpetual doubt because of a relatively small number of users and developers. The commercial packages have a large library of

finite elements and excellent GUIs to enable efficient and detailed modeling of structural responses to fire and also allow user subroutines for modeling special features of behavior. Despite obvious advantages commercial packages require substantial recurring investment for purchase and maintenance that often make them unaffordable for researchers and deter new entrants to the field. Furthermore the development of commercial codes is not in the hands of the user and users have little control over the direction the development takes. This is usually dictated by the needs of the largest commercial subscribers and rarely addresses the needs of discounted subscription paying researchers.

An alternative to commercial software is open source software, where the source code for the software is made available for anyone to download, modify, and use (mostly for free). In successful open source projects many outside developers contribute new developments and bug fixes back to the project to further its capabilities. Examples of successful open source projects include Mozilla Firefox, GNU Linux and the Apache HTTP server software. In the structural engineering field, OpenSees [169] is an open source object-oriented software framework developed at UC Berkeley and supported by PEER and Nees. OpenSees has so far been focussed on providing an advanced finite-element computational tool for analysing the non-linear response of structural and geotechnical systems subjected to seismic excitations. In contrast to algorithm based programs, object-oriented programs are composed of objects, each with a number of attributes and methods, and can be viewed as the interaction between objects by the sending of messages due to the support of abstraction, encapsulation, modularity and inheritance [170]. These features of object-oriented programs make OpenSees computationally efficient, flexible, extensible and portable [169, 171]. This means a developer can combine and reuse the existing classes in OpenSees to create an application to solve one's own specific problem. Given that OpenSees is open source and has been available for best part of this decade, it has spawned a rapidly growing community of users as well as developers who have added to its capabilities over this period. For the analysis of structural and geotechnical systems it now has capabilities developed by researchers that have yet to appear in commercial software. OpenSees offers the potential of a common community owned research program with large and growing modelling capability in many areas of structural engineering. It will enable researchers to collaborate freely across geographical boundaries with a much greater potential longevity of research and development efforts.

In contrast to SAFIR and VULCAN, which are both purpose-built packages for analysis of structures in fire, OpenSees is a general purpose finite element software framework for structural analysis. Furthermore, SAFIR and VULCAN are both FORTRAN programmes and associated with small university based research groups, but OpenSees uses C++ Object Oriented Programming which allows the framework to be used as a community code and facilitates collaboration between multiple research groups regardless of geographical proximity. This offers an almost unlimited potential for improvement and enables shared development and maintenance of the framework thus ensuring longevity.

As OpenSees was developed initially for simulating structural response to earthquakes it is an ideal platform for multi-hazard simulation, such as for modelling the effect of fire on earthquake damaged structures which is one of the main aims of this thesis project. This is currently not possible with SAFIR and VULCAN.As a member of the research team at the University of Edinburgh the author has been working to add a "structures in fire" modelling capability to OpenSees. Eventually this capability will involve a heat transfer model, a structural model and an interface between them to map the temperature data automatically from the heat transfer analysis to the structural analysis, without losing the spatial and temporal resolution of the temperatures when applied to the structural elements. Further work is planned to link OpenSees to the open source CFD model OpenFOAM (capable of modelling compartment fires) leading to a fully automated software framework for modelling fire, heat transfer and structural response (as illustrated in Figure 4.1).

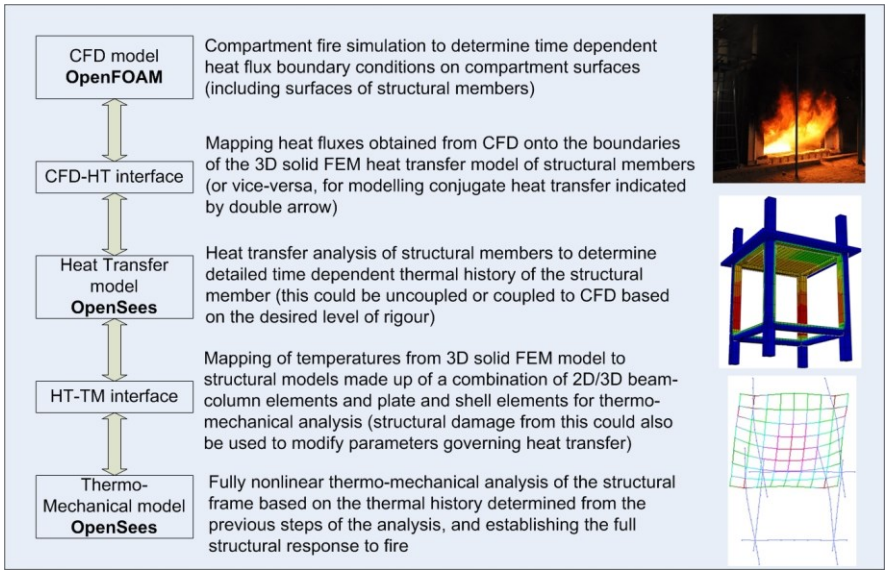

Figure 4.1: An open software framework for modelling structures in fire

This Chapter presents the extensions to OpenSees to enable 2D thermomechanical analysis. This involved creating a new thermal load pattern, modifying existing material classes to include temperature dependent properties and modifying methods in element and section classes in OpenSees. The algorithm used for thermomechanical analysis of structures is given first followed by class diagrams describing the hierarchy and architecture of the development in OpenSees. Based on the algorithm and class hierarchy, sequence diagrams are presented to illustrate the interaction between thermal load classes and material, section and element classes. The sequence diagrams provide an overview of important aspects of how to apply thermal load and obtain element forces.

4.2 Thermomechanical Algorithm

In an incremental-iterative nonlinear analysis, three phases can be identified: Predictor, corrector and convergence check [172]. The predictor needs to predict an initial out of balance force and calculate the displacement increment due to this unbalanced force given the stiffness matrix at the previous step. For thermomechanical analysis, in addition to the general external load increment, the unbalanced force should include the equivalent fixed end force due to thermal load and material softening. The corrector is concerned with the recovery of element force increment from the displacement increment obtained in the predictor phase. Equilibrium of the structure is checked at the end of each iteration to ensure that convergence is achieved in the new deformed configuration.

4.2.1 Predictor

The unbalanced force resulting from thermal load and material softening should be calculated in the predictor phase. The thermal load can be considered as elemental load derived from the temperature distribution along the section. In the finite element analysis, the elemental load should be transformed into equivalent nodal load. Figure 4.2 shows a general fibre section, which is subdivided into longitudinal fibres, with the geometric properties and temperature conditions, as defined by a uniform temperature increment, ΔT_{r}, and a through-depth thermal gradient, $(T_{,\mathrm{z}})_{\mathrm{r}}$, for a given fibre, r. Thermal gradient has not been implemented in OpenSees (one fibre corresponds to one temperature, and the temperature gradient across the fibre section is not considered), only mean temperature is used for simplicity, however this can conceivably be implemented in the future to model very steep thermal gradients with fewer fibres. If the

beam that the section belongs to is fully restrained, each fibre will have a force and moment associated with it. Integrating the forces in each fibre gives section force $F_{\text{sec}} = \left[\bar{F} \quad \bar{\text{M}}\right]$, defined as in [173]

$$\bar{F} = \sum_r E_r A_r \alpha_r \Delta T_r \tag{4.1}$$

$$\bar{M} = \sum_r F_r \left(z_r - \bar{z}\right) + \sum_r E_r I_r \alpha_r \left(T_{,z}\right)_r \tag{4.2}$$

Where the subscript r represents the *rth* fiber; E_r and A_r are the Young's modulus and area of the fiber; I_r is the second moment of area; and is the axial force and moment of the section; F_r is the axial force; α_r is the thermal elongation coefficient; z_r is the location of fiber *r* through the thickness of the section; $\bar{z}$ is the centroid of the section given by

$$\bar{z} = \frac{\sum_r A_r E_r \times z_r}{\sum_r A_r E_r} \tag{4.3}$$

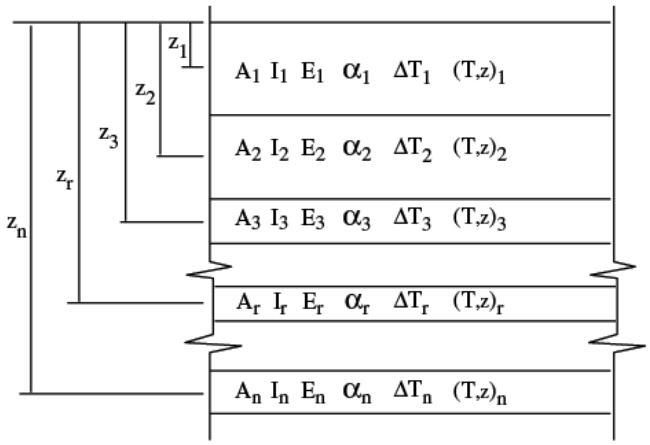

Figure 4.2: A general section divided into n fibres

Another source of unbalanced force is the material softening or material degradation due to the increment of the temperature. The imbalance between the applied external load and reduced resisting force leads to further deformation of the structure. Therefore, at the beginning of each thermal load step, the temperature-dependent material properties should be updated given current temperature and then the resisting force should be calculated again given the converged deformation at the previous step using the updated material properties. It should be noted that the centroid of the section is regarded as fixed in the implementation of OpenSees and the numerical analysis in the following chapters, so that equation (4.3) is not used further.

The out of balance force F_u^1 at the beginning of each load step is determined by

$$F_u^1 = F_{ex} + F_{th} - F_{re} \tag{4.4}$$

Where F_{ex} is the external load; F_{th} is the elemental thermal force by integration of section force F_{sec} along the element; F_{re} is the updated resisting force due to material softening.

4.2 Corrector

Once the initial displacement increment is obtained due to the updated out-of-balance force F_u^1, iterations are needed to determine the converged displacements for the nonlinear problem. In this case, when forming the out of balance force, there is no need to consider thermal force F_{th}, i.e.

$$F_u = F_{ex} - F_{re} \tag{4.5}$$

Where F_{u} is the out-out-balance force calculated for the iterations after the first iteration (i.e. F_u^1 in Equation 4.4) where the temperature-induced elemental resisting force F_{th} is not considered. Remember that the stress state depends only on the mechanical strain

$$\varepsilon_{mechanical} = \varepsilon_{total} - \varepsilon_{thermal} \tag{4.6}$$

where $\varepsilon_{\text{mechanical}}$, $\varepsilon_{\text{total}}$ and $\varepsilon_{\text{thermal}}$ are the mechanical strain, total and thermal strain respectively. The total strain can be obtained from the strain-displacement relation and the thermal strain can be calculated as $\varepsilon_{\text{thermal}} = \alpha \Delta T$.

With these two modifications, the corrector phase of thermomechanical analysis can follow the general procedure of mechanical analysis of structures [174]. Figure 4.3 shows the flow chart of element state determination for thermomechanical analysis.

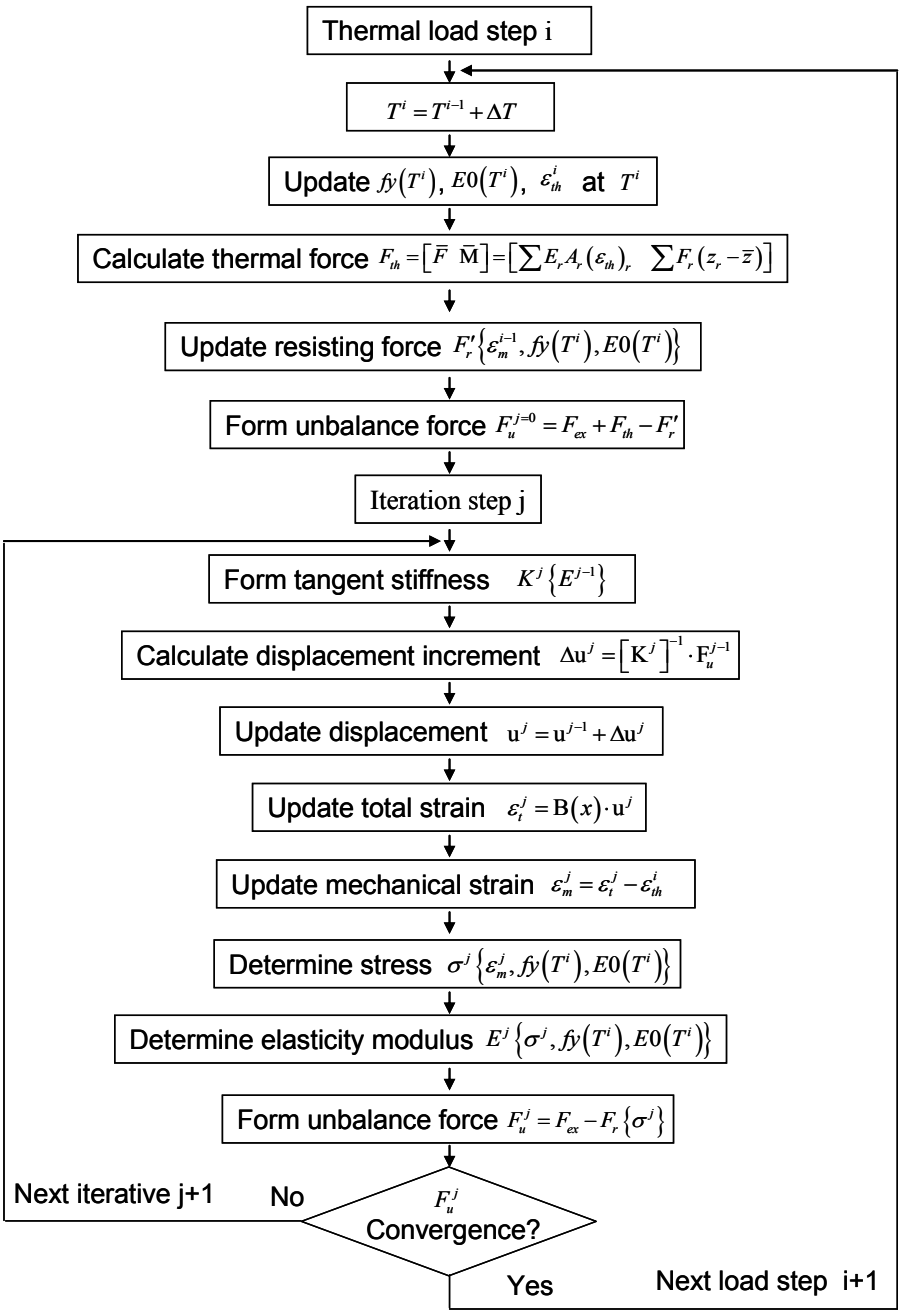

Figure 4.3: Flow chart for thermal-mechanical analysis

4.3 Class Diagrams for Thermomechanical Analysis in OpenSees

In order to implement the aforementioned solution algorithm in OpenSees, new subclasses were implemented and new methods were developed that derive behavior from existing components in OpenSees. These involved creating a new thermal load pattern class, and modifying existing material classes to include temperature dependent properties. Figure 4.4 shows the class hierarchy of new classes added in OpenSees using the graphical Unified Modeling Language notation [175]. The class ThermalLoadPattern was created to store the temperature distribution in the structure and can be used as an interface. It paralleled other load patterns such as earthquake. The

temperature distribution stored can be either retrieved from the output of the heat transfer analysis or directly input by the user according to standard codes and experimental data. The data transfer between heat transfer and structural model was designed to account for the disparity in spatial and temporal scales and different element types. One of the functions of ThermalLoadPattern was to call the class Beam2dThermalAction to pass the temperature distribution across the section. It can then be retrieved by the element class such as DispBeamColumn2dThermal and be passed to material classes (e.g. Steel01Thermal) through section classes such as FiberSection2dThermal. The material properties at elevated temperature will be updated corresponding to the temperature input. Beam2dThermalAction can also be used independently to define simple temperature profiles such as uniform and linearly distributed temperature distribution. The temperature distribution in the structural element can be considered as elemental load. Therefore the class Beam2dThermalAction defining the temperature distribution in the element was created as a subclass of ElementalLoad. The detailed attributes and implementation of these classes will be presented in the following sections.

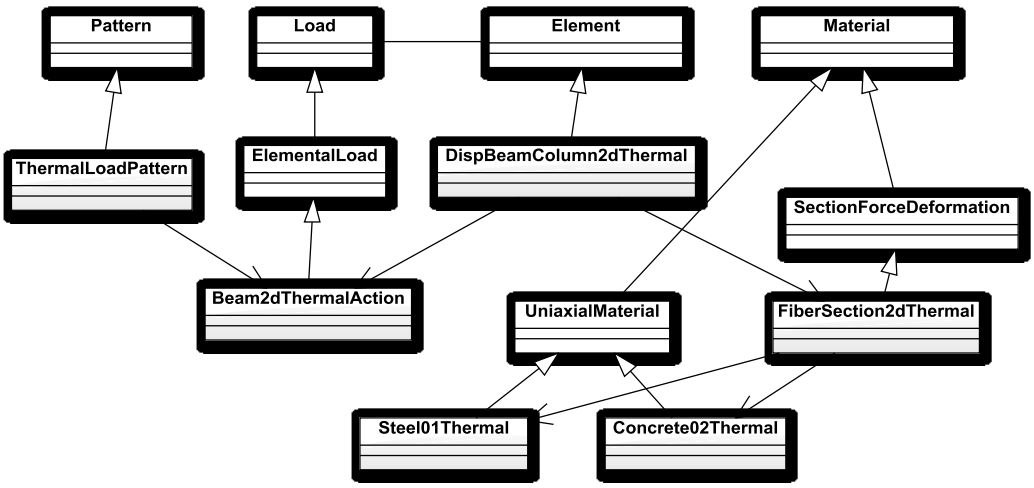

Figure 4.4: Class diagram for thermomechanical analysis in OpenSees

Thermal actions in the form of an average temperature and linear temperature gradient through a beam or column section are applied simply through the Beam2dThermalAction class. More general and realistic thermal actions are applied using fibres across the section, with the temperature history of each fibre being provided through the Beam2dThermalAction class and processed through the FireSection2dThermal and SectionFDThermal classes.

ThermalField is an abstract class, whose instance invokes the thermal analysis modules, which are also being developed for OpenSees. This class is able to provide detailed temperature distribution for each structural element either from direct user input or from carrying out complete fire and heat transfer analyses. The class diagrams for these modules are shown in Figures 4.5, 4.6 and 4.7 below.

A HeatTransferDomain object represents the state of heat transfer model by aggregating essential FE components, such as HeatTransferNode*, HeatTransferElement, HeatTransferMaterial,* TemperatureBC*, HeatFluxBC* and *BoundaryPattern*. Each HeatTransferDomain object is also associated with a HeatTransferModelBuilder object, a HeatTransferAnalysis object and a HeatTransferRecorder object, for the purpose of creating and analyzing the model and recording the solutions respectively.

The TemperatureBC and the *HeatFluxBC* objects specify where Dirichlet and Neumman boundary conditions are imposed respectively for the heat transfer analysis. The *BoudaryPattern* class is introduced to define the transient behavior of boundary conditions. As shown in Figure 4.6, by subclassing the *BoundaryPattern* class, both transient Dirichlet and Neumman boundary conditions can be defined. The *HeatFluxPattern* class is an abstract class, whose subclasses provide the implementation methods. Two subclasses of *HeatFluxPattern* are provided. The first, TimeSeriesPattern object, which is associated with a *HeatFluxBC* object and a TimeSeries object, can be used to define any arbitrarily time-varying flux boundary condition. The second, FireImposedPattern object, which is associated with the *HeatFluxBC* object and a *FireModel* object, is designed to impose flux boundary conditions determined by different types of fire models.

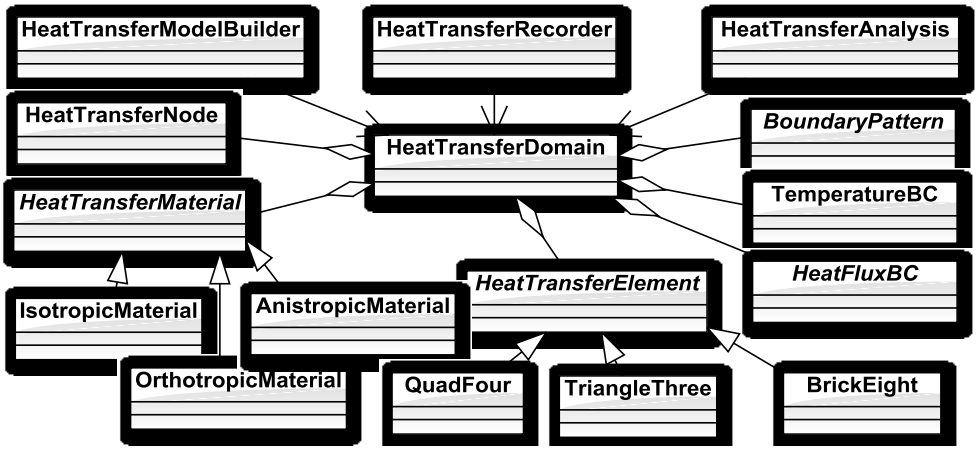

Figure 4.5: Class diagram for representing heat transfer FE components

The “strategy pattern” technique [160] will be adopted to implement the fire models. In this case, the strategy is the *FireModel*, which declares interfaces common to all of its subclasses. Using this software design pattern allows encapsulation of different algorithms for calculating heat flux at structural boundaries. The encapsulated algorithms are interchangeable at run time and the client (*e.g.* FireImposedPattern) has no need to know about the implementation details. This loose coupling makes the *FireModel* class greatly extensible and addition of new models does not require corresponding changes in the client classes.

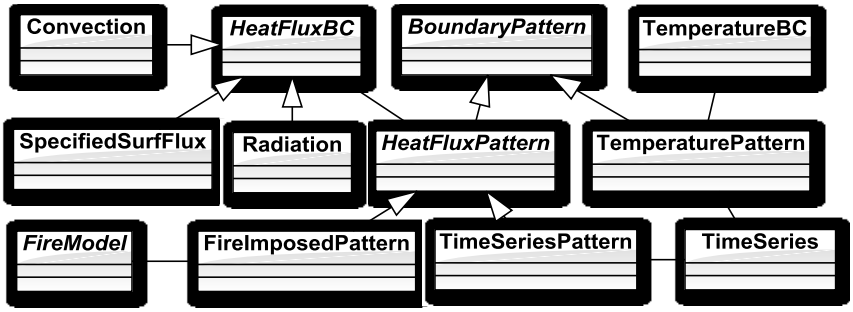

Figure 4.6: Class diagram for representing time-dependent boundary conditions

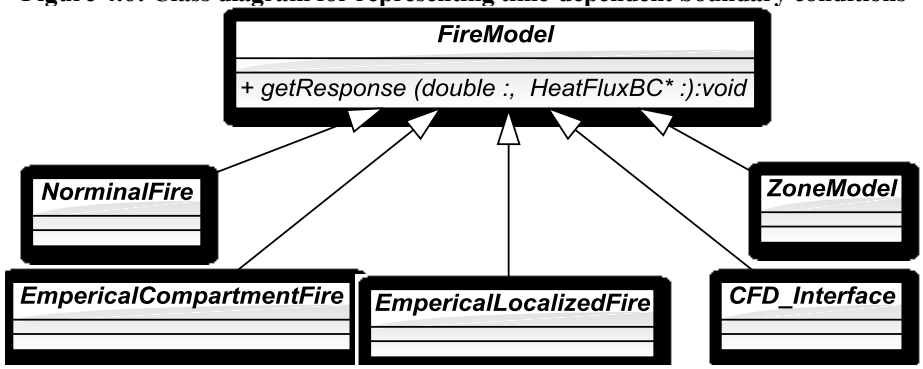

Figure 4.7: Class diagram for fire model

An abstract method which takes two arguments is provided in the *FireModel* class: *getResponse(double time ,HeatFluxBC* theHeatFluxBC) = 0* and any instantiable subclasses must redefine this method. The message passing between a *FireModel* object and a FireImposedPattern object happens in this way: first, a FireImposedPattern object invokes the *getResponse* operation on a *FireModel* at a specific time instant, which then computes necessary quantities to calculate the boundary heat flux at this time instant and invokes operations on the *HeatFluxBC* object to pass it those quantities. Some subclasses such as *EmpericalLocalizedFire* and *CFD_Interface* may require geometric information of the target location in order to achieve correct mapping of boundary heat flux. This information can be obtained with assistance from *theHeatFluxBC* object which carries an element tag and a face tag. With those two unique tags, the locations of target element faces can be determined and the corresponding coordinates can then be

mapped correctly. The development of the heat transfer classes (including Figure 4.5, 4.6 and 4.7) has been completed by another member of the OpenSees team at the University of Edinburgh [211].

Thermal Load Class

Figure 4.8 shows the class diagram of thermal load classes created in OpenSees and their implementations are shown in Figure 4.9.

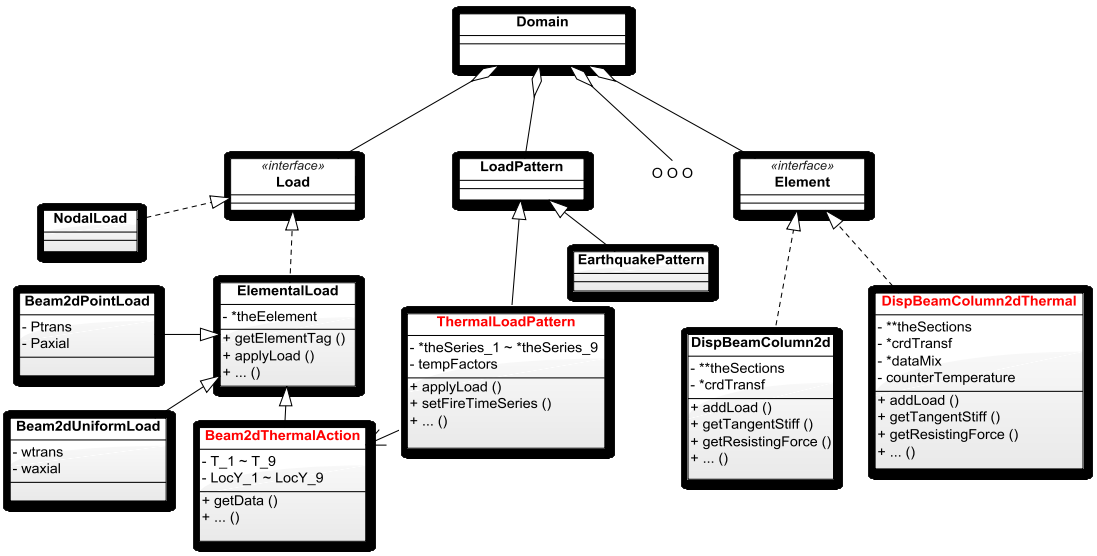

Figure 4.8: Class diagram of thermal load classes in OpenSees

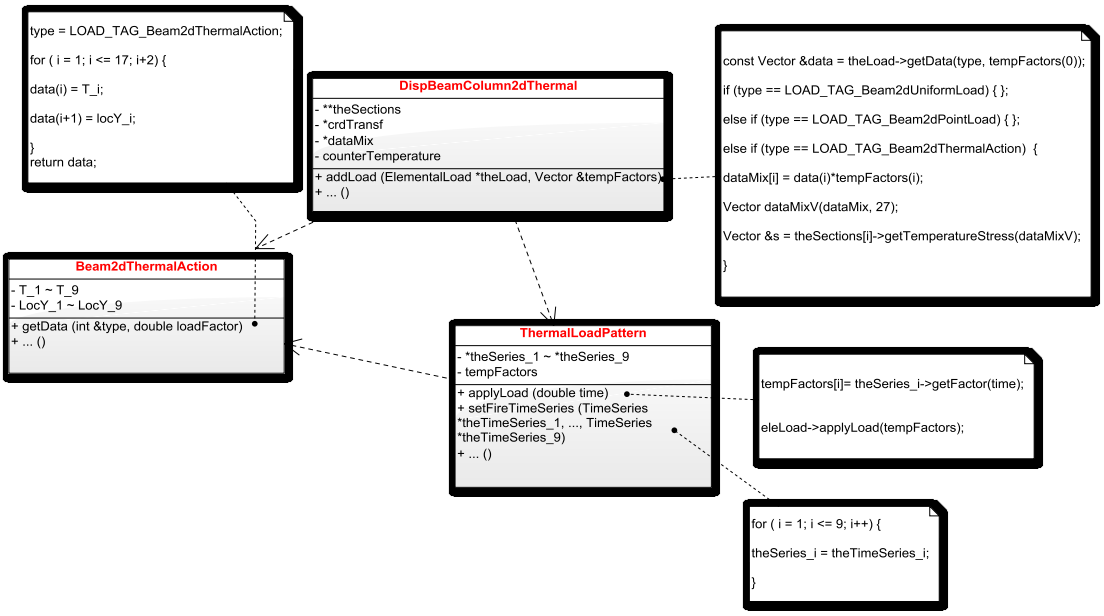

Figure 4.9: Implementation of functions defined in thermal load classes in OpenSees

Thermal load class Beam2dThermalAction was defined as a subclass of ElementalLoad ranked with point load and uniform load. Beam2dThermalAction was created to store the temperature distribution through the depth of the beam section defined by coordinate (*LocY*) and corresponding temperature (*T*). The temperature of each fibre located along the depth of beam section will be determined by interpolating the

temperature at the nearest coordinate point according to its location. At this stage three kinds of constructors were defined in Beam2dThermalAction to deal with the input of 2, 5 and 9 temperature points through the height of beam section respectively. Uniform and linearly distributed temperatures can be defined using 2 temperature points defined at the top and bottom of the section respectively.

Thermal load pattern ThermalLoadPattern was created to define detailed and highly varying time-dependent temperature distributions in structural members. It can be used as an interface to transfer the temperature distribution from the heat transfer model to the structural model where the structural responses will be predicted. The thermal analysis and structural analysis are uncoupled in OpenSees so far which means that temperature distribution along the element should be provided as input before the structural analysis. Parallel work is under progressing on automatically generating time varying structural temperature data from a heat transfer analysis within OpenSees [176] however direct inputs will always be required for modelling of experiments. A series of parameters containing time points and corresponding temperature for the nine temperature points along the height of the section respectively are defined as the input of ThermalLoadPattern. The maximum temperature at each temperature point through the whole fire duration will be defined first and the temperature can then be defined as a ratio of its absolute value to the corresponding maximum temperature. This scheme can accommodate both heating and cooling scenarios.

Modified Material Class

There are many types of material models available in OpenSees for steel and concrete, defining their mechanical constitutive relationships, however, some of these needed to be modified to include temperature dependent properties. New temperature dependent material classes Steel01Thermal (for steel) and Concrete02Thermal (for concrete) were created by modifying the existing material class steel01 and Concrete02. These new classes while they share the same stress-strain relations in absence of thermal effects (thus our choice of names) are not be derived from the existing classes as no re-use of any of the existing class methods was possible. The temperature dependence added in these two material classes were based on Eurocode stipulations [177, 178]. Figure 4.10 shows the class diagram of temperature dependent classes created in OpenSees with implementations shown in Figure 4.11.

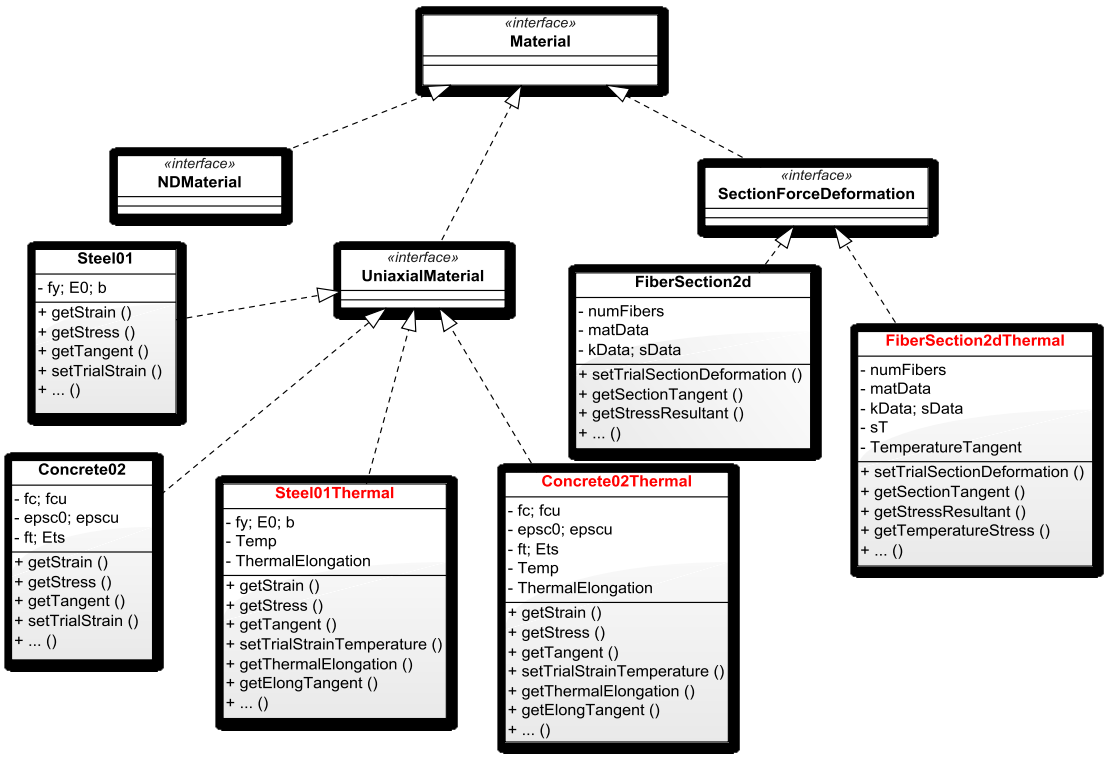

Figure 4.10: Class diagram of temperature-dependent material classes in OpenSees

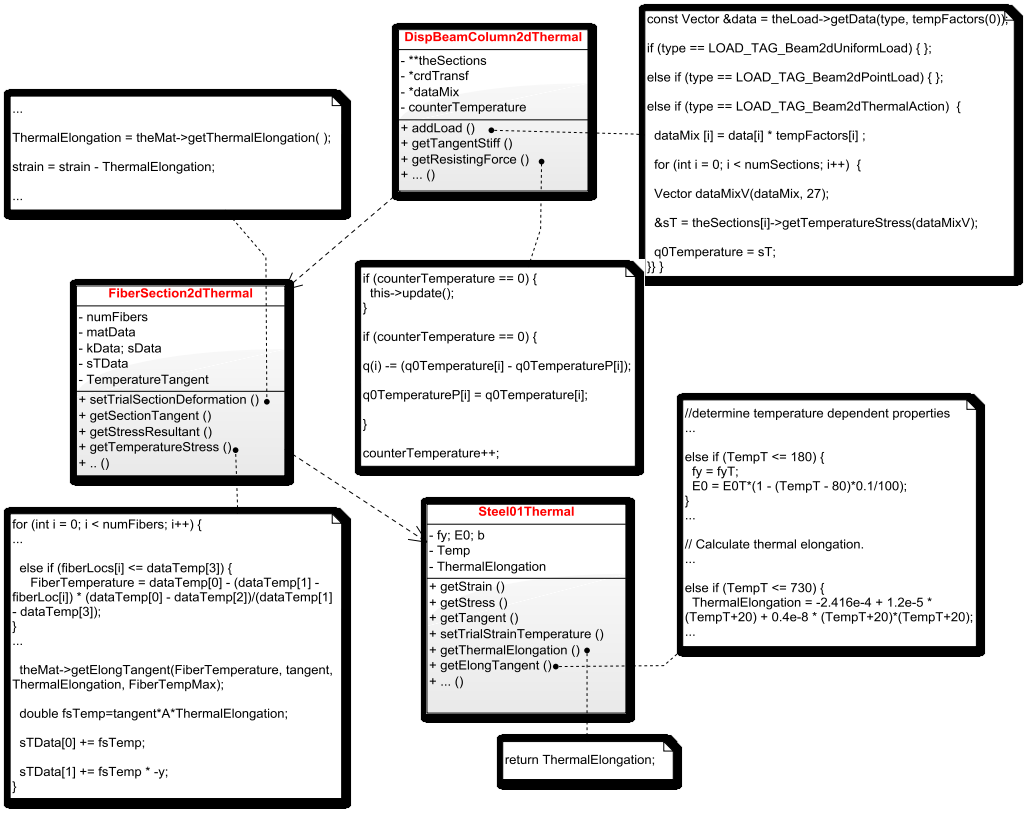

Figure 4.11: Implementation of functions defined in temperature-dependent material classes in OpenSees

Sequence Diagram for Thermomechanical Analysis in OpenSees

The previous section presented a static view of the new classes contributed to OpenSees. To describe how these objects interoperate to conduct thermomechanical analysis, this

section presents sequence diagrams (as shown in [171] for existing OpenSees) showing how to apply thermal load and obtain element resisting force.

Figures 4.12 and 4.13 show the sequence diagrams for applying thermal load to beam element through thermal load classes. The thermal load is applied by invoking method *applyLoad*() in class ThermalLoadPattern. This method is primarily responsible for two operations. The first responsibility is to retrieve temperature ratio of each temperature point according to current time point from object LinearSeries by calling method *getFactor*(). The second step is to invoke the method *addLoad*() in the associated DispBeamColumn2dThermal object to add thermal load to the beam element as shown in Figure 4.12. The temperatures and their distributions (dataMix) at current time are calculated and then passed to the section class by invoking the method *getTemperatureStress*() which in turn will invoke the method *getElongTangent*() in the materials. The method *getElongTangent*() has two operations. One is to update the material properties according to the current temperature. The other function is to send back the temperature dependent elastic modulus (*tangent*) and thermal elongation (*ThermalElongation*) of each fibre material to the section class. These temperature-dependent properties are then used to calculate the force of each fibre through which the section thermal force (*sT*) can be calculated by integration. The thermally induced resisting force of the element can be calculated by integration through sections.

Figure 4.14 shows the procedure for obtaining elemental resisting force. As mentioned in Section 2, the out-of-balance force of an element at the beginning of each load step comes from three sources including mechanical load, thermal load and reduced resisting force due to material degradation. In the method *getResistingForce*(), a parameter (*counterTemperature*) is set to determine whether it is the first iteration of each load step. If *counterTemperature*=0 (means first iteration), the method *update*() is invoked to update the element state due to the material degradation and the thermally induced resisting force is considered to calculate the total out-of-balance force (*s*+*sT*). For the next iteration, only mechanically induced out-of-balance force is considered.

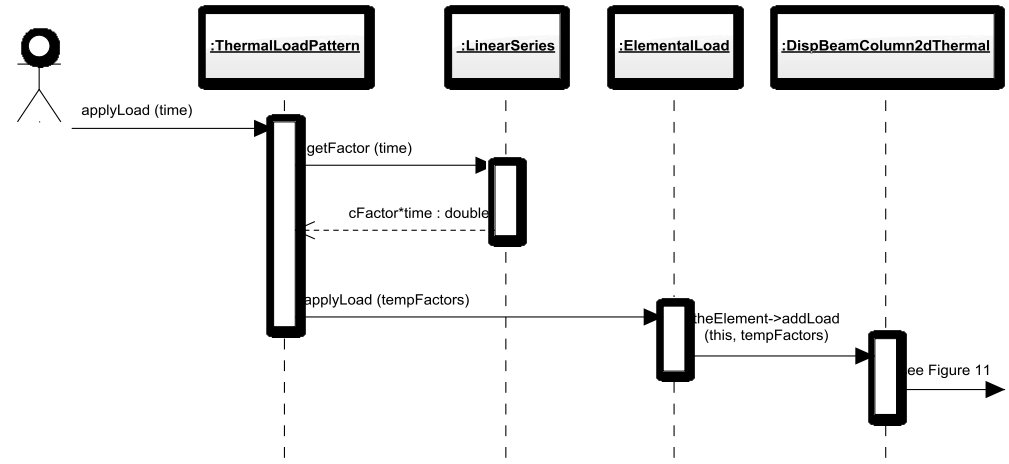

Figure 4.12: Sequence diagram for applying thermal load in thermal load classes

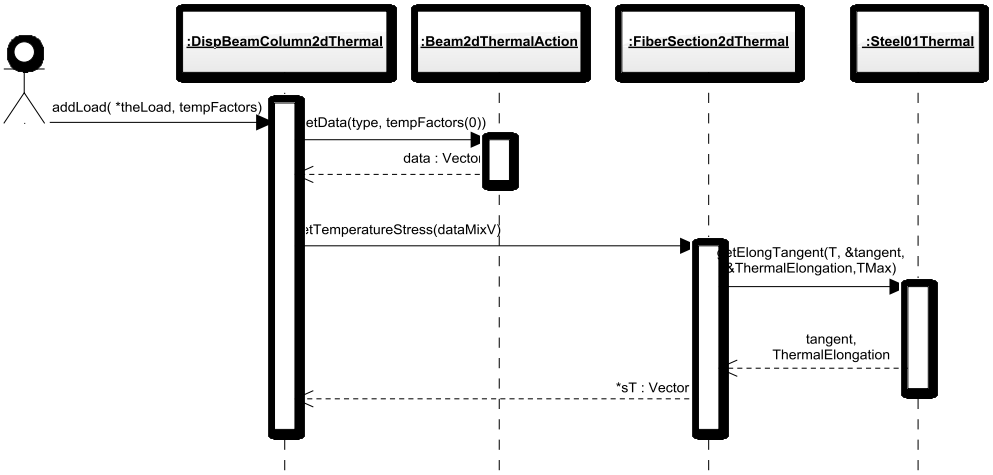

Figure 4.13: Sequence diagram for adding thermal load in beam element

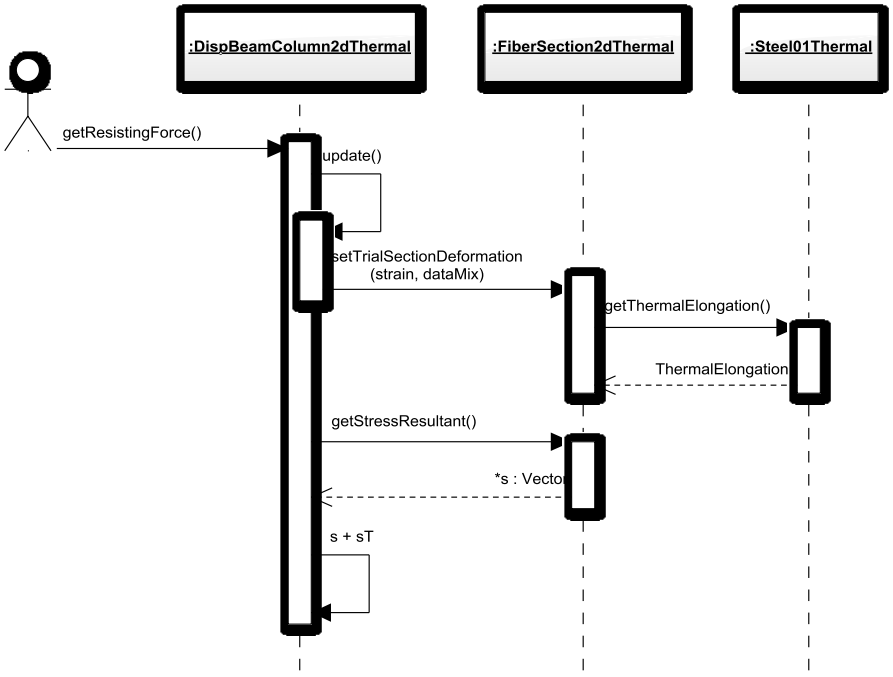

Figure 4.14: Sequence diagram for obtaining element resisting force

4.4 Summary

The open source object-oriented finite element based structural engineering framework OpenSees was extended to perform thremomechanical analysis. The class and sequence diagrams presented provide a logical overview of the hierarchy and relationship between the newly created and modified classes in OpenSees. The more detailed instruction of the themomechanical analysis flow chart and validation of new modules are presented in the next chapter.

Chapter 5 - Developing and Validation of OpenSees

This chapter describes more details of the development of the thermo-mechanical analysis module of OpenSees for carrying out numerical analyses, as well as the testing of the newly developed module. As OpenSees uses object oriented programming (OOP) features of the C++ language and it also uses the tcl-tk scripting language to build the user interface for the software framework [179, 180], it was important to become conversant in both of these programming languages before the development work could start. The new classes developed for thermomechanical analysis include separate classes for materials (steel and concrete), calculating section forces and deformations, beam column elements for 2D frame analysis, and thermally induced loading. The developed classes were initially tested against analytical solutions of number simple problems, which were also solved using ABAQUS. OpenSees and ABAQUS results match well with each other and with analytical solutions (where available). A real fire test has also been modelled using OpenSees, the results show that the development so far has been reasonably successful.

5.1 Introduction

OpenSees is developed at UC Berekeley and currently supported by NEES. Given that OpenSees is open source (available for free download at opensees.berkeley.edu) and has been available for best part of this decade it has spawned a rapidly growing community of users as well as developers who have added to it's capabilities over this period. For instance it has significant geotechnical modelling capabilities developed by this community so that the seismic response analyses can include full soil structure interaction if required. It also has a structural reliability and sensitivity analysis capability offering many reliability calculation tools. Furthermore it has an HPC or parallel version for solving large problems on high-performance computing hardware. In addition to its availability as an analysis tool OpenSees is also the software platform of choice for the US NEES network that enables earthquake engineers to organise and share data, participate in remote experiments, and perform hybrid simulations. It therefore represents the largest community of this kind in structural engineering and has the potential to bring together the best structural engineering computational modelling capabilities under one platform accessible to all facilitating new collaborations across geographical boundaries to solve ever more challenging problems.

The decades since the 60s saw explosive growth in computing power and its affordability leading to the kind of ubiquity where access to network computing is now seen as practically at par with services such as the electricity grid or the water and sewerage networks. Structural Engineers were one of the earliest exploiters of the opportunity offered by digital computers driven very much by the need of solving larger and larger systems of linear equations to analyse structures such as whole aircraft or building frames. This led to a great deal of legacy code being written, primarily developed in Fortran. This activity however peaked in the 80s and much of the development founds its way into the many currently available commercial codes such as SAP, ANSYS, ABAQUS etc. Much of the millions of lines of special purpose research codes written in this period (representing thousands of man-years of effort) are now very likely unusable not just because of the dramatic changes in operating systems, interface software, storage media etc. but the change in the whole working environment brought about by information technology. The potential offered by this explosion in information technology is immense for structural engineers (as it is for all other type of engineers) however so far there is a relative lack of imagination from our profession in taking on this challenge. Structural engineers who were once the pioneers in exploiting the new digital computing technologies emerging in the 60s and 70s, are now at risk of being seen as dinosaurs, perhaps because of, rather than despite, that early success.

The picture is not however uniformly dismal as there have been a number of very forward looking developments starting incidentally from that most productive of places, California. Among the most imaginative examples of a structural engineering project is the NEES network [120], bringing together 15 earthquake engineering research labs in universities across the USA. The key vision of this network is to enable hybrid testing of structures, where one (or more) part(s) of a structure is constructed in a lab and the rest exists virtually as a computer model in a separate (geographically remote) location, perhaps on a high performance computing platform. The two are then made to interact in real time via sensors and actuators acting on the real model in the lab exchanging information with the virtual model over the internet or Grid. The NEES network recommends the use of the software framework OpenSees [121] for simulating virtual components of hybrid testing. OpenSees is another example of an excellent imaginative project that addresses some of the issues discussed earlier. It takes a different route to software development from the traditional research codes that routinely die and commercial packages which are by definition restricted access (both in terms of

affordability and more importantly in terms of adding functionality for problems that can not be adequately dealt with by the package as it stands). The OpenSees route is not in itself new and the most ubiquitous and successful expression of it is the linux movement, *i.e.* an open source "community" code offering free access to all developers wishing to add new functionality to the core framework.

The structural engineering community is clearly considerably smaller than the linux community and it remains to be seen if OpenSees will be as successful, however the potential it offers is arguably very attractive. The potential is that of a common community owned research code with a large and growing collection of modelling capability in many areas of structural engineering enabling researchers to collaborate freely across geographical boundaries and being secure in the knowledge that the fruits of their effort will continue to exist in a living code (until superseded by a better version). Other strengths of the OpenSees framework is the inclusion of a high performance computing (or parallel) version [181] and the adoption of the object oriented paradigm of software development using C++, which enforces a discipline on the developers and ensures that the framework will develop in a manner that is manageable and easy to maintain and most of the its components are "reusable" by other developers.

In this chapter an overview is also presented of the work to add a "structures in fire" modelling capability in OpenSees which will be consistent with the ethos of the other components of OpenSees in terms of being object oriented and enabling the use of HPC hardware. Furthermore, this work will also enable the modelling of earthquake damaged structural frames subjected to a subsequent fire. The development of this capability involves work in the following areas:

- Fire load modelling to provide boundary conditions for the subsequent heat transfer into structural components

- Analysis of heat transfer to structural components accounting for local changes in thermal properties as a result of seismic damage

- Implementing temperature dependent material properties for the main material models available in OpenSees and adding new temperature dependent material models

- Implementing temperature dependent transient thermal strain or LITS (load induced thermal strain) type effects

- Modification of beam and shell element classes available in OpenSees to develop new classes that account for thermal effects

This chapter provides a summary of the work carried out on each of the topics above and present results from a number of test problems solved using the new code developed within the OpenSees framework.

5.2 Fire Load Modelling

The aim of this part of the work is to allow a wide range of heterogeneous and homogeneous fire boundary conditions to be applied to the boundaries of the structural model. To this end, it is proposed that the following methods for simulating fire loading conditions will be developed in this work (see [182] for a good summary):

1. Post-flashover standard compartment fires evolving according to time-temperature curves established in various codes and standards (such as ISO 834 and ASTM E119)
2. Post-flashover natural compartment fires evolving according to various parametric time-temperature relationships recommended in the research literature and codes (such as EN1991-1-2)
3. In addition to the code based standard fires and parametric natural fires, simple energy balance laws can be used to create "zone models" to produce relatively more realistic representations of temperatures in a fire compartment.
4. Localised fires and travelling fires, such as in large compartments where whole compartment involvement (flashover) is unlikely to occur. EN1991-1-2 offers useful empirical approaches for dealing with small and large localised fires. There are no current guidelines for moving fires, however NIST investigation [183] of the collapse of the WTC 7 building on September 11, 2001 offers interesting insights (based on CFD modelling),
5. Fires impinging on the structure from external sources. Some guidelines for this are provided in EN1991-1-2 for flames emerging out of compartment windows. This however could be a common situation in the case of fires following an earthquake and façade fires for high rise buildings, for which there is no current guidance.

The first three types of fire loading produce spatially homogeneous compartment temperatures where a single temperature is supposed to represent the temperatures at all points in the compartment at a specific instant of time (in case of zone models this applies to one or more zones used to model the compartment). The last two types of loading conditions could produce both spatially and temporally non-uniform temperatures. All types of fire loading will be implemented by applying radiation and convective flux boundary conditions to the structure.

The most realistic heterogeneous temperature distributions in the compartment can be produced using a computational fluid dynamics (CFD) based model. Addition of a full CFD model to OpenSees is not feasible however an interface will be developed in OpenSees based on the work of Jowsey [184] which will enable a time dependent and non-uniform heat flux boundary condition to be derived from CFD computations, which can be applied to the structure.

5.3. Modelling of Heat Transfer to Structural Components

Once the fire boundary conditions have been determined, the heat transfer to the structural components must be computed to establish the time evolution temperatures within the structure. This will be done by adding a 3D conduction heat transfer modelling capability in OpenSees. It will be possible to reuse parts of existing OpenSees framework to create a new "main()" heat transfer function in C++, not least the virtual domain class, geometric meshing classes, brick element and the assembly and solver classes. Some early work on an object-oriented heat transfer code available to the developers will be also used [185].

The heat transfer module will take advantage of the "fibre section" beam elements used in OpenSees. Heat transfer in building structures as a result of a fire typically has a character that naturally suits fibre type modelling of structural members because the greatest thermal gradients exist in the cross-section of the member rather than along its length. A finite element mesh that has the same character will therefore be best suited to heat transfer modelling. Figure 5.1 shows a schematic sketch of such a mesh of 3D brick elements with fine discretisation in the cross-section and coarse along the length of the member.

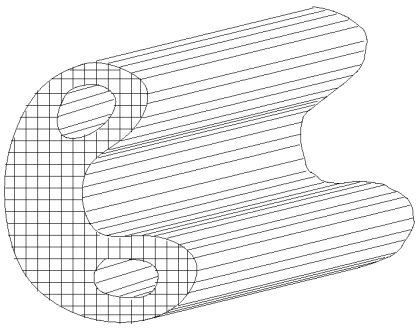

Figure 5.1: Schematic of a 3D brick element mesh for an arbitrary length of an arbitrary structural member

In the cases where heat transfer along the longitudinal direction can be neglected, a 2D heat transfer modelling capability for the structural section will also be developed, which can save computational resources and offer additional flexibility to users.

The proposed modelling of fire and heat transfer as described above will enable the most general fire loading conditions to be modelled in a relatively straightforward manner. The temperature history from the heat transfer module could be stored or recorded for reproduction if only a heat transfer analysis is to be carried out. If a mechanical analysis is to follow, a temperature history file will automatically be generated for all fibres of beam-column (and slab) fibre elements if the fibre definitions are identical to the heat transfer discretisation, otherwise the temperatures will be mapped to the mechanical fibre definitions.

In traditional "structures in fire" analysis typically only a one-way coupling is assumed between the heat transfer and the thermo-mechanical analysis, *i.e.* there is no feedback to the heat transfer calculation from the mechanical analysis, thus the structural deformation is not considered in heat transfer modelling [186]. This assumption is reasonable for the global structural behaviour modelling that is the aim of this work. Local detailed investigation of, for instance, concrete spalling behaviour typically requires a fully coupled thermo-mechanical analysis also including mass transport of multi-phase fluids in the concrete matrix, for example [187]. Though important, there is no plan so far to include this kind of analysis in this work. But as we are explicitly considering the modelling of earthquake damaged structures in fire in this work, some effect of mechanical damage must be included in the heat transfer model. Recently some experiments have been carried out [188] to investigate the influence of tensile cracking type damage (in a four point bending test on an RC beam) on the local diffusivity of heat, however the results are so far inconclusive. It is anticipated that local

thermal conductivity could be made a function of the damage state in the structure. It seems reasonable that damage will create preferred directions of heat transfer (promoting heat transfer along the cracks and perhaps inhibiting it across cracks) as shown in Figure 5.2.

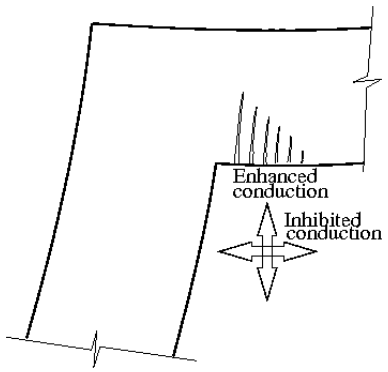

Figure 5.2: Thermal conductivity change depending on mechanical damage

5.4. Temperature Dependent Material Properties

There are many types of material models available in OpenSees for steel and concrete, defining their mechanical constitutive behaviour, however some of these need to be modified to include temperature dependent stress and strain including effects such as LITS. At this stage temperature dependence will only be added to the uniaxial concrete and steel models and this data is not reliably available for the multiaxial case. This also naturally suits the fibre beam and shell models where the section behaviour can be derived from integrating fibre stress, strain and temperature states. The uniaxial properties for steel and concrete will be primarily based on Eurocode stipulations. For concrete additional information from the literature, such as [189, 190], will be used to take into account LITS type effects.

A new set of material properties (also temperature dependent) will need to be added for the heat transfer model as well. These in the first instance will be based on Eurocode data for steel and concrete. As mentioned earlier, the thermal properties, particularly thermal conductivity will be related to a localised strain measure representing damage.

5.5 Application of Thermal Action to Beam-column Elements

The class diagrams of newly developed modules have bee described in the last chapter. Further details of the implementation of thermomechanical analysis in OpenSees and properties of new classes are introduced in this section.

5.5.1 Methods to Apply Thermal Loads

Thermal action applied on structures has two effects, changing of material properties (Young's Modulus and strength) and causing thermal expansion. Normal gravity loads can also change material properties when materials become inelastic, however they cannot produce "pure strain" (unaccompanied by mechanical stress) as thermal loads do. The methods (remember in OOP classes are data structures that define their own "data" and "methods") used in OpenSees classes and their implementation in the program are based on normal gravity loads, hence the method to apply thermal loads has to be compatible with the existing procedures.

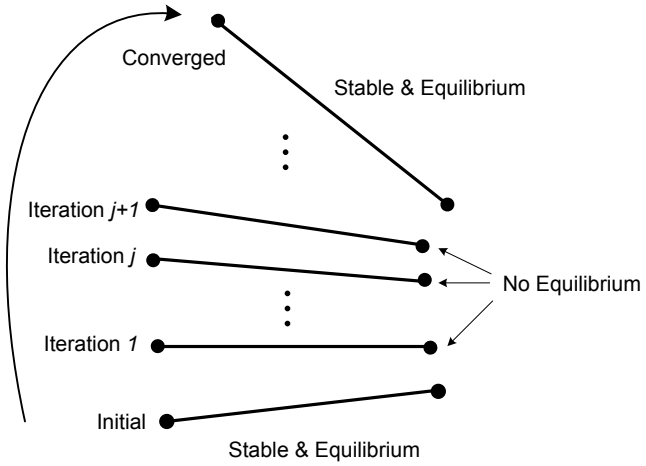

Figure 5.3: The procedure achieving convergence for an element performing nonlinear analysis

The nonlinear analysis procedure is from stable & equilibrium state to another stable & equilibrium state in an incremental step for structures under loading, as shown in Figure 5.3. First order elastic analysis can share the procedure with first order nonlinear analysis, but one iteration step can satisfy it compared with two or more iteration steps for thermomechanical analysis.

Thermal action in beam-column elements is introduced as a one-dimensional thermal strain along the element axis by this thermal strain method. Firstly, predicted thermal forces are calculated according to the increase of the temperatures and the material properties under these temperatures across the integration sections of the element. Then these forces are applied to the structure as equivalent nodal loads. Deformations can be derived by solving the equilibrium equation and the associated thermal strains are part of the total strains. Setting thermal forces to be zero, another iteration step starts until force balance is reached for this incremental step.

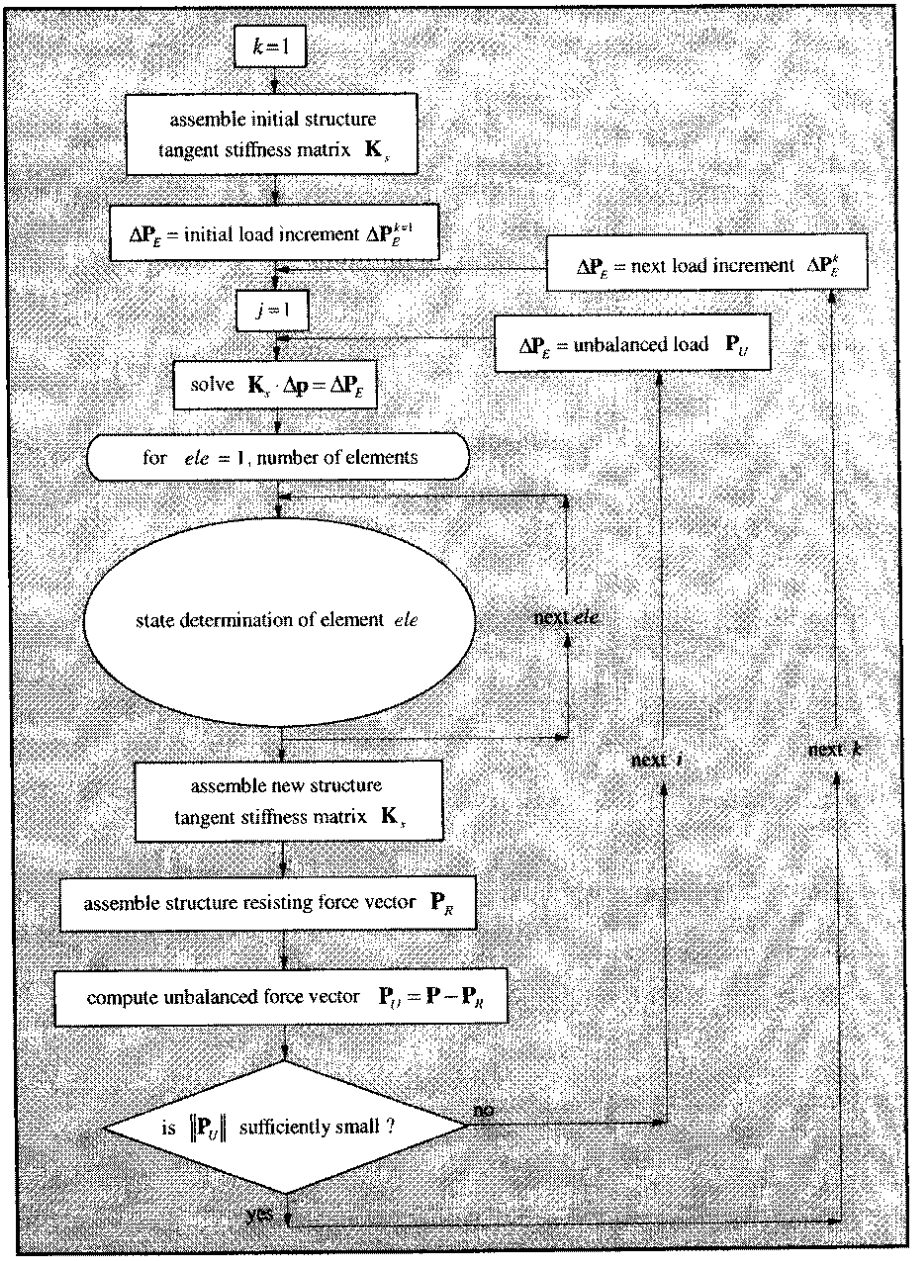

Figure 5.4: Flow chart of structure state determination. [191]

5.5.2 Flow Chart of Thermomechanical Analysis

The flow chart of the solution process of equilibrium equations in OpenSees is shown in Figure 5.4. Element tangent stiffness matrices are determined first followed by the assembly of the global tangent stiffness matrix K_s. Load increment ΔP_E is then applied to determine the nodal displacements Δq:

$$K_s \Delta q = \Delta P_E \tag{5.1}$$

Element section deformations can then be determined from the kinematic equations since nodal displacements are now known, followed by the determination of mechanical

stress based on the constitutive equations. Section tangent stiffnesses are integrated to determine updated element tangent stiffness, which is used to assemble the new structure tangent stiffness matrix K_s. At the same time section forces are calculated from section stresses. Integrating the section forces along the element (using Gauss-Lobatto rule) yields internal forces. The internal forces are used to assemble the global resisting force vector P_R which allows the "unbalanced" force to be determined,

$$P_U = P - P_R \tag{5.2}$$

where P is the applied force. If the norm of the unbalanced force is sufficiently small, the analysis proceeds to the next increment, if not, P_U will be regarded as the applied force for the next iteration. This process is repeated until the norm of P_U is less than the prescribed tolerance.

The solution scheme for structures under thermal actions requires modifications to the process described above and is shown in Figure 5.5 ignoring the assembly steps.

The transformation of thermal load to equivalent nodal load is more involved in comparison to gravity loads, as described in the last section. The external load F_{ex}, includes any directly applied nodal loads and the equivalent nodal loads transformed from distributed gravity load on the element (F_{ele}) and the thermal loads on it (F_{th}). The internal force (F_{in}) of each element contributes to the resisting force F_{re} (after appropriate transformations). Knowing resisting force and external force, the residual or unbalanced force can be calculated as: $R = F_{ex} - F_{re}$.

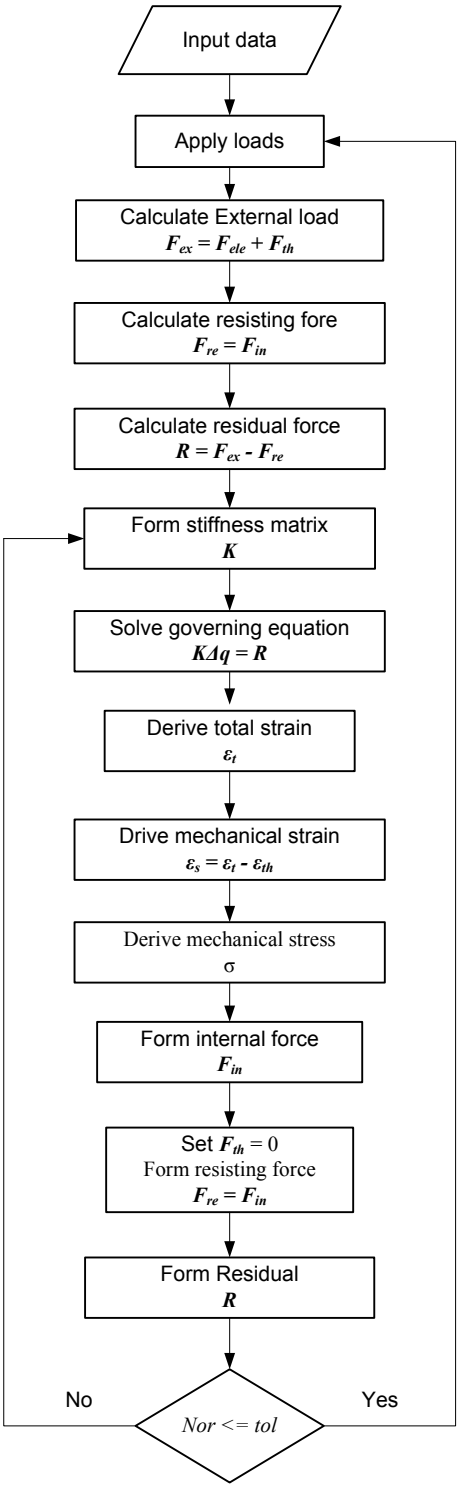

Figure 5.5: The flow chart of solution process of structures under thermal loading

Next, the tangent stiffness matrix K is updated taking into account to the changed properties of the materials fibre cross sections, and forces in the element. With residual force and stiffness matrix, the displacements of all the nodes Δq of the structure can be obtained by solving the equilibrium equation: $K\Delta q = R$. For a beam-column element, if the displacements of the two end nodes are known, the total strain ε_t of any section along the element can be derived according the kinematic equations. It should be noted

that the total strain includes thermal strain ε_{th} and mechanical strain ε_{σ}, therefore the mechanical strain is obtained from $\varepsilon_{\sigma} = \varepsilon_{t} - \varepsilon_{th}$. So the corresponding stress σ of the section can be obtained based on the temperature-dependent constitutive behaviour of the material. Numerically, the element internal forces F_{in} can be determined by Gauss-Lobatto integration rule, and only the section stresses on a few selected integration points are needed (five integration points are used as the default in the beam-column element in OpenSees). The residual or unbalanced force is calculated again using the equation $R^{i} = R^{i-1} - F_{re}$, where the R^{i-1} on the right side of the equality is the previous residual. Following this, the norm is calculated based on the updated residual. If the norm is less than a pre-set tolerance, the algorithm will go to the next increment of load, if not, an updated stiffness matrix will be formed and the next iteration is performed (see Figure 5.5), and so on, until convergence is achieved.

5.5.3 Developing the software OpenSees for thermomechanical analysis

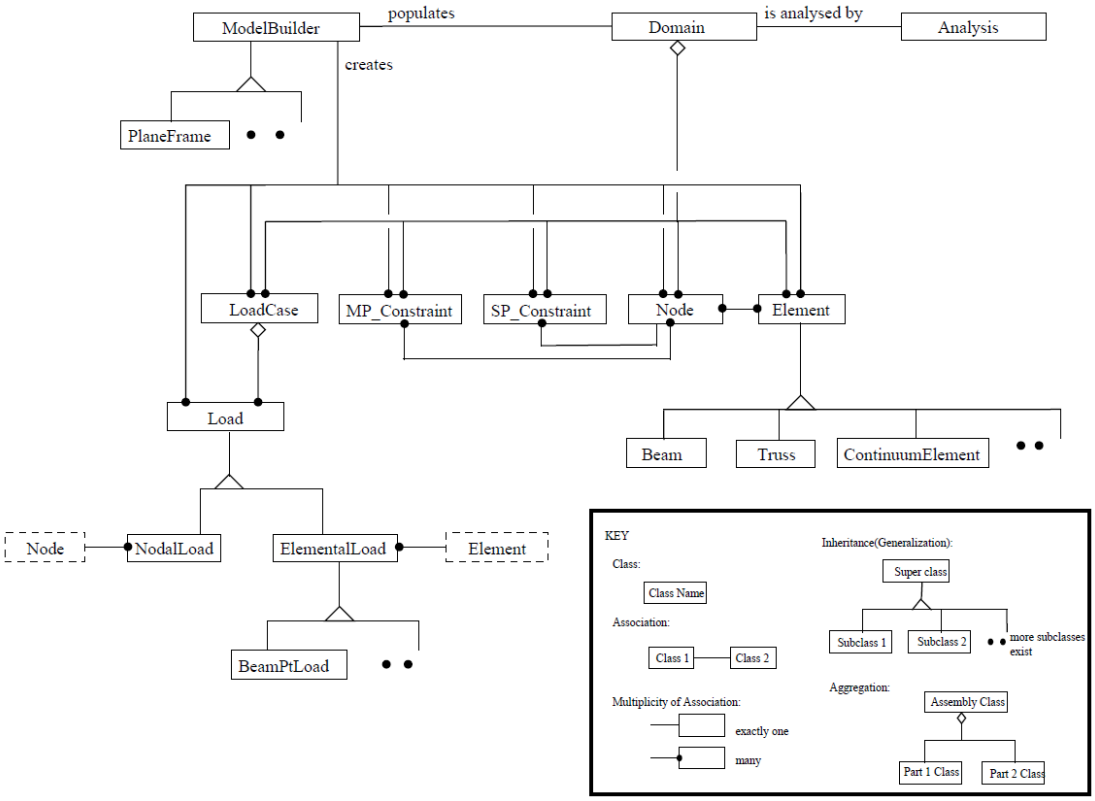

Figure 5.6: Class diagram for the finite element method [192]

The original development of the OpenSees was mainly focussed on developing a library of finite element method classes. The classes and the relationship amongst them can be graphically seen in Figure 5.6, which shows the class diagram for the analysis using Rumbaugh notation. In Rumbaugh notation, a class is represented by a rectangle, and

the relationships between classes are represented by lines between the classes. There are three types of relationships in object-oriented programming: knows-a, is-a and has-a, illustrated in Figure 5.6. Further details about this can be found in McKenna's thesis. [192]

The ModelBuilder class is used to construct the models, and these models are saved in the domain class. A domain object is a container responsible for holding all the components of the finite element model, i.e. the Node, Element, Constraint, and Load objects. It is associated with a ModelBuilder object and an Analysis object. The Analysis object forms and solves the governing equations for the finite element model. The type of the analysis that can be performed by the analyst depends on the analysis classes provided.

ThermalAction

ThermalAction class is used to apply temperatures to the members of the structure, as a type of Load. Thermal loads produce strain in the elements, and only if the element nodes are constrained stresses will be produced. ThermalField is the parent class of the ThermalAction class. ThermalField class is designed to receive both 2D and 3D data.

The temperature data is imposed across the sections of the element, which can be uniform or variable, but for this work the temperature is assumed to be uniform along the axial direction of the element.

For the nonlinear analysis of structures under gravity loads, the loading progress is usually divided into incremental steps. However, for a structural member subjected to heating from a fire, the temperatures do not usually change at constant rate at different locations in the member. Especially for the materials with low thermal conductivity, such as concrete or timber, every point across the section of an element will have its own temperature evolution with time. Figure 5.7 shows time-temperature curve of the points across the section of a concrete slab, which has a depth of 120mm, under the standard fire [210]. Thermal loading classes have been developed to achieve realistic loading for the 2D beam-column elements for this work.

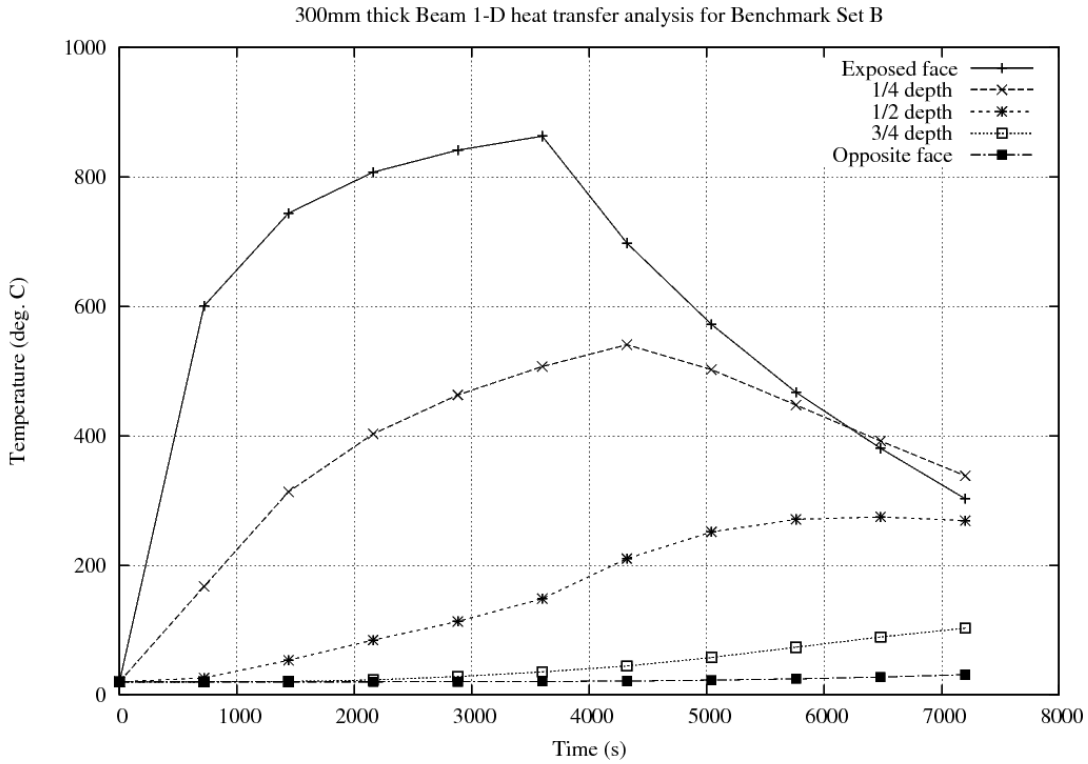

Figure 5.7: Time-temperature curves across the depth of the concrete slab under fire

Element

The basic function of the original Element classes was to provide the current linearized stiffness, mass, and damping matrices, and residual force vector due to the current stress and element loads [192]. For the thermomechanical analysis, two further components which have been added to the element class, for calculating thermal loads and the resisting force. Resisting force is the assembled vector of the transformed element internal forces induced by the combination of mechanical strains and thermal strains.

Figure 5.8 shows the calculation of the thermal force. The temperatures and coordinates available from "Beam2dThermalAction" are transferred to the fibre section class without any change. Each fibre interpolates its temperature based on the location of its central point in relation to nearest temperature points. The fibre section class obtains the Young's Modulus and thermal strain from the material class based on the fibre temperature. The fixed-end axial force in the fibres is calculated in the fibre section class and from which the element thermal forces are integrated in the DispBeamColumn2dThermal (element) class.

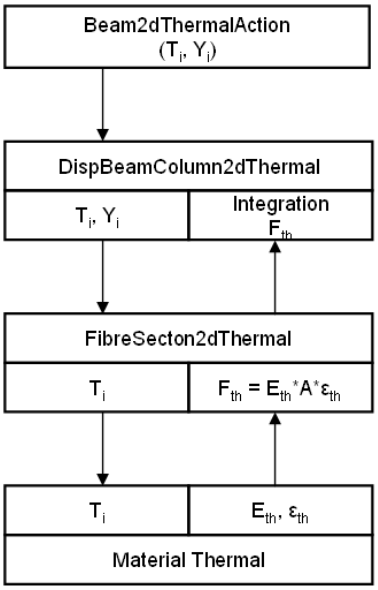

Figure 5.8: Flow chart for the calculation of thermally induced load

Section

The Section class defines the stress resultant force-deformation response at a cross section of a beam-column or plate element [192]. Figure 5.9 shows the representation of the section which is specified over a number of integration points along the length of the element There are three types of sections which include elastic, resultant and fibre setion.

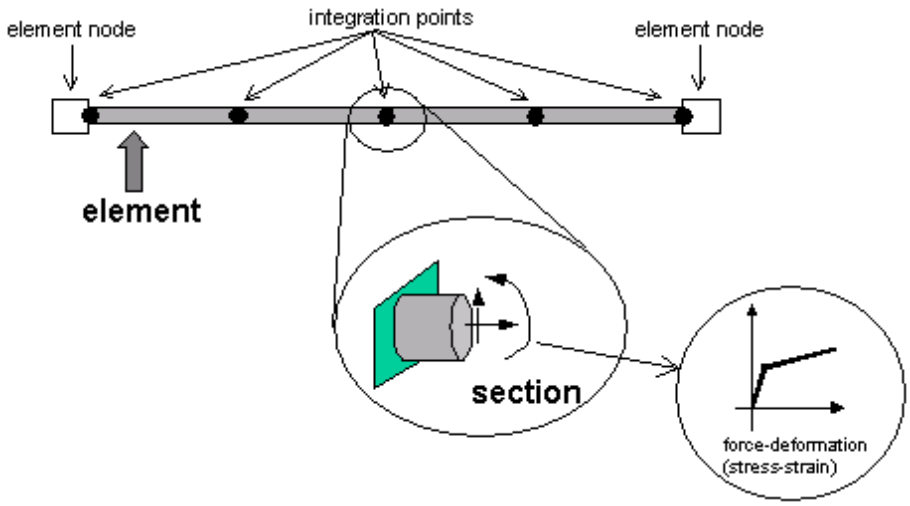

Figure 5.9: Section representation [192]

To calculate the thermal force, the element class calls the fibre section class, and assigns the measured temperature points into the selected section. Using linear interpolation, every single fibre finds its own temperature. Section class calls the material class and sends the fibre temperature, the material tangent modulus and thermal elongation at this

temperature is returned. The axial thermal force in the fibre is calculated as, from $s_i = E_i A_i \varepsilon_{i_{th}}$. The contribution to section moment of the fibre can be calculated as, $m_i = s_i y_i$, where y_i is the distance between the fibre and the centroid of the section. The section force is then,

$$\begin{bmatrix} s \\ m \end{bmatrix} = \sum_{i=1}^{n} \begin{bmatrix} s_i \\ m_i \end{bmatrix} \tag{5.3}$$

All the section forces are returned to element class, where the element end-forces are obtained by numerical integration. It should be noted that the integrated axial force from the fibre sections compares well with theory, the integrated moment does not match perfectly and depends upon the number of fibres used for the section, the greater the better.

Temperature-dependent materials

The material class in the original OpenSees simply provides constitutive laws for the materials used in the model, consisting of a number of 1D and nD classes [16]. The section class calls the material class with a deformation (strain), and the corresponding Young's Modulus and stress are derived and returned to the section. Under ambient temperatures, the stress-strain relationship is a single curve for 1D materials, but for the material at elevated temperatures, the stress-strain relationship requires many more curves to adequately represent the constitutive behaviour.

New material classes were created which accept the deformation (strain) and temperature from the fibre section class and return corresponding mechanical stress, Young's Modulus and thermal elongation. Among the material classes developed for elevated temperatures, *conctrete02thermal* and *steel02thermal* comply with the Eurocodes, and *steel01thermal* has a bilinear curve which is a common simplified model used for describing the stress-strain relationship of the steel.

5.6 Program Validation

The code developed as part of this work was tested against other software to ensure that the simulations are reasonably accurate before applying to the real problem of modelling the fire resistance of earthquake damaged reinforced concrete frames (in the next chapter).

5.6.1 General test

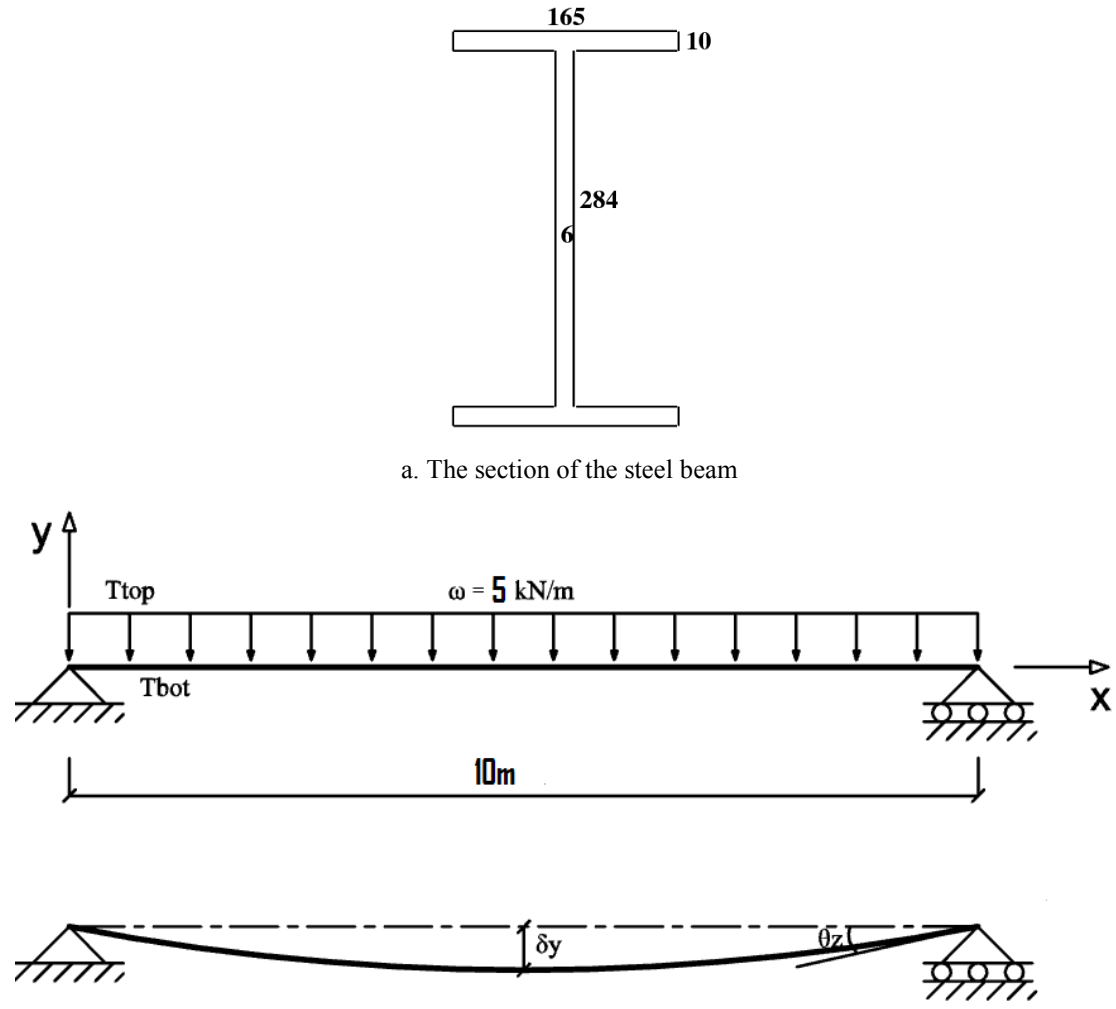

a. The section of the steel beam

b. Simply supported beam with UDL and temperature loading

Figure 5.10: Deflection of a beam subjected to UDL and thermal loading

The first analysis is that of a beam subjected to a UDL and thermal loading as shown in Figure 5.10. The beam is simply supported with a length of 10 metres and the uniformly distributed load on the beam w = 5000 N/m. The maximum temperature of the bottom of the I-section steel beam is increased to 800ºC, and the top temperature reaches 750ºC. Simple calculations show that the beam would collapse before it reaches the specified temperatures. To simplify the modelling, the temperatures are applied uniformly from ambient to the specified values.

In this test, the deflection of the mid-span of the beam is plotted against the increments of temperature as shown in Figure 5.11. The deflection increases relatively uniformly before the temperature reaches around 660ºC, after which it increases dramatically (suggesting "runaway" collapse) due to loss of bending capacity of the steel section because of the reduction in material stiffness.

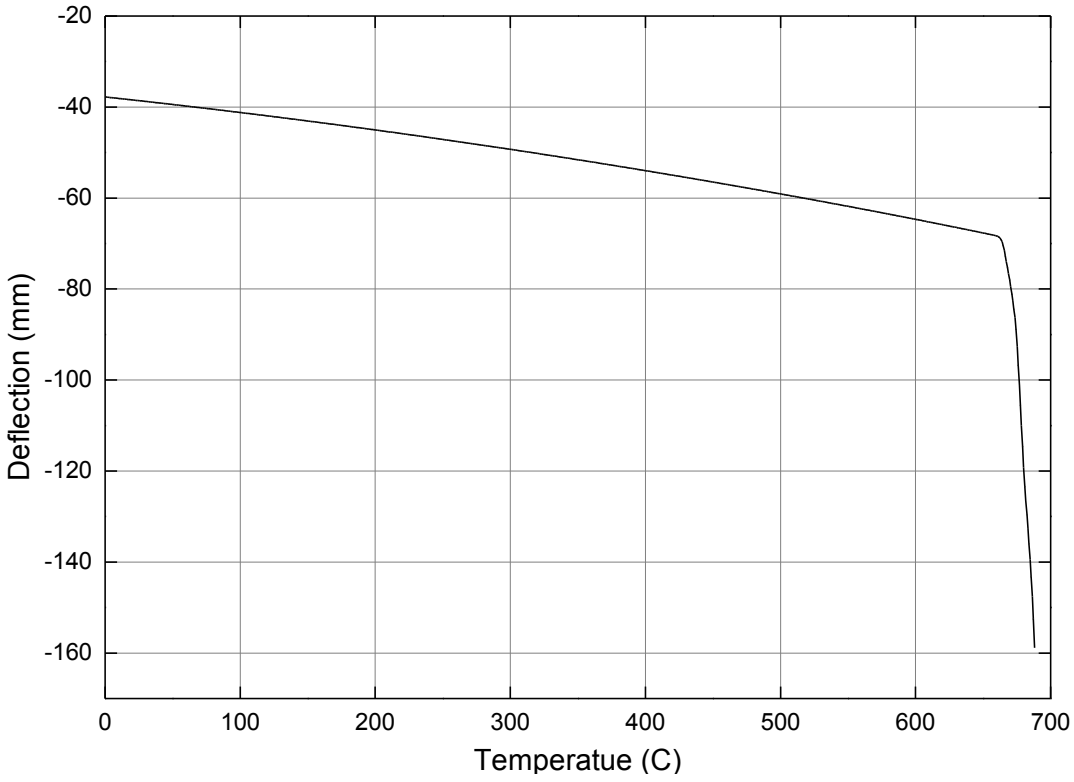

Figure 5.11: The mid-span deflection of the simply supported beam under thermal load

For comparison with the previous model, another beam is analysed with the same loading, except that the ends of the beam are fully fixed (see Figure 5.12). Figure 5.13 shows the deflection plot against temperature, from which we can see that the deflection increases greatly at a temperature of 130ºC, because the ends of the beam section yield. The beam experience thermal expansion because of elevated temperatures but is unable to expand due to the constraints from the fixed boundary, which lead first to yielding of the ends and then to very large deflections. Another point is that despite the much larger deflection of around 440mm, compared to 160mm of the simply supported beam, this particular beam has not collapsed and can sustain even greater deflections by essentially "hanging" from the boundary restraints as a catenary.

The results of the above models are compared with simple theory and are found to be reasonable and they also make sense intuitively. Further tests are carried out and compared against theory and other software.

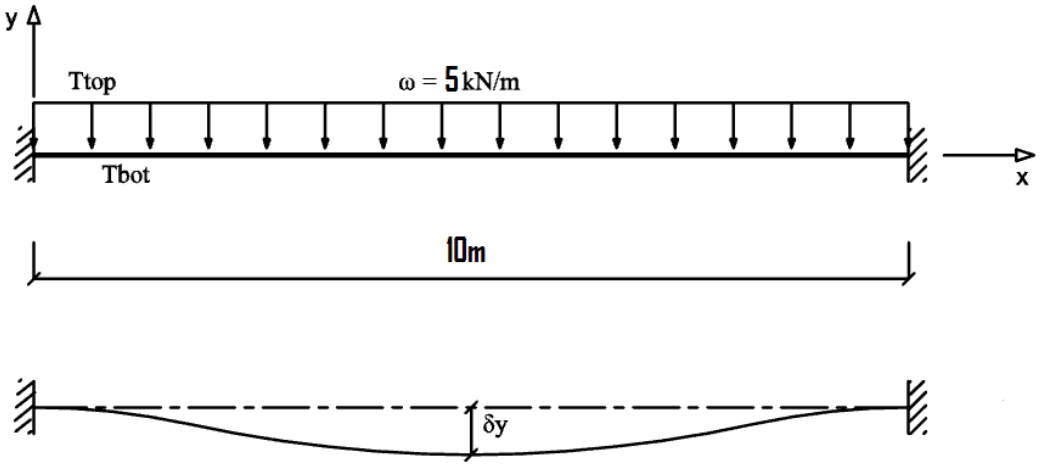

Figure 5.12: Deflection of a fixed ends beam subjected to UDL and thermal loading

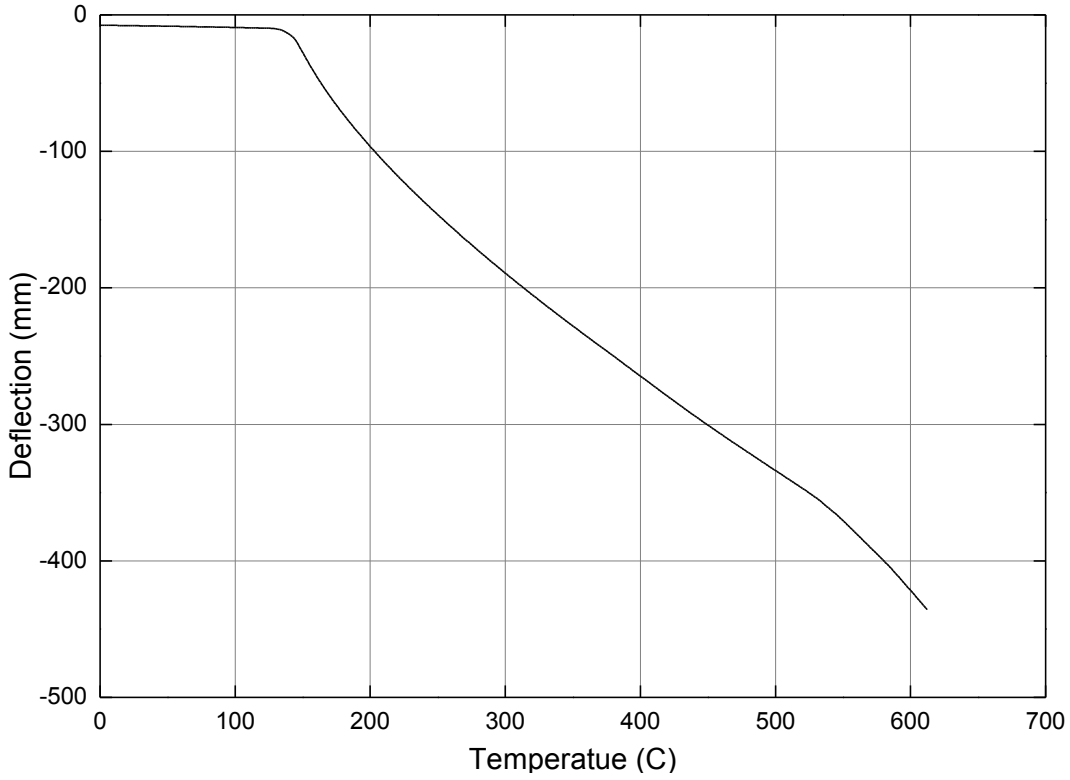

Figure 5.13: The mid-span deflection of the fixed-end beam under thermal load

5.6.2 Benchmark Problems

In this section, a few benchmark problems are analysed and the results are compared with theory and commercial software.

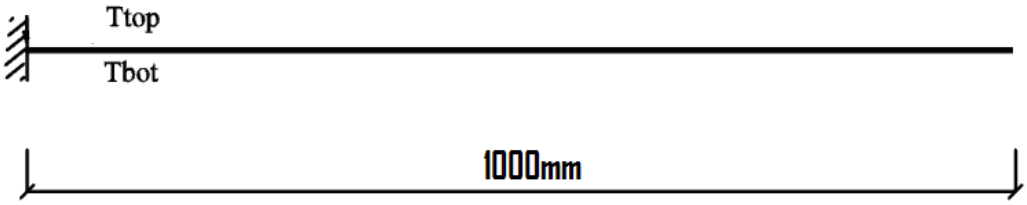

a). The cantilever subjected to a uniform thermal gradient

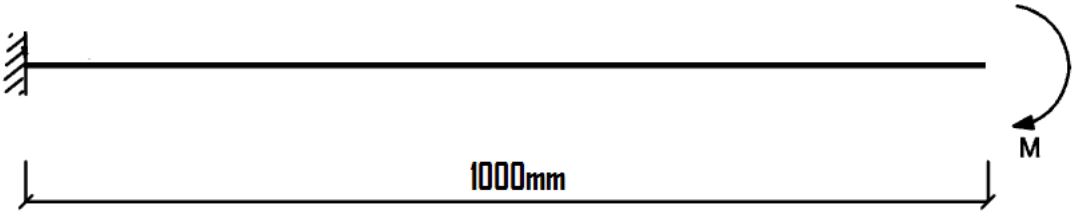

b). The cantilever subjected to a pure moment

Figure 5.14(a): The cantilever subjected to a uniform thermal gradient or pure moment at the free end

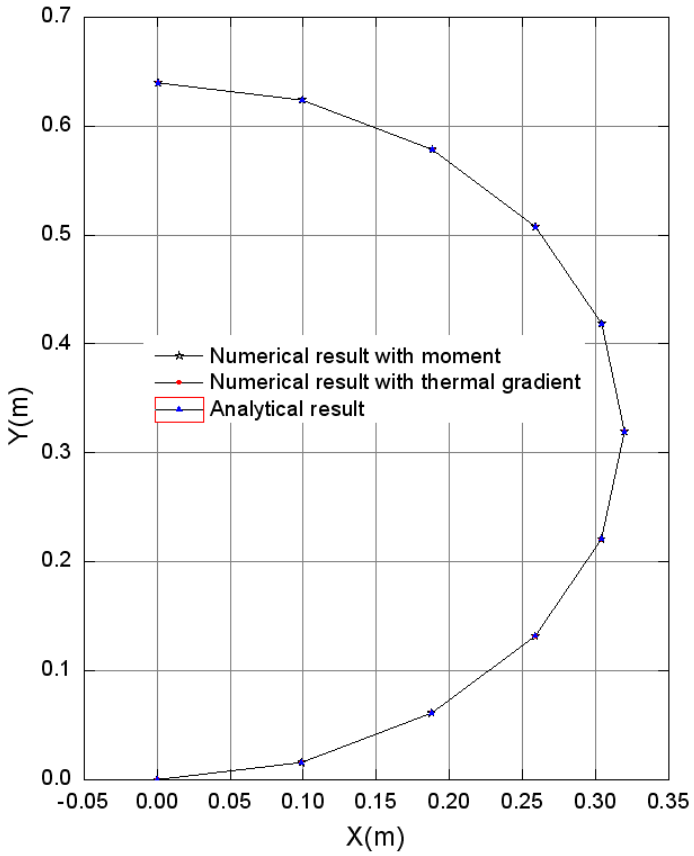

Figure 5.14(b): The shape of the cantilever beam subjected to a uniform thermal gradient or pure moment at the free end

(1) Cantilever

Theoretically, if a nonlinear model of a cantilever beam is subjected to a very high temperature at the bottom and a very low temperature at the top, the curvature of the cantilever will become larger and larger until the deflected shape resembles a circle. The

temperature gradient and the equivalent moment required to achieve a semi-circular or circular deflected shape can be easily calculated, making for useful benchmark test.

Figure 5.14(a) shows a one metre long steel cantilever subjected to a uniform thermal gradient. The cross section of the cantilever is square with a side length 0.1 metre. An equivalent analysis is performed using a pure moment applied at the free end of the cantilever. The results are shown in Figure 5.14(b). The shapes of the cantilever subjected to the uniform thermal gradient and the pure moment are exactly the same producing a perfect half circle.

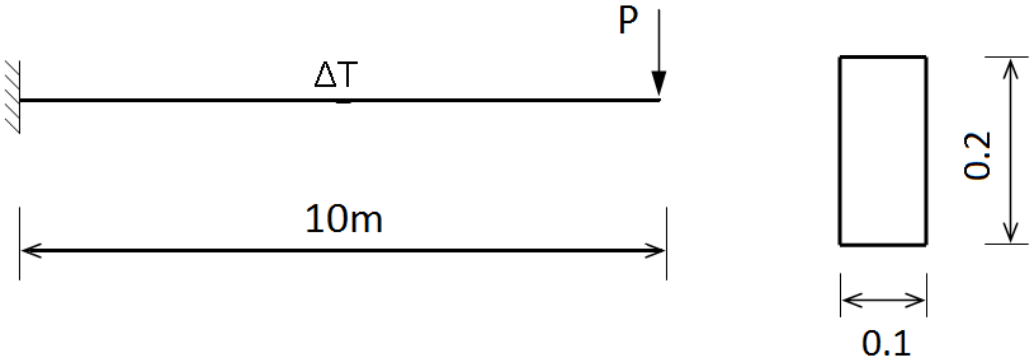

Figure 5.15 (a): The cantilever subjected to pointed load and uniform thermal load

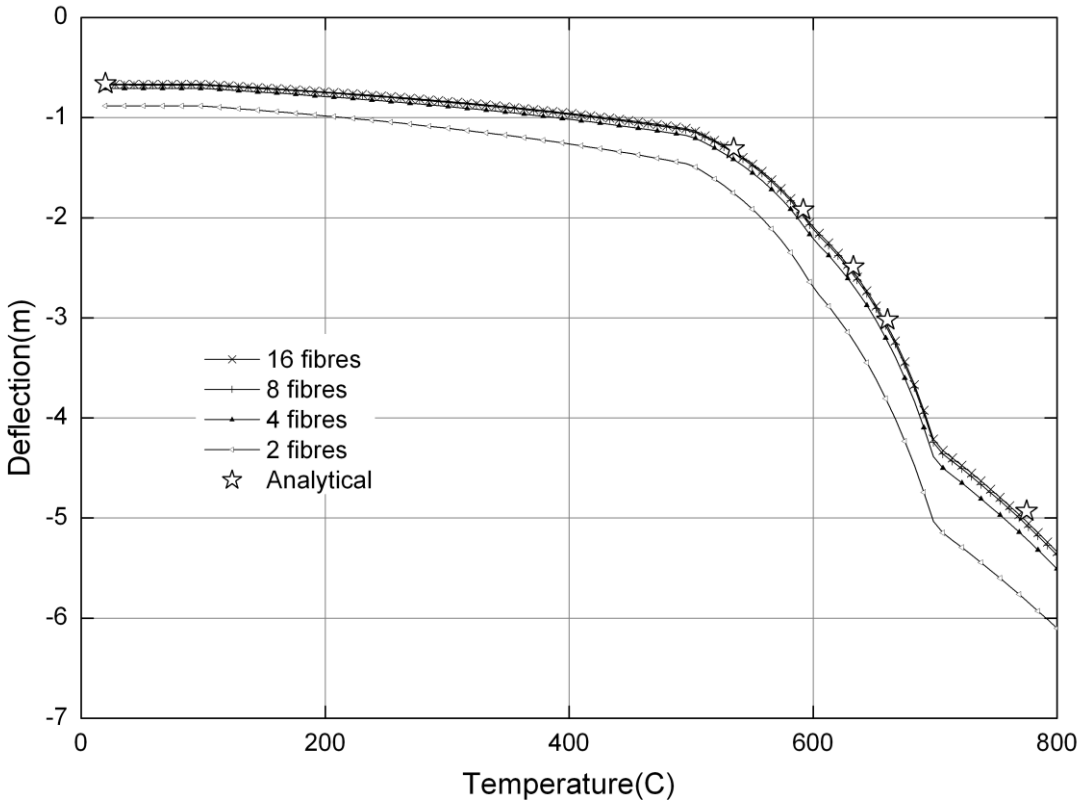

Figure 5.15 (b): The deflection of the cantilever subjected to point load and uniform thermal load

Another cantilever beam is shown in Figure 5.15(a). The Young's modulus of the beam material is assumed to change with the increase of temperature but never yield. The beam is analysed for a uniform temperature increase across the section and the results are compared against a closed-form solution obtained using the classical beam theory considering geometric nonlinearity [212]. To test the sensitivity of numerical results to the segmentation of the beam cross-section, beam sections with 2 fibres, 4 fibres, 8 fibres and 16 fibres are analysed. From Figure 5.15(b) we can see the numerical and analytical results match very well, and when the member of fibres used for the section is 8 the error is negligible.

(2) Half Heated Beam

The next example is a benchmark test of modelling restrained thermal expansion in and axial member, only a half of which is subjected to an increased temperature (see Figure 5.16 below).

A bi-linear stress-strain curve of the steel is used for this example, which has a yield stress 280MPa and an initial Young's modulus of 20,000 MPa. The temperature dependence of both these parameters vary according the relevant Eurocode (EN 1993 1-2-1) while undergoing constant temperature increments from ambient to 1000ºC. The temperature-displacement curve for node 2 from both OpenSees and ABAQUS solutions is shown in Figure 5.17.

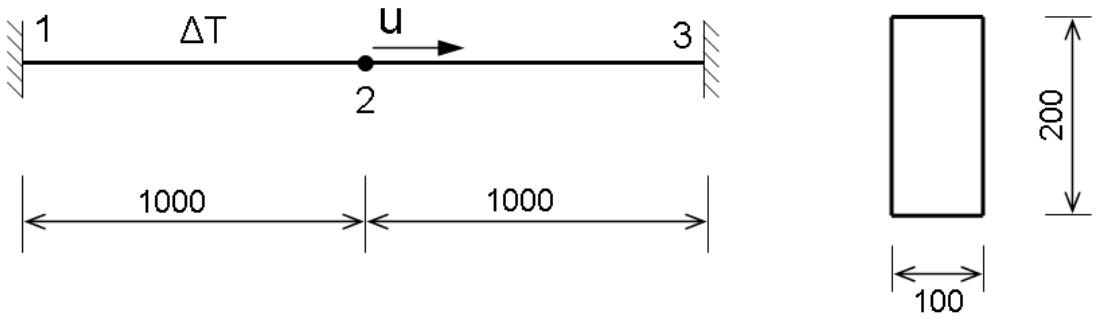

Figure 5.15: Rigidly restrained steel beam of rectangular section with one half heated

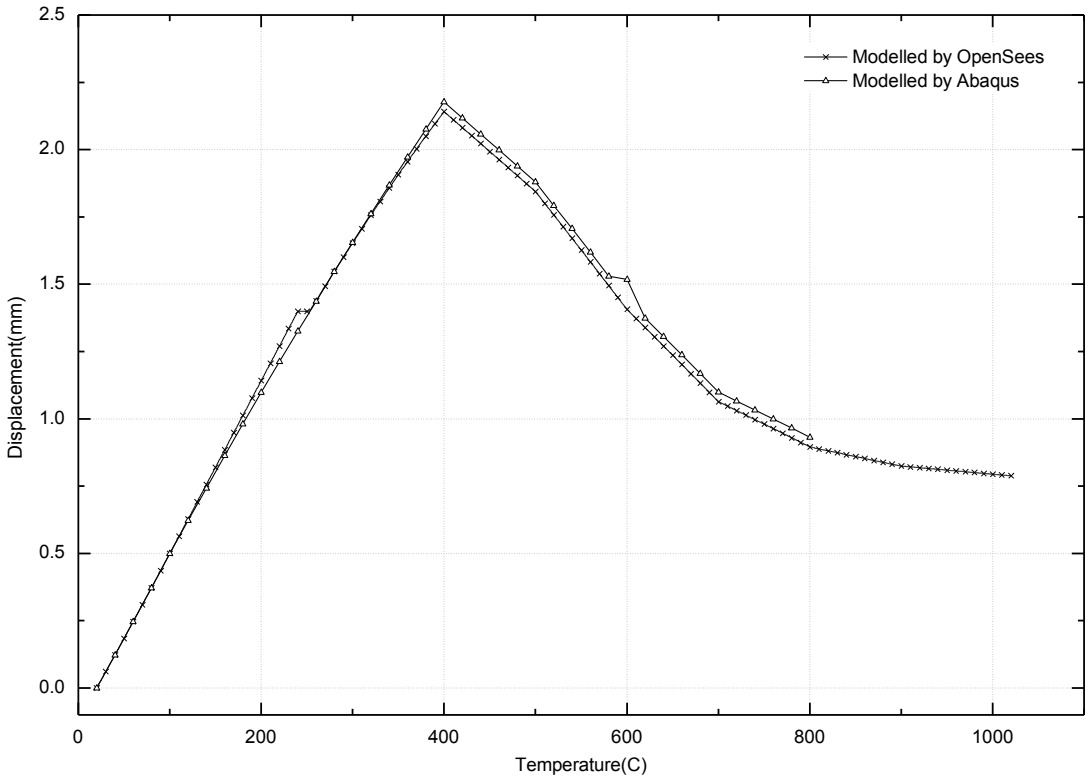

Figure 5.16: Displacement at node 2

From ambient to 400ºC, the displacement of node 2 increases linearly, even though the two halves yield at 253ºC (the yield stresses remain unchanged until 400ºC). At roughly 400ºC, node 2 begins to move from right to left due to the drop in yield stress in the heated half leading to elastic unloading of the unheated half. However, the curve asymptotes to a finite displacement resulting from the plastic strain in the right half stored during the post yield phase (between 253ºC to 400ºC).

(3) Frame in Elevated Temperature

Figure 5.18 shows the schematic of a single beam model which is extracted from a framed structure. The beam in the middle of the frame is subjected to uniformly distributed load (UDL) and is restrained by one beam and two columns at both ends. The restraining forces offered by these surrounding elements can be represented by equivalent rotational and translational springs. Therefore the framed structure can be transformed to an equivalent single beam with finite end restraints. The dimensions of beams and columns in Cardington Restrained Beam test [193] are used (i.e. 305×165×40UB for beam and 254×254×89UC for column). The corresponding second moment of area of column (I_c) and beam (I_b) cross-section can be calculated as

I_c=1.4×10^{-4}m^4, I_b=0.8×10^{-4}m^4. The equivalent stiffness of rotational spring (K_r) and translational spring (K_t) can be calculated as $K_r=8EI_c/l+4EI_b/l$ and $K_t=2EA_b/l+48EI_c/l^3$ with values of K_r=4.8×10^{4}kN.m/rad and K_t=3.8×10^{5}kN/m.

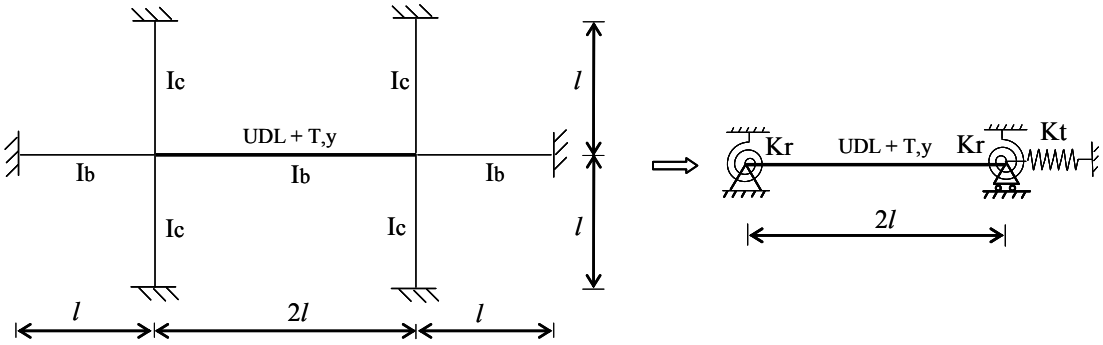

Figure 5.17: Beam with translational and rotational springs at the ends

Based on fundamental structural mechanics, the analytical solution of the response of the beam subjected to UDL and thermal gradient $T_{,y}$ can be given as

$$\delta = \frac{5ql^4}{384EI}\left(1-0.8\varphi_r\right)+\frac{\alpha T_{,y} l^2}{8}\left(1-\varphi_r\right) \tag{5.7}$$

$$\theta = \left(\frac{ql^2}{12}+EI\alpha T_{,y}\right)\frac{1}{K_r+2EI/l} \tag{5.8}$$

$$u = \alpha \Delta T l\left(1-\varphi_t\right) \tag{5.9}$$

Where δ, θ and u are the mid-span deflection, end rotation and horizontal displacement of the beam respectively; φ_r=1/(1+2$EI/K_r l$) and φ_t=1/[1+(EA/l)/K_t] is a factor due to the rotational and translational end restraint, respectively.

OpenSees was used to analyse the response of a 6m beam (l=3m) with finite end restraints (K_r=4.8×10^{4}kN.m/rad and K_t=3.8×10^{5}kN/m) subjected to UDL and thermal gradient. The UDL is assumed to be 30kN/m and the temperature at the top of the beam was assumed to be 0^{o}C and it varied linearly over the depth of the beam from temperatures of 100^{o}C to 1000^{o}C. Steel01Thermal was used to model the steel material. A finite large value was assigned to yield stress in order to make the material behaviour elastic but still temperature-dependent. The elastic modulus at ambient temperature is 200GPa and a constant coefficient of thermal elongation α = 1.2×10^{-5}/^{o}C was assumed. Three different analyses were conducted including materially and geometrically linear analysis, materially nonlinear but geometrically linear analysis as well as both materially and geometrically nonlinear analysis. Material nonlinearity is

limited to elastic modulus being dependent on temperature. Figure 5.19 shows good agreement between OpenSees and analytical solutions using Equations 5.7-5.9 for the linear case.

The responses of the beam subjected to UDL and thermal load for the three analyses in OpenSees are shown in Figure 5.20-5.22. The symbol "MatL" represents materially linear analysis and "MatNL" for materially nonlinear analysis. Similarly, "GeoL" represents geometrically linear analysis and "GeoNL" for geometrically nonlinear analysis. The material nonlinearity has an obvious effect on the end rotation and horizontal movement of the beam end. In contrast, the effect of the geometrical nonlinearity is obvious on the mid-span deflection but negligible on the rotation and horizontal displacement of the beam. The mid-span deflection of the beam continued to increase and experienced a larger slope after about 600°C for nonlinear analysis. This is because the beam deflection, as temperature increases, is dominated by the thermal bowing effect and this downward bending is accelerated by material degradation at high temperature. As shown in Figure 5.21 and 5.22, the rotation and horizontal displacement of the beam increased first driven by the thermal elongation (and thermal gradient) until 500°C and then began to decrease as the decreasing of modulus of elasticity of the beam is unable to resist the stored strain energy and elastic rebound of the unheated rotational and translational spring respectively.

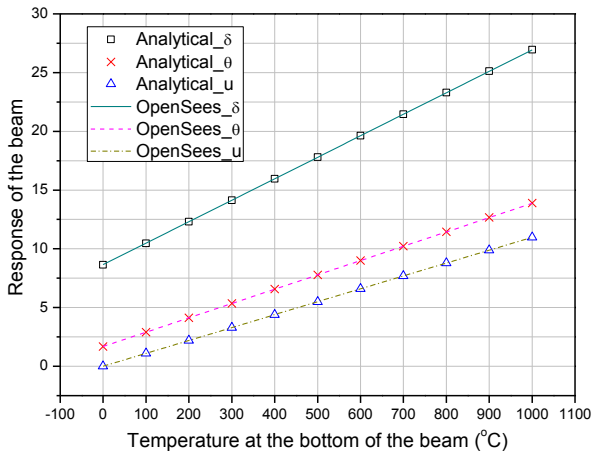

Figure 5.18: Responses of the beam from OpenSees compared with analytical solution (δ, u: mm; θ: 10^{-3}rad)

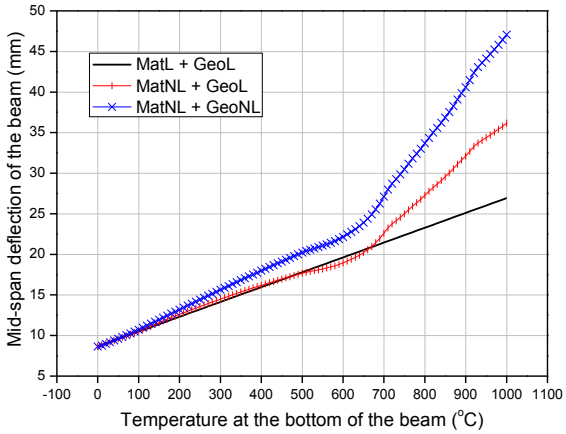

Figure 5.19: Mid-span deflection of the beam against temperature

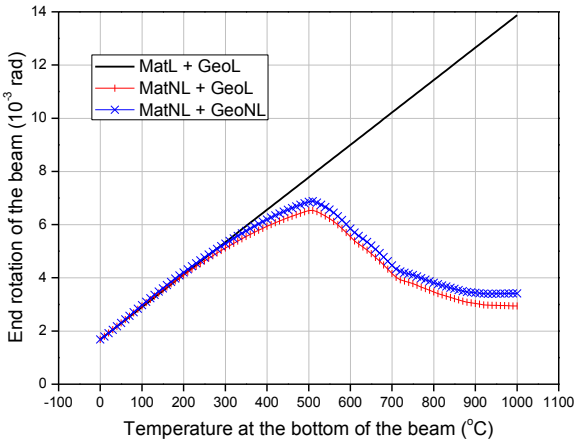

Figure 5.20: End rotation of the beam against temperature

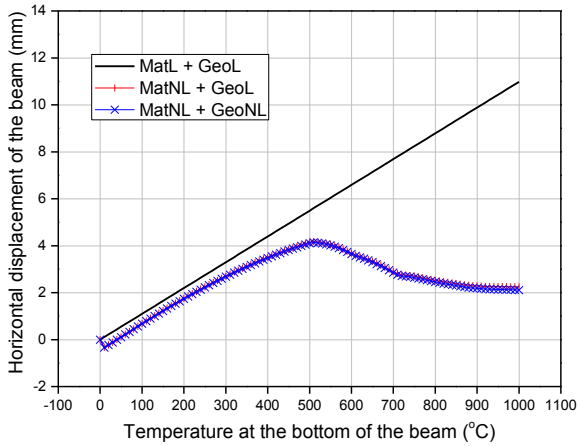

Figure 5.21: Horizontal displacement of movable end of the beam against temperature

5.6.3 Modelling real experiments

(1) ZSR1

The modelling in this section is a steel frame (ZSR1) tested and analyzed by Rubert [194]. The frame with dimensions is shown in Figure 5.23. All structural elements are made of IPE80 I-sections. Different material properties have been used to model the experiment, including steel properties given in EN 1993-1-2-1 (Eurocode 3) and ST37

[194] (see Figure 5.24). The yield stress and Young's modulus of the steel are 355MPa and 21,000MPa at ambient temperature. The left bay of the frame including the middle column is uniformly heated at a constant rate by electrical elements and the remaining two members are kept at room temperature. A comparison of test and modelling results is shown in Figure 5.25.

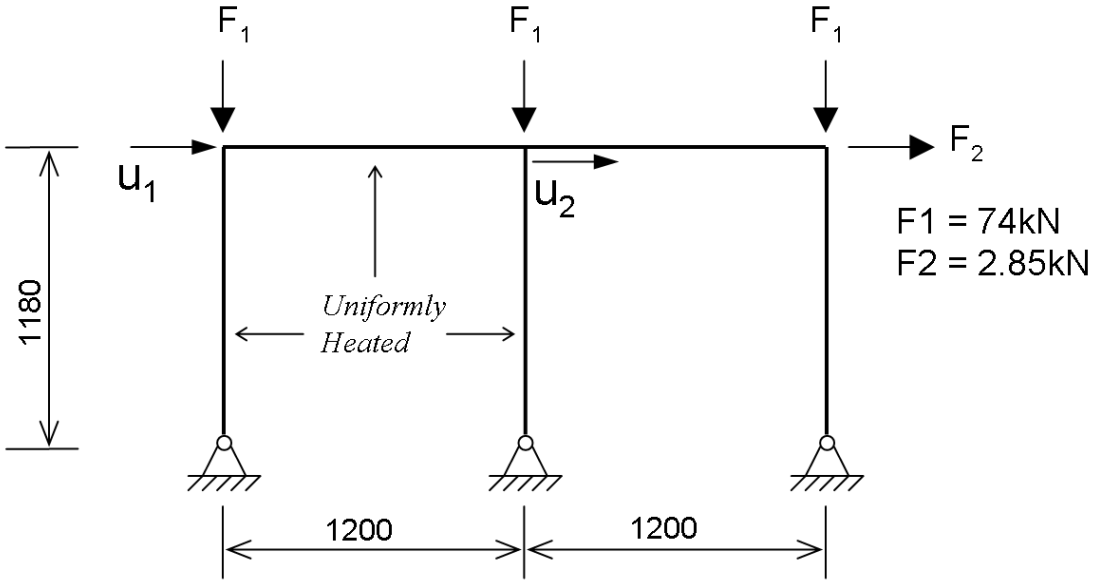

Figure 5.22: Schematic of the ZSR1 frame test

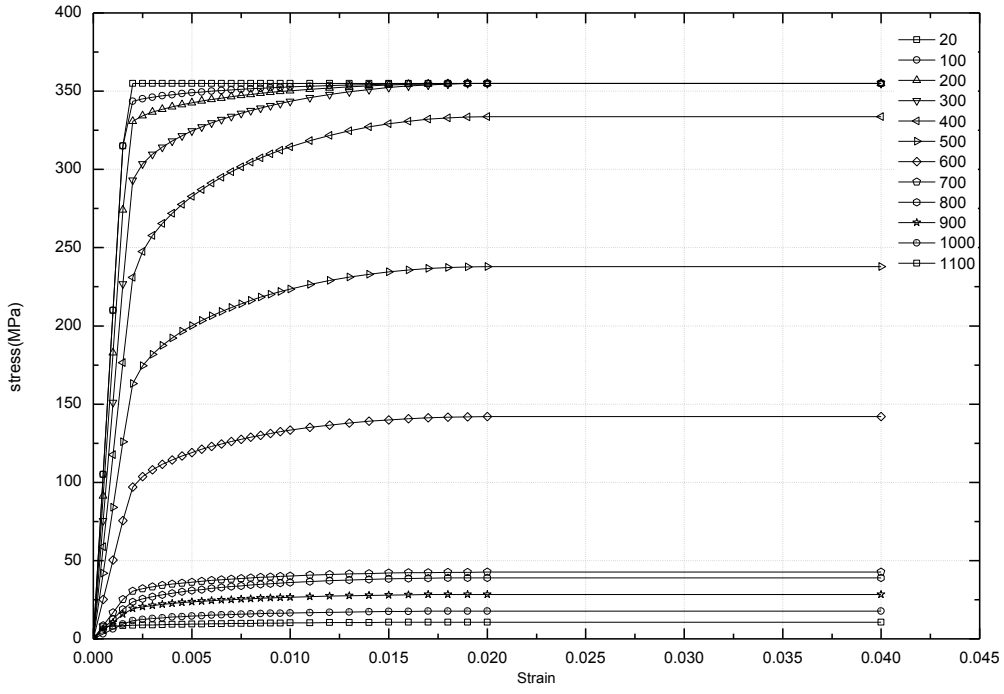

a. Stress-strain curve of steel in EN 1993 1-2-1 without hardening

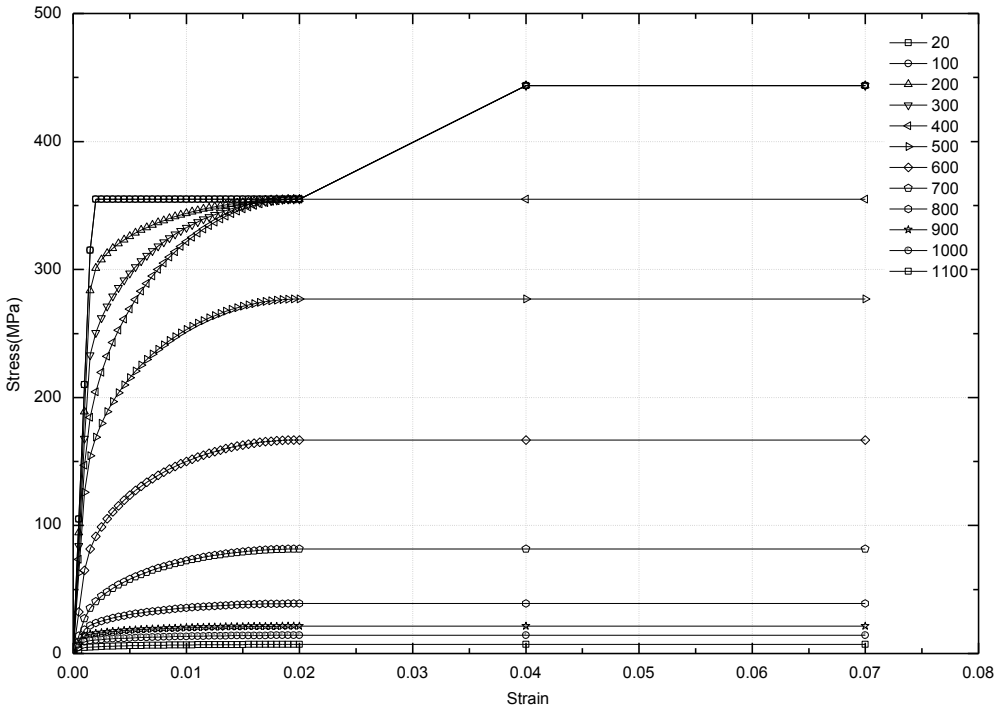

b. Stress-strain curve of steel in EN 1993 1-2-1 with hardening

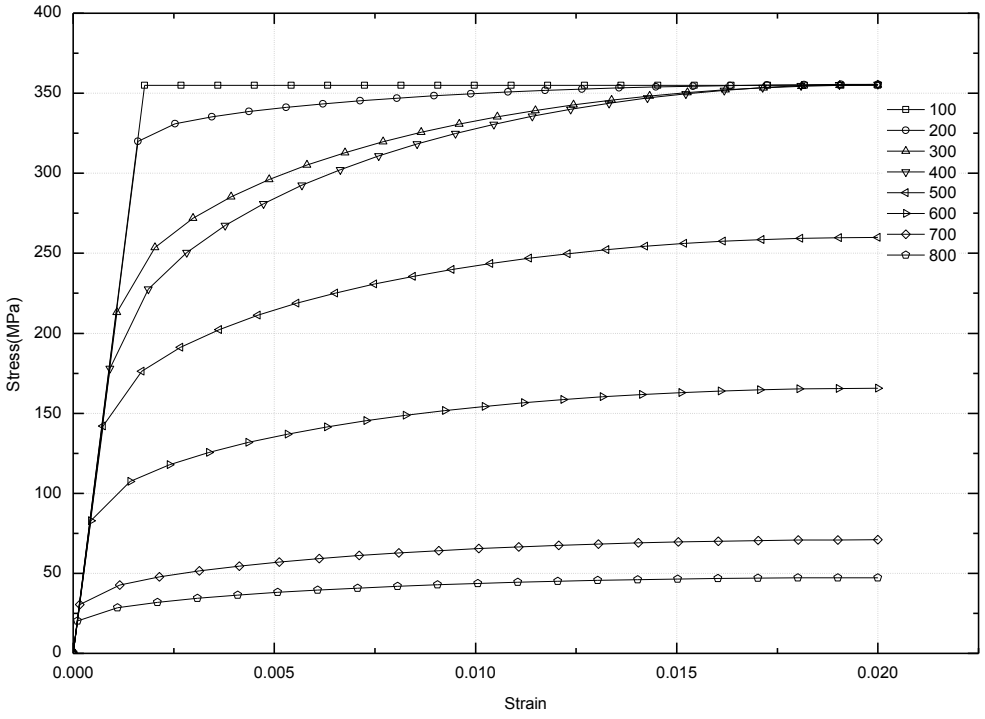

c. Stress-strain curve of ST 37

Figure 5.23: Stress-strain curves of steel used in the ZSR1 frame analysis

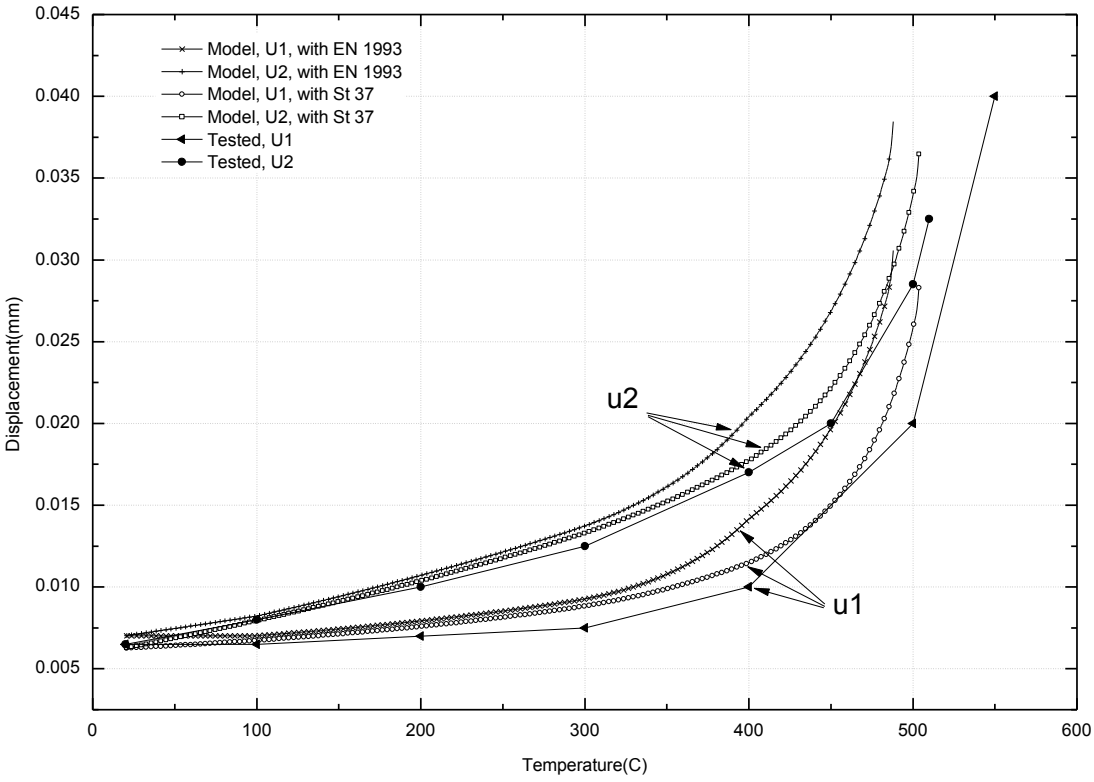

Figure 5.24: Comparison of results between test and models using different steel properties

The material properties were a key factor in this simulation. The displacements stay at a low level until around 500ºC if a bilinear stress-strain curve is used for steel, but they increase sharply around 300ºC when using a multi-linear curve (both curves were based on Eurocode recommendations). If the steel temperature dependent property variation specified by EN 1993 1-2-1 is used, the results are not very close to the test (as shown in Figure 5.25 - results were identical for both with and without hardening versions). When ST 37 properties are used, the results show satisfactory agreement. This is encouraging as the test frame was constructed using ST37 steel.

(2) Cardington Restrained Beam Test

The next example chosen to validate the programme is derived from the restrained beam test in the composite steel frame at Cardington [195]. Although this experiment was initially meant to test one of the internal secondary beams only, it offered considerable insights into the behaviour of steel frame composite structures in fire [193, 196]. The test showed true 3D behaviour and considerable interaction between the longitudinal section of the composite beam (as shown in Figure 5.26) and the transverse deck slab

(in the direction of the slab ribs). However as using a 2D element here, only the longitudinal section shown in Figure 5.26 will be modelled as a fully composite section.

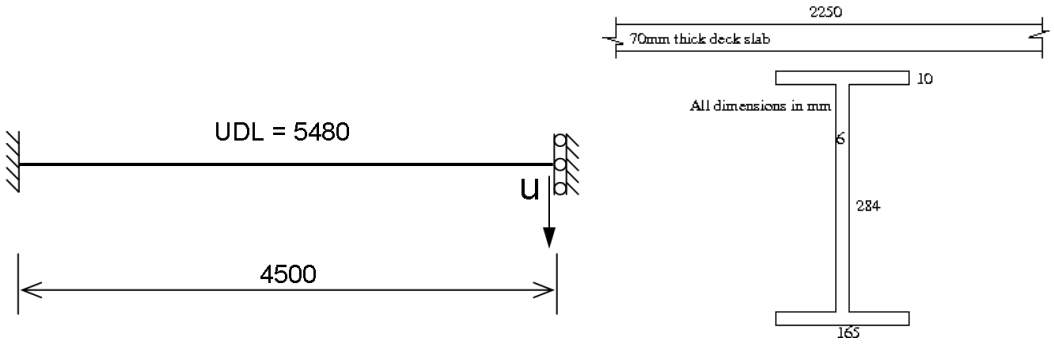

Figure 5.25: Example problem (derived from the restrained beam test at Cardington)

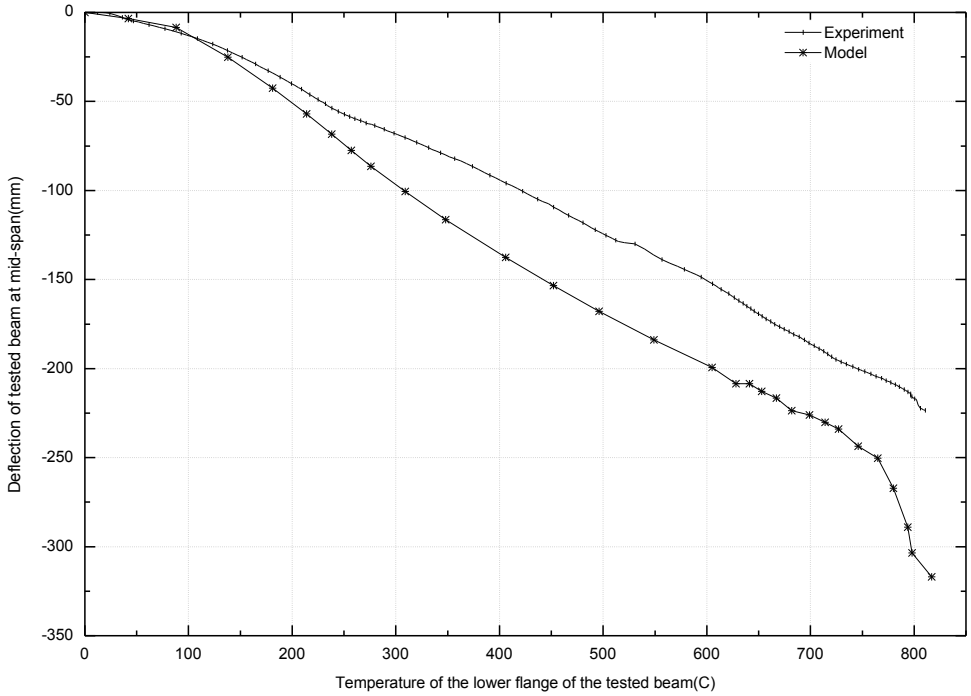

Figure 5.26: Comparison of OpenSees model against restrained beam test results

The composite beam was modelled using 9 DispBeamColumn2dThermal elements (taking advantage of symmetry, so only half the beam length of 9m was modelled), and further for the sake of simplicity, the analysis uses a single section, which includes the I-section steel, concrete, and rebar. The gap (60mm depth) is also in placed within the section. The two end nodes are restrained against all translation and rotation except for the vertical translation at midspan. Because of the composite nature of the beam, even with end rotations free, the composite section is able to generate resisting moments at the end, justifying the fixed-end conditions used here. The beam was first loaded using the

gravity load used in Cardington. Both parts of the beam were divided into eight fibres (or layers) each and the full temperature history at each fibre was applied in a number of thermal loading stages.

The analysis result is shown in Figure 5.27 against the actual test result. The deflections are low at the start however they accelerate after 100ºC because of yielding in the steel bottom fibres and large tensile strains in the top concrete layers. The curve dips sharply at around 760ºC, due to sharply reducing yield stress and Young's modulus beyond this temperature. The test trace also shows a drop after 800C, but it is much smaller because the ribs perpendicular to the beam continue to support it and this is also why the deflections from this analysis are much greater than the test. Convergence problems occur in between 600 to 800ºC which were solved by replacing the Newton-Raphson algorithm with Modified Newton-Raphson. As reported in [196], the gravity loading contributes little to the total deflection and it only increases or decreases a few millimeters with double or half the udl respectively. The deflections are larger in this model compared to the actual test, as the model is 2D and does not have any resistance to the thermally induced deflections from the orthogonal (out-of-plane) direction.

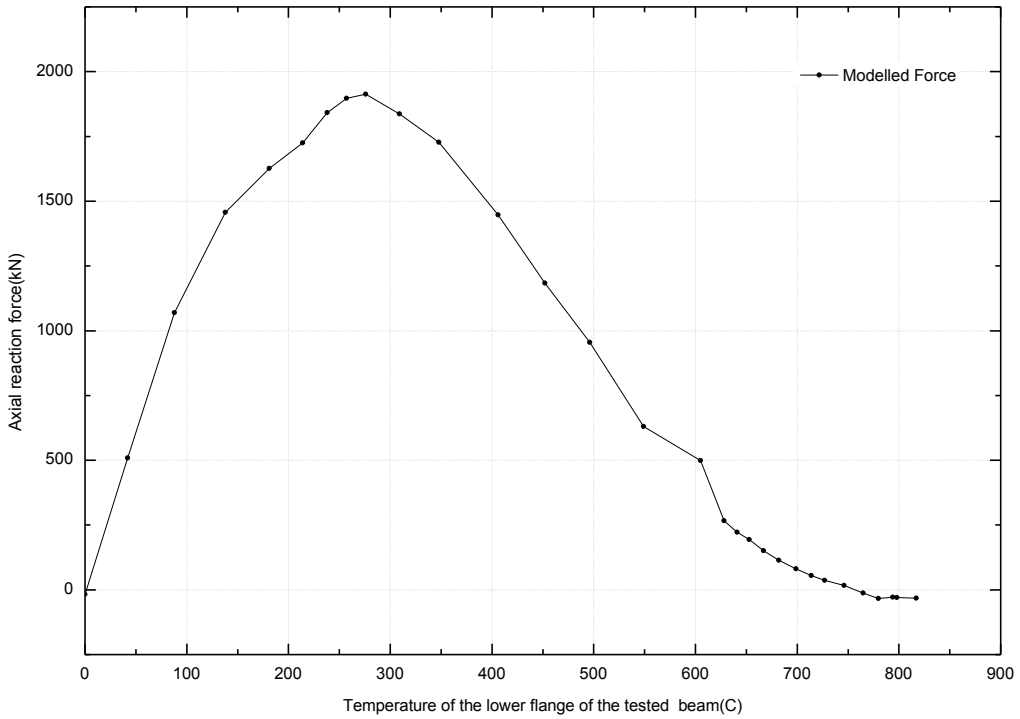

Figure 5.27: Axial reaction at end support

Figure 5.28 shows the variation of the axial reaction force at the end support with temperature. This also shows good agreement with other reported analyses of this test, *e.g.* [196].

5.7 Summary and Conclusion

This chapter has described the developments implemented in OpenSees for thermomechanical analyses, with details of some of the main developments, such as the Element, Section, Load and Material classes, but this does not represent the full extent of the work undertaken. To test the new developments, a number of challenging theoretical problems and experiments were modelled. The results from the tests performed in the previous section suggest that the developments undertaken have been successful and therefore we conclude that the updated OpenSees software can be used to analyse 2D structural frames subjected to elevated temperatures, e.g. from a fire.

Chapter 6 - Modelling of a RC Frame Subjected to Post Earthquake Fire

This chapter reports the 2D modelling of a RC frame subjected to cyclic loading and a following fire. Full-scale fire tests on reinforced concrete frames were undertaken in India as part of a project funded by UKIERI. The results from the tests are introduced briefly followed by the description of a finite element model of the experiments using OpenSees. The results from the modelling work are analysed and compared with the experimental results. In this chapter, the modelling work has been completed by the author but the experimental works were carried out by other team members at University of Edinburgh and IIT Roorkee in India.

6.1 Introduction

Earthquakes can and do cause extreme damage to buildings and infrastructure. However, secondary disasters often present as much of a risk as the earthquake itself. For example fire following earthquake (FFE) is a relatively common secondary disaster as well as tsunamis, landslips and so on. The fire in San Francisco following the 1906 earthquake was the largest urban fire in history up to that time, and the fire following the 1923 Tokyo earthquake is considered to be the largest urban conflagration to date. In fact both of the fires led to major conflagrations and widespread devastation and caused far more damage than the original shaking. Although not all of the earthquakes cause fires, there have been many major earthquakes followed by fires since 1923. For example, 116 ignitions were reported following the 1971 San Fernando earthquake, and 200 fires were reported within 24 hours after 1985 Mexico city earthquake. There were 89 fires in the first 14 minutes and more than 400 in the following few days after the 1995 Kobe earthquake, and 69,000 buildings were destroyed over an area of 65 hectares. These post earthquake fire events can be found in Botting's report and paper, in which he described the impact of many more FFE events in buildings and the environment, and analysed them from the point of view of ignition sources, fire spread, fire fighting activities, damage to fire protection systems and lifelines [197, 198].

However, many recent earthquakes were not followed by widespread fire events, for example, there were no significant fires reported following 1999 Izmit, 2001 Gujrat, 2005 Kashmir and 2008 Wenchuan earthquakes. All of these earthquakes happened in

rural rather than urban areas, which suggests that the occurrence of FFE events may depend on the level of urbanization and industrialization of the earthquake affected regions. If this is indeed the case then the risk of FFE to urban infrastructure, life and livelihoods must be considered as a serious threat due to the rapidly increasing trend towards urbanization in the world. This risk is increased significantly by the hindrance to intervention by emergency crews from extreme traffic congestion, collapsed houses and buildings and rubble in the streets. The existence of multiple fires at the same time and the possible damage to water supply is like to further add to the risk that FFE events pose to urban infrastructure and populations [199]. With increasing globalisation and integration of the world economy, major disasters of the future could have repercussions far beyond the local region. FFE events have the potential to create such disasters and should certainly be considered in the overall disaster mitigation strategies by governments and agencies with such a remit [200]. Further discussion about the FFE events can be found here [197, 201-203].

To develop a comprehensive earthquake and fire research programme based on exploiting the complementary strengths of the collaborating institutions, a project funded by UKIERI was undertaken by a University of Edinburgh team with involving this author and a team at IIT Roorkee in India. The key aim of the project was to carry out the first ever full-scale tests to understand the behaviour of earthquake damaged reinforced concrete frames in fire. Considerable new understanding was gained on the behaviour of steel framed composite structures in fire from the Cardington test in the mid 1990s [204] and a large collaborative project on the computational modelling of the tests. It was expected that these tests would also help generate similarly useful information on the behaviour of damaged and undamaged RC structures subjected to fire.

This chapter also describes the modelling of the tests using OpenSees. At first the modelling work provided useful predictions for fine tuning the proposed tests and the test set up. Post-test modelling was used to compare the key features of response in the tests, including: pushover reaction force; hysteretic based on the initially designed cyclic displacement history (in order to produce simulate seismic damage); and finally the deformation of the damaged frame in a fire. The modelling was repeated to take account of the real displacement and temperature history (measured in the test), and the modelling results are compared with the tested results. Modelling of the second test of the series of experiments is also presented.

6.2 Large scale testing of damaged RC frames

Tests are planned on a number of identical reinforced concrete frames consisting of four columns (3m apart in plan) supporting four beams and a slab, all monolithically constructed, at a dedicated testing facility on the campus of IIT Roorkee in India. These frames will then be subjected to cyclic quasi-static loading against a reaction wall which will provide a reasonable simulation of the damage expected to occur under real seismic loads. Table 6.1 shows the planned fire tests with different levels of simulated seismic damage.

Table 6.1: Frame tests originally planned [206]

Test no.	Simulated seismic damage	Fire loading	Aftermath
1	Displacement beyond peak lateral force	900^{o}C -1000^{o}C*	Residual lateral capacity test*
2	None	900^{o}C -1000^{o}C for 1 hr	Residual lateral capacity test
3	"intermediate" damage (x% of the displacement corresponding to peak lateral force)	900^{o}C -1000^{o}C for 1 hr	Residual lateral capacity test

**for as long as considered safe*

Since it was not feasible to test a full-scale monolithic RC frame, it was decided to use a frame sub-assemblage for the experimental programme. The plan and elevation of the simple and symmetrical 4 storey RC framed building from which the sub-assemblage was extracted is presented in Figure 6.1 which also shows the configuration of the sub-assemblage.

The "intermediate" damage level was intended to correspond to a certain percentage of the horizontal slab displacement achieved at peak lateral force. Efforts were made to keep the fire exposure for all tests broadly similar. Figure 6.2 shows a schematic of the front elevation of the test frame setup with key dimensions. The frames were erected on a 1.2 m thick raft of dimensions 6.75m x 8.55 m and subjected to an increasing cyclic lateral displacement (as shown in Figure 5.3) applied through jacks reacting against a stiff, 1.2m thick reaction wall (monolithic with the base of the raft). The cyclic displacements were applied at the slab level.

Detailed thermal and mechanical histories were to be recorded. A set of selected displacements were to be measured by erecting a secondary steel frame around the test frame, during both the damage inducing phase and the fire phase. During the lateral

displacement phase (to induce damage) a good number of strain gauges were installed to obtain a detailed picture of strains at key locations.

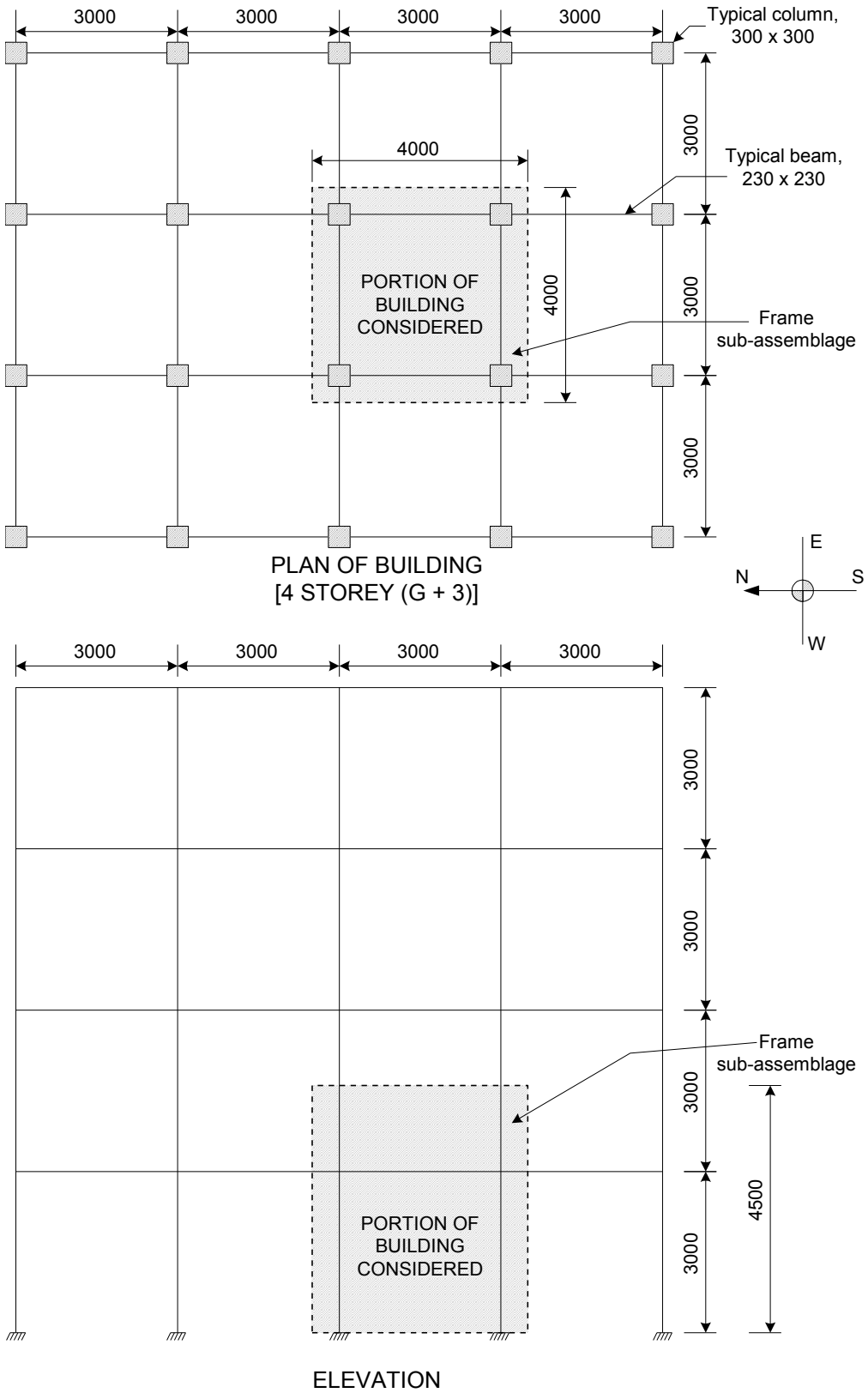

Figure 6.1: Building configuration and the frame sub-assemblage. All dimensions in mm [206]

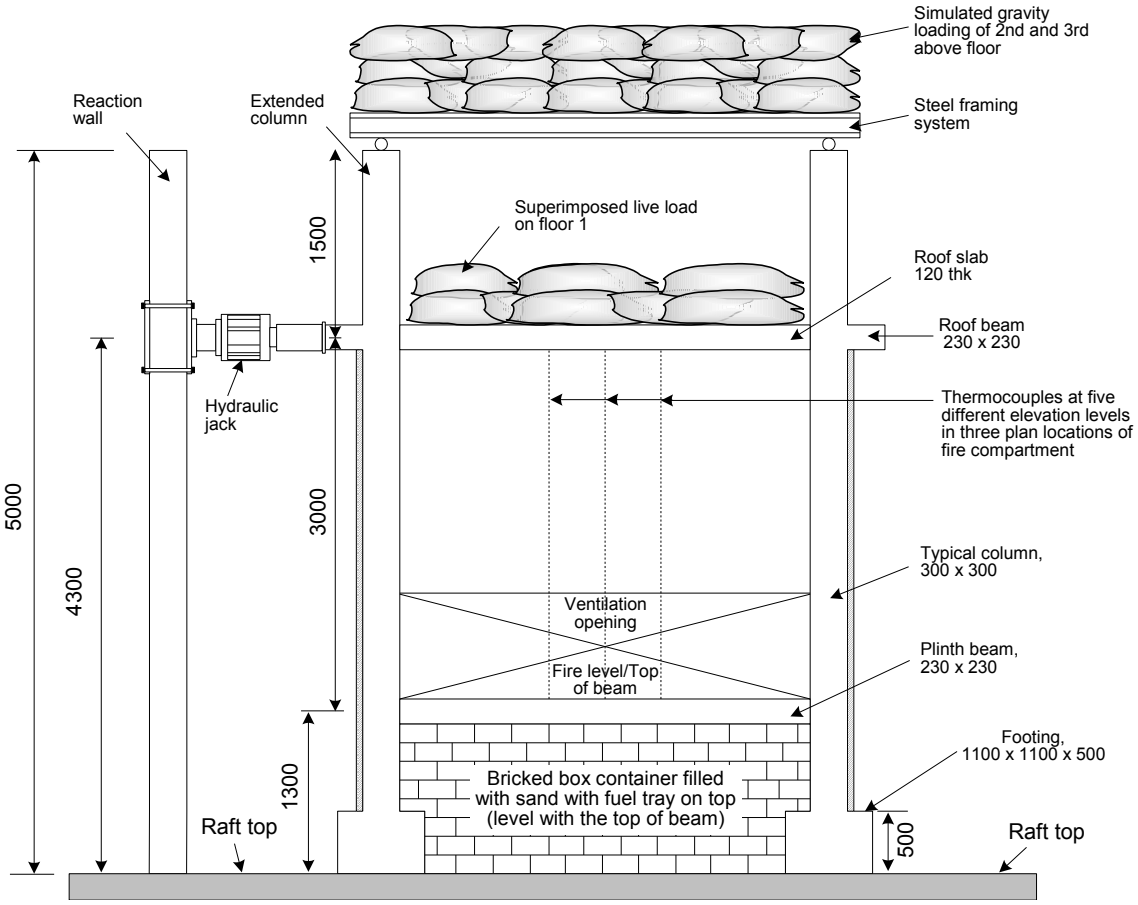

Figure 6.2: Schematic view of the test setup (all dimensions in mm) [206]

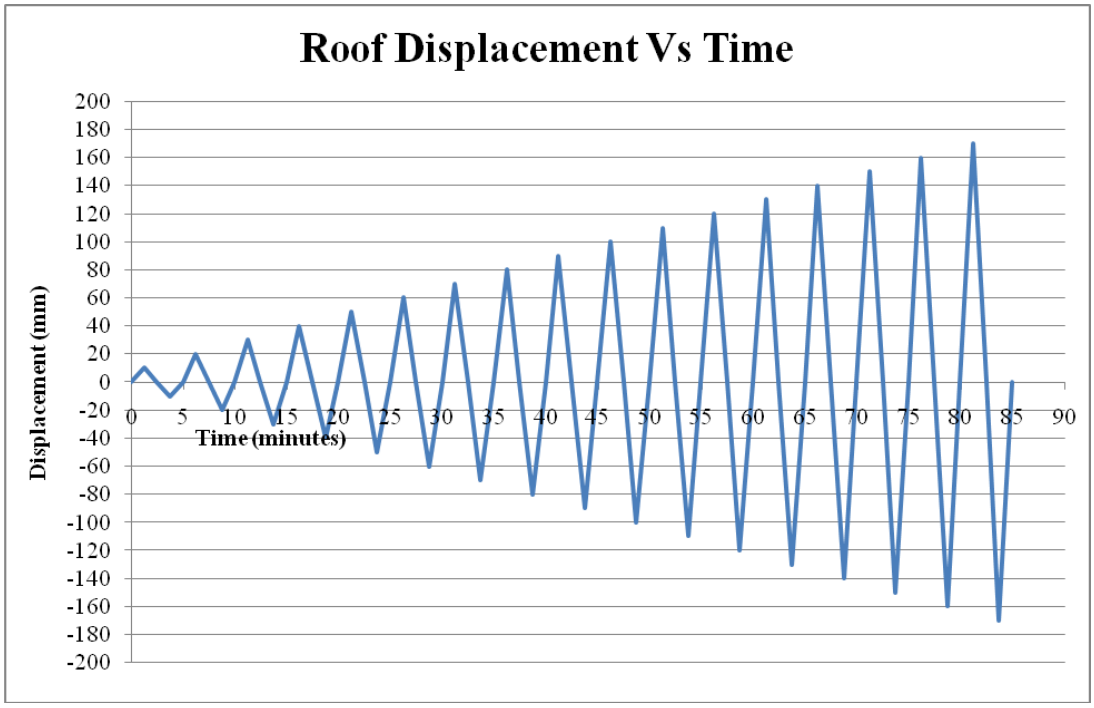

Figure 6.3: Incremental cyclic loading of the frame [206]

Fire Testing

The fire compartment was constructed using detachable panels made of fire-proof materials commonly used in brick kilns in India. This allowed repeated use of the panels for the whole testing programme and beyond. The fire was continuously fed by a 1m square tray of kerosene in a roughly 3m cube compartment with a 1m high opening along the full length of the wall at the bottom of one side (see Figure 6.2). To maintain a post flashover temperature of 900^{o}C to 1000^{o}C the peak burning rate for the chosen opening configuration is approximately 0.117 kg/m^{2}s. This required a peak flow rate of kerosene into the tray of 1.43 x 10^{-4} m^{3}/s which was maintained using a fixed head. About 0.51m^{3} of kerosene was required for maintaining the post flashover temperatures within the above range for 1 hour. The chosen configuration was designed to achieve flashover within 5 minutes.

Thermal instrumentation consisted of three thermocouple trees in the fire compartment to capture the gas temperature history inside the compartment during the fire testing phase. Adequate numbers of thermocouples were also embedded in the structural members to obtain detailed structural temperature evolution for the whole heating and cooling cycle.

A number of mock fire tests were carried out at the location of the test to ensure that the expected fire behaviour is achieved and is repeatable. The first mock test carried out in July 2009 did not succeed as the brickwork walls were very damp because of rain and much of the radiant heat from the fire was being absorbed by the wall leading to an inordinate delay in flashover and low peak temperatures. The test was repeated in November 2009 and this time the results were as expected as shown in Figure 6.4. This however was not an issue for the actual tests as the compartment was made up of waterproof insulating panels.

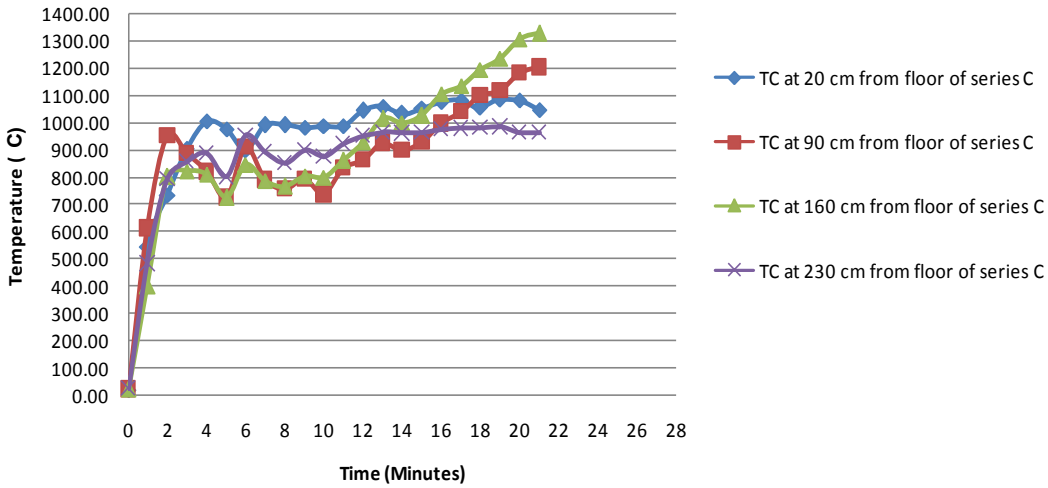

Figure 6.4: Temperatures inside the fire compartment (near the centre of the back wall opposite to opening) [206]

6.3 Predictive Modelling

Predictive modelling of the tests was carried out to refine the loading magnitudes and displacements and fine-tune the test set up.

6.3.1 Material model

The material property models (for both concrete and steel rebars) under elevated temperature was derived from Eurocodes 2 and 3 [22, 205]. The mechanical properties of concrete and steel rebars at ambient temperatures are provided in Tables 6.2 and 6.3.

Table 6.2: Mechanical property of the concrete at ambient temperature [206]

Compressive stress (MP)	-30
Strain corresponding to Compressive stress	-0.0025
ultimate stress (MP)	-0.00001*
strain at ultimate stress	-0.02
tensile strength (MP)	1.5

*ultimate Stress changed from 0 to 0.00001 as zero stress value cannot be used for ABAQUS

Table 6.3: Mechanical property of the steel rebar at ambient temperature [206]

Yield stress (MP)	420
Ultimate stress (MP)	550
Yield strain	0.002
ultimate strain	0.015
Young's Modulus (MP)	210000

6.3.2 Elements and sections

In this chapter, 2D analysis is performed, therefore a simplification of the test frames is necessary. The numerical model of the frames is shown in Figure (6.5). Due to the simplification from 3D frame to 2D frame, the slab and roof beams are considered as one structural member as shown in Section 1-1. Similarly, two lower beams are regarded as one beam as in Section 2-2, and the columns are modelled as "double columns" as in Section 3-3.

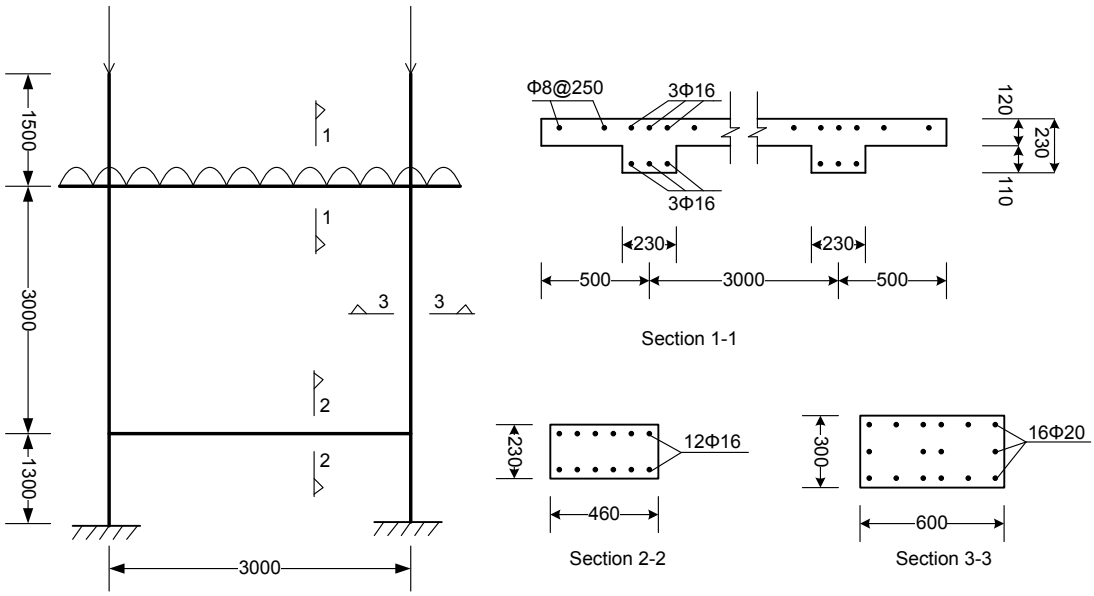

Figure 6.5: 2D frame model and member sections.

Non-linear beam-column elements are used to model the frame. To get adequate precision in the calculation of displacements, stresses and strains in sections of each member, every member of the frame is divided into 10 elements.

6.3.3 Gravity and Cyclic Loading

The one storey test frame represents a sub-assemblage of a multi-storied structure consisting of ground + 3 floors. To simulate gravity loads of the upper floors on the columns of the test frame, a grillage of orthogonally oriented rolled steel I-beams was constructed on the top of the frame. The grillage was loaded with sand-filled hessian bags to simulate the specified dead and live loads from the stories above the ground floor in the RC building. The self-weight of the columns, beams and slab are also considered, which can be derived from the dimensions and the density.

Displacement control method is used in the modelling, so that a series of increasing maximum displacement values of the frame are applied in suitable increments. The left joint of roof beam and column is considered as control nodal point.

6.3.4 Temperature distribution

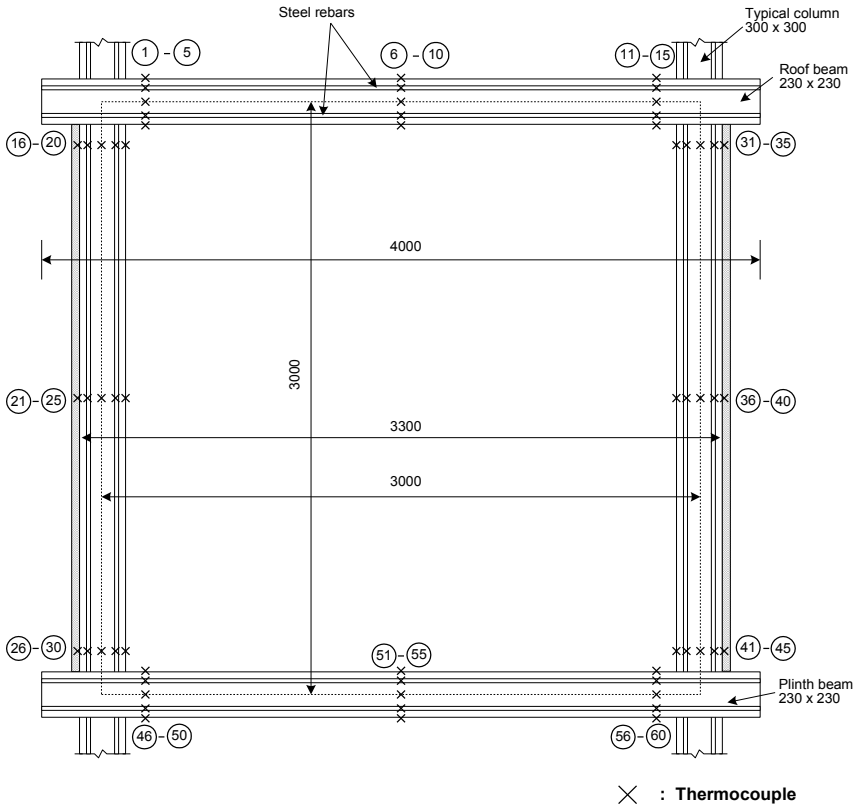

Figure 6.6: Typical location of thermocouples in beam and column [206]

In the experiment, the temperature of concrete at different locations in the structural members was recorded through 0.5 mm diameter K-type thermocouples embedded along the depth and width as shown in Figure 6.6. Thermocouples were fixed at three sections in each member – near end supports and at the mid span. Each section consisted of nine thermocouples. Five thermocouples were embedded along the depth in the roof slab at five different locations to record the thermal profile as shown in Figure 6.6, respectively.

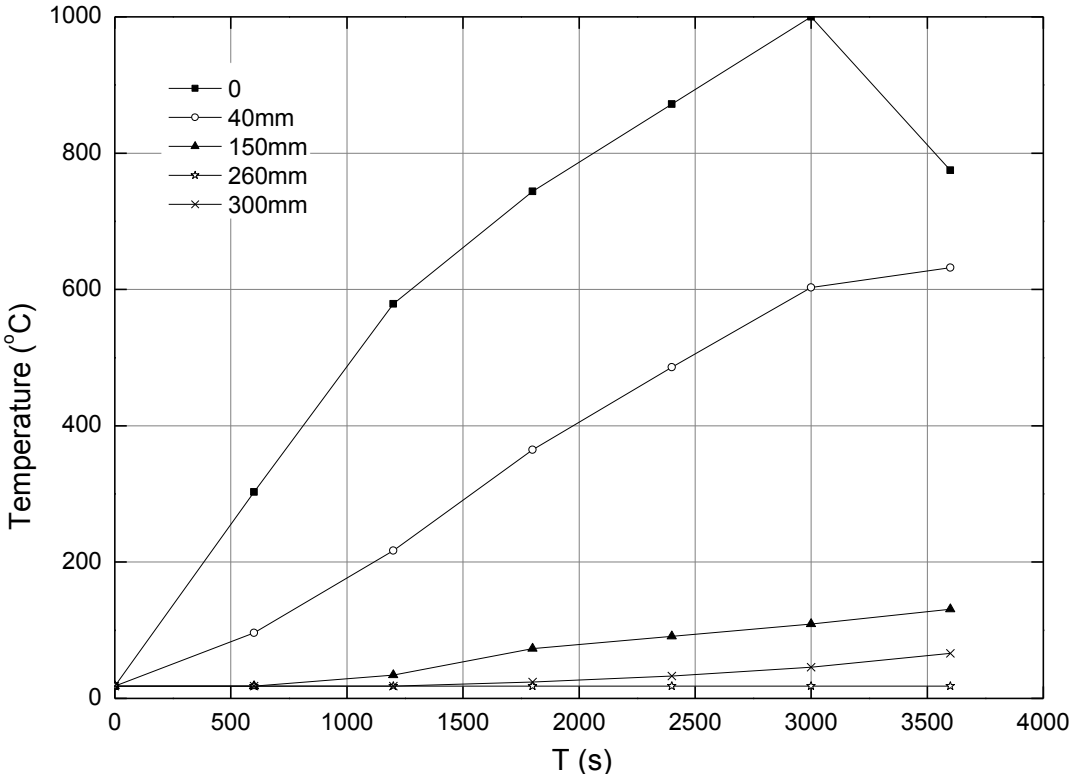

Figure 6.7: Time-Temperature curves for the heated column through its depth [206]

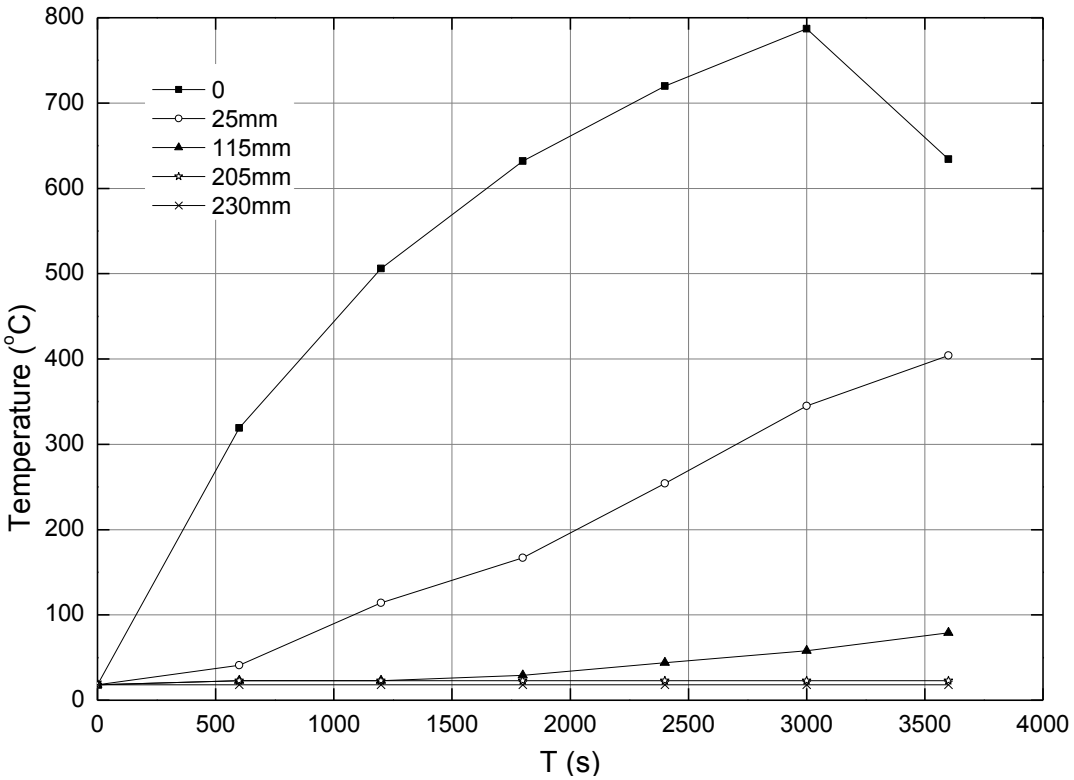

Figure 6.8: Time-Temperature curves for the lower beam (B1) through its depth [206]

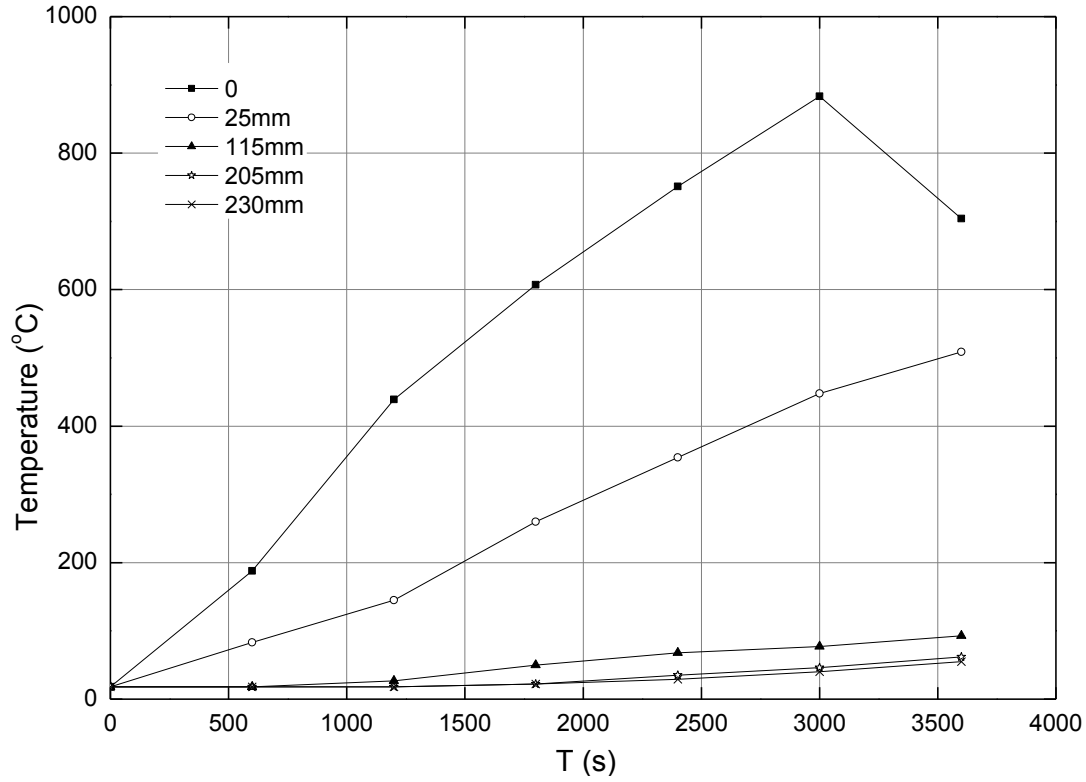

Figure 6.9: Time-Temperature curves for the upper beam (B2) through its depth [206]

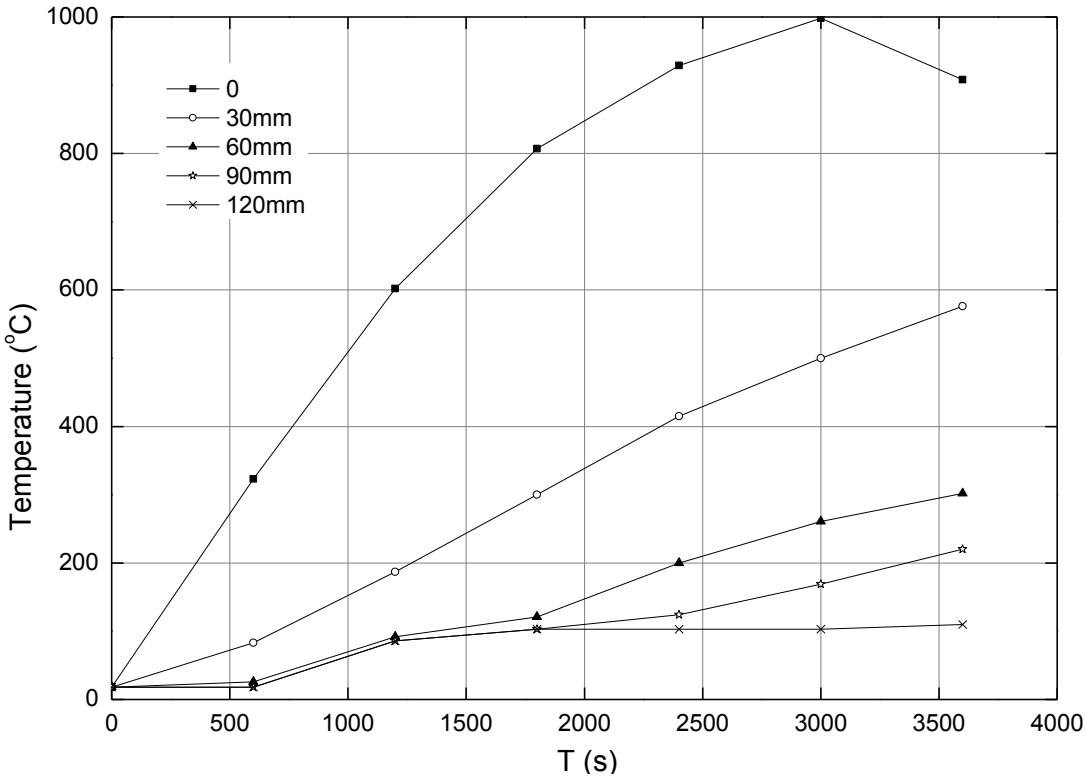

Figure 6.10: Time-Temperature curves for the slab through its depth [206]

For the numerical analysis, average temperatures for each structural member were derived from the test data, as shown in Figures 6.7, 6.8, 6.9 and 6.10, where the

temperature evolution within the member with time is presented for locations measured through the depth from the exposed face.

6.4 Results Analysis

6.4.1 Peak Load and Displacement of The Push Over Model

A pushover model for the frame was developed to predict the lateral load resistance capacity of the frame as designed, to assist the members of team preparing for test. The results were used to estimate the peak load applied to the test frame and the corresponding displacement. This was especially important since the quasi-static cyclic tests were to be carried out in load-controlled mode.

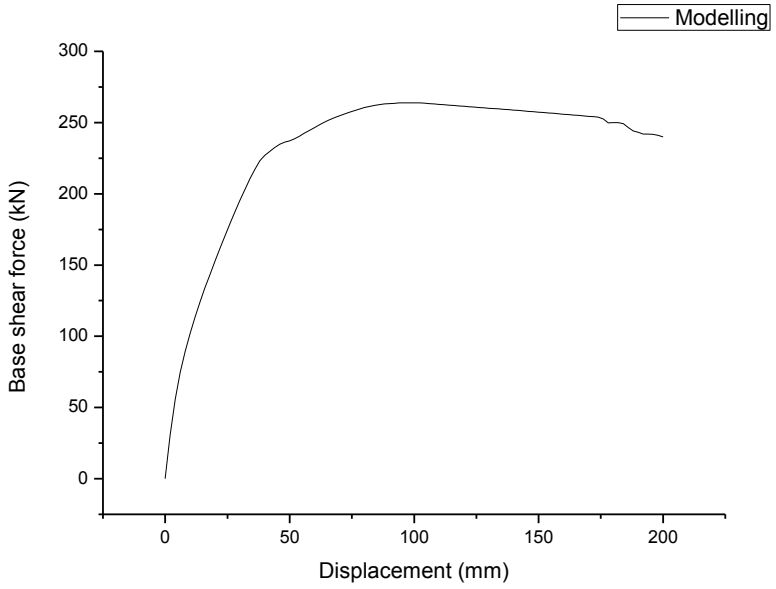

Figure 6.11: Base shear force – roof displacement curve

The base shear force – displacement curve of the frame, which has a maximum displacement of 200mm, is shown in Figure 6.11. The base shear force, equalling the lateral applied force, reaches the peak when the roof displacement is around 100mm. After the peak displacement is reached, the base shear decreases gradually, showing that the lateral strength of the frame has begun deteriorate.

In the first set of tests, the maximum displacement of the frame under cyclic loading is less than 100mm. To compare the modelling and test results, half of the curve in Figure 6.11 was cut out and compared with the base shear – roof displacement curve of the test, which is shown in Figure 6.12. The two curves match well before the displacement reaches 60mm, and then the base shear of the modelled curve has a milder increase than the base shear of the tested frame which is more than 300 kN.

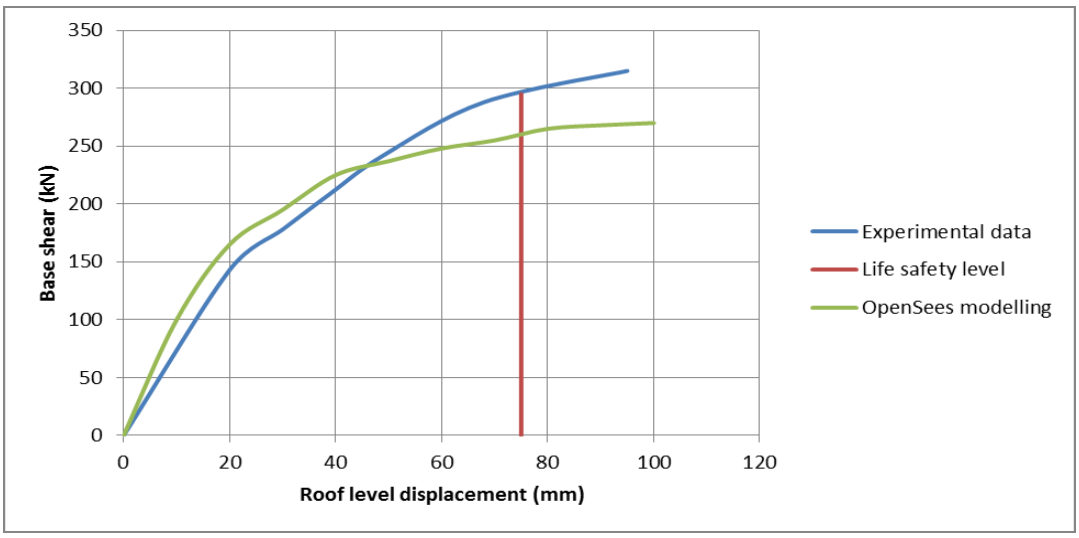

Figure 6.12: Base shear force – roof displacement curve

6.4.2 Tested Results of The Frame Under Cyclic Loading

The proposed cyclic displacements that the frame was to be subjected to (in order to create damage similar to a seismic event) is shown in Figure 6.13. The maximum targeted roof level lateral displacement for the test frame was 76 mm which corresponds to a roof drift ratio of 2 %, corresponding to life safety structural performance level according to FEMA 356:2000.

The measured displacement history of the frame did not match time-displacement curve in Figure 6.13 perfectly, due to the limitations of the jacks used and because the pressure in the jacks was controlled manually to mimic displacement control, although the jacking system was load controlled. The actual lateral load and displacement history from the test is shown in Figure 6.14, and the hysteretic response of the test frame is shown in Figure 6.15.

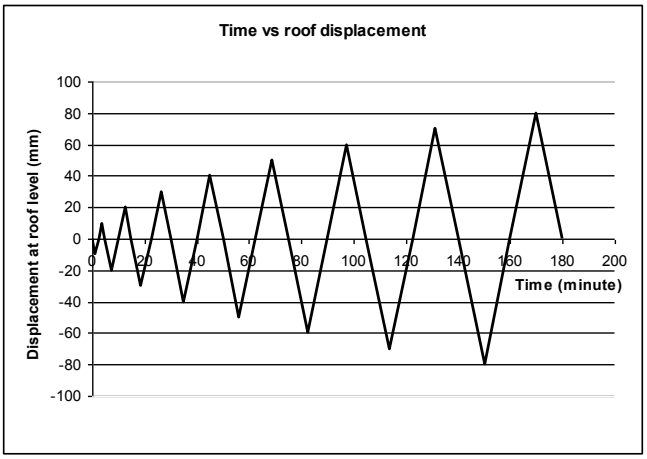

Figure 6.13: Proposed displacement-time history of the test frame [206]

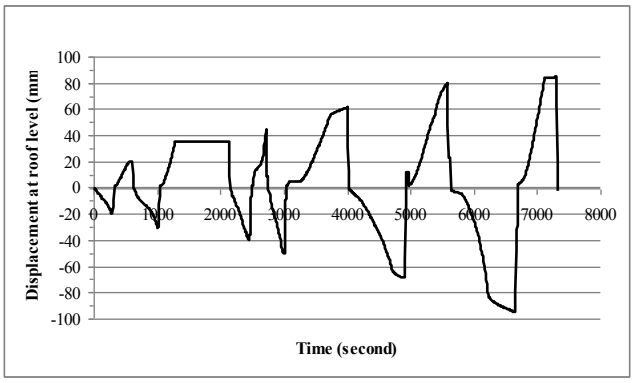

(a) Measured displacement-time history.

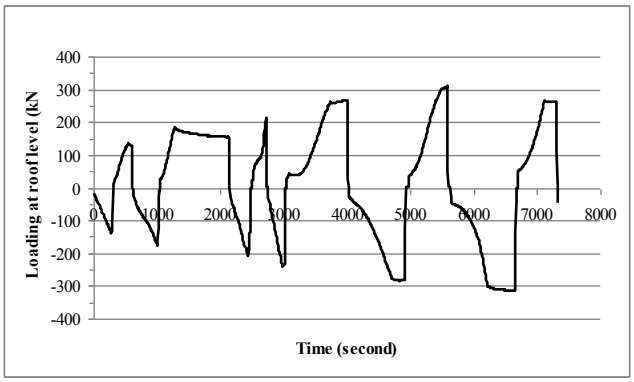

(b) Measured loading history.

Figure 6.14: Measured load and displacement behaviour of the test frame [206]

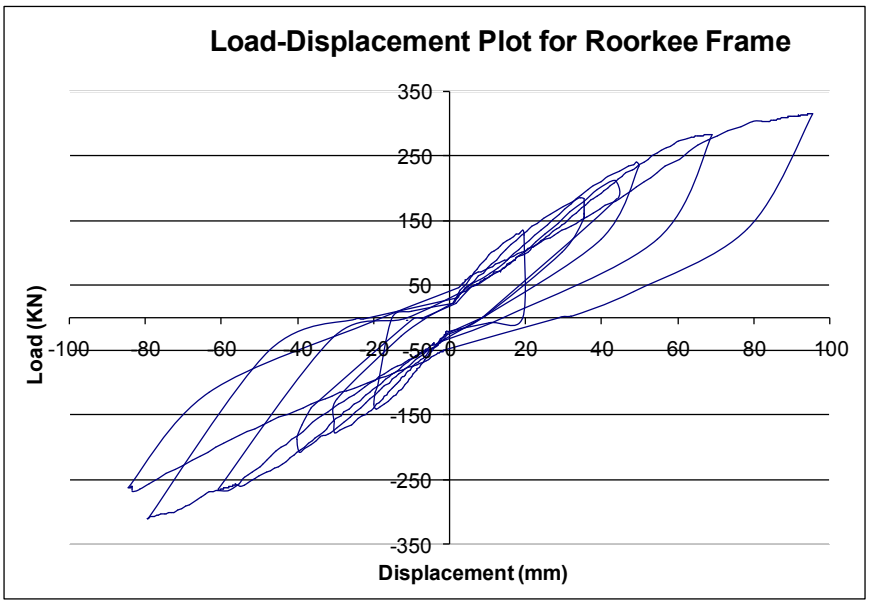

Figure 6.15: Hysteretic curve of the test frame [206]

6.4.3 Modelling Without Considering The "Pinching"Effect

A numerical analysis was carried out to predict the actual test behaviour of the frame using OpenSees. This analysis simulated the cyclic loading procedure, where the

displacements were to be applied in both directions in increasingly larger increments until the displacement corresponding to the peak load had been achieved. The simulation was then continued to the fire loading phase based on the temperatures obtained in the mock tests (see Figure 6.4).

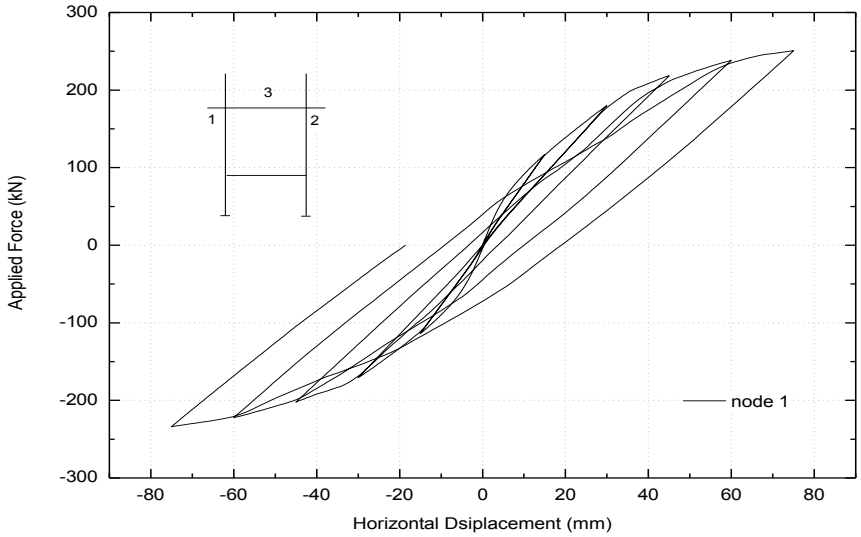

Figure 6.16: Horizontal displacement of node 1 under quasi-static cyclic loading

The fire loading was based on a considerable simplification of the temperature field shown in Figure 6.4. The fire was assumed to be represented by a constant temperature of 1000^{o}C at the boundaries of the structural members applied for 1 hour. A 1D heat transfer analysis was carried out to determine the temperature evolution in the structural members, which was then used to determine the mechanical response (after the damage inducing cycle).

Figure 6.16 shows the lateral (or horizontal) displacement of the frame through 5 cycles of loading, which produces a peak load of roughly 250 kN corresponding to a displacement of approximately 75mm, which agrees reasonably well with the SAP "pushover" analysis [206].

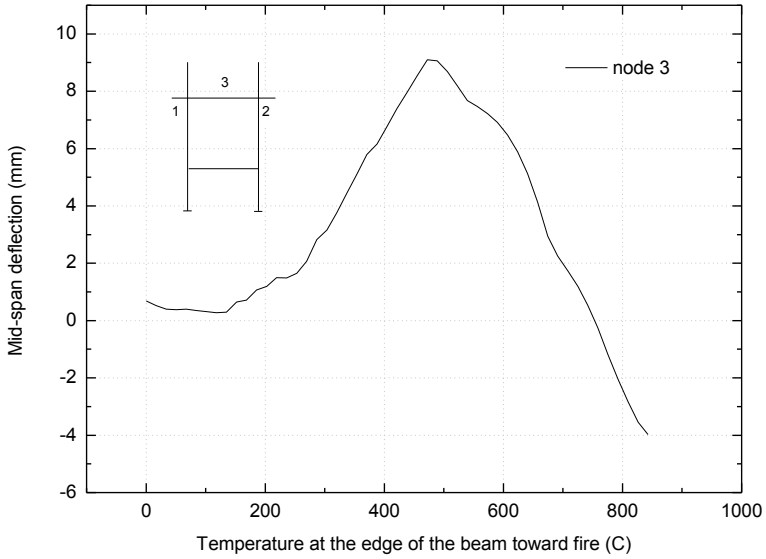

(a)

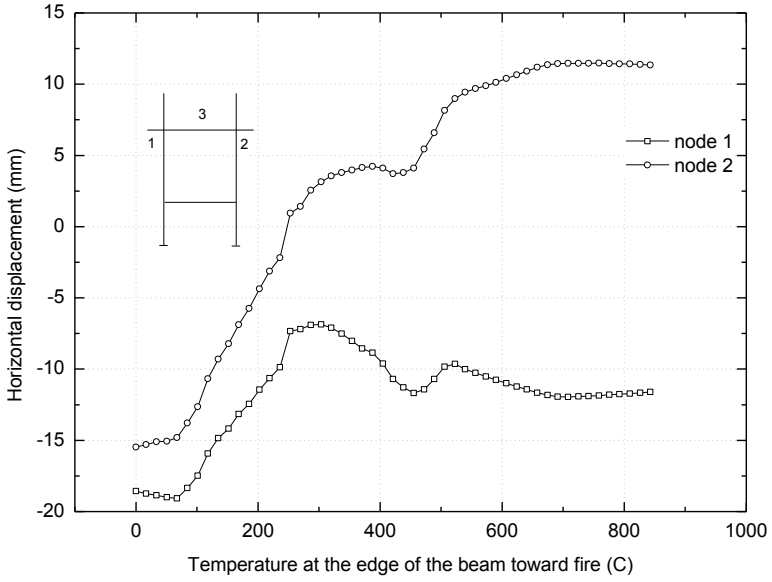

(b)

Figure 6.17: Displacements during the fire loading phase, (a) node 3 at midspan of top beam, and (b) at nodes 1 and 2

Figure 6.17(a) shows the vertical displacement of the midspan of the top beam during the fire loading phase and Figure 6.17(b) shows the horizontal displacement of the end nodes of the top beam during the fire phase (both continuing from the permanent residual displacements at the end of the cyclic displacement). An interesting and counterintuitive feature of behaviour from this analysis is that during the early phase of

the fire, the frame as whole moves towards becoming more "upright". The permanent lateral "drift" at the end of the cyclic loading of about 18mm is initially reduced to about 7mm when the exposed surface of the beam reaches approximately 300^{o}C, which suggests a "stiffening" of the frame. After this, however the drift begins to increase again but plateaus out by the end of the heating.

6.4.4 Modelling With The "Pinching" Effect Included

It is obvious that the hysteretic curves of the prediction model and the test frame do not match well. The "pinching" effect clearly present in the test can not be observed in the model result. The pinching phenomenons have been always observed in experiments on reinforced concrete structures under cyclic lateral loading. Pinching behaviour occurs because of the loss of stiffness due to opening of cracks in the tension zones of the concrete member and loss of bond between concrete and rebars resulting in a flatter response upon unloading and reloading in the opposite direction until the structure returns to the position where cracks close and the zones previously in tension begin to experience increasing compression upon further reloading, which results in increased stiffness. This alternating tension and compression behaviour produces the classic "pinching" effect.

To model this effect, a 'pinching' material is used in the sections of the elements around the joints of beams and columns to simulate the cracking and bond slip. Pinching material is a uniaxial material in OpenSees that reproduces a 'pinched' load-deformation response and exhibits degradation under cyclic loading. Cyclic degradation of strength and stiffness occurs in three ways: unloading stiffness degradation, reloading stiffness degradation, strength degradation [207, 208]. The degradation of the stiffness and strength of the pinching material under cyclic loading is shown in Figure 5.18.

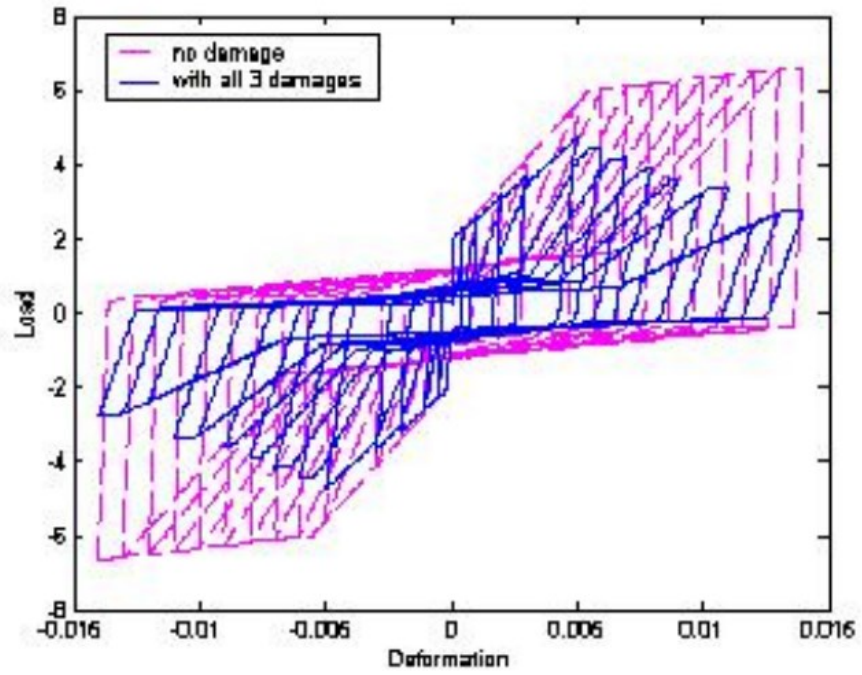

Figure 6.18: The degradation of the stiffness and strength of the pinching material [208]

The model mentioned in the previous section was rerun with an OpenSees "pinching material" used for all elements adjacent to the joints. This produced a more realistic comparison with the test as shown in Figure 6.19 below. The "pinching" can be observed from the hysteretic curve, and the final horizontal displacement of the control point is 20.8mm when the applied lateral force (base shear force) is zero at the end of the pushing and pulling. The residual displacement from the model is found to be close to that obtained in the test.

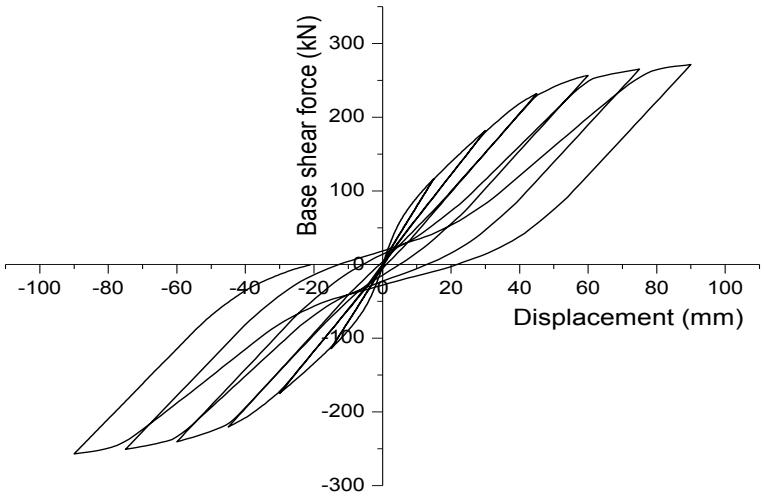

Figure 6.19: Load-displacement curve with pinching material

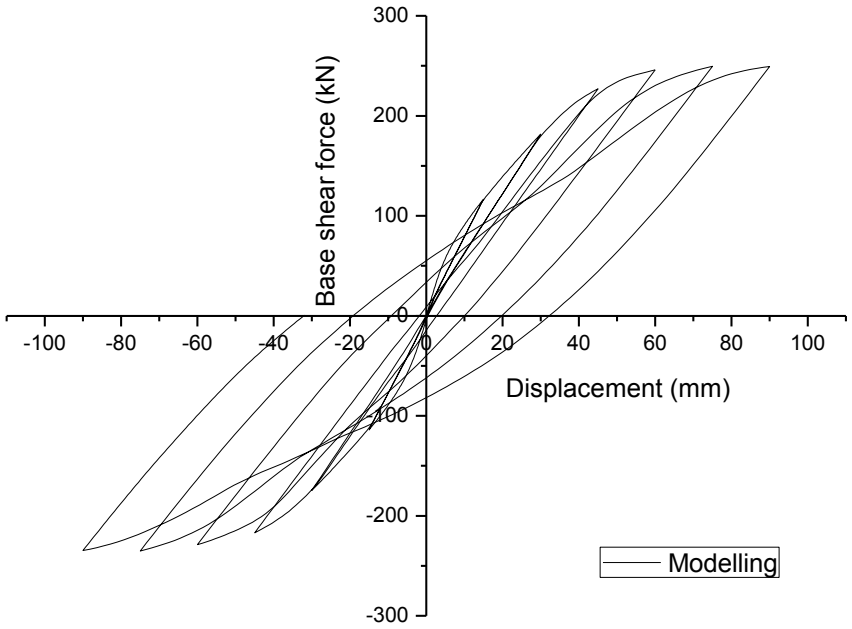

Figure 6.20: Load-displacement curve without pinching material

Figure 6.20 shows the modelling results of the displacement-force curve of the frame without using pinching material in the elements near the joints. Compared with Figure 6.16 which produced a 20mm residual displacement, Figure 6.20 was subjected more applied cyclic loading. The curves of Figure 6.19 and Figure 6.20 have same displacement history, but the final displacement in the curve of Figure 6.20 is greater than that in Figure 6.19. The area of the envelope of the hysteretic curve in Figure 6.20 is 25942.6 kNmm, compared with 28388 kNmm in Figure 6.19, which indicates that the former consumed more energy than the latter.

6.4.5 Modelling The Frame Using The Cyclic Displacement Obtained From The Test

The actual cyclic displacement history was different from that used in the predictive modelling because of the limitations of the loading jacks as discussed earlier (see Figure 6.14).

The model developed was rerun with the displacements obtained from the test. The results are shown in Figure 6.21which produces a better comparison with the test compared to the model with the idealised cyclic displacements (Figure 6.20), because the pinching phenomenon can be observed, and the hysteretic curve is much closer to the tested curve.

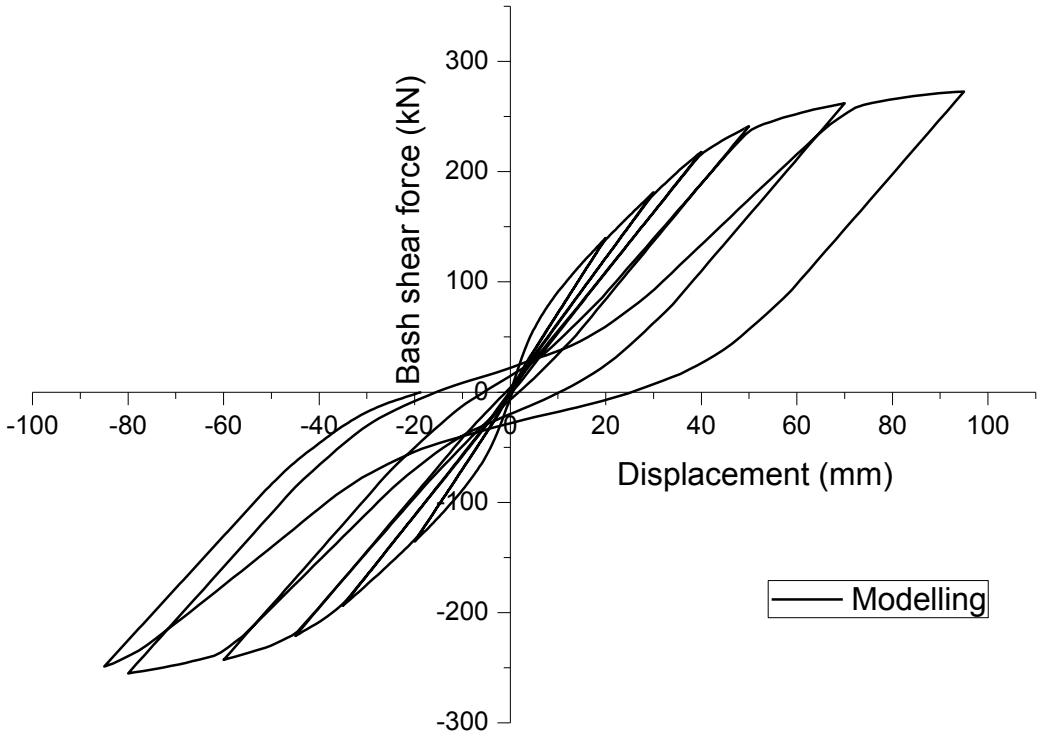

Figure 6.21: Modelling hysteretic curve of the frame following measured displacements

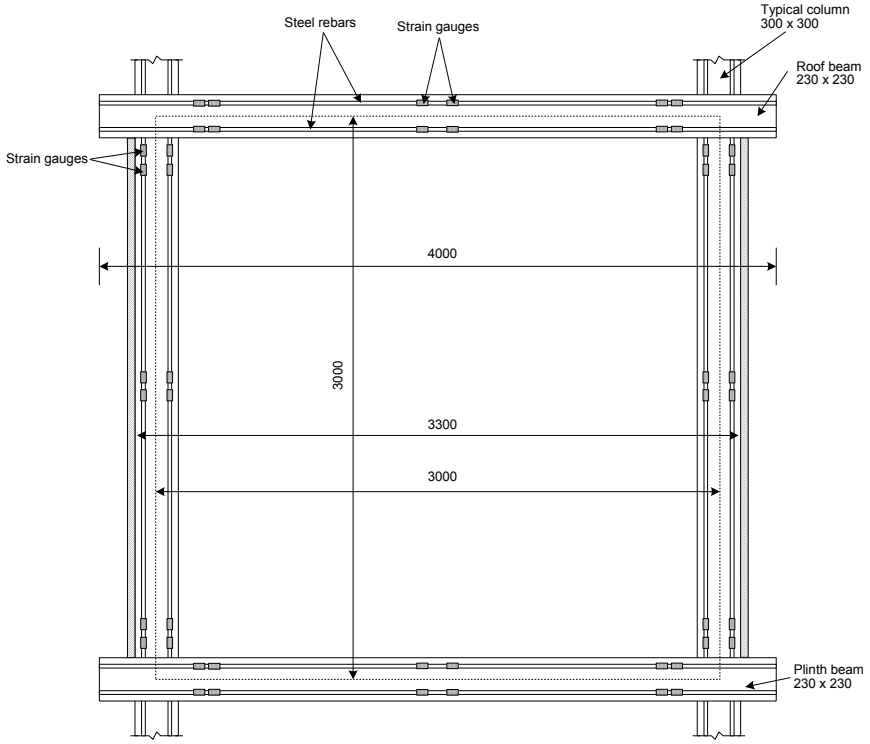

Figure 6.22: Location of the electrical resistance strain gauges

A comparison of the tested and modelled strains is now presented. Figure 6.22 shows the location of strain gauges embedded inside the concrete. Figure 6.23 depicts the nomenclature used for identifying the locations in the RC frame.

Figure 6.23: Nomenclature of the frame

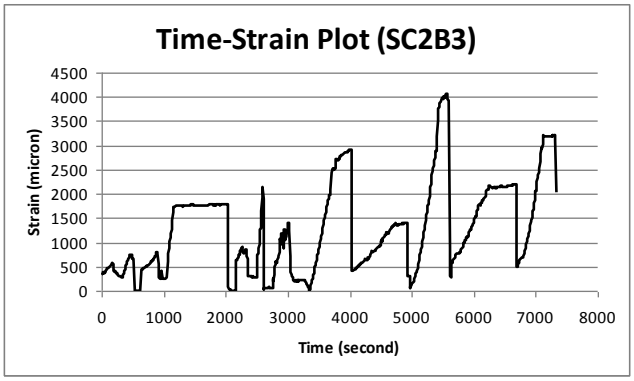

(a) Corner rebar located near the bottom face outside in Column C2

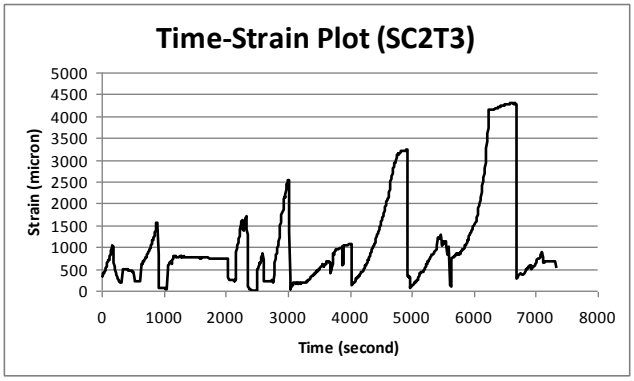

(b) Corner rebar located near the top face outside in Column C2

Figure 6.24: Measured strain in Column C2

The measured data for the strains at the bottom and top of column C2 is shown in Figure 6.24. It should be pointed out there are only positive values measured by strain gauges, that is to say the measured compressive and tensile strain are all in the same

side of the horizontal axis. Therefore the measured data needs processing to separate the compressive and tensile strains before it can be compared with the modelling results.

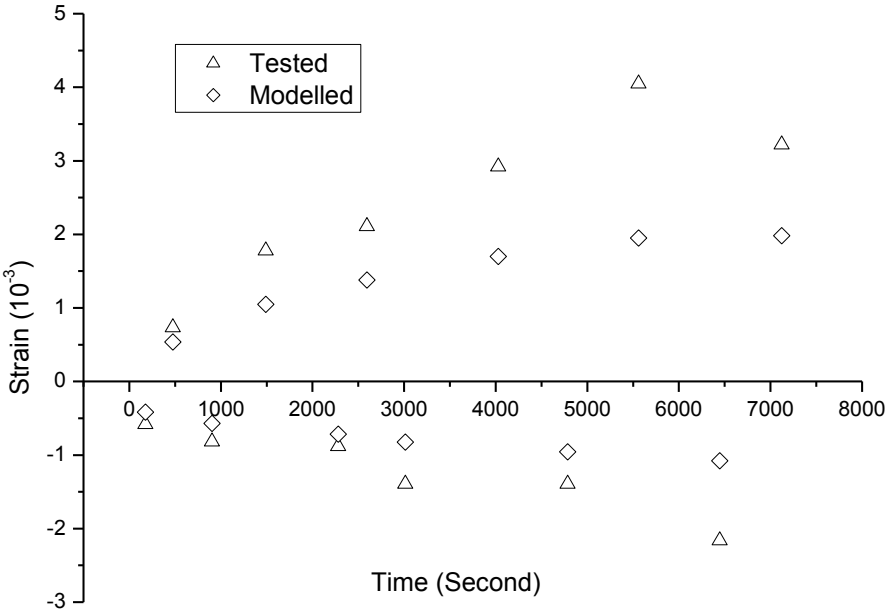

Figure 6.25: The tested and modelled peak strains

The test and model results of peak strains is shown in Figure 6.25. The peak strains increase smoothly following the loading cycles for both the test and model results. The strains are not symmetric for a single cycle (as the displacement cycles are not symmetric) and the compressive strain is less than the tensile strain.

6.4.6 Modelling of The Fire Loading After The Cyclic Loading

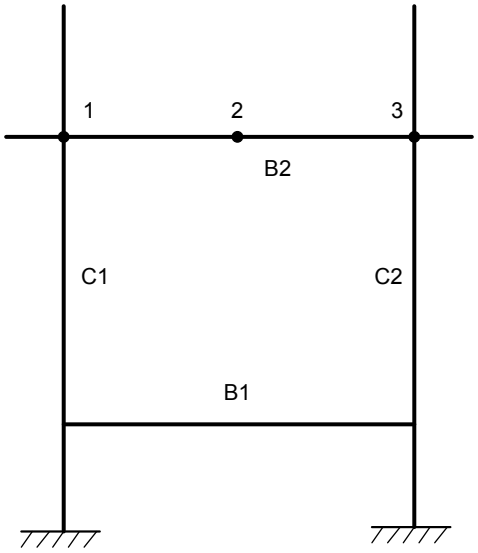

Figure 6.26: Monitored nodes and members on the frame

The frame was subjected to heating from a one hour fire after applying the gravity and cyclic loading steps. To describe the effects of all these applied loads, the joints and the

middle point of the roof beam are monitored at locations 1, 2, and 3 as shown in Figure 6.26. Table 6.4 shows the displacements of these nodes, from which it can be observed that the displacements from the gravity load were very small, as expected. The deflection of the roof beam is only 0.3 mm, however this is an artificial result because the two-dimensional nature of the model. This deflection did not increase too much after the cyclic loading, although the frame had a lateral displacement of nearly 20mm. The frame deformed shape after the cyclic loading is shown in Figure 6.27 magnified by a factor of 20.

Table 6.4: Displacements of Node 1, 2, and 3

Load type	Node	Displacement (m)	
		Horizontal	Vertical
Gravity	1	4.46409e-007	-0.000153673
	2	-4.46409e-007	-0.000153673
	3	0	-0.000338581
Cyclic	1	-0.0186142	8.49923e-005
	2	-0.0165225	9.4229e-005
	3	-0.0174277	-0.000520878

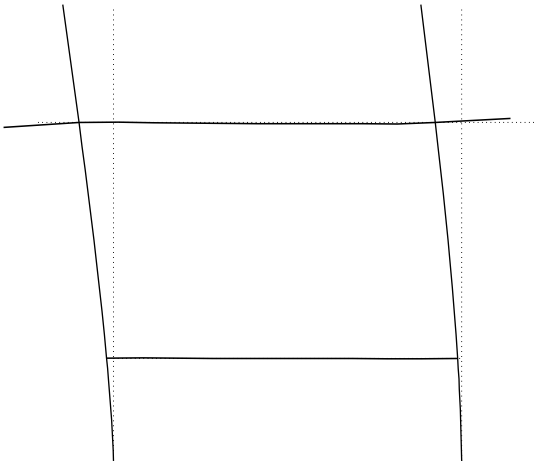

Figure 6.27: Frame displaced shapes at the end of the cyclic displacements

Spalling occured approximately 15 minutes after the start of the firewhich caused small reductions in the section dimensions of the structural members, however, these effects are not considered in this work.

The fire was set from inside of the frame, therefore only C1, C2, B1 and B2 (Figure 6.26) were considered to be heated, and the rest of the members of the frame were assumed to be at ambient temperature during the test (see Figure 6.28(a), heated members are in red). The final deformed shape of the frame, after being subjected to cyclic loading and then the one hour fire, is shown in Figure 6.28(b) magnified 20 times.

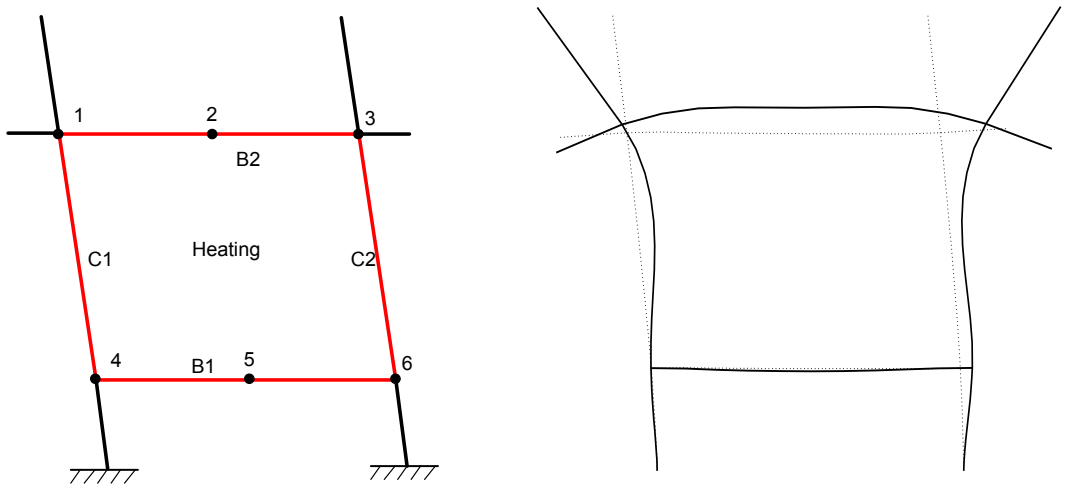

Figure 6.28: The shape of the frame after cyclic loading (dotted line) and heating (solid line)

In Figure 6.28(b) thermal bowing can be observed for columns C1 and C2, which causes the rotation of joint nodes 1, 3, 4 and 6. The deflection of beams B1 and B2 is caused by both thermal bowing and the joint rotation. Thermal expansion of beam B1 was partly restrained by the columns and the fixed restraints, however, the beam B2 was relatively less restrained and shows greater thermal expansion.

The deflection of the beams keeps changing with the increase of the temperature while the frame is heating. Figure 6.29 shows curves of the deflection of various nodes in the roof-beam against time of heating, where I is the distance from the current node to the edge of the beam, and L is the whole beam length. It can be seen from this figure that the deflection of the roof beam was downward initially reaching the lowest point at around 600 seconds after that the deflection was upward, until the end of heating. All the curves intersected at around 1400 seconds, which means that the roof-beam became nearly straight at this point.

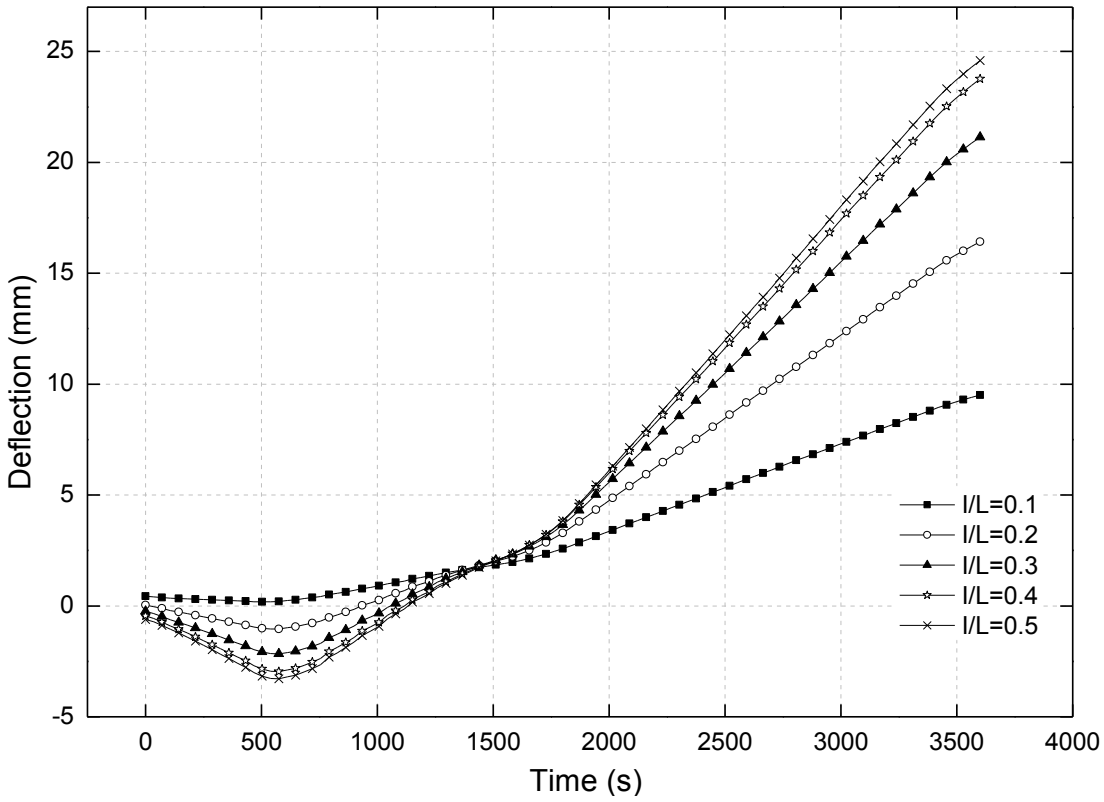

Figure 6.29: Deflection of various nodes in the roof-beam (B2) in fire

Initial downward deflection of the roof beam is caused by thermal bowing while the upward deflection is induced by the rotation of the columns (C1 and C2) which is also caused by thermal bowing.

It should be noted that the modelling results of the deflection of the roof-beam does not really represent the test results, due the use of a 2D model to simulate a 3D frame. However, the modelling does represent the behaviour of a damaged reinforced concrete frame in fire and is worth further exploration here.

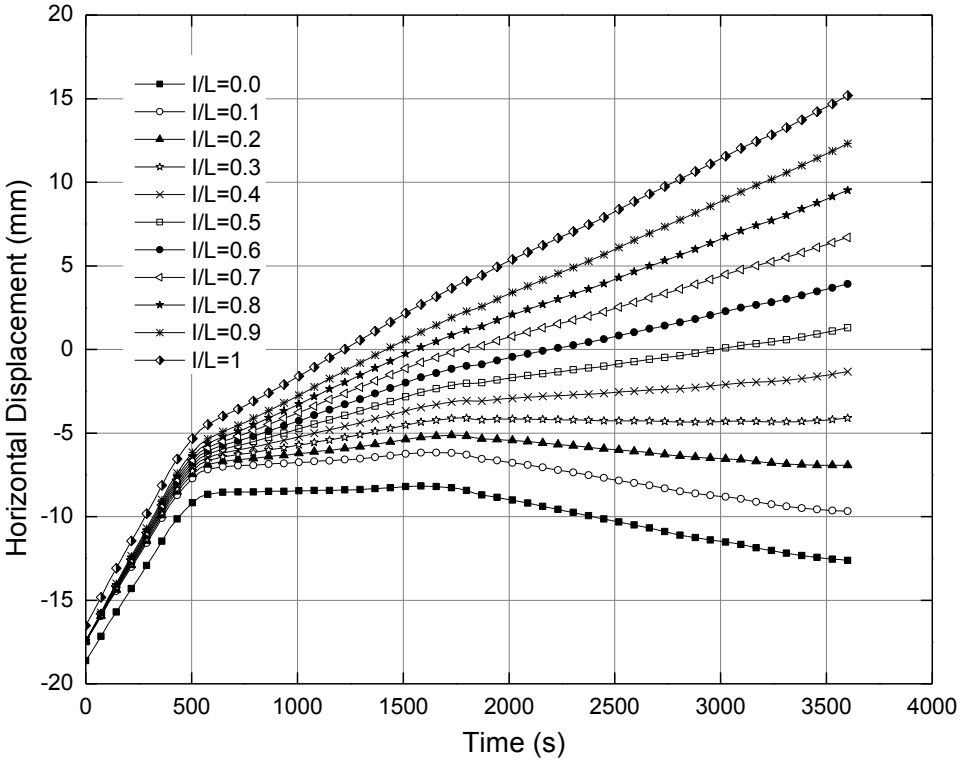

Figure 6.30: Horizontal Displacement of various nodes in the roof-beam (B2) in fire

Figure 6.30 shows the horizontal displacement of the nodes in beam B2 over an hour of heating. The frame moved back towards its original position in the first 500 seconds of heating, the possible explanation of this is that the heating induced thermal expansions closed the cracks and made the frame stiffer during this period. After 500 seconds, the central node of beam B2 experienced much smaller horizontal displacement until the end of heating. The main feature of behaviour after 500 seconds is the gradual increase in the relative distance between all nodes, suggested that the beam B2 undergoes significant thermal expansion.

Figure 6.31 shows how the distance between the two end nodes of the roof-beam changed during the frame over the one hour of heating.

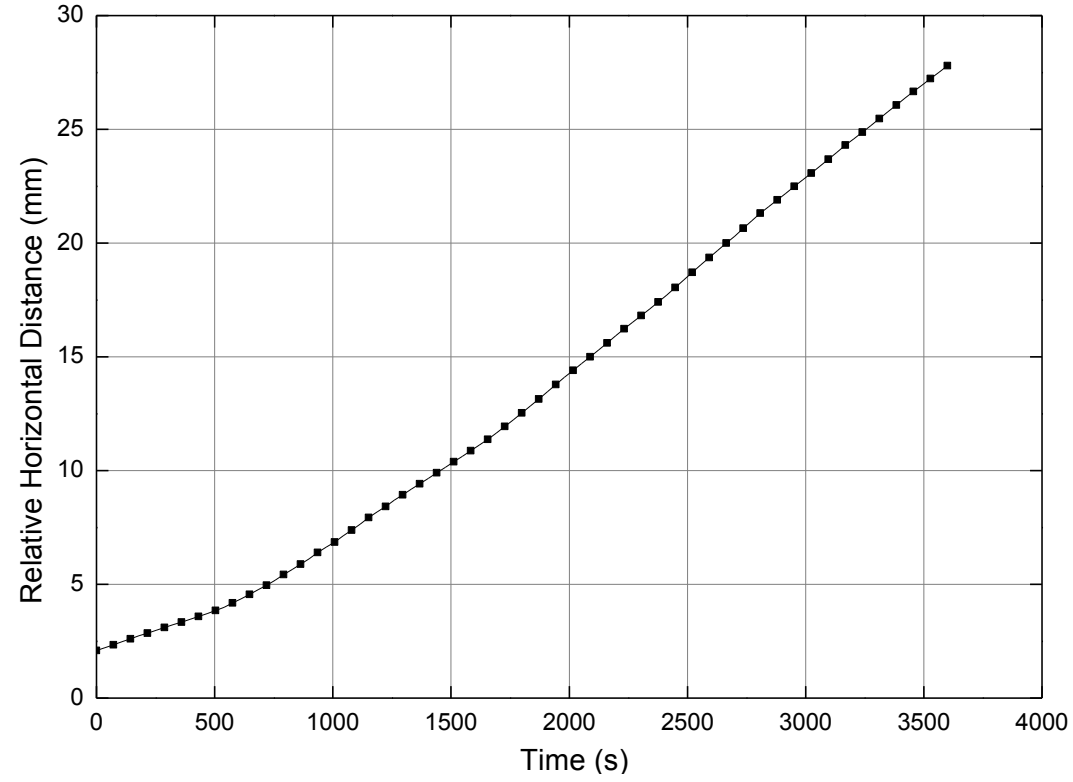

Figure 6.31: Relative horizontal displacements between the two joint nodes of the roof-beam while heating

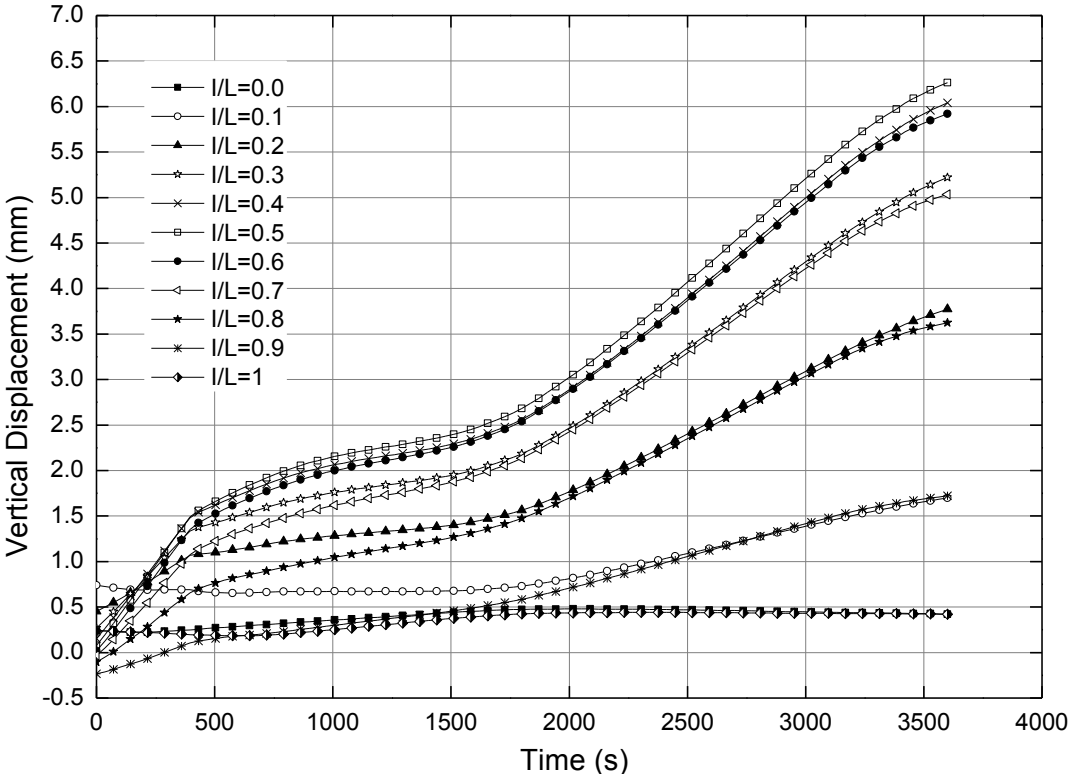

Figure 6.32: Vertical displacement of various nodes in the lower beam (B1) in fire

Figure 6.32 shows the vertical displacement of the nodes of the lower beam over the one hour heating period, where l/L represents how far the node is from the left end of the beam. The two joint nodes (l/L=0, l/L=1) had very little movement in the vertical

direction, which can be seen from the figure. These two nodes were also the top nodes of the lowest support columns, and they were not heated at all by the fire. The two nodes with l/L=0.1 and 0.9, which were closest to the end nodes, had the largest vertical displacement before the frame was heated, however their displacement became the smallest except for the end nodes at the end of heating. The vertical displacement of the mid point (l/L=0.5) of the beam increased sharply up to 500 seconds, and then increased gradually up to 1500 seconds, followed by another sharp increase.

The deflection of the lower beam did not show the first downward then upward behaviour seen in the roof beam, instead it kept deflecting upward through the whole heating period. In this case both the joint rotation caused by the column bowing and the thermal bowing of the lower beam itself caused upward deflection of beam B1. The ***P-δ*** effect caused by the restraint to thermal expansion also added to the upward deflection.

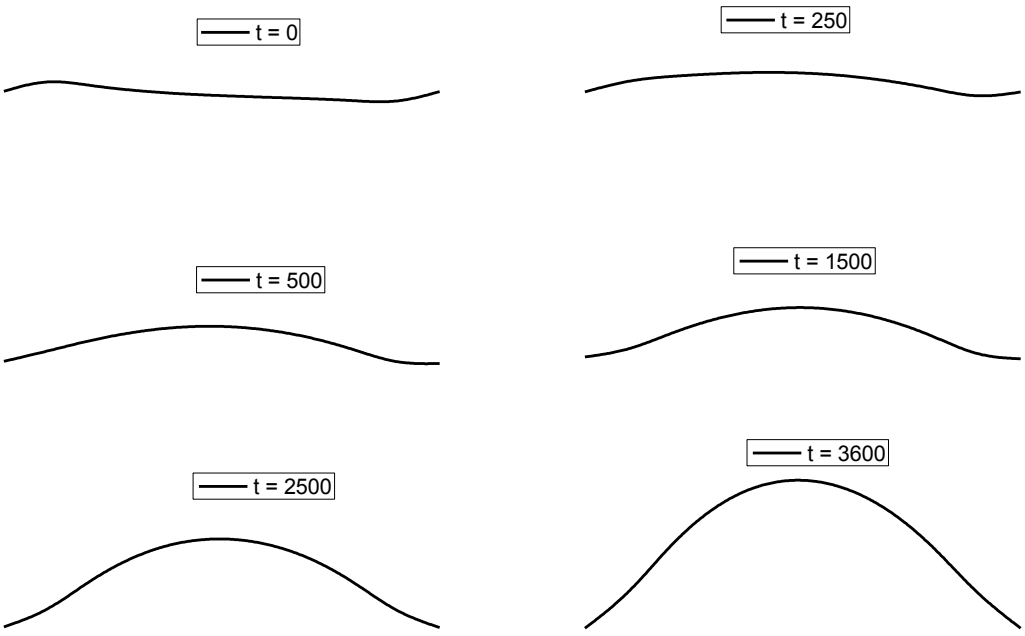

Figure 6.33: Shapes of the lower beam at different time of heating

The exaggerated deflected shapes of the lower beam (B1) at different times of heating are shown in Figure 6.33. The beam had an "s" shape before it was heated, because the frame had been subjected to lateral cyclic load and the lower beam experience two end-moments in the same direction. However at 250 seconds, the deflection of all the nodes of the beam was upward. These deflections continued to grow thereafter.

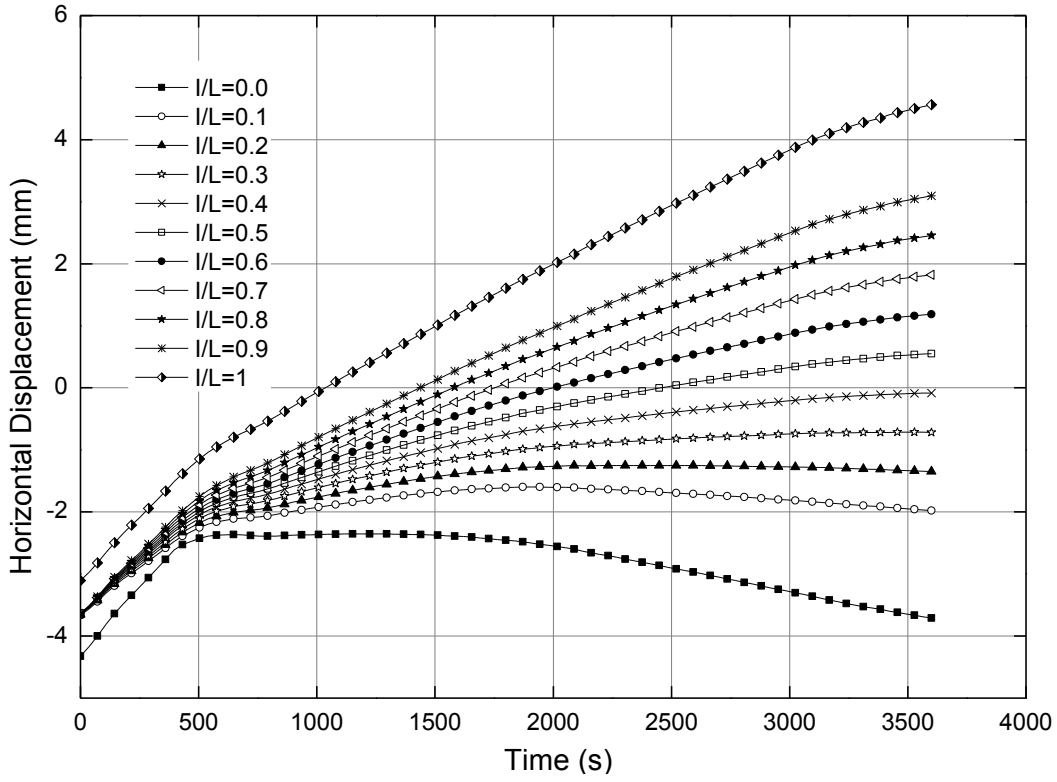

Figure 6.34: Horizontal Displacement of various nodes in the lower beam (B1) in fire

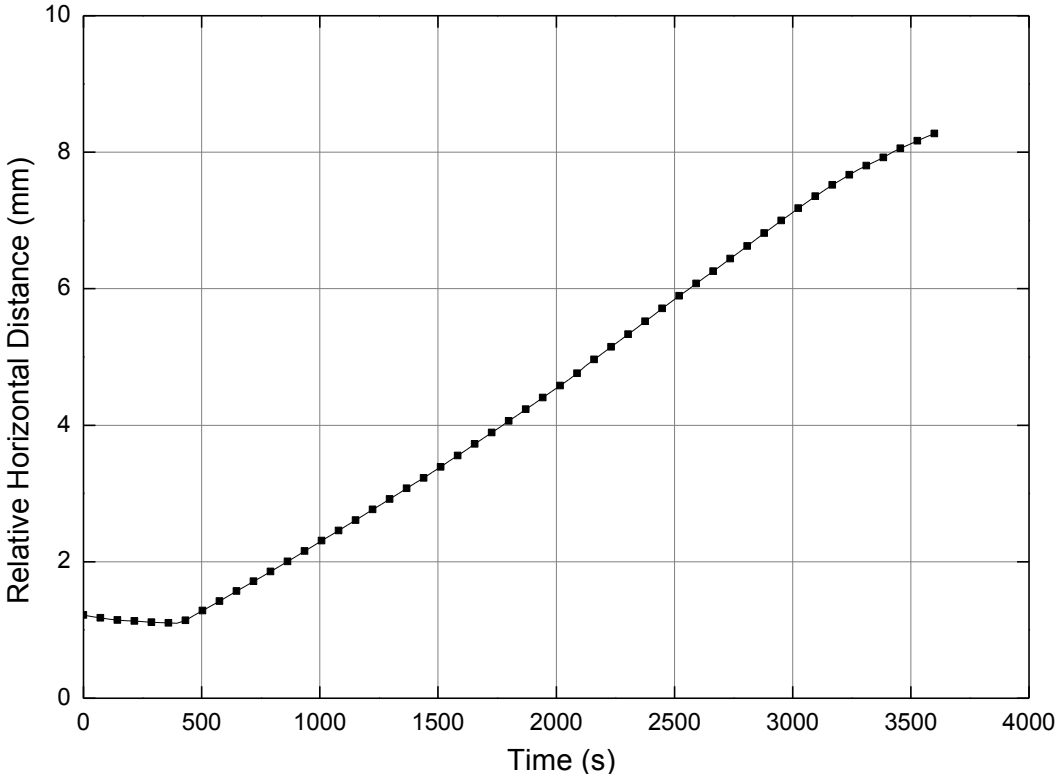

Figure 6.35: Relative horizontal displacements between the two joint nodes of the lower beam while heating

Figure 6.34 shows the horizontal displacement of the nodes on B1 in an hour of heating. Figure 6.34 has a similar pattern to Figure 6.30 however the magnitude of relative displacements between the beam nodes was much less than the roof beam.

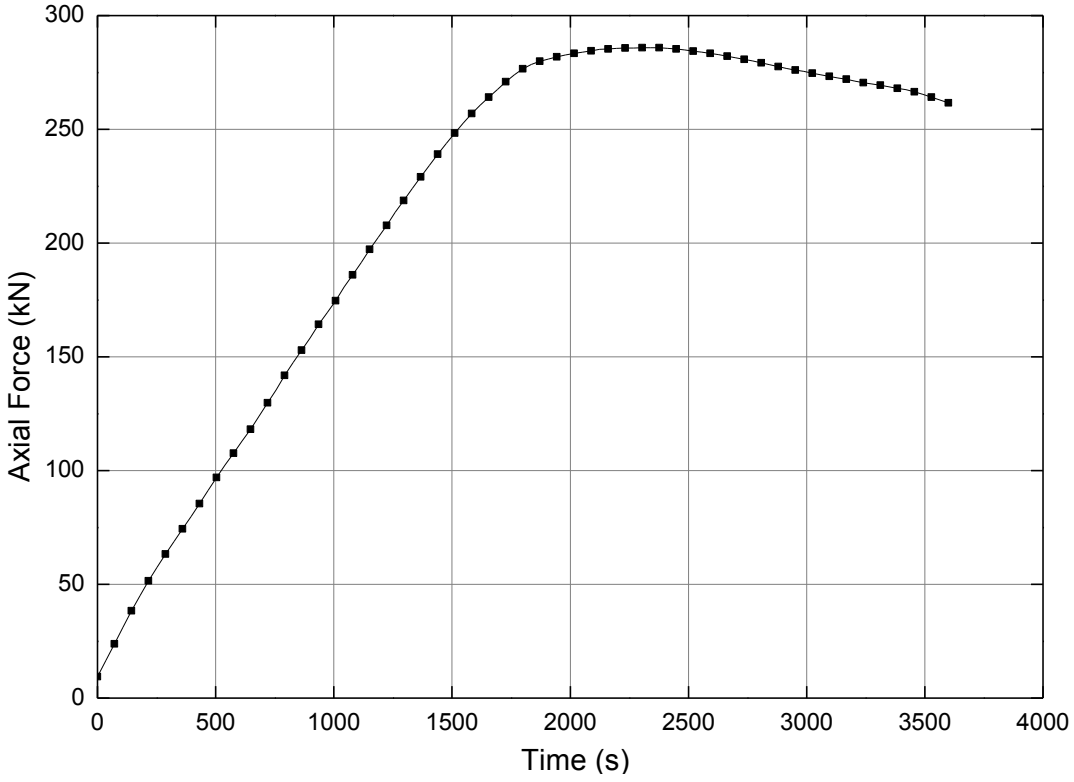

Figure 6.36: Axial force in the lower beam while heating

The axial force in the lower beam increased with time of heating, as shown in Figure 6.36. The axial force was only 9.4kN (compression) at the end of the cyclic loading. It increased rapidly when the frame was heated because the thermal expansion of the lower beam was significantly more restrained that the roof beam. The force reached its peak, 285.9kN, after 2000 seconds and then it decreased gradually because of the increased deflection and upward thermal bowing.

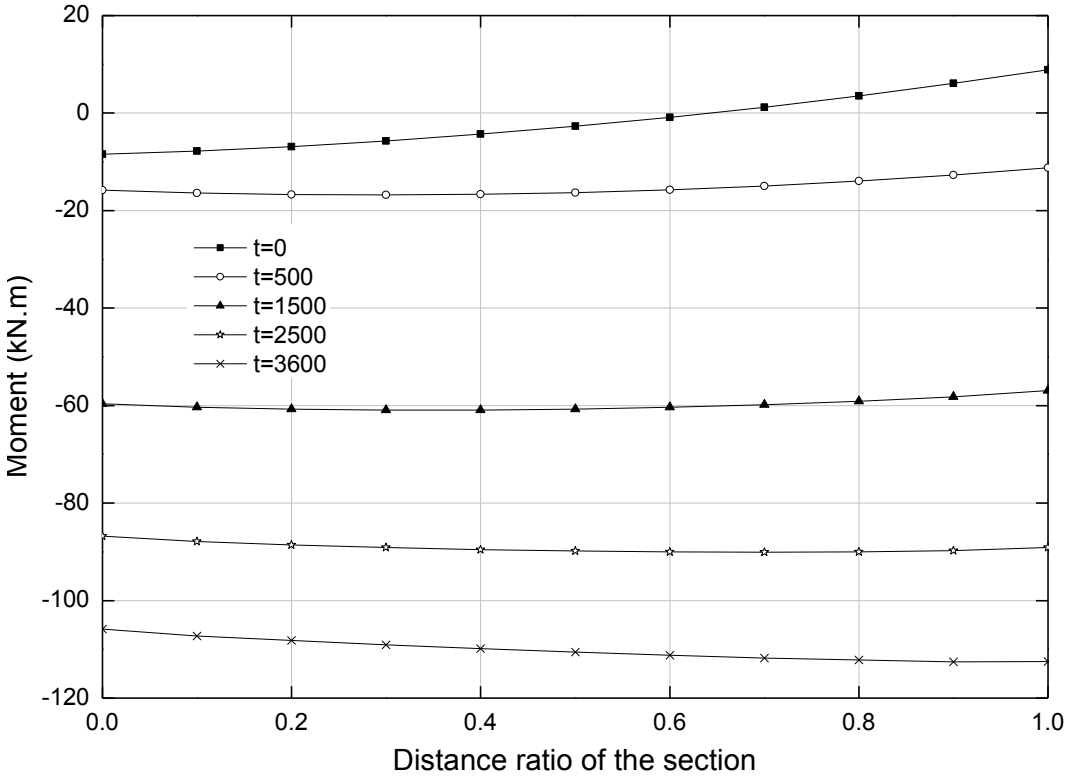

Figure 6.37: Section moment of lower beam at various time of heating

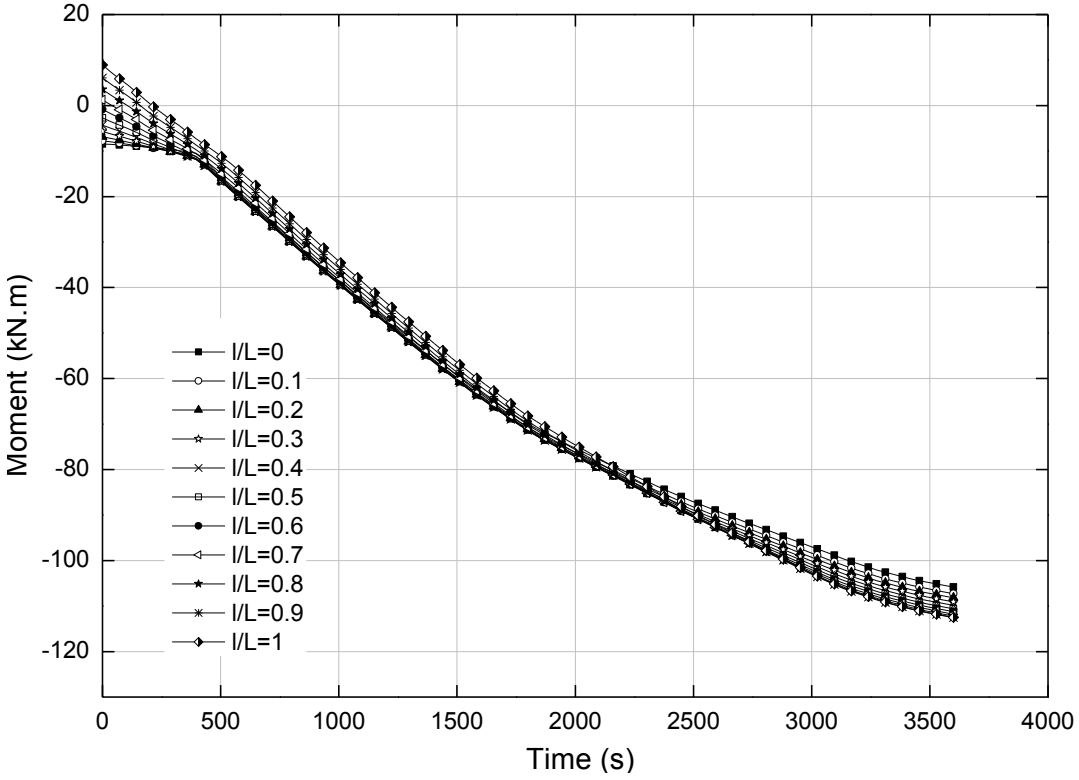

Figure 6.38: Moment at various section along the lower beam during the heating

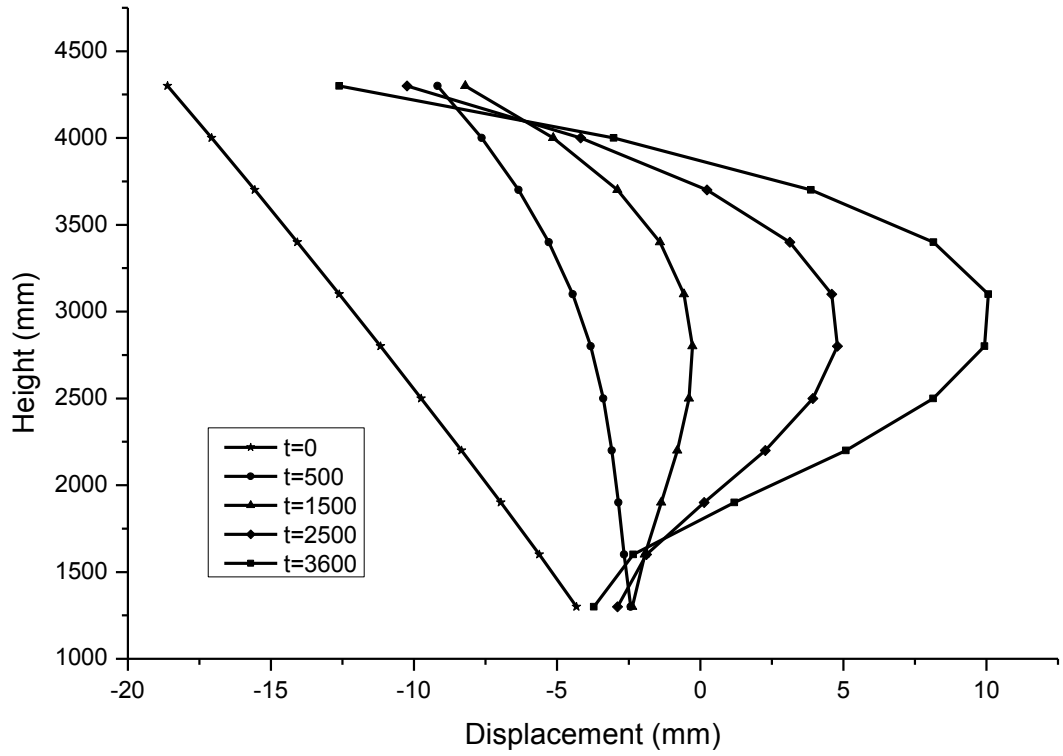

Figure 6.39: Deformed shapes of the column C1 during heating

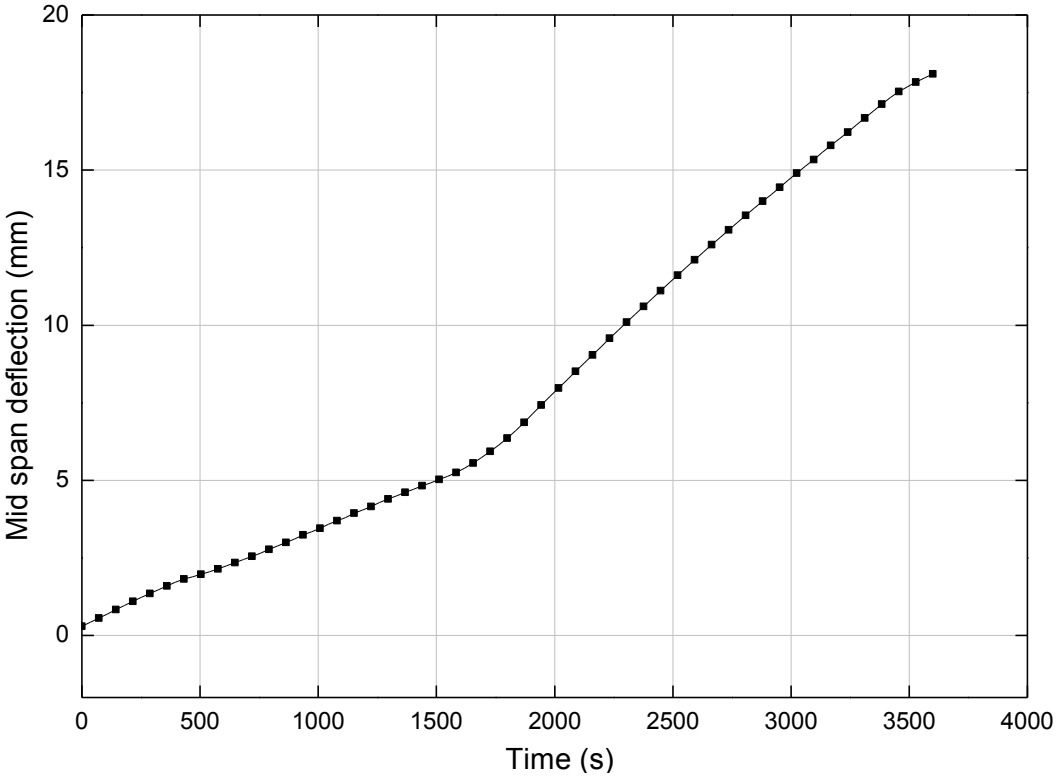

Figure 6.40: Mid span deflection of C1 during heating

Figure 6.37 shows the section moments along the lower beam (B1) when the frame was heated at 0, 500, 1500, 2500 and 3600 seconds. The moments are consistent with the

deflected shape before the start of heating (negative moment on the left portion and positive on the right portion). The section moments beam kept increasing during the heating (see Figure 6.38), and there was very little difference in their relative magnitude, as these moments were caused by the restraint to rotation at the ends inducing an increasing negative moment in the beam which was approximately constant over the length of the beam (the beam was not subjected to much shear as there was no load on it).

Figure 6.39 shows how the shape of the column C1 changed during the heating phase. It should be noted that the shape had been exaggerated. The column was almost straight after the cyclic loading phase. The top of the column C1 moved right and then moved back during the heating, but the central deflection (out-of-straightness) of the column kept increasing over the whole heating phase. Figure 6.40 shows the maximum deflection of column C1 over the full heating period, this deflection is relative to the column end points not including the "rigid body displacement" of the column.

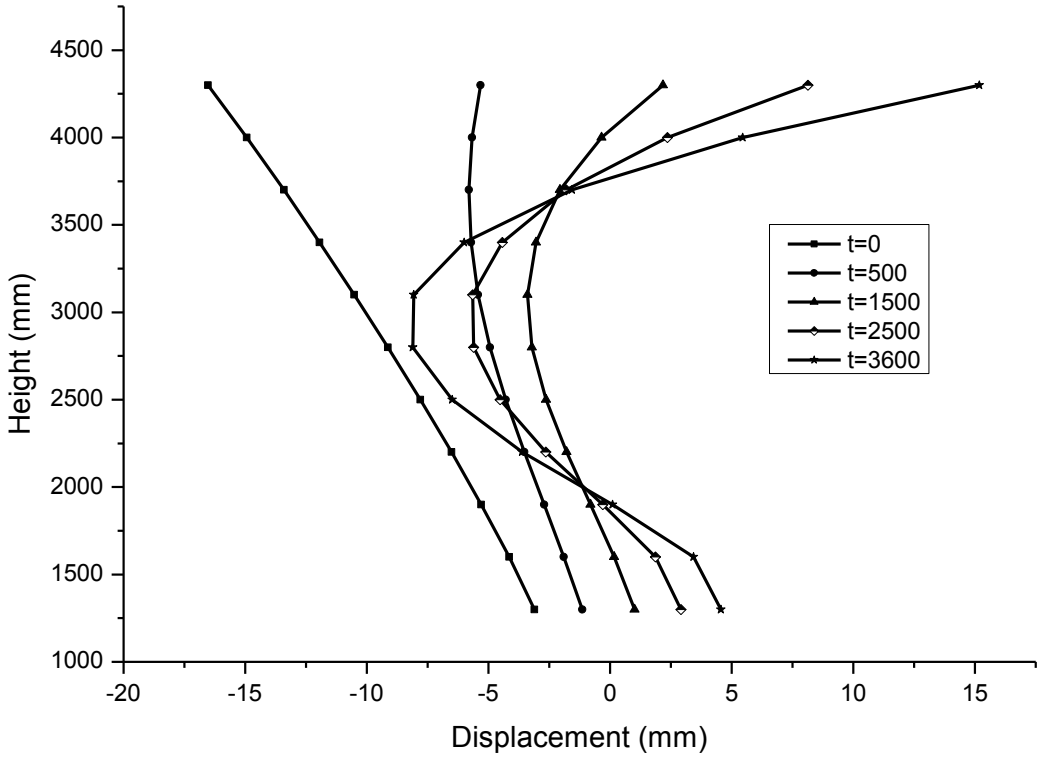

Figure 6.41: Deformed shapes of the column C2 during heating

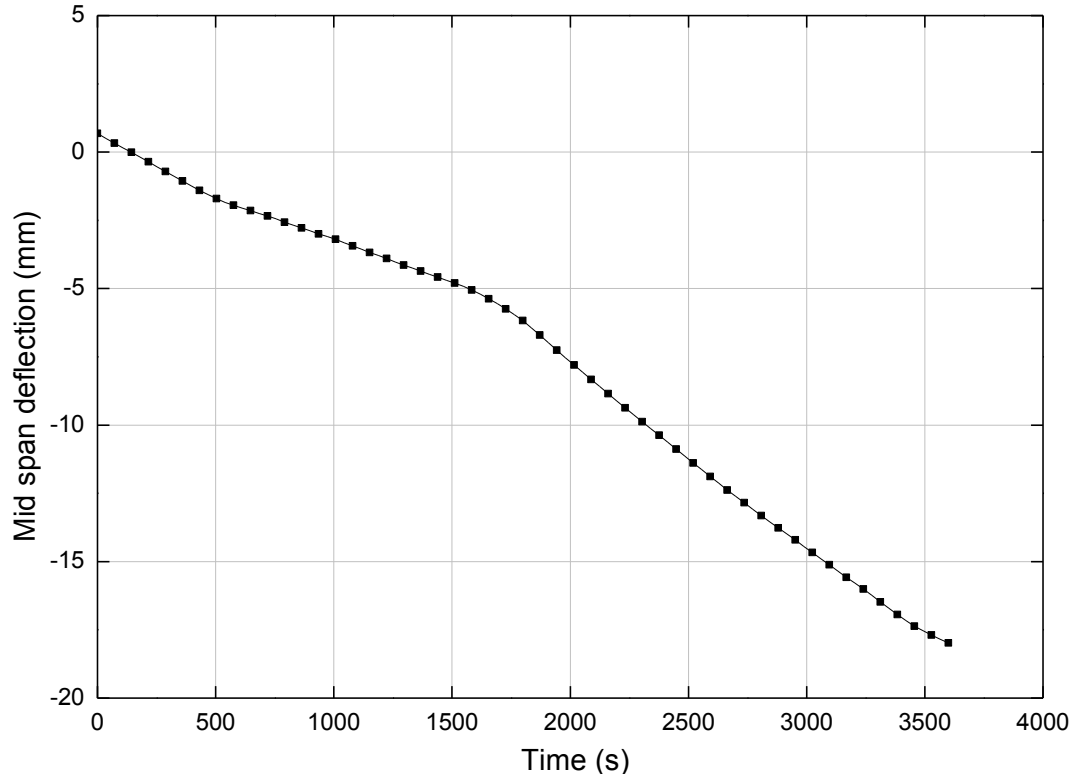

Figure 6.42: Mid span deflection of C2 during heating

Figures 6.41 and 6.42 show exaggerated deformed shape and mid span deflection of the column of C2 during the heating. These two figures are similar to the previous figures for column C1 but in the opposite direction.

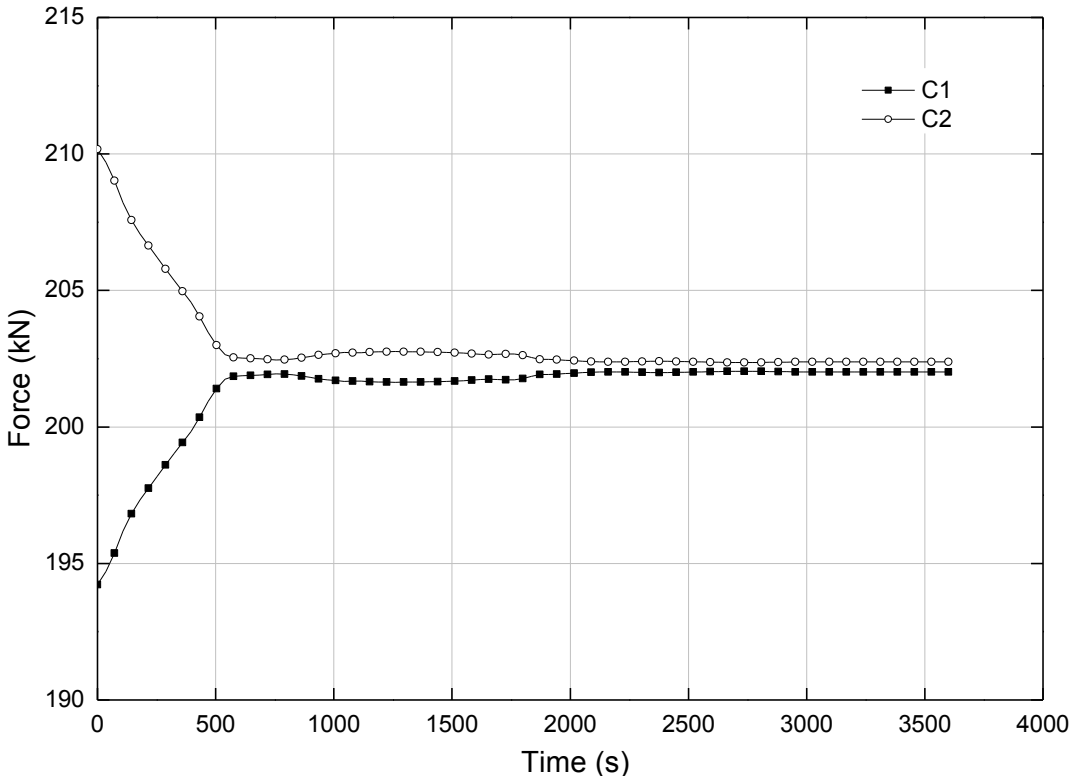

Figure 6.43: Axial force in C1 and C2 during the heating

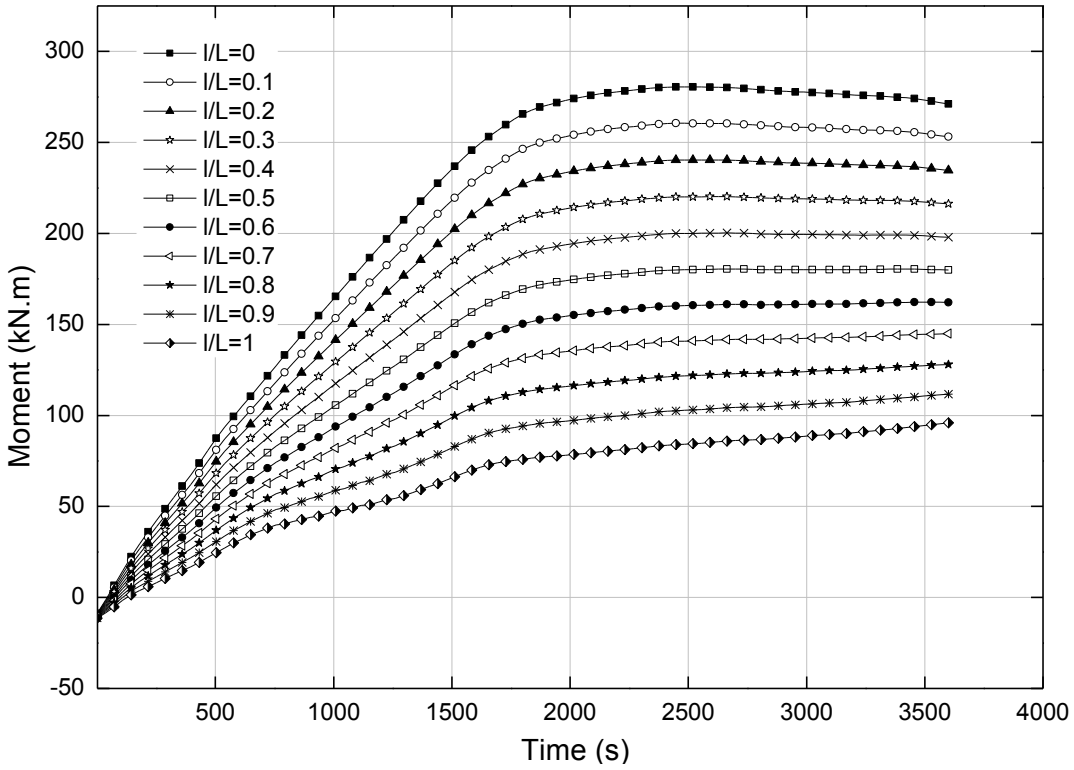

Figure 6.44: Moments at various sections along the column C1 during heating

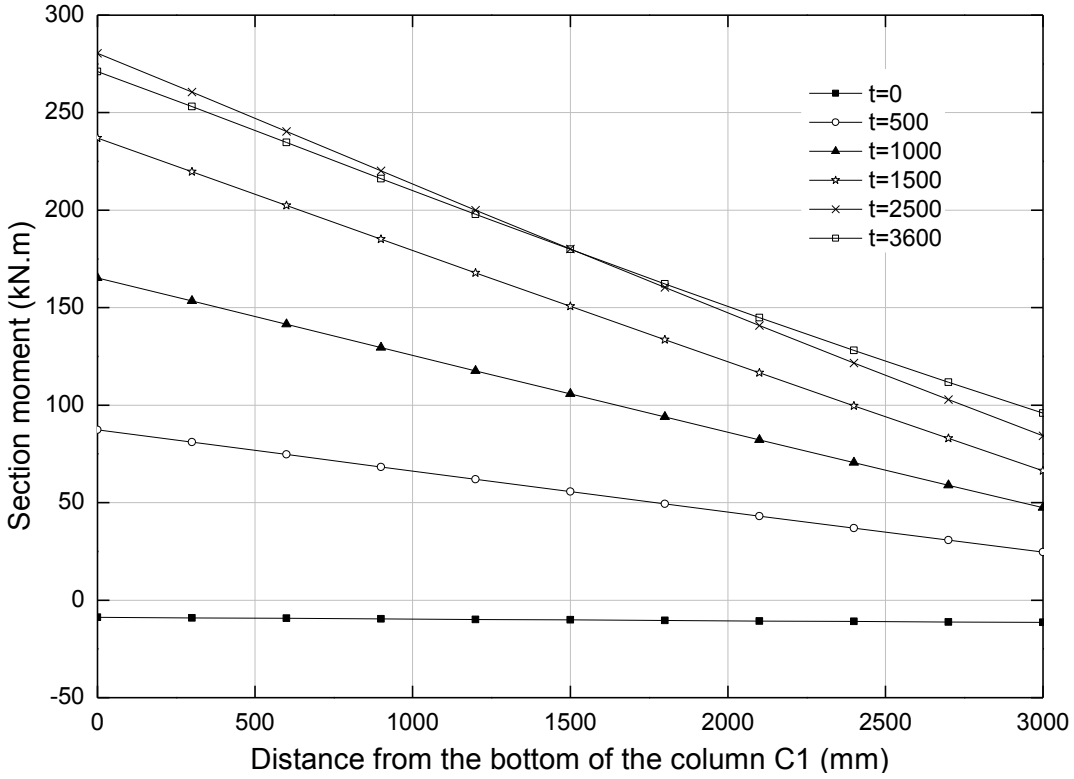

Figure 6.45: Section moments in the column C1 during heating

The axial force in the midspan section of column C1 and C2 while the frame was heated is shown in Figure 6.43. During the minor horizontal movement of the frame while it was heated, the gravity centre of the frame moved slightly, which caused a redistribution of the axial force between the two columns C1 and C2. The force increase of one column was equal to the force decrease of the other one, therefore the two axial force – time figures were symmetric.

Compared with axial force, the moments along the column C1 varied dramatically during the heating phase. Figure 6.44 shows how the moment in the sections changed along column C1. The moment in the column increased sharply before the heating time reached 2000 seconds after which it remained approximately constant. The initial increase is greatest at the bottom of the column (l/L = 0) as this is where the column was most restrained in rotation, resulting in the development of large moments. The top of the column had relatively lower restraint to rotation therefore the moments there are lower. Figure 6.45 shows the moment along the whole column at a given time of heating.

From a low and nearly constant value in the beginning, the moment over the column increases rapidly with heating, primarily because of restrained thermal bowing (from restraints to rotation at the column ends, as explained earlier). The slope of the moment diagram also increases with heating, indicating that a significant amount of shear is generated by the difference in thermal expansion in the lower and roof beams. There is a very small reduction in the shear at the end of heating.

The horizontal reaction forces in the columns are illustrated separately in Figures 6.46, 6.47 and 6.48, corresponding to the phases of cyclic loading through displacement control; release of the boundary restraint used for inducing cyclic displacement; and heating. The reaction forces reached a maximum at the final “push” of the cyclic loading, 145kN in the left column and 104kN in the right column. When the boundary restraint used for applying cyclic displacements to the frame was released, the reaction reduced with the left column reaching a residual horizontal reaction force of 7.4kN and the right column -7.4kN to satisfy equilibrium. During the heating, the reaction forces increased again during the first 2000 seconds, following by a slight decline due to the material degradation at elevated temperatures (Figure 6.48). The initial increase can be attributed to the restraint provided to the expanding plinth beam. The highly symmetric

nature of the column reactions during heating suggests that either both columns were damaged equally or the effects of damage were masked by the thermal strains.

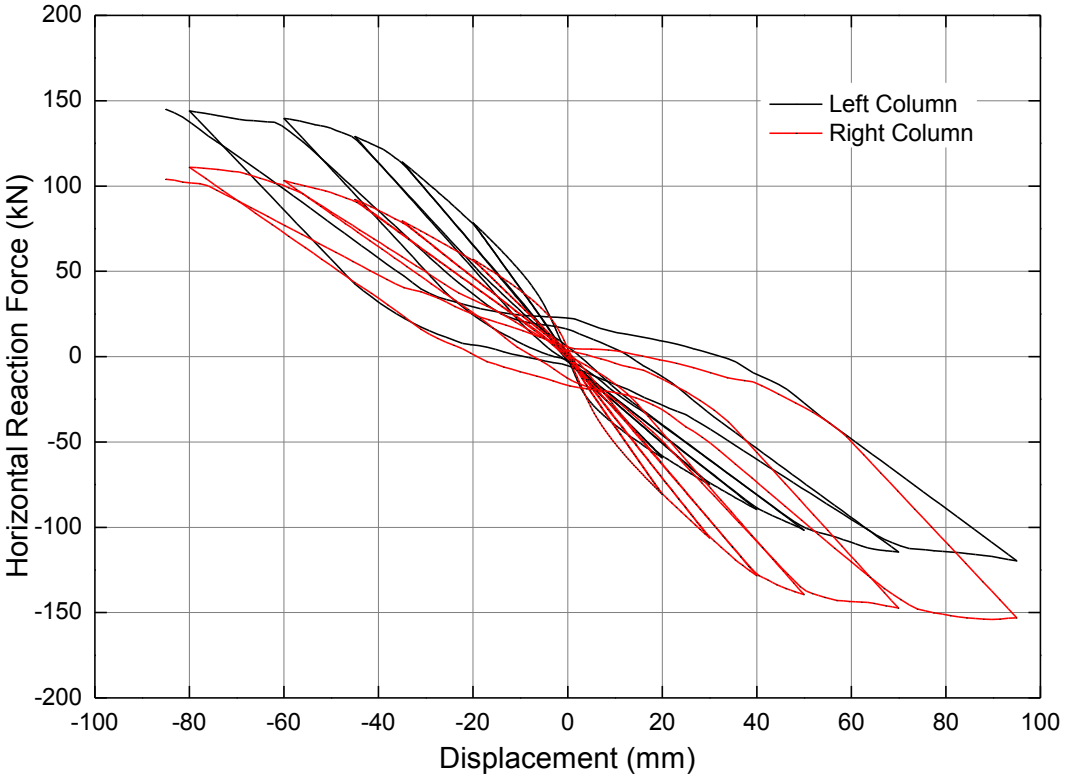

Figure 6.46: The curve of displacement against horizontal reaction forces in the columns under cyclic loading

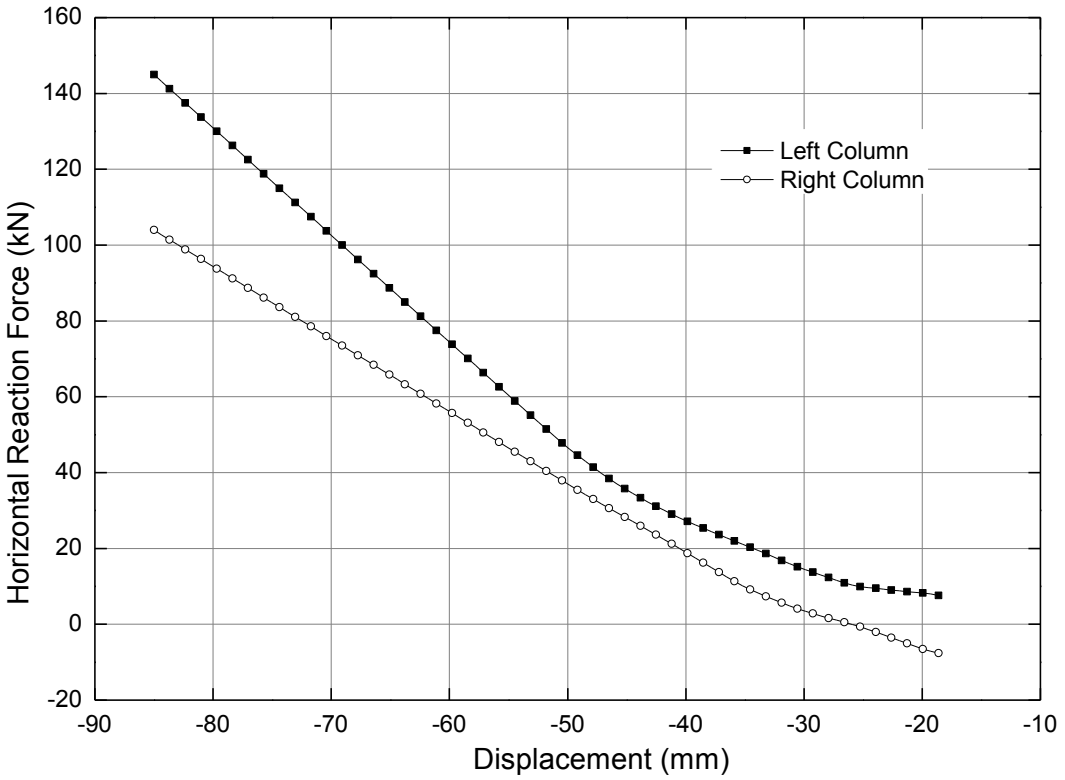

Figure 6.47: Horizontal reaction forces in the columns after "release"

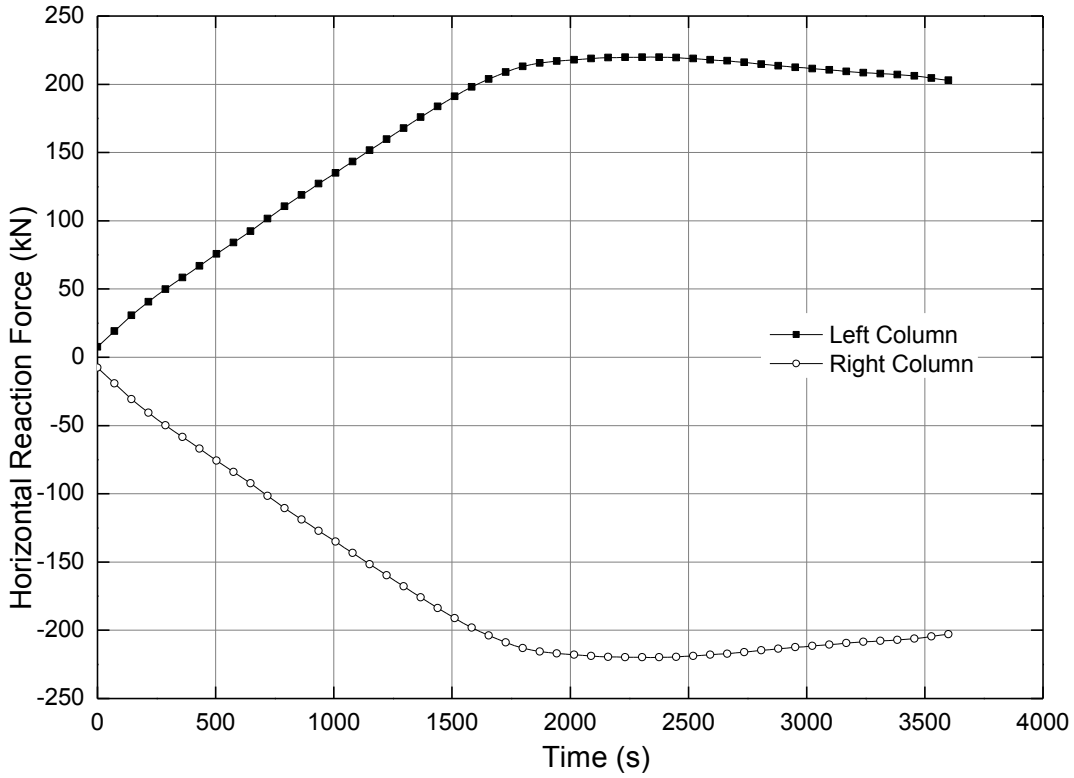

Figure 6.48: Horizontal reaction forces in the columns during the heating

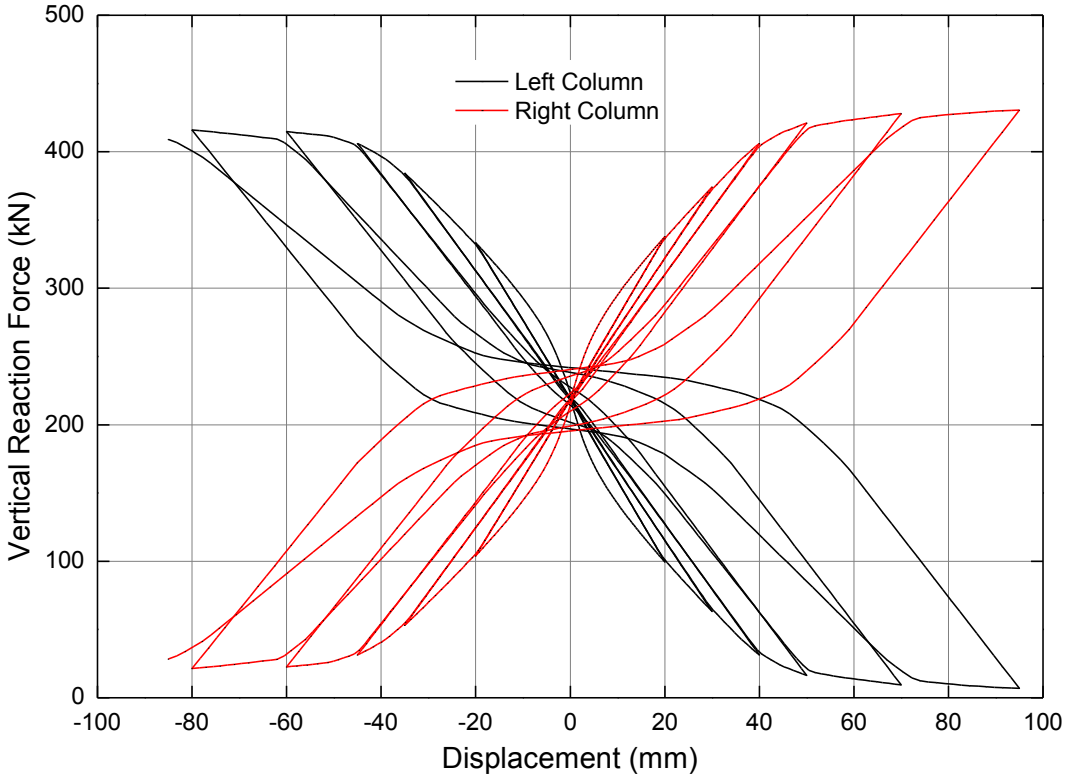

Figure 6.49: The curve of displacement against vertical reaction forces in the columns under cyclic loading

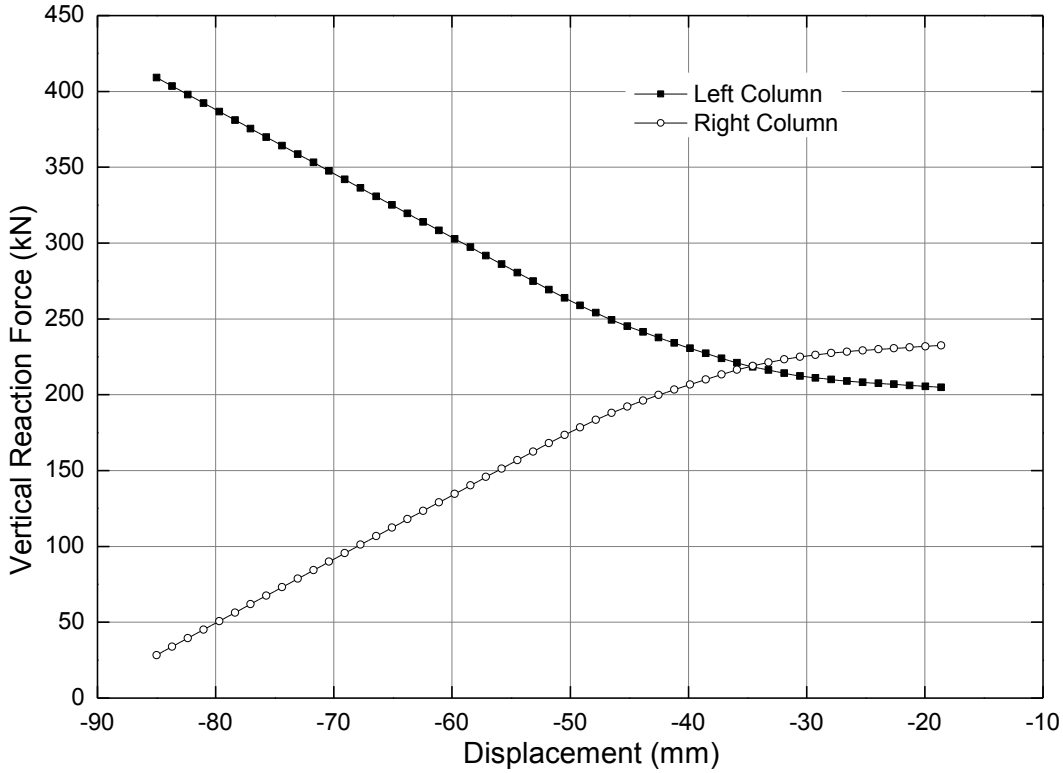

Figure 6.50: Vertical reaction forces in the columns after "release"

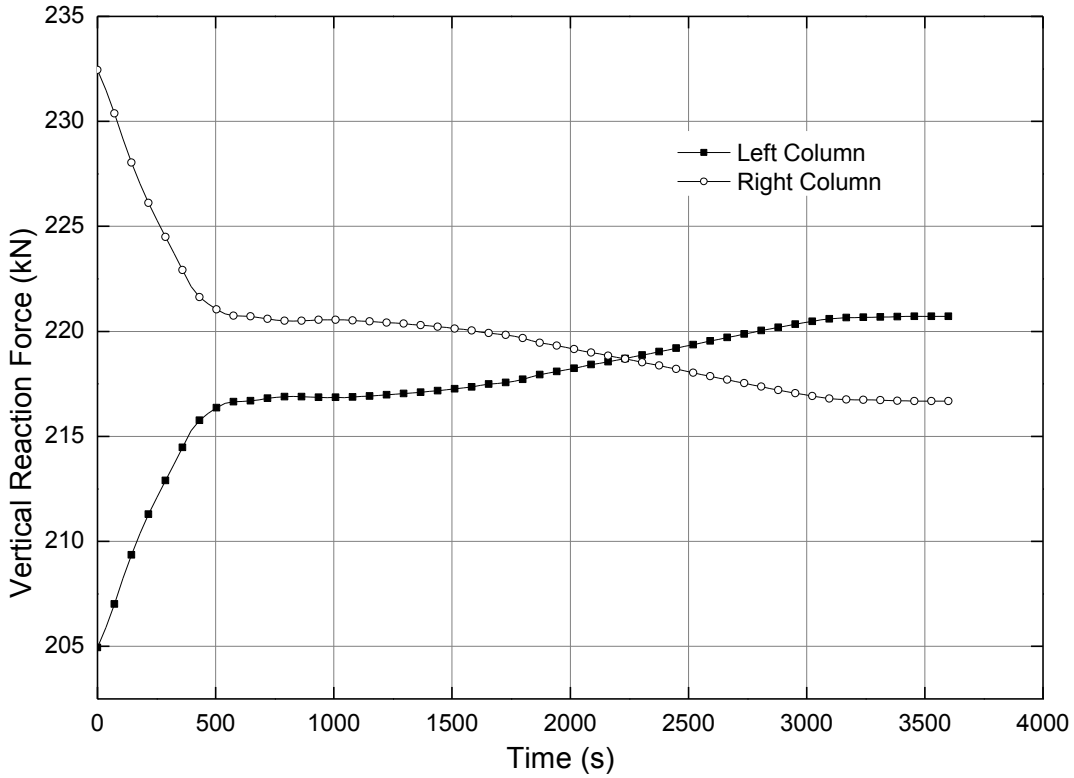

Figure 6.51: Vertical reaction forces in the columns during heating

The vertical reaction forces at the base of the columns are illustrated separately in Figures 6.49, 6.50 and 6.51, corresponding to the phases of cyclic loading through

displacement control; release of the boundary restraint used for inducing cyclic displacement; and heating. When completing the final cycle, the reaction forces reached a maximum, 409kN in the left column and 28kN in the right column, because of the large lateral force (applied as displacement). When the boundary restraint used to apply the cyclic displacements is released the vertical reactions in both columns equalise a lateral displacement offset of 35mm. Interestingly however, the vertical reaction in the right column overshoots that in left column thereafter until the frame comes to stop at a permanent left-leaning offset of 18mm (Figure 6.50). Upon heating the difference in vertical reactions reduced rapidly again during the first 500 seconds with the curves intersecting at 2200 seconds, after which the reaction in the left column became larger than that in the right column.

6.4.7 Modelling of The Undamaged Frame in Fire

To further understand the effect of the mechanically simulated seismic damage on the RC frame's fire resistance a further analysis is carried out excluding the cyclic loading stage, while all the rest of the loading (gravity and then fire) remains exactly the same.

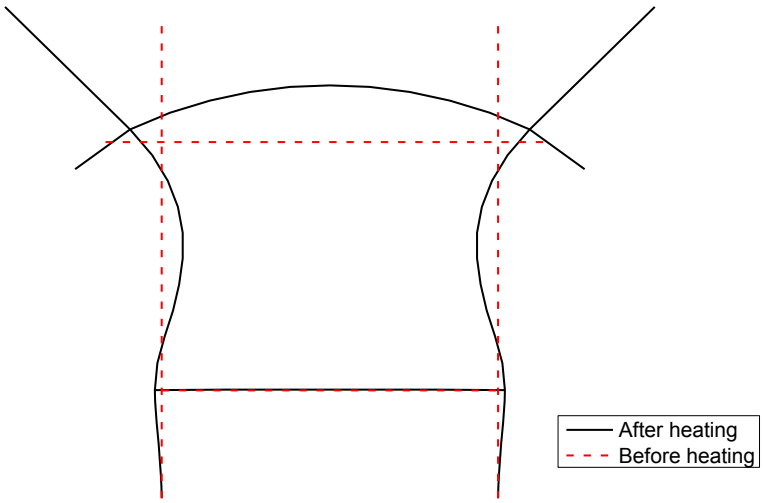

Figure 6.52: The shape of the frame before and after heating

Figure 6.52 shows the exaggerated deformed shape of the frame after applying the gravity load and the fire loading in two load steps. As expected the deformed shape is almost perfectly symmetric. Perhaps an analysis with various degrees of distributed geometrical and material imperfections would have produced more natural looking

results, however this was considered out of scope for this project as the purpose here is only to establish a base line response of the frame to the fire loading.

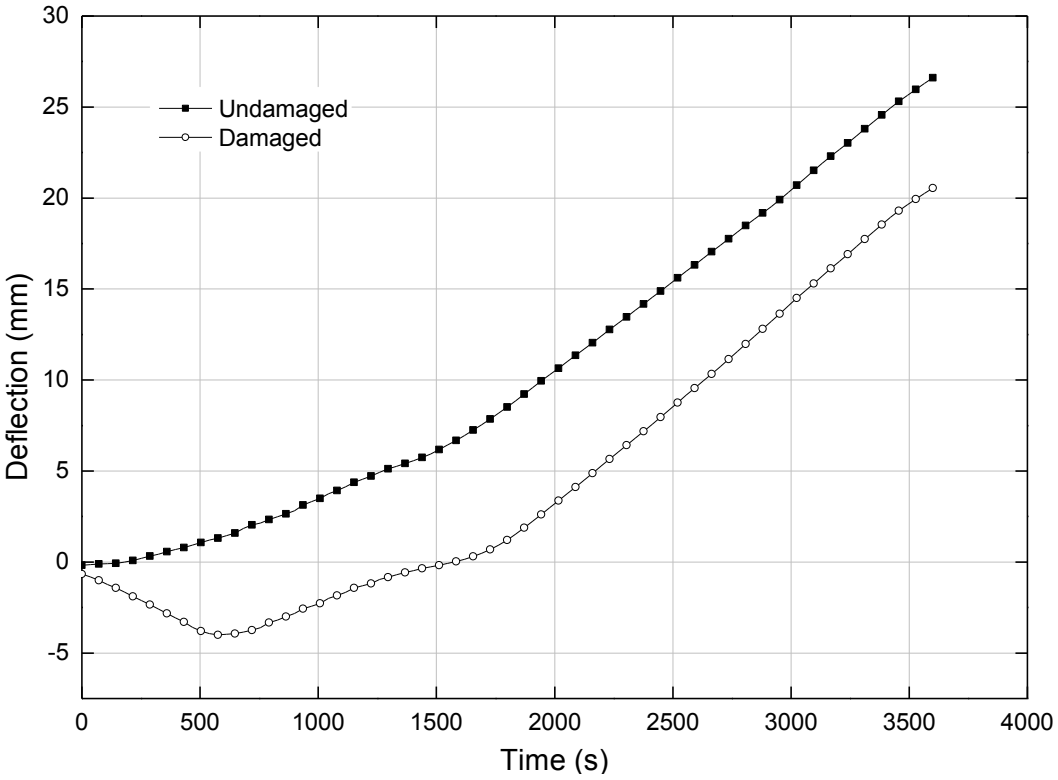

Figure 6.53: Mid span deflection of the roof beam (B2) during heating for both the damaged and undamaged models

Figure 6.53 shows the mid span deflection of the roof beam during the heating phase for both the frames, with and without cyclic loading. It is clear that roof beam in the undamaged structure undergoes upward deflections right from the beginning of the heating, while in the damaged frame it experiences downward deflections at first which begins to reverse after 500 seconds. This suggests that the damaged columns where not able to impart as much rotation to the ends of the roof beam (as a result of thermal bowing) as the undamaged columns. However after a degree of heating the damaged columns regain stiffness and are able to transfer rotations to the roof beam.

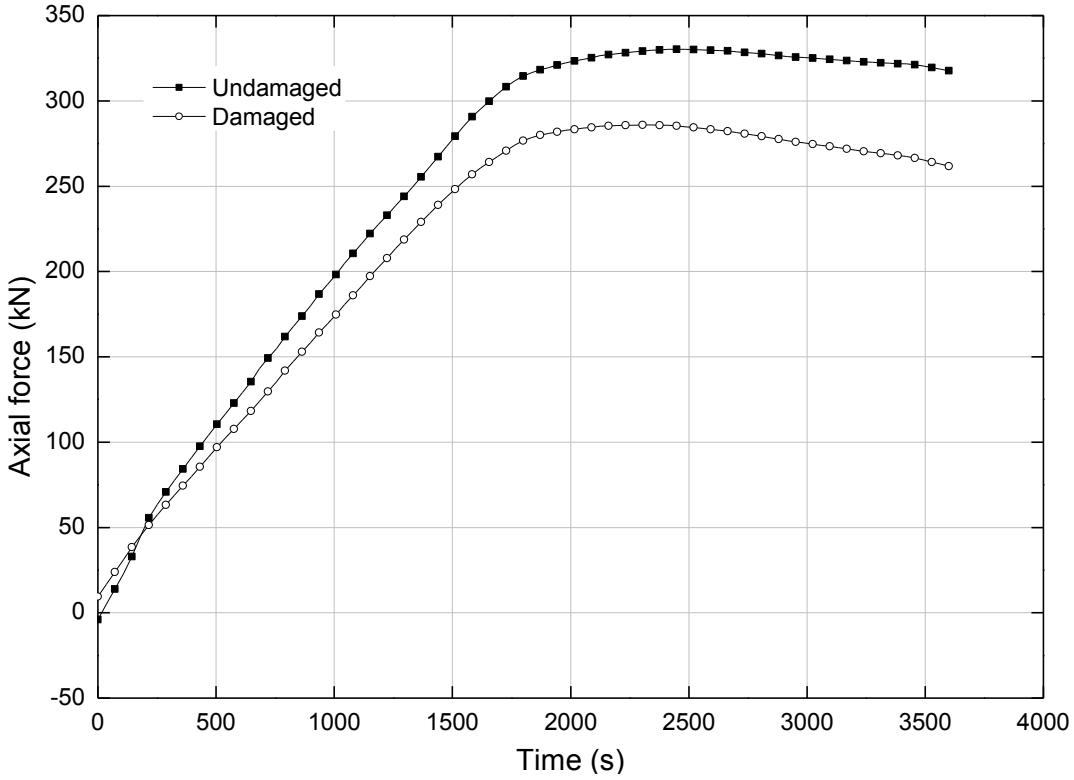

Figure 6.54: Axial force of the lower beam (B1) during the heating for both the damaged and undamaged models

Figures 6.54 and 6.55 show the axial force and moment in the lower beam during the heating phase for both the models. Both of these graphs indicate that the undamaged model had a larger stiffness than the damaged model and therefore attracted larger forces because of the restraints to thermal expansion (axial force) and thermal bowing (moment).

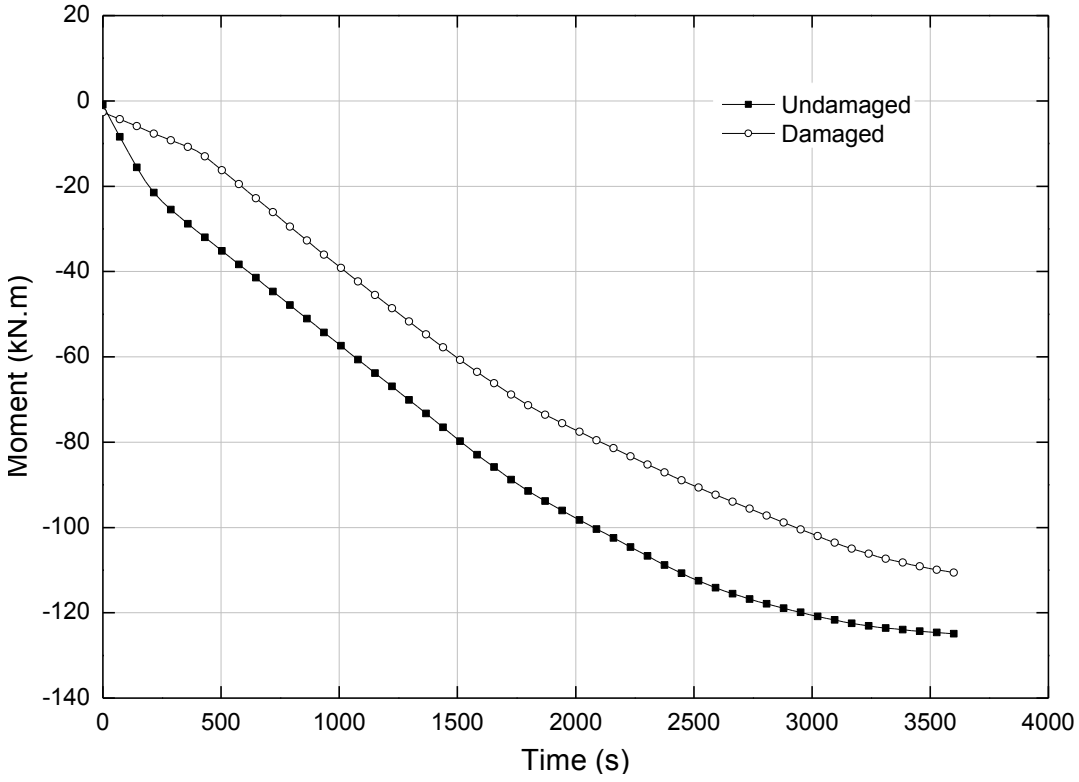

Figure 6.55: Mid span moment of the lower beam (B1) during the heating for both the damaged and undamaged models

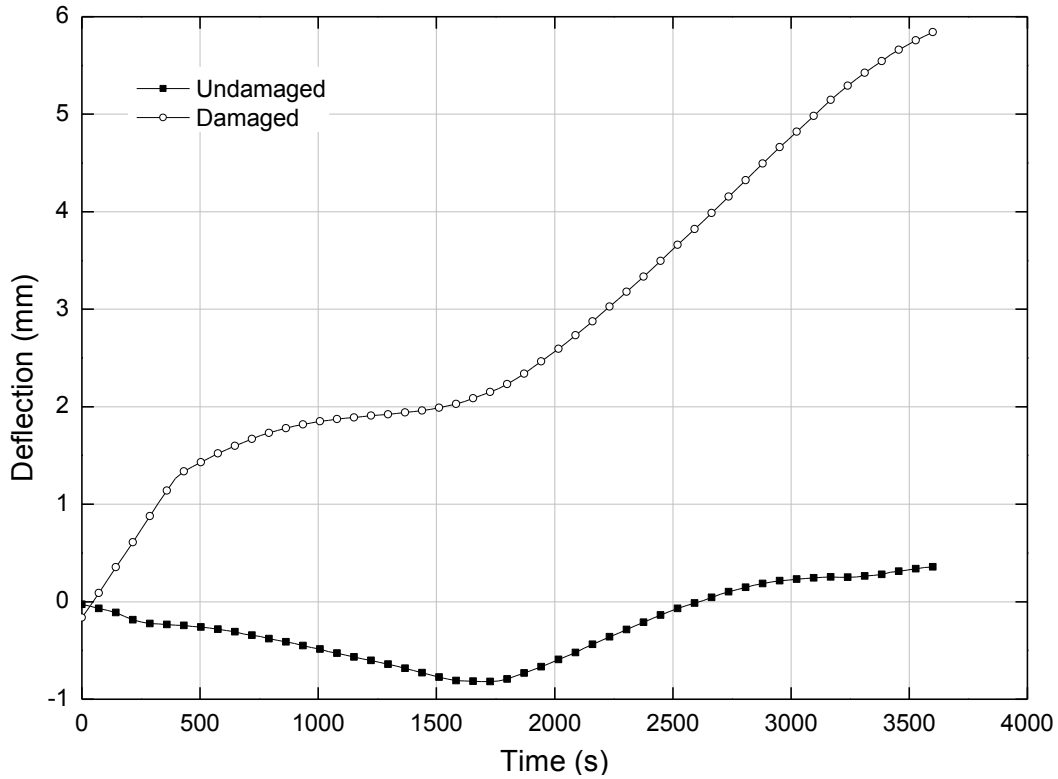

Figure 6.56: Mid span deflection of the lower beam (B1) during the heating for both the damaged and undamaged models

Figure 6.56 shows the deflections of the lower beam in fire for the damaged and undamaged models. The lower beam had a much smaller deflection for the undamaged model than the damaged model. The difference is primarily because of the asymmetry in the damaged frame before fire loading commenced, while the undamaged frame

showed a perfectly symmetric response. Furthermore as the deformed shape showed in Figure 6.52, there is very little rotation in the columns at the beam ends in this case.

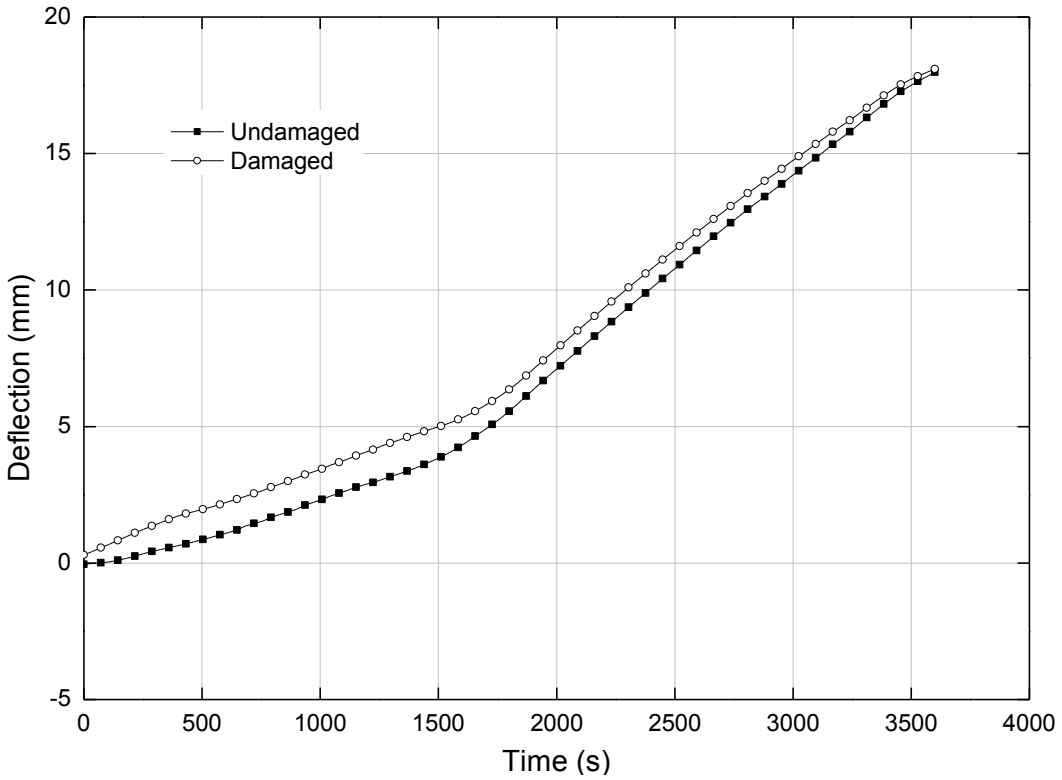

Figure 6.57: Mid span deflection in the column (C1) during the heating for both the damaged and undamaged models

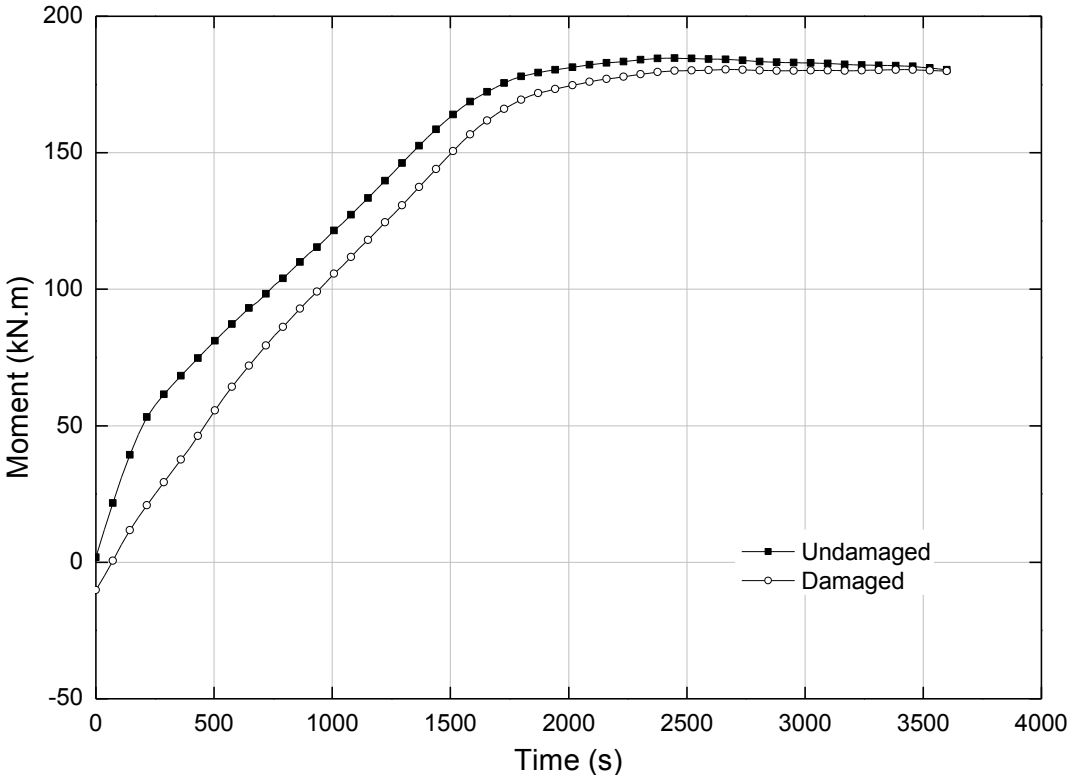

Figure 6.58: Mid-height moment in the column (C1) during the heating for both the damaged and undamaged models

The deflection of the column C1 did not show much difference between the damaged and undamaged model during the heating, as shown in Figure 6.57. This difference was greater in the first 1500 seconds than the rest of the time of heating.

Figure 6.58 shows the moment in the column at mid-height during the heating for the two models, the evolution is similar with larger values in the undamaged column as expected.

Based on the modelling of the undamaged frame, it can be concluded that in general, the beams were affected more than the columns by the damage, which seems a little counter-intuitive, however it should be remembered that the frame was designed to ensure that in case of overload hinges form in the beams first and then in the columns, based on the principles of good seismic design. This meant that the columns were had greater bending capacity than the beams, therefore the results are not surprising.

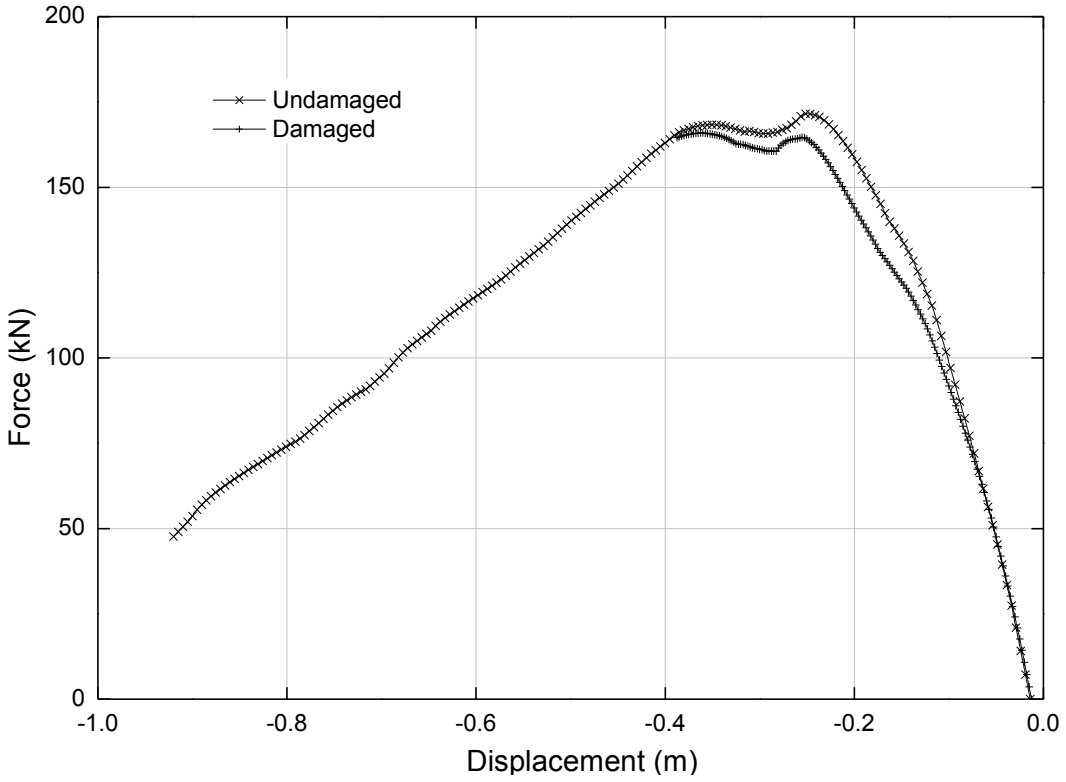

Figure 6.59: Displacement against reaction force during post fire pushover for the damaged and undamaged models (using displacement control)

Pushover Capacity after Heating

To understand to what extent the concrete frame in fire was affected by the cyclic loading applied previously, a pushover analyses were performed using the same

numerical models with and without cyclic loading induced damage. These analyses were carried out subsequent to the thermomechanical analyses. The damaged model was pushed laterally in the direction that the frame was leaning towards at the end of the cyclic loading stage. The undamaged model was pushed in the same direction as the damaged model, for convenience of comparison. Each model was analysed using both load control and displacement control separately. Figure 6.59 shows the plot of the reaction force against the displacement of the control point for the pushover analyses using displacement control for both models. Surprisingly, the maximum reaction force from the two models did not show a great difference, 165.9kN for the model with damage and 171.5kN for the model without damage, indicating that the lateral reaction force capacity was not affected greatly by the cyclic loading induced damage. However the pushover analysis could not be carried beyond a lateral displacement of less 0.4m for the damaged model because of convergence difficulties. This does suggest that the damaged model exhibited greater susceptibility to the pushover displacement than the undamaged model.

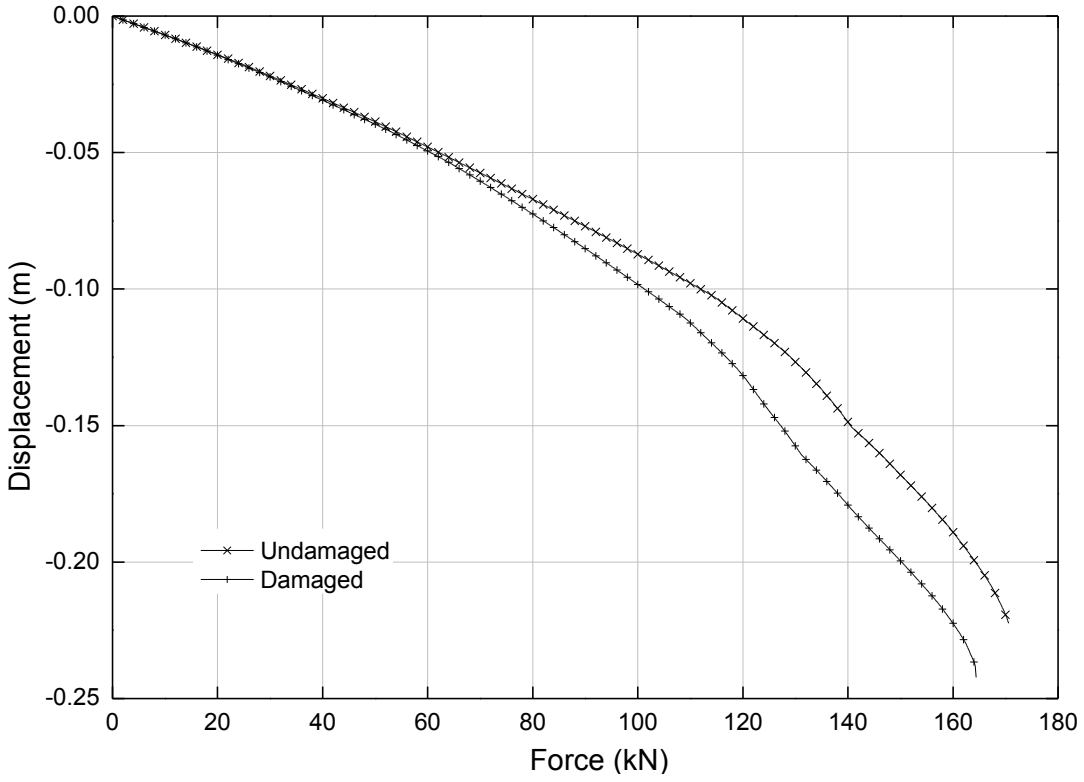

Figure 6.60: Applied force against displacement during post fire pushover for the damaged and undamaged models (using load control)

The results from both analyses are similar and corroborate each other, however because of the nature of load control post-peak response could not be traced.

The force-displacement plots for both models are nearly linear and overlapping at an early stage of the pushover loading, indicating that the lateral stiffness of the damaged and undamaged models was very similar in this period. It can be concluded from this analysis that the damage caused by the cyclic loading to the reinforced concrete frame affected the pushover capacity, but this effect was fairly small.

6.5 Conclusion

The key conclusions are:

Modelling the response of the reinforced concrete frame to cyclic loading requires the use of a "pinching" model to obtain the correct hysteresis behaviour and generate results that would be comparable to real tests.

Although for the tested and modelled frame sub-assemblage, the beams are not constrained horizontally by the adjacent (cold) structural members, however, the internal axial forces and moments generated in the beams, caused by the restraint to thermal deformation, are still very large.

The thermal bowing of the columns affected greatly the overall deformation of the frame during the heating phase.

The deformation of the frame in fire is affected only slightly by the damage caused by cyclic loading (consistent with a life safety level of story drift).

The pushover capacity of the damaged frame after having experienced a significant fire load was reduced only slightly, which was initially surprising, however this is explained by the practice of good seismic design which tries to ensure that the first hinges form in beams and not columns.

Chapter 7 - Conclusion and Further work

7.1 Introduction

This research has developed thermo-mechanical analysis modules for the finite element software OpenSees, and the new code development has been tested and has proven to be successful by analysing a number of theoretical benchmark problems and modelling the real experiments and comparing the results with commercial software ABAQUS. Real concrete frames first subjected to cyclic loading (in order to induce simulated seismic damage) and a subsequent fire (as part of a series of tests carried out at IIT Roorkee in collaboration with University of Edinburgh) were also been modelled using the new developed program and provided useful insights into the fire resistance of seismically damaged RC frames. This was the first case of systematic large-scale research on structures subjected to fire following an earthquake and has helped develop a much better understanding of the behaviour of damaged RC frames in fire than previously available.

The purpose of this chapter is to evaluate critically the methods used during the course of the project, discuss the implications of the results and then to draw conclusions from the research. Further more, some thoughts will be given on the direction of future work in this area.

7.2 Summary and Conclusions

- This work was the first attempt at introducing a thermomechanical analysis capability in OpenSees and it has produced a useful and free tool for engineers and researchers interested modelling structural frames subjected to elevated temperatures. Furthermore the tool is completely free of cost and can be downloaded from the University of California Berkeley and University of Edinburgh OpenSees web pages.

- Adding new classes into OpenSees turned out to be much more convenient than adding subroutines to the sequential algorithm centred programs most of the currently used FEM software is written in. By contrast OpenSees is a C++ based

object oriented program, with an open source code with reusable classes, making it easier less error prone to modify and add new capabilities into it.

- The newly developed thermo-mechanical analysis classes have been accepted by the team and Berkeley, and the included in version 4.0 in October 2012. All the new developments can be downloaded, used, and revised and improved if freely, since they are all open source.

- The original OpenSees proved more efficient for modelling RC frames subjected cyclic loading compared to the commercial software ABAQUS as it had been specifically developed for analysis structures subjected to earthquakes. Even for thermomechanical analyses OpenSees is better in some respects. Such as for the beam-column element, up to 9 temperature points can be specified over the depth of the element section, and the locations of these points can be defined by the users. This enables the modelling the highly realistic temperature gradients particularly RC sections, currently not straightforward to do in ABAQUS beam elements.

- Given a perfectly ideal material, and applying uniform temperature gradient across the section of the cantilever, the theoretical half circle was achieved using OpenSees. The shape of the half circle is exactly the same for the cantilever under equivalent pure moment at the free end, which shows that the new development allows accurate geometric nonlinear analysis.

- Modelling of a half heated fully restrained axial member reproduced results fully consistent with theory and showed that material behaviour including plasticity and elastic unloading can also be modelling correctly.

- The modelling result of ZSR1 steel frame showed reasonable comparison with experiment.

- Modelling of the Cardington restrained beam test, a composite structure showed good qualitative comparison with test results, with the difference attributable to 2D modelling of a 3D problem.

- The fire following earthquake problem is considered important but there is little research on this field. This author was involved with the team that carried out the first ever large-scale tests to study the behaviour of earthquake damaged RC frames subjected to a subsequent fire. Predictive modelling using OpenSees was carried out before the test to assist the team in setting up the test properly, followed by detailed modelling to reproduce and simulate observed behaviour in the tests.

- To predict the capacity of the test RC frame while applying a large lateral load of displacement, a push over analysis was performed. The modelling result of shear force – displacement curve was quite similar to the experimental result (obtained from an increasing cyclic displacement).

- The initially modelled hysteretic curve as a result of increasing cyclic displacements of the top of the RC frame seemed to suggest significant energy dissipation capacity and did not exhibit the "pinching" phenomenon commonly seen in testing RC member structures under cyclic loads. The use of OpenSees "pinching material" on the joints of the frame was able to reproduce this phenomenon and provided and improved comparison with the test.

- The strain results between the model and the frame were qualitatively similar with the same trends but not very accurate quantitatively, this was found to be true in previous modelling as well, such as the Cardington fire tests.

- After the application of cyclic loading (through increasing displacements of the top of the frame) the frame was "released" and exhibited a residual displacement as was expected. The magnitude of this displacement is also an indicator of the "damage" that the post-peak loading induced in the frame. The models produced residual displacements very similar to that obtained in the test.

- The modelling showed that initially the frame "stiffened" with heating and moved towards its original position (i.e. the residual displacement was reduced). However with further heating this displacement reversed and after the full hour of heating the frame ended up roughly in the same place as it was at the start of the heating. Unfortunately this behaviour could not be confirmed from the test as the displacement transducers had malfunctioned because of the fire. Furthermore, as the

magnitude of these displacements compared to the overall dimensions of the frame were very small (2 orders of magnitude lower) it was also not noticeable in the videos or photographs or to any of those who witnessed the tests on site.

- The modelling showed that there was considerable interaction between the columns and beams, not only during the cyclic loading (as expected) but also during the fire loading. The overall behaviour showed that the thermal bowing in the column was the most dominant feature and beam deformations were significantly affected by this. Furthermore, thermally induced deformations were much greater in the top beam/slab as it was relatively less strongly restrained, while the bottom (plinth) beam showed significantly lower deformations and therefore correspondingly higher axial forces and moments.

- Before the frame was heated, the vertical force on the left and right column had some difference, but this difference became very little in around ten minutes of heating. After that, the vertical forces kept steady.

- To further explore the behaviour of RC frames in fire, an undamaged frame was modelled under the same fire. One of the key differences found was that the top beam deformations were monotonic with increasing upward deflections with increasing temperature driven by column thermal bowing (the top beam in the damaged frame first deflected downward and then upward – suggesting that in that model the column damage had reduced their stiffness and therefore column bowing was not strong enough to rotate the beam ends in the beginning, however as this stiffness increased with heating the top beam began to deflect upwards). The restraint forces generated in the lower beam (both axial forces and moments) of the undamaged frame were larger than in the damaged frame as expected, which also corresponded to lower deformations. Push over analyses were carried out on both the damaged and the undamaged frame to determine their residual capacities for lateral force resistance. It is interesting to note that until the displacements reached over 0.1m both models showed similar capacity and stiffness, however beyond this the undamaged frame showed greater capacity.

7.3 Further work

- Developing the capability to analyse 3D frames in fire in OpenSees is the obvious next step. This has already been undertaken by other members of the group, including the development of nonlinear shell elements. This also includes much more thorough thermal loading classes, including that for analysing more realistic fires which lead to non-uniform temperatures distributions in the structural members. This would ultimately require the coupling of CFD models of fire with 3D heat transfer and thermomechanical analysis to enable modelling of real fire scenarios, with automatic transfer of information from one model to another.

- Further development of good reinforced concrete models including bond-slip and cracking behaviour to model the damage from cyclic loading accurately. Models of reinforced concrete at high temperatures are often simple extrapolations of ambient temperature models based on uniaxial constitutive behaviour at elevated temperature. Research is required to determine if this approach is reasonable.

Using Opensees for Structures in Fire

by

Asif Usmani, Jian Zhang, Jian Jiang, Yaqiang Jiang and Ian May

Reprinted from

Journal of
Structural Fire Engineering

Volume 3 · Number 1 · March 2012

Multi-Science Publishing
ISSN 2040-2317

Using Opensees for Structures in Fire

Asif Usmani[1], Jian Zhang[2], Jian Jiang[1], Yaqiang Jiang[1] and Ian May[2]
[1]School of Engineering, The University of Edinburgh, Edinburgh EH9 3JF, United Kingdom
[2]School of Built Environment, Heriot-Watt University, Edinburgh EH14 4AS, United Kingdom email: asif.usmani@ed.ac.uk

ABSTRACT

In this paper we report the progress of our work so far on extending of the OpenSees framework so that it can be used to model structures subjected to fire. The work has focussed on understanding the C++ based object oriented structure of the OpenSees framework, so that all developments remain consistent with it. New classes have been added to introduce temperature dependent material properties for steel and concrete materials. New element classes have also been added to analyse 2D truss and frame structures subjected to fire. This paper will provide an overview of the developments already implemented and present results from using the implemented code to solve a number of benchmark problems and from modelling real fire tests.

1. INTRODUCTION

OpenSees is an open source object oriented software framework developed at UC Berekeley and currently supported by NEES. OpenSees has so far been focussed on providing an advanced computational tool for analysing the non-linear response of structural frames subjected to seismic excitations. Given that OpenSees is open source (available for free download at opensees.berkeley.edu) and has been available for best part of this decade it has spawned a rapidly growing community of users as well as developers who have added to it's capabilities over this period. For instance it has significant geotechnical modelling capabilities developed by this community so that the seismic response analyses can include full soil structure interaction if required. It also has a structural reliability and sensitivity analysis capability offering many reliability calculation tools. Furthermore it has an HPC or parallel version for solving large problems on high-performance computing hardware. In addition to it's availability as an analysis tool OpenSees is also the software platform of choice for the US NEES network that enables earthquake engineers to organise and share data, participate in remote experiments, and perform hybrid simulations. It therefore represents the largest community of this kind in structural engineering and has the potential to bring together the best structural engineering computational modeling capabilities under one platform accessible to all facilitating new collaborations across geographical boundaries to solve ever more challenging problems.

The decades since the 60s saw explosive growth in computing power and its affordability leading to the kind of ubiquity where access to network computing is now seen as practically at par with services such as the electricity grid or the water and sewerage networks. Structural Engineers were one of the earliest exploiters of the opportunity offered by digital computers driven very much by the need of solving larger and larger systems of linear equations to analyse structures such as whole aircraft or building frames. This led to a great deal of legacy code being written, primarily developed in Fortran. This activity however peaked in the 80s and much of the development founds its way into the many currently available commercial codes such as SAP, ANSYS, ABAQUS etc. Much of the millions of lines of special purpose research codes written in this period (representing thousands of man-years of effort) are now very likely unusable not just because of the dramatic changes in operating systems,

Draft submitted to J. of Structural Fire Engineering on 7 Dec 2010

interface software, storage media etc. but the change in the whole working environment brought about by information technology. The potential offered by this explosion in information technology is immense for structural engineers (as it is for all other type of engineers) however so far there is a relative lack of imagination from our profession in taking on this challenge. Structural engineers who were once the pioneers in exploiting the new digital computing technologies emerging in the 60s and 70s, are now at risk of being seen as dinosaurs, perhaps because of, rather than despite, that early success.

The picture is not however uniformly dismal as there have been a number of very forward looking developments starting incidentally from that most productive of places, California. Among the most imaginative examples of a structural engineering project is the NEES network [1], bringing together 15 earthquake engineering research labs in universities across the USA. The key vision of this network is to enable hybrid testing of structures, where one (or more) part(s) of a structure is constructed in a lab and the rest exists virtually as a computer model in a separate (geographically remote) location, perhaps on a high performance computing platform. The two are then made to interact in real time via sensors and actuators acting on the real model in the lab exchanging information with the virtual model over the internet or Grid. The NEES network recommends the use of the software framework OpenSees [2] for simulating virtual components of hybrid testing. OpenSees is another example of an excellent imaginative project that addresses some of the issues discussed earlier. It takes a different route to software development from the traditional research codes that routinely die and commercial packages which are by definition restricted access (both in terms of affordability and more importantly in terms of adding functionality for problems that can not be adequately dealt with by the package as it stands). The OpenSees route is not in itself new and the most ubiquitous and successful expression of it is the linux movement, *i.e.* an open source "community" code offering free access to all developers wishing to add new functionality to the core framework.

The structural engineering community is clearly considerably smaller than the linux community and it remains to be seen if OpenSees will be as successful, however the potential it offers is arguably very attractive. The potential is that of a common community owned research code with a large and growing collection of modelling capability in many areas of structural engineering enabling researchers to collaborate freely across geographical boundaries and being secure in the knowledge that the fruits of their effort will continue to exist in a living code (until superseded by a better version). Other strengths of the OpenSees framework is the inclusion of a high performance computing (or parallel) version [3] and the adoption of the object oriented paradigm of software development using C++, which enforces a discipline on the developers and ensures that the framework will develop in a manner that is manageable and easy to maintain and most of the its components are "reusable" by other developers.

This paper presents an overview of the work currently underway in Edinburgh to add a "structures in fire" modelling capability in OpenSees which will be consistent with the ethos of the other components of OpenSees in terms of being object oriented and enabling the use of HPC hardware. Furthermore, this work will also enable the modelling of earthquake damaged structural frames subjected to a subsequent fire. The development of this capability will involve work in the following areas:

- Fire load modelling to provide boundary conditions for the subsequent heat transfer into structural components
- Analysis of heat transfer to structural components accounting for local changes in thermal properties as a result of seismic damage
- Implementing temperature dependent material properties for the main material models available in OpenSees and adding new temperature dependent material models
- Implementing temperature dependent transient thermal strain or LITS (load induced thermal strain) type effects

- Modification of beam and shell element classes available in OpenSees to develop new classes that account for thermal effects

This paper will provide a summary of the work carried out on each of the topics above and present results from a number of test problems solved using the new code developed within the OpenSees framework.

2. FIRE LOAD MODELLING

The aim of this part of the work is to allow a wide range of heterogeneous and homogeneous fire boundary conditions to be applied to the boundaries of the structural model. To this end, it is proposed that the following methods for simulating fire loading conditions will be developed in this work (see [4] for a good summary):

1. Post-flashover standard compartment fires evolving according to time-temperature curves established in various codes and standards (such as ISO 834 and ASTM E119)
2. Post-flashover natural compartment fires evolving according to various parametric time-temperature relationships recommended in the research literature and codes (such as EN1991-1-2)
3. In addition to the code based standard fires and parametric natural fires, simple energy balance laws can be used to create "zone models" to produce relatively more realistic representations of temperatures in a fire compartment.
4. Localised fires and travelling fires, such as in large compartments where whole compartment involvement (flashover) is unlikely to occur. EN1991-1-2 offers useful empirical approaches for dealing with small and large localised fires. There are no current guidelines for moving fires, however NIST investigation [5] of the collapse of the WTC 7 building on September 11, 2001 offers interesting insights (based on CFD modelling),
5. Fires impinging on the structure from external sources. Some guidelines for this are provided in EN1991-1-2 for flames emerging out of compartment windows. This however could be a common situation in the case of fires following an earthquake and façade fires for high rise buildings, for which there is no current guidance.

The first three types of fire loading produce spatially homogeneous compartment temperatures where a single temperature is supposed to represent the temperatures at all points in the compartment at a specific instant of time (in case of zone models this applies to one or more zones used to model the compartment). The last two types of loading conditions could produce both spatially and temporally non-uniform temperatures. All types of fire loading will be implemented by applying radiation and convective flux boundary conditions to the structure.

The most realistic heterogeneous temperature distributions in the compartment can be produced using a computational fluid dynamics (CFD) based model. Addition of a full CFD model to OpenSees is not feasible however an interface will be developed in OpenSees based on the work of Jowsey [6] which will enable a time dependent and non-uniform heat flux boundary condition to be derived from CFD computations, which can be applied to the structure.

3. MODELLING OF HEAT TRANSFER TO STRUCTURAL COMPONENTS

Once the fire boundary conditions have been determined, the heat transfer to the structural components must be computed to establish the time evolution of temperatures within the structure. This will be done by adding an object oriented 3D conduction heat transfer modelling capability in OpenSees [7]. It will be possible to reuse parts of the existing OpenSees framework to create a new heat transfer analysis system, not least the graph numbering classes, the numerical classes, and the solver classes.

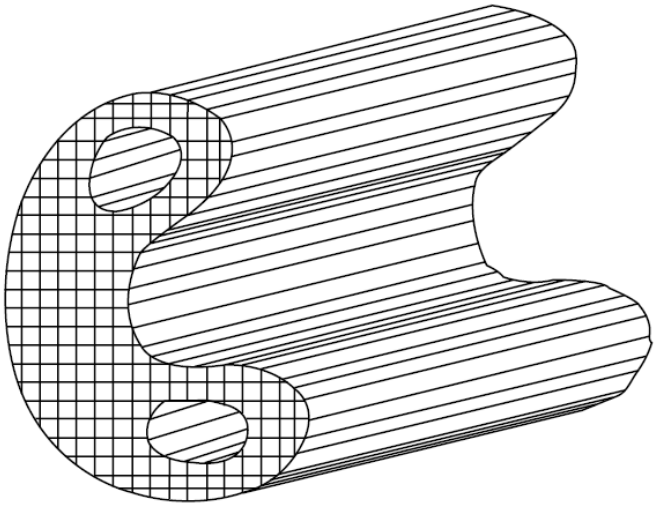

Figure 1. Schematic of a 3D brick element mesh for an arbitrary length of an arbitrary structural member.

The heat transfer module will take advantage of the "fibre section" beam elements used in OpenSees. Heat transfer in building structures as a result of a fire typically has a character that naturally suits fibre type modelling of structural members because the greatest thermal gradients exist in the cross-section of the member rather than along its length. A finite element mesh that has the same character will therefore be best suited to heat transfer modelling. Figure 1 shows a schematic sketch of such a mesh of 3D brick elements with fine discretisation in the cross-section and coarse along the length of the member.

In the cases where heat transfer along the longitudinal direction can be neglected, a 2D heat transfer modelling capability for the structural section will also be developed, which can save computational resources and offer additional flexibility to users.

The proposed modelling of fire and heat transfer as described above will enable the most general fire loading conditions to be modelled in a relatively straightforward manner. The temperature history from the heat transfer module could be stored or recorded for reproduction if only a heat transfer analysis is to be carried out. If a mechanical analysis is to follow, a temperature history file will automatically be generated for all fibres of beam-column (and slab) fibre elements if the fibre definitions are identical to the heat transfer discretisation, otherwise the temperatures will be mapped to the mechanical fibre definitions.

In traditional "structures in fire" analysis typically only a one-way coupling is assumed between the heat transfer and the thermo-mechanical analysis, *i.e.* there is no feedback to the heat transfer calculation from the mechanical analysis, thus the structural deformation is not considered in heat transfer modelling [8]. This assumption is reasonable for the global structural behaviour modelling that is the aim of this work. Local detailed investigation of, for instance, concrete spalling behaviour typically requires a fully coupled thermo-mechanical analysis also including mass transport of multi-phase fluids in the concrete matrix, for example [9]. Though important, there is no plan so far to include this kind of analysis in this work. But as we are explicitly considering the modelling of earthquake damaged structures in fire in this work, some effect of mechanical damage must be included in the heat transfer model. Recently some experiments have been carried out [10] to investigate the influence of tensile cracking type damage (in a four point bending test on an RC beam) on the local diffusivity of heat, however the results are so far inconclusive. It is anticipated that local thermal conductivity could be made a function of the damage state in the structure. It seems reasonable that damage will create preferred directions of heat transfer (promoting heat transfer along the cracks and perhaps inhibiting it across cracks) as shown in Figure 2.

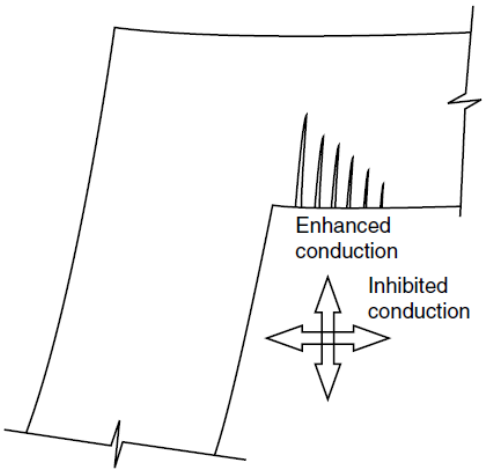

Figure 2. Thermal conductivity change depending on mechanical damage.

4. TEMPERATURE DEPENDENT MATERIAL PROPERTIES

There are many types of material models available in OpenSees for steel and concrete, defining their mechanical constitutive behaviour, however some of these need to be modified to include temperature dependent stress and strain including effects such as LITS. At this stage temperature dependence will only be added to the uniaxial concrete and steel models and this data is not reliably available for the multiaxial case. This also naturally suits the fibre beam and shell models where the section behaviour can be derived from integrating fibre stress, strain and temperature states. The uniaxial properties for steel and concrete will be primarily based on Eurocode stipulations. For concrete additional information from the literature, such as [11, 12], will be used to take into account LITS type effects.

A new set of material properties (also temperature dependent) will need to be added for the heat transfer model as well. These in the first instance will be based on Eurocode data for steel and concrete. As mentioned earlier, the thermal properties, particularly thermal conductivity will be related to a localised strain measure representing damage.

5. THERMO-MECHANICAL MODELLING AND PROPOSED CLASS DIAGRAMS

This work has started by creating new versions of existing OpenSees nonlinear beam-column elements. OpenSees has two main types of these elements, one based on the traditional displacement formulation and the other seemingly more efficient set of elements based on flexibility or force formulation [13]. Considerable team effort has to be invested in understanding C++ and object oriented programming concepts along with the structure of the OpenSees framework. Figure 3 below shows the new classes that have been implemented within the existing framework (the original OpenSees classed are identified by the greyed boxes).

Most of the work so far has gone towards implementing new classes shown above. The existing abstract class *Element* and its children have been generalised to an abstract class *ElementThermal* and its corresponding children ElasticBeam2dThermal, ElasticBeam3dThermal and the nonlinear beam element class DispBeamColumn2dThermal. More of the existing OpenSees elements will be generalised for thermal actions in course of this work. The DispBeamColumn2d Thermal element has been created by modifying DispBeamColumn2d, to enable thermal loading to be applied. The thermal loading is calculated by integrating thermal expansion of the fibres (or layers in 2D) over the depth of the section taking into account the temperature dependent properties of the fibre. The tangent stiffness matrix terms of the beams are also modified based on temperature dependent properties. Temperature dependent properties have been added for uniaxial steel and concrete models (Steel01, Steel02 and Concrete02), creating new temperature dependent versions of these materials (Steel01Thermal, Steel02Thermal and Concrete02Thermal).

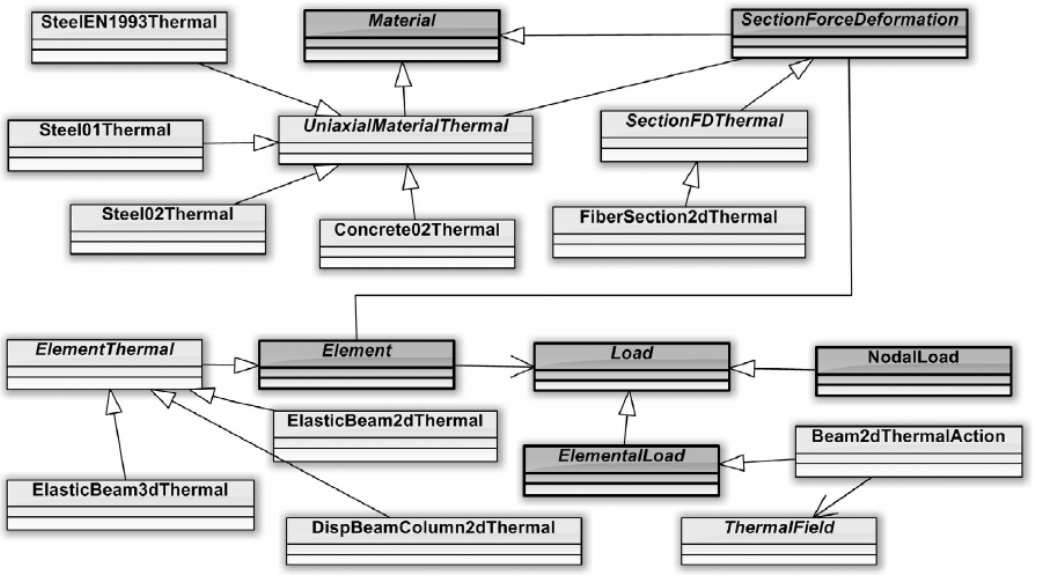

Figure 3. New classes introduced to the current OpenSees framework for performing thermo-mechanical analyses.

Thermal actions in the form of an average temperature and linear temperature gradient through a beam or column section are applied simply through the Beam2dThermalAction class. More general and realistic thermal actions are applied using fibres across the section, with the temperature history of each fibre being provided through the Beam2dThermalAction class and processed through the FiberSection2dThermal and SectionFDThermal classes.

ThermalField is an abstract class, whose instance invokes the thermal analysis modules, which are also being developed for OpenSees. This class is able to provide detailed temperature distribution for each structural element either from direct user input or from carrying out complete fire and heat transfer analyses. The class diagrams for these modules are shown in Figures 4, 5 and 6 below.

As shown in Figure 4, a HeatTransferDomain object represents the state of the heat transfer model by aggregating essential FE components, such as HeatTransferNode, *HeatTransferElement, HeatTransferMaterial,* TemperatureBC, *HeatFluxBC* and *BoundaryPattern*. Each HeatTransferDomain object is also associated with a HeatTransferAnalysis object for the purpose of analyzing the finite element model. Currently 2D quadrilateral and 3D brick elements have been introduced. Temperature dependent materials have also been implemented based on information given in Eurocode 2 and 3. The TemperatureBC and the *HeatFluxBC* objects specify where Dirichlet and Neumman boundary conditions are imposed respectively for the heat transfer analysis. The *BoudaryPattern* class is introduced to define arbitrarily transient behavior of boundary conditions. Subclass FireImposedPattern, whose instances are associated with FireModel objects, has been implemented to specify temporal heat flux boundary conditions determined by different types of fire models.

The "strategy pattern" technique [14] is adopted to implement the fire models. In this case, the strategy is the *FireModel*, which declares interfaces common to all of its subclasses. Using this software design pattern allows encapsulation of different algorithms for calculating heat flux at structural boundaries. The encapsulated algorithms are interchangeable at run time and the client (*e.g.* FireImposedPattern) has no need to know about the implementation details. This loose coupling makes the *FireModel* class greatly extensible and addition of new models does not require corresponding changes in the client classes.

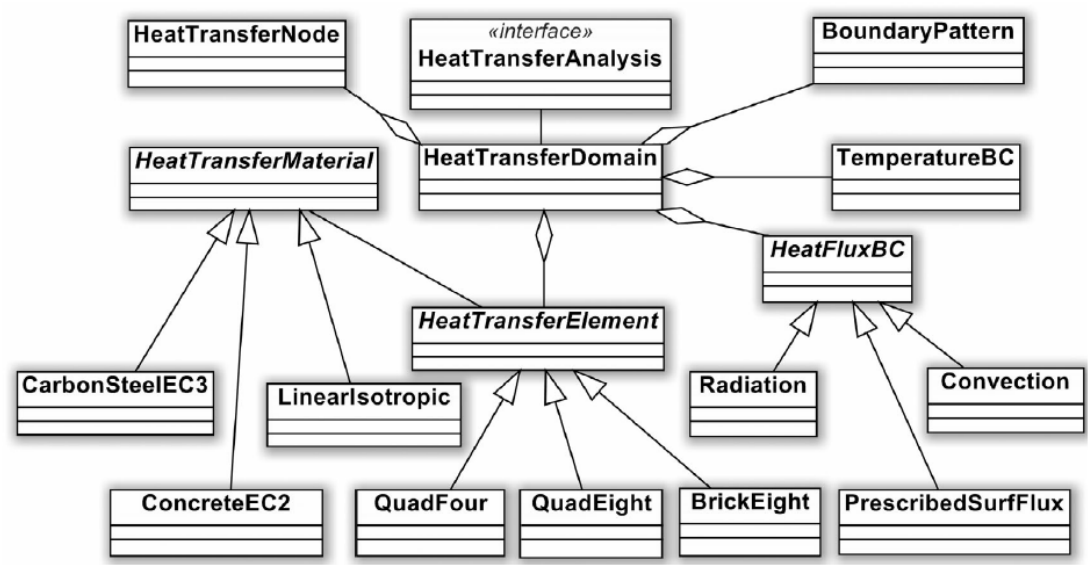

Figure 4. Class diagram representing heat transfer FE components.

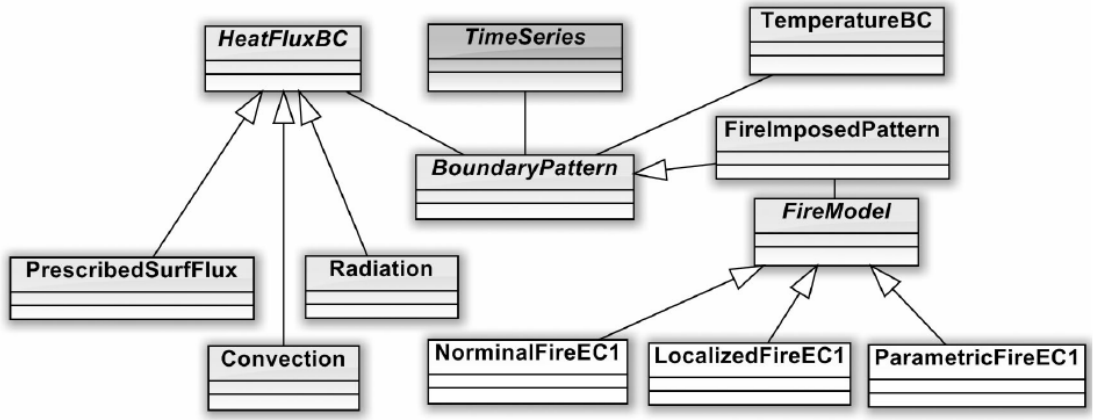

Figure 5. Class diagram representing time-dependent boundary conditions and the fire models.

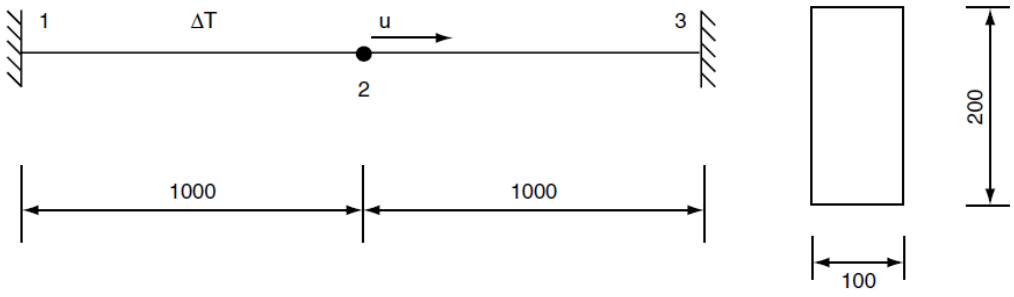

Figure 6. Rigidly restrained steel beam of rectangular section with one half heated.

An abstract method which takes two arguments is provided in the *FireModel* class: `applyFluxBC` (*HeatFluxBC* theHeatFluxBC, double time*) = 0 and any instantiable subclasses must redefine this method. The message passing between a *FireModel* object and a FireImposedPattern object happens in this way: first, a FireImposedPattern object invokes the `applyFluxBC` operation on a *FireModel* at a specific time instant, which then computes necessary quantities to calculate the boundary heat flux at this time instant and invokes operations on the *HeatFluxBC* object to pass it those quantities. Some subclasses such as those for localized fire models may require geometric information of the target location in order to achieve correct mapping of boundary heat flux. This information can be obtained with assistance from *HeatFluxBC* object which carries an element tag and a face tag. With those two unique tags, the locations of target element faces can be determined and the corresponding coordinates can then be mapped correctly. Some fire models suggested by Eurocode 1 have been implemented so far as given in Figure 5.

6. TEST EXAMPLES

The work done so far has been tested on a number of problems some which are presented in this section. The first example is a simple test of modelling restrained thermal expansion in a steel beam, half of which is subjected to an increased temperature (see Figure 6 below). The beam is rigidly restrained at both ends, however the heated of the beam must expand against the cold half, which will lead to the midpoint of the beam displacing towards the right hand side while generating increasing compressive stresses in both halves of the beam.

The stress-strain curve of the steel used in this example is elastic-perfectly plastic with a yield stress of 280 MPa and an initial Young's modulus of 200,000 MPa. The temperature dependence of both these parameters varies according the relevant Eurocode (EN 1993 1-2-1) while undergoing constant temperature increments from ambient to 1000°C. The temperature-displacement curve for node 2 from both OpenSees and ABAQUS solutions is shown in Fig. 7.

From ambient to 400°C, the displacement of node 2 increases linearly, even though the two halves yield at 253°C (the yield stresses remain unchanged until 400°C). At roughly 400°C, node 2 begins to move from right to left due to the drop in yield stress in the heated half leading to elastic unloading of

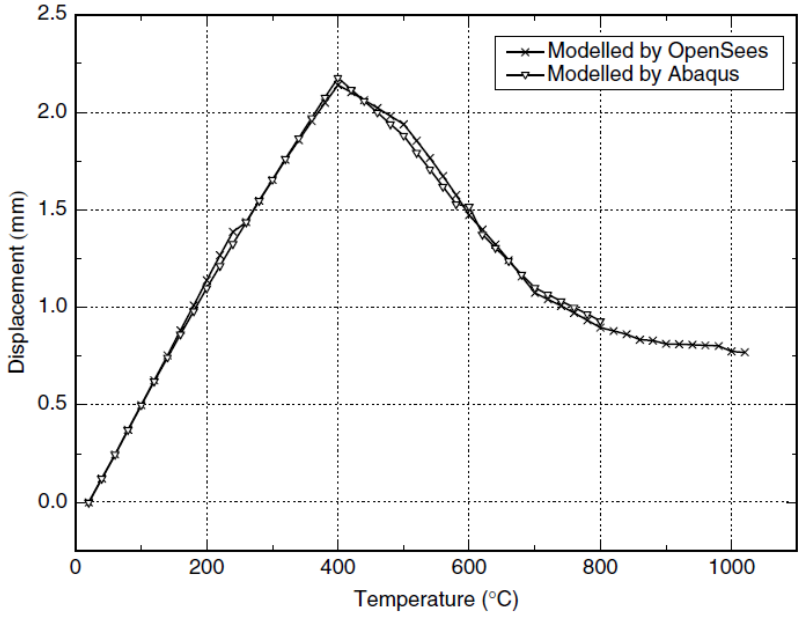

Figure 7. Displacement at node 2.

the unheated half. However, the curve asymptotes to a finite displacement resulting from the plastic strain in the right half stored during the post yield phase (between 253°C to 400°C).

The second example is a steel frame (ZSR1) tested and analyzed by Rubert [15]. The frame with dimensions is shown in Figure 8. All structural elements are made of IPE80 I-sections. Different material properties have been used to model the experiment, including steel properties given in EN 1993-1-2-1 (Eurocode 3) and ST37 [15] (see Figure 9). The yield stress and Young's modulus of the steel are 355 MPa and 210,000 MPa at ambient temperature. The left bay of the frame including the middle column is uniformly heated at a constant rate by electrical elements and the remaining two members are kept at room temperature. A comparison of test and modeling results is shown in Figure 10.

The material properties were a key factor in this simulation. The displacements stay at a low level until around 500°C if a bilinear stress-strain curve is used for steel, but they increase sharply around 300°C when using a multi-linear curve (both curves were based on Eurocode recommendations). If the steel temperature dependent property variation specified by EN 1993 1-2-1 is used, the results are not very close to the test (as shown in Figure 11 - results were identical for both with and without hardening versions). When ST 37 properties are used, the results show satisfactory agreement. This is encouraging as the test frame was constructed using ST37 steel.

The third example (see Figure 11), is chosen to illustrate the progress so far is derived from the restrained beam test in the composite steel frame at Cardington [16]. Although this experiment was initially meant to test one of the internal secondary beams only, it offered considerable insights into the behaviour of steel frame composite structures in fire [17, 18]. The test showed true 3D behaviour and considerable interaction between the longitudinal section of the composite beam (as shown in Figure 12) and the transverse deck slab (in the direction of the slab ribs). However as we are only using a 2D element here, only the longitudinal section shown in Figure 11 will be modelled as a fully composite section.

The composite beam was modelled using 9 DispBeamColumn2dThermal elements (taking advantage of symmetry, so only half the beam length of 9 m was modelled), and further for the sake of simplicity, the analysis uses a single section, which includes the I-section steel, concrete, and rebar. The gap (60 mm depth) is also in placed within the section. The two end nodes are restrained against all translation and rotation except for the vertical translation at midspan. Because of the composite nature of the beam, even with end rotations free, the composite section is able to generate resisting moments at the end, justifying the fixed-end conditions used here. The beam was first loaded using the gravity load used in Cardington. Both parts of the beam were divided into eight fibres (or layers) each and the full temperature history at each fibre was applied in a number of thermal loading stages.

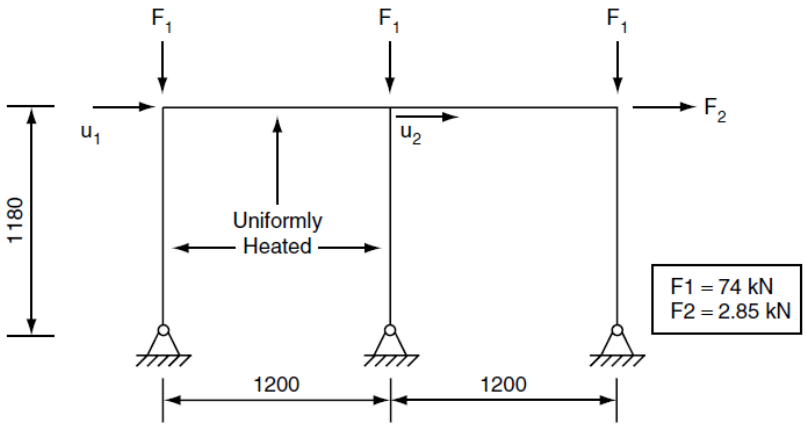

Figure 8. Schematic of the ZSR1 frame test.

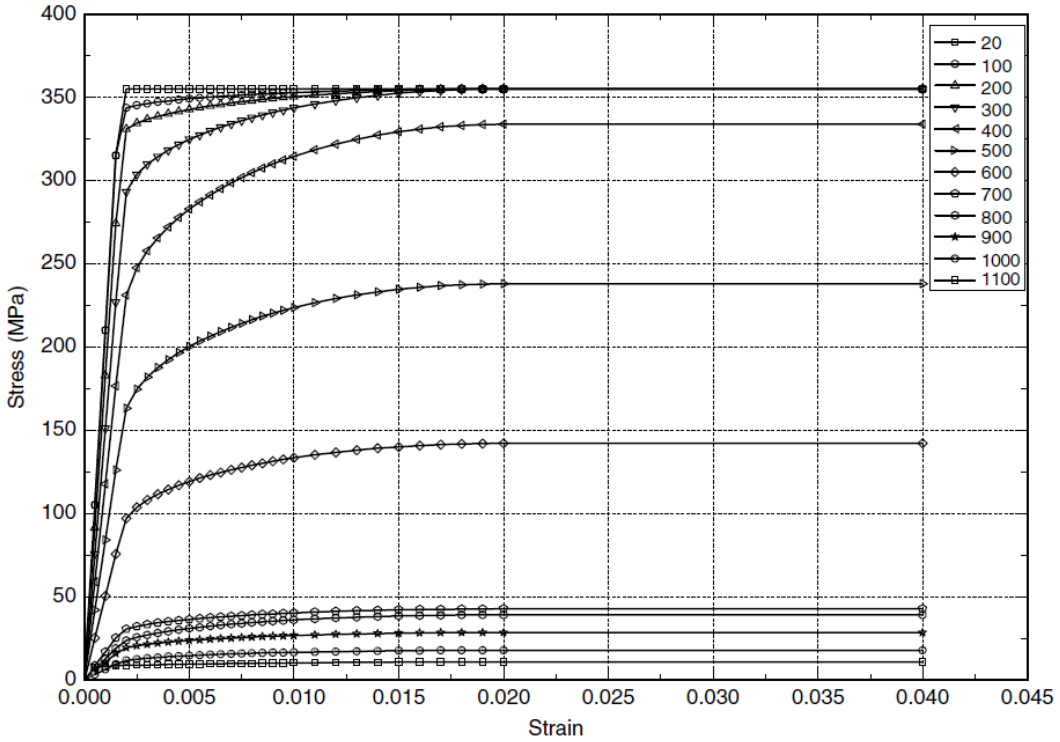

(a) Stress-strain curve of steel in EN 1993 1-2-1 without hardening

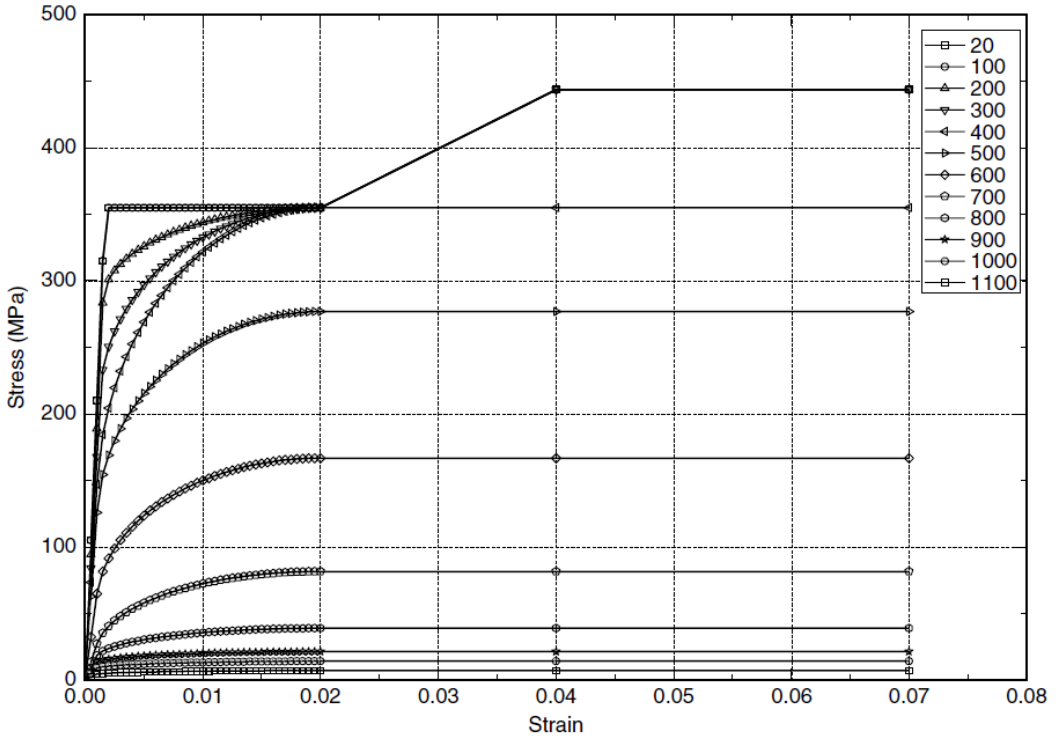

(b) Stress-strain curve of steel in EN 1993 1-2-1 with hardening

Figure 9. (*Continued*)

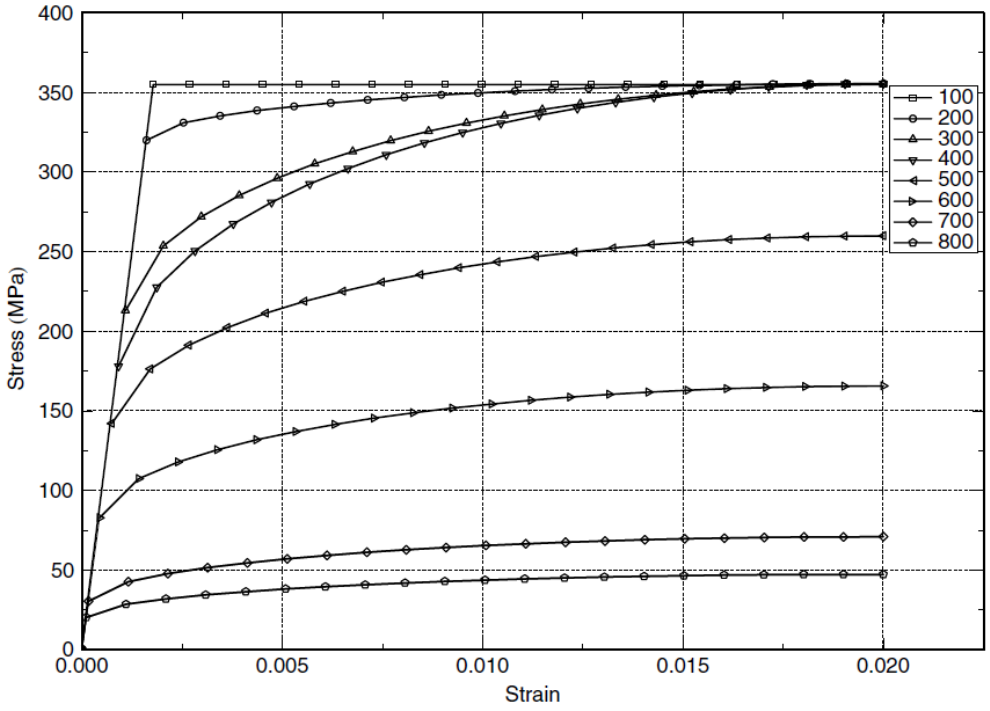

Figure 9. Stress-strain curves of steel used in the ZSR1 frame analysis.

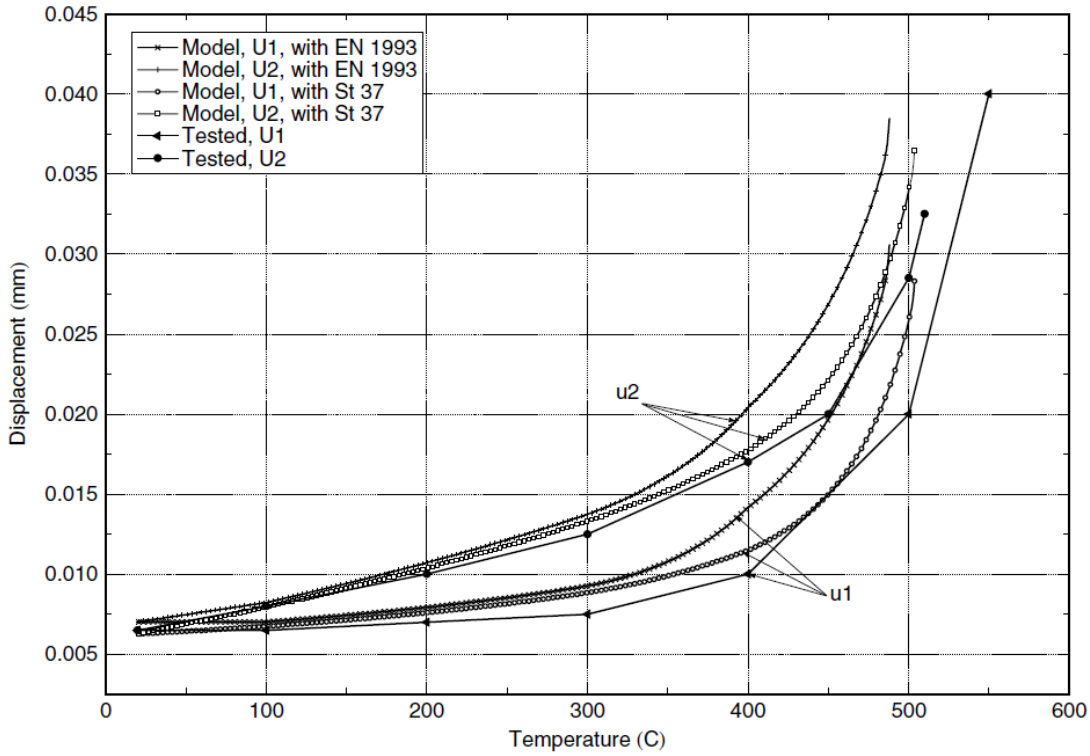

Figure 10. Comparison of results between test and models using different steel properties.

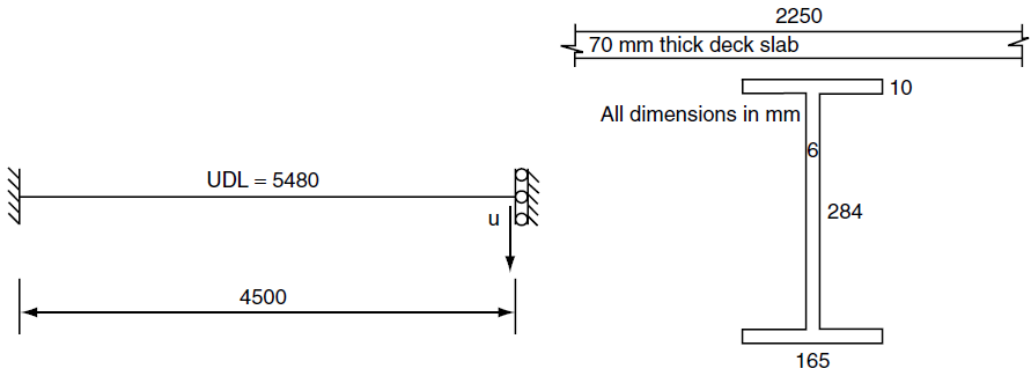

Figure 11. Example problem (derived from the restrained beam test at Cardington).

The analysis result is shown in Figure 12 against the actual test result. The deflections are low at the start however they accelerate after 100°C because of yielding in the steel bottom fibres and large tensile strains in the top concrete layers. The curve dips sharply at around 760°C, due to sharply reducing yield stress and Young's modulus beyond this temperature. The test trace also shows a drop after 800°C, but it is much smaller because the ribs perpendicular to the beam continue to support it and this is also why the deflections from this analysis are much greater than the test and therefore the simulation reported here cannot does not offer a good comparison.

Convergence problems occur in between 600 to 800°C which were solved by replacing the Newton-Raphson algorithm with Modified Newton-Raphson. As reported in [17], the gravity loading contributes little to the total deflection and it only increases or decreases a few millimeters with double or half the udl respectively. Figure 13 shows the variation of the axial reaction force at the end support with temperature. This also shows good agreement with other reported analyses of this test, *e.g.* [17].

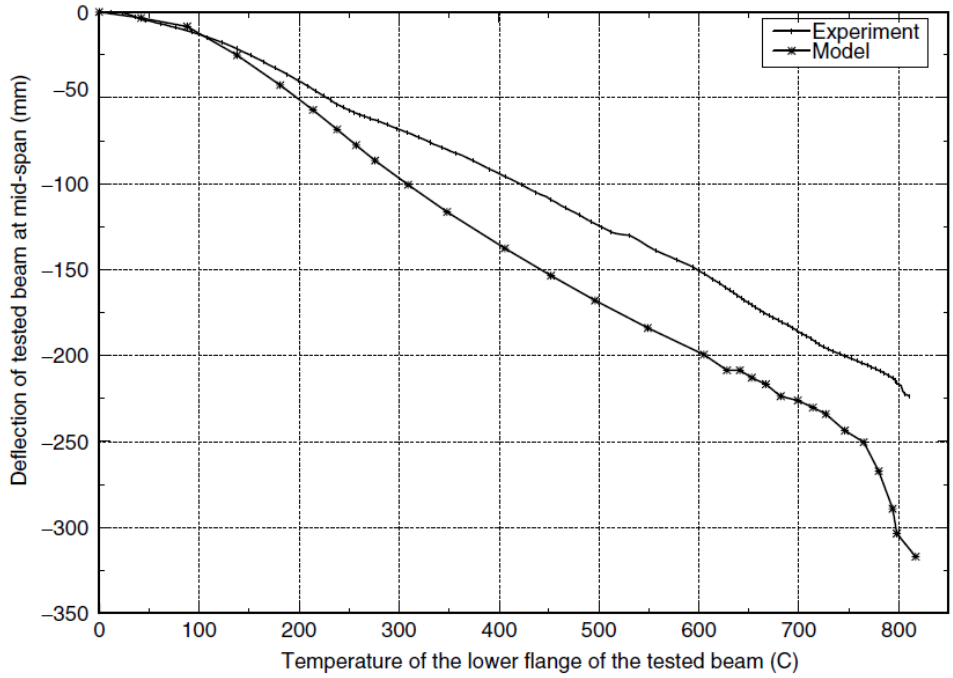

Figure 12. Comparison of OpenSees model against restrained beam test results.

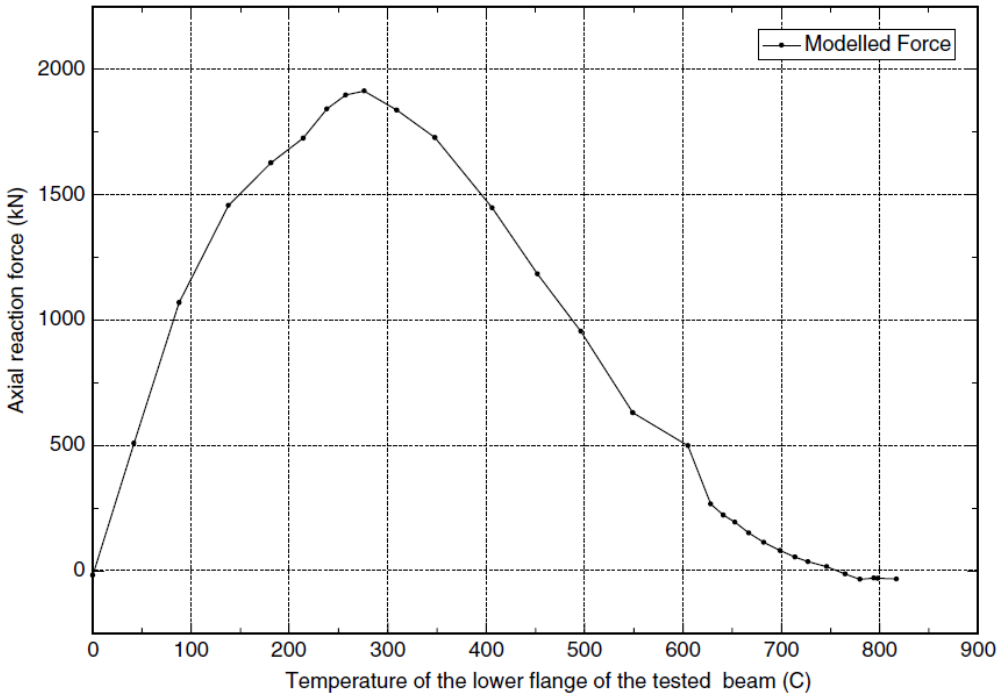

Figure 13. Axial reaction at end support.

7. CONCLUSIONS

It is still very early in the life of this work to make definite conclusions, however a good start has been made in developing an understanding of the OpenSees framework and a comprehensive plan for developing all the new modules has been developed. The code implemented so far has been restricted to mechanical behaviour and this mainly involves creating new classes out of existing OpenSees classes. Even this work is far from complete and early results were presented in the previous section. The work on fire loading and heat transfer will require the addition of an entirely new set of classes to the framework, and this must be done very carefully to remain consistent with OpenSees philosophy and existing structure.

ACKNOWLEDGMENTS

This work is made possible by co-funding of Mr Jian Zhang by the BRE Centre for Fire Safety Engineering (University of Edinburgh) and by Heriot-Watt University. The collaboration between the two universities is organized under the umbrella of the Edinburgh Research Partnership. Thanks are also due to Dr Frank McKenna of UC Berkeley and PEER for his assistance in the developments so far.

REFERENCES

[1] NEES Consortium, Inc. webpage http://www.nees.org

[2] McKenna, F. T., Object-Oriented Finite Element Programming: Frameworks for Analysis, Algorithms and Parallel Computing, PhD thesis, University of California, Berkeley (1997).

[3] Scott, M. H., Fenves, G. L., McKenna, F. and Filippou, F. C., Software patterns for nonlinear beam-column models, *Journal of Structural Engineering*, ASCE, 134:562–571 (2008).

[4] Drysdale, D., An Introduction to Fire Dynamics, John Wiley and Sons 1998.

[5] Collapse of the World Trade Center Building 7, final report, NIST NCSTAR 1–9, WTC Investigation, 2008.

[6] Jowsey, A., Fire Imposed Heat Fluxes for Structural Analysis, PhD thesis, University of Edinburgh (2006).

[7] Masters, I., Usmani, A. S., Cross, J. T. and Lewis, R. W., Finite element analysis of solidification using object-oriented and parallel techniques, *International Journal for Numerical Methods in Engineering*, 40:2891–2909 (1997).

[8] Welch, S., Miles, S. D., Kumar, S., Lemaire, T. and Chan, A., "FIRESTRUC - Integrating advanced three-dimensional modelling methodologies for predicting thermo-mechanical behaviour of steel and composite structures subjected to natural fires", *Fire Safety Science*, 9: 1315–1326 (2009).

[9] Gawin, D., Pesavento, F. and Schrefler, B. A., Modelling of hygro-thermal behaviour of concrete at high temperature with thermo-chemical and mechanical material degradation, *Comput. Methods Appl. Mech. Engrg.*, 192:1731–1771 (2003).

[10] Ervine, A. A., The effect of tensile cracking on thermal diffusivity, internal communication, University of Edinburgh (2009).

[11] Khoury G. A., Grainger B. N. and Sullivan P. J. E., Strain of concrete during first heating to 600ºC under load, *Magazine of Concrete Research*, 37:195–215 (1985).

[12] Neilsen, C. V., Pearce, C. J. and Bicanic, N., Theoretical model of high temperature effects on uniaxial concrete member under elastic restraint, *Magazine of Concrete Research*, 54:239–249 (2002).

[13] Neuenhofer, A. and Filippou, F. C., Geometrically nonlinear flexibility-based frame finite element, *Journal of Structural Engineering*, ASCE, 124:704–711 (1998).

[14] Gamma, E., Helm, R., Johnson, R., & Vlissides, J. (1995). *Design patterns: elements of reusable object-oriented software* (p. 395). Addison-Wesley, Reading, MA.

[15] Rubert, A. and Schaumann, P., Structural steel and plane frame assemblies under fire action, Fire Safety Journal, 10:173–184 (1986).

[16] O'Connor, M. A., Martin, D. M., Behaviour of a multi-storey steel framed building subjected to fire attack *Journal of Constructional Steel Research*, 46:1–3 (1998).

[17] Sanad, A. M., Rotter, J. M., Usmani, A. S. and O'Connor, M. A., Composite beams in large buildings under fire numerical modelling and structural behaviour, *Fire Safety Journal*, 35: 165–88 (2000).

[18] Usmani, A. S., Understanding the Response of Composite Structures to Fire, *Engineering Journal*, AISC, 42:83–98 (2005).

Structures and Buildings
Volume 165 Issue SB7

Full-scale testing of a damaged reinforced concrete frame in fire
Sharma, Bhargava, Singh *et al.*

ice | proceedings

Proceedings of the Institution of Civil Engineers
Structures and Buildings 165 July 2012 Issue SB7
Pages 335–346 http://dx.doi.org/10.1680/stbu.11.00031
Paper 1100031
Received 21/03/2011 Accepted 02/12/2011
Keywords: concrete structures/fire engineering/seismic engineering, safety and hazards

ice Institution of Civil Engineers publishing

Full-scale testing of a damaged reinforced concrete frame in fire

1 **Umesh Kumar Sharma** PhD
Assistant Professor, Department of Civil Engineering, Indian Institute of Technology (IIT), Roorkee, India

2 **Pradeep Bhargava** PhD
Professor, Department of Civil Engineering, IIT, Roorkee, India

3 **Bhupinder Singh** PhD
Assistant Professor, Department of Civil Engineering, IIT, Roorkee, India

4 **Yogendra Singh** PhD
Associate Professor, Department of Earthquake Engineering, IIT, Roorkee, India

5 **Virendra Kumar** MEng
PhD Student, Department of Civil Engineering, IIT, Roorkee, India

6 **Praveen Kamath** MS
PhD Student, Department of Civil Engineering, IIT, Roorkee, India

7 **Asif Usmani** PhD, CEng
Professor, School of Engineering, University of Edinburgh, Edinburgh, UK

8 **Jose Torero** PhD, FREng
Professor, School of Engineering, University of Edinburgh, Edinburgh, UK

9 **Martin Gillie** PhD, CEng
Lecturer, School of Engineering, University of Edinburgh, Edinburgh, UK

10 **Pankaj Pankaj** PhD
Senior Lecturer, School of Engineering, University of Edinburgh, Edinburgh, UK

11 **Ian May** PhD, CEng
Professor, School of Built Environment, Heriot-Watt University, Edinburgh, UK

12 **Jian Zhang**
PhD Student, School of Built Environment, Heriot-Watt University, Edinburgh, UK

Fires are a relatively likely event following earthquakes in urban locations and in general are an integral part of the emergency response strategies, which are focused on life safety in most developed economies. Similarly, building regulations in most countries require engineers to consider the effect of seismic and fire loading on structures to provide an adequate level of resistance to these hazards; however, this is only on a separate basis. To the authors' knowledge there are no current regulations that require buildings to consider these hazards in a sequential manner to quantify the compound loading and design for the required resistance. This paper provides a first and early report from a novel set of tests on a full-scale reinforced concrete frame subjected to simulated earthquake and fire loads. The results from the first test indicate that the test frame could withstand a pre-damage corresponding to a seismic performance level and subsequent 1 h fire exposure without collapse. Important observations have been made about the development of temperatures and displacements in the various structural elements during the mechanical loading and subsequent fire excursion.

1. Introduction

The risk of fires in the aftermath of earthquakes is well known. The fires following the 1906 San Francisco and the 1923 Tokyo earthquakes led to major conflagrations and widespread devastation, resulting in far greater damage than caused by the original shaking. Fortunately, the scale of those events has not been repeated; however, there have been many major earthquakes that have been followed by fires. Nearly all major Californian earthquakes have been followed by multiple ignitions, most notably the 1971 San Fernando and 1994 Northridge earthquakes, which were both followed by over 100 ignitions. The 1995 Hanshin (Kobe) earthquake was also followed by over 100 ignitions in Kobe city and a similar number of fires in other cities in a highly populated area (over

2 million people), and several conflagrations developed. Scawthorn *et al.* (2005) provide a relatively comprehensive treatment of the post-earthquake fires from an emergency response, societal preparedness and disaster mitigation point of view and include discussions of the major historical fire-following-earthquake (FFE) events.

Another fact that emerges rather starkly from the study of FFE events is that the risk of FFE is very non-uniform. Many recent earthquakes were not followed by widespread fire events, for example 1999 Izmit (Turkey) (although a number of crude and naphtha tanks burned), 2001 Gujarat (India), 2005 Kashmir (Pakistan and India) and 2008 Wenchuan (China) earthquakes were not followed by significant fire events. The level of urbanisation and industrialisation is an obvious factor which possibly explains this anomaly (most certainly for the relatively remote and backward mountainous regions of Kashmir – even here, however, the main market in the town of Uri suffered a major fire following the earthquake, which caused extensive damage). If urbanisation (and concomitant density of gas, fuel and electrical supply networks) is indeed one of the key reasons, the risk of fire after earthquakes must then be considered as a rapidly increasing risk to life, livelihoods and to the sustainability of growth and development in some of the world's most densely populated regions. With an increasing integration of the world economy, major disasters of the future could have repercussions far beyond the local region. FFE events have the potential to create such disasters and should certainly be considered in the overall disaster mitigation strategies by governments and agencies with such a remit. Considerable new research effort is required to properly address the challenge posed by FFE events, some of which are discussed by Botting (1998), Cousins *et al.* (1991), Robertion and Mehaffey (2000) and Usmani (2008).

This paper will describe the progress on a collaborative project involving a number of institutions in India and the UK (2008–2011). The key aim of this project has been to carry out possibly the first ever large-scale tests to understand the behaviour of damaged reinforced concrete (RC) frames in fire. Considerable new understanding was gained on the behaviour of steel-framed composite structures in fire from the Cardington test in the mid-1990s (British Steel, 1999) and a large collaborative project on the computational modelling of the tests (Lowes *et al.*, 2004). It is expected that these tests will help generate similarly useful information on the behaviour of damaged and undamaged RC structures subjected to fire.

After a great deal of preparation, these tests began in February 2011 and the full test programme is intended to end by summer 2011. The programme is expected to produce a great deal of new information and experimental data on the behaviour of damaged RC structures in fire, which should be of considerable international interest to researchers and practitioners in structural engineering. The project team has, therefore, set up a round-robin modelling exercise. The exercise requires participants to predict aspects of behaviour witnessed in the test programme described above. It is hoped that all those who attempt to model the test will in due course also participate in a workshop to be organised in India and present their results (which will be published in a compendium). The full experimental results will be made available to all participants at the workshop (and published on the workshop webpage).

2. The plan for large-scale testing of damaged RC frames

Tests were planned on a number of identical RC frames consisting of four columns (3 m apart in plan) supporting four beams and a slab, all monolithically constructed, at a dedicated testing facility on the campus of the Indian Institute of Technology (IIT), Roorkee in India. These frames were proposed to be subjected to cyclic quasi-static loading against a reaction wall, which would provide a reasonable simulation of the damage expected to occur under real seismic loads. Table 1 shows the planned tests. The first frame test was aimed to subject the frame to displacement beyond the peak lateral force. The frame would then be exposed to fire capable of attaining a temperature up to 1000°C or beyond. The frame would subsequently be subjected to further loading to evaluate its residual capacity in each case. While the second frame test aims to evaluate the fire damage on an undamaged frame, the third test is planned to introduce an 'intermediate' damage level that would correspond to a certain (x) percentage of the horizontal slab displacement achieved at the peak lateral force obtained in the first test.

The first test on the frame has already been carried out as planned.

Test no.	Simulated seismic damage	Fire loading	Aftermath
1	Displacement beyond peak lateral force	900–1000°C[a]	Residual lateral capacity test[a]
2	None	900–1000°C for 1 h	Residual lateral capacity test
3	'Intermediate' damage (x% of the displacement corresponding to peak lateral force)	900–1000°°C for 1 h	Residual lateral capacity test

[a] For as long as considered safe.

Table 1. Frame tests planned

Initially, the frame was subjected to a simulated seismic damage. The initial seismic damage was achieved by inducing a pre-planned lateral displacement through applying lateral cyclic load. The planned lateral displacement corresponds to the life safety level of FEMA 356:2000 (FEMA, 2000). Figure 1 shows a schematic diagram of the front elevation of the test frame set-up with key dimensions. The frame was tested on a 1·2 m thick raft of dimensions 6·75 m × 8·55 m (Figure 1a). The lateral load was

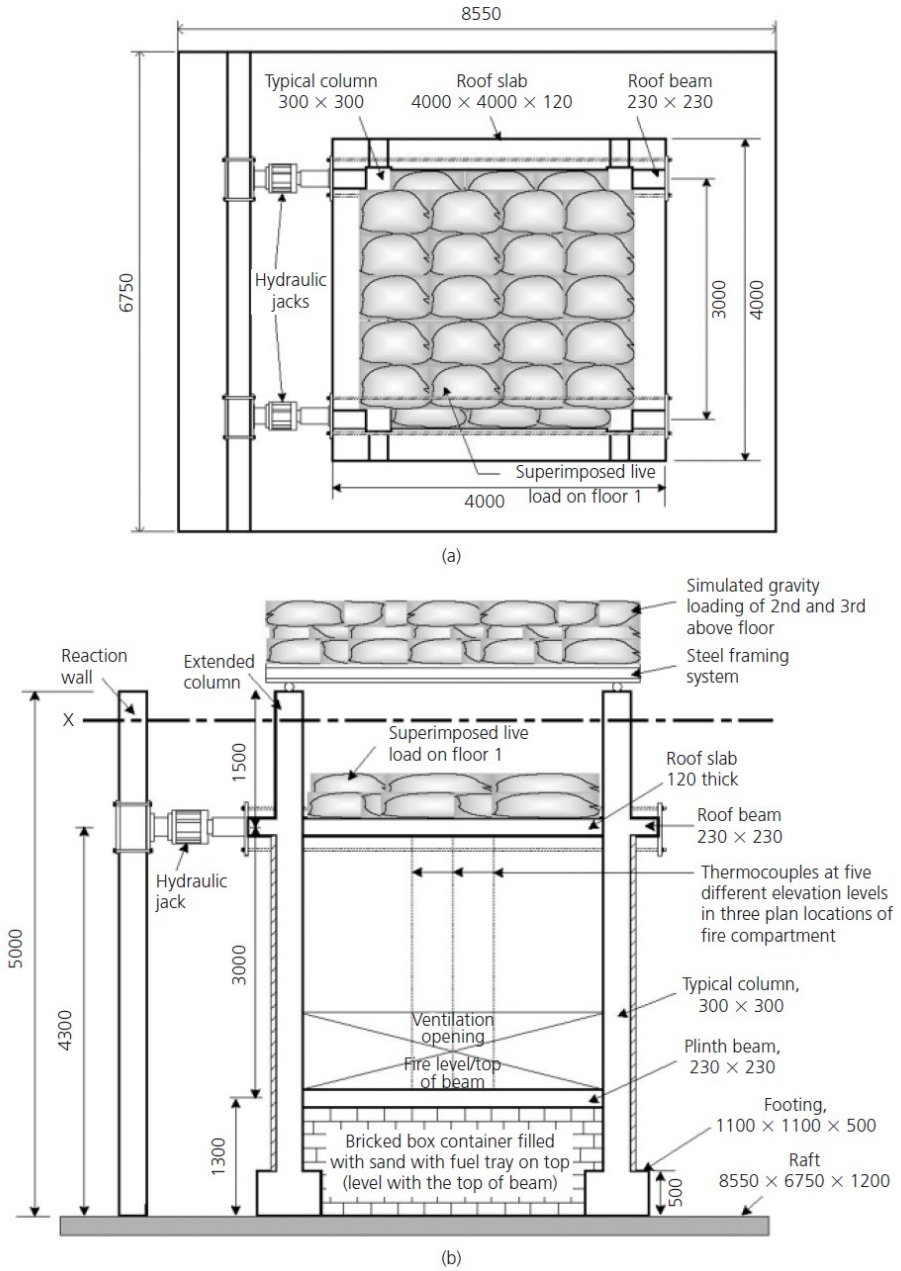

Figure 1. Schematic view of the test set-up: (a) plan of the test set-up; (b) elevation of the test set-up (all dimensions in mm)

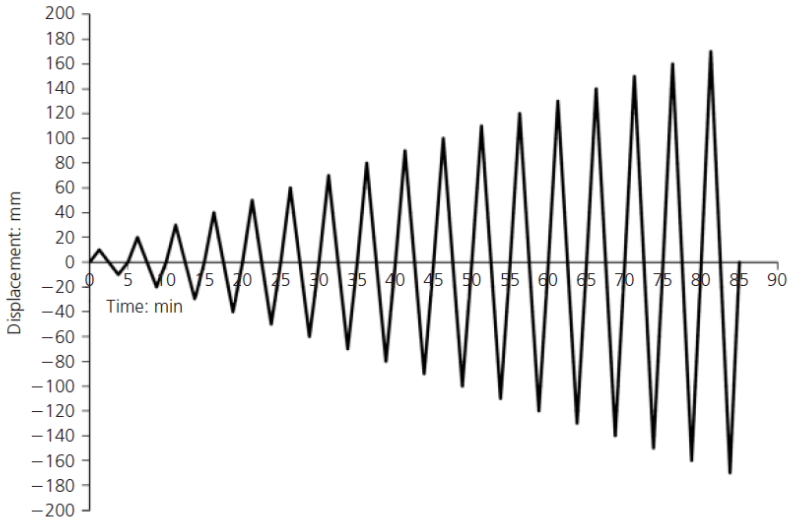

Figure 2. Incremental cyclic loading of the frame; roof displacement plotted against time

applied through jacks, which were mounted on a vertical reaction wall. Subsequently, the frame was exposed to fire of 1 h duration. Detailed thermal and mechanical histories were recorded during the initial loading and subsequent fire. Thermocouples embedded at three different locations in plan and at five layers along the section of the beams recorded the temperature history. The displacements were also measured by erecting a secondary steel frame around the test frame, during both the initial damage-inducing phase and the fire phase. Particle image velocimetry (PIV) equipment (high-resolution digital camera and image analysis software) was also used to create an independent set of data for comparison with the mechanical data using traditional methods.

3. Fire testing

The fire compartment of size 3 m × 3 m × 3 m was constructed using detachable panels made of fire-proof materials commonly used in brick kilns in India. This was expected to allow repeated use of the panels for the whole testing programme and beyond. The fire was continuously fed by a 1 m square tray of kerosene in the compartment with a 1 m high opening along the full length of the wall at the bottom of one side (Figure 1). To maintain a post flashover temperature of 900–1000°C the peak burning rate for the chosen opening configuration was approximately 0·117 kg/m^{2}s. This required a peak flow rate of kerosene into the tray of $1{\cdot}43 \times 10^{-4}$ m^3/s which was maintained using a fixed head. About 0·51 m^3 of kerosene was required for maintaining the post-flashover temperatures within the above range for 1 h. The chosen configuration was designed to achieve flashover within 5 min.

Thermal instrumentation for the compartment consisted of three thermocouple trees in the fire compartment to capture the gas temperature history inside the compartment during the fire testing phase. Adequate numbers of thermocouples were also embedded in the structural members to obtain detailed structural temperature evolution for the whole heating and cooling cycle. A number of mock fire tests were carried out at the location of the test to ensure that the expected fire behaviour was achieved and was repeatable. The first mock test was carried out in July 2009, and did not succeed, as the brickwork walls were very damp because of rain, so much of the radiant heat from the fire was absorbed by the wall, leading to an inordinate delay in flashover and low peak temperatures. The test was repeated in November 2009 and this time the results were as expected, as shown in Figure 3. This, however, was not expected to be an issue for the actual tests as the compartment was made up of waterproof insulating panels.

4. Computational modelling

The frame was designed as part of a four-storey building frame located in seismic zone IV according to Indian Standard IS 1893: Part 1 (BIS, 2002). India has been divided into four earthquake-prone zones: Zone II–Zone V, based on their occurrence. Zone IV corresponds to a severe intensity zone prone to major property damage and a zone factor of 0·24 is considered. The beam and column reinforcement detail obtained from the first design cycle is shown in Figure 4. The design was also checked against Eurocode 8 (CEN, 1998) and found to be sufficiently ductile to withstand the assumed earthquake loading.

To ensure that the design did indeed provide adequate ductility, a number of different numerical models of the test frame were developed to investigate the expected behaviour of the frame under the imposed quasi-static displacements (Figure 2).

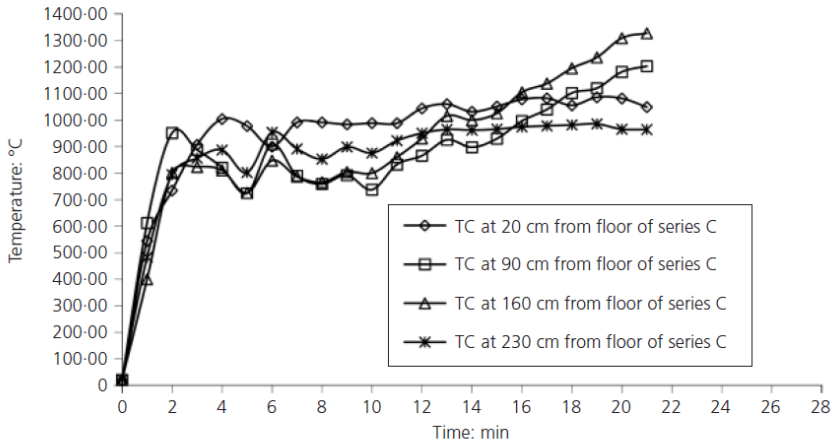

Figure 3. Temperatures inside the fire compartment (near the centre of the back wall opposite to opening)

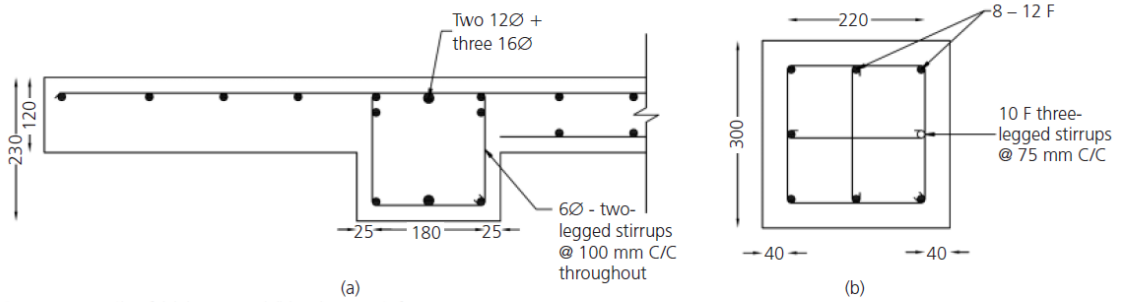

Figure 4. Details of (a) beam and (b) column reinforcement (dimensions in mm)

Although not explicitly stated in the standard, it was expected that if the code-based design recommendations were followed, strong-column weak-beam type behaviour would be obtained, that is the first hinge would form in the beams. A simple plastic analysis showed that this was not the case for the one-storey test structure and this was later confirmed by more detailed finite-element frame analyses, as shown in Figure 5.

There are two main reasons for this discrepancy: first, the design is based on a four-storey structure where the beam moments at the joints are balanced by the sum of moments in two columns (upper and lower), while for the single-bay single-storey structure the moments in the beam and column must be the same; second, frame analysis, which is the usual method for analysing structures under earthquake loads, does not fully account for the significant additional moment capacity from the monolithic slab acting compositely with the beam.

This issue was discussed in detail between the UK and Indian teams and it was decided to revise the design to produce a more desirable 'seismic' behaviour and ensure that first hinge formation occurs in the beam. The reinforcement in the column was increased (to eight 20 mm dia. bars) and that in the beam was decreased (to three 16 mm dia. bars top and bottom). Now the results from a single-storey frame model analysis in the SAP2000 software package (SAP) showed that first hinges formed in the beams; however, a more detailed Abaqus finite-element model (using brick elements for columns, beams and slabs) was still inconclusive, with plastification starting at joints (as shown in Figure 6) where the beam is composite with the slab (lower beams without slabs clearly formed hinges first). The revised design was, however, adopted.

5. Peak load and displacement

The computational models also allowed estimates of peak lateral load and displacement curves to be made. The peak load from a plastic analysis calculation for the original frame (before the modification mentioned above) was found to be approximately 140 kN. Figure 7 shows the results from 'pushover' type analyses

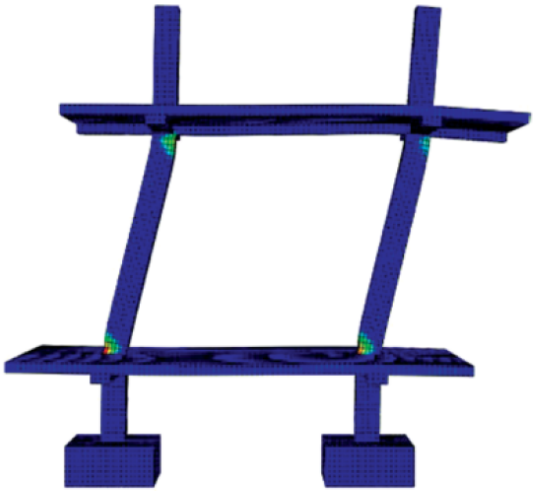

Figure 5. Finite-element model of the frame showing hinges in columns

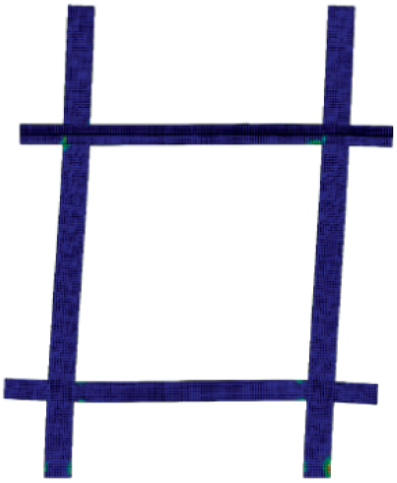

Figure 6. Finite-element model of the modified RC frame (with stronger columns and weaker beams)

carried out using two different software packages and using different types of models based on the modified design. Figure 7(a) shows the results from a quasi-static non-linear SAP frame model and Figure 7(b) shows the results from two non-linear dynamic finite-element models (using Abaqus). The two Abaqus analyses (with the same data) were carried out using the 'implicit' dynamic procedure and the conditionally stable 'explicit' dynamic procedure, both of which produced similar results (with the explicit procedure taking significantly large computing

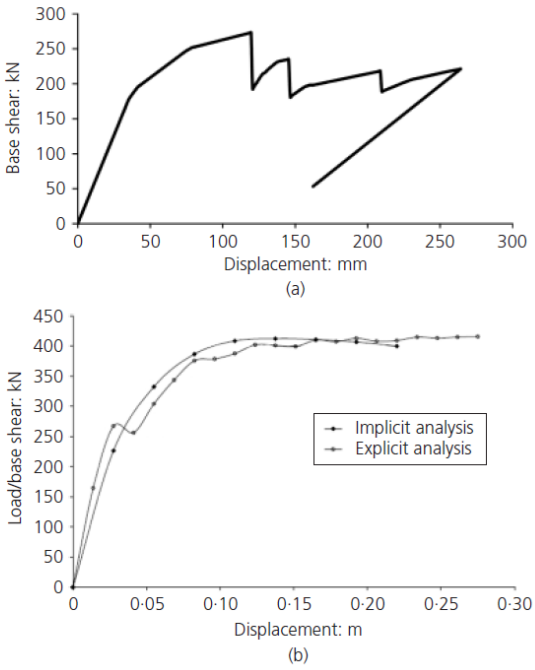

Figure 7. Load–displacement curves from (a) frame model and (b) detailed finite-element model

time). The Abaqus models seem to overestimate the peak load considerably; however, at a displacement of roughly 50 mm the two models are somewhat in agreement (200 kN and 260 kN); the displacements at peak load are also similar (~100 mm). It is likely that the Abaqus model, constructed of brick elements, is over-stiff (despite using non-conforming elements and a relatively fine mesh). An Abaqus beam and shell model provided results comparable to the SAP model. These two preliminary analyses were primarily carried out to obtain upper and lower bound estimates of the frame load displacement response for planning the experiment properly and to obtain useful data on the capacity and stroke lengths of the loading jacks required to carry out the damage-inducing cyclic loading for the frame. A more detailed predictive analysis is reported in the next section.

6. Predictive models

A number of further analyses are also being carried out to predict the actual test behaviour of the frame. This is being done using software such as Abaqus and OpenSees (modified by the University of Edinburgh team to include thermal loading). These analyses are simulating the cyclic loading procedure, where the displacements will be applied in both directions in increasingly larger increments (Figure 2) until the displacement corresponding to the peak load has been achieved. The simulations are then continued to the fire loading phase based on the temperatures

obtained in the mock tests (Figure 3). This work will be reported in much more detail in a number of separate reports and papers; however, brief results from one of the predictive models (using OpenSees) are presented here.

The fire loading was based on a considerable simplification of the temperature field shown in Figure 3. The fire was assumed to be represented by a constant temperature of 1000°C at the boundaries of the structural members applied for 1 h. A one-dimensional heat transfer analysis was carried out to determine the temperature evolution in the structural members, which was then used to determine the mechanical response (after the damage-inducing cycle).

Figure 8 shows the lateral (or horizontal) displacement of the frame through five cycles of loading, which produces a peak load of roughly 250 kN, corresponding to a displacement of approximately 76 mm, which agrees reasonably well with the SAP 'pushover' analysis of Figure 7. Figure 8 also shows that a permanent 'drift' of approximately 19 mm (leftward) occurred at the end of the cyclic loading.

Figure 9(a) shows the vertical displacement of the mid-span of the top beam (node 3) during the fire loading phase, and Figure 9(b) shows the horizontal displacement of the end nodes (nodes 1 and 2) of the top beam during the fire phase (both continuing from the permanent residual displacements at the end of the cyclic displacement). Both figures are plotted to start from the point where the nodes were located at the end of the gravity and cyclic loading stages. Therefore, node 3, in Figure 9(a), was displaced in the positive direction (upward) and nodes 1 and 2, in Figure 9(b), were displaced in the negative direction (leftward) at the end of the cyclic loading. The initial displacement of node 1 in Figure 9(b) is the same as the drift mentioned for Figure 8, above. An interesting and counterintuitive feature of behaviour from this analysis is that during the early phase of the fire, the

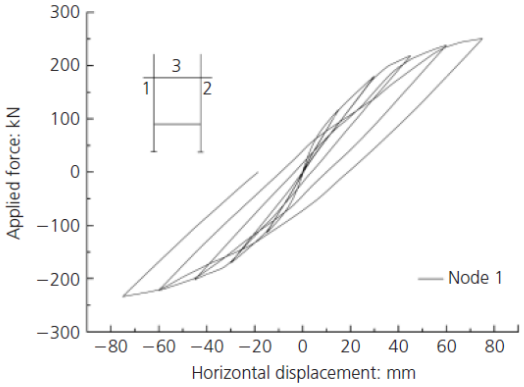

Figure 8. Horizontal displacement of node 1 under quasi-static cyclic loading

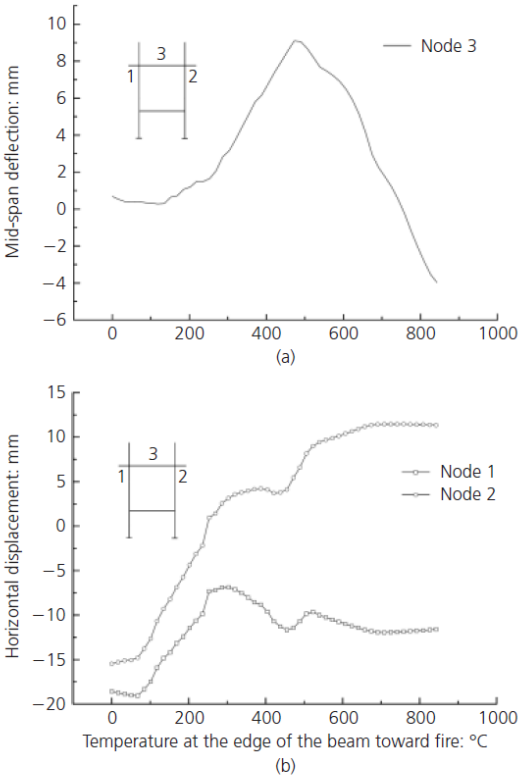

Figure 9. Displacements during the fire loading phase: (a) node 3 at mid-span of top beam; (b) at nodes 1 and 2

frame as a whole moves towards becoming more 'upright'. The permanent lateral 'drift' at the end of the cyclic loading of about 19 mm is initially reduced to about 7 mm when the exposed surface of the beam reaches approximately 300°C, which suggests a 'stiffening' of the frame. After this, however, the drift begins to increase again, but plateaus out by the end of the heating.

7. Preliminary test results

This section presents some key results of the first test conducted in March 2011. A pre-planned mechanical damage in the form of 2% of the storey height (FEMA 356, FEMA, 2000) was introduced in the frame by applying lateral quasi-static cyclic loading. Seven incremental lateral displacement cycles of equal push and pull were applied using the loading jacks, as explained earlier. Figure 10 shows the recorded lateral load–displacement response of the test frame. A maximum displacement of 95 mm in push and 85 mm in pull was registered, corresponding to load levels 316 kN and 267 kN, respectively. After each cycle of push and pull, a careful visual inspection was carried out to locate cracks and spalls, if any. All the cracks were graded with permanent markers. No cracks were noticed up to a lateral displacement of

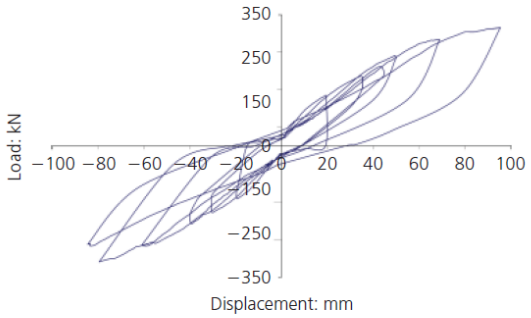

Figure 10. Test load–displacement response of frame

20 mm. However, first visible cracks were observed at the ends of the roof beams aligned parallel to the direction of loading after the third cycle of push and pull and at a displacement of 30 mm. In subsequent cycles, these cracks propagated and further cracks were observed in beams and columns as well. The cracks were observed to be more pronounced at the beam–column joints. However, the frame remained structurally stable after the initial mechanical test.

Although the permanent residual displacement after the cyclic loading phase matched well with the OpenSees prediction of approximately 20 mm, the 'pinching' effect clearly visible in the test results was not predicted by the computer model. The model was rerun with an OpenSees 'pinching material' (Lowes *et al.*, 2004) used for all elements adjacent to the joints. This produced a more realistic comparison with the test, as shown in Figure 11. Figure 12 shows exaggerated displaced shapes of the frame after (a) cyclic loading and (b) fire loading. Figure 12 shows the frame displaced shapes at the end of the cyclic displacements and at the end of fire. The displaced shape (b) is more reliable than (a), as the fire-induced displacements cannot be modelled properly by a two-dimensional model (more comprehensive three-dimensional models are currently being developed and will be reported in due course). Nevertheless, Figure 12 clearly shows that the frame as a whole does move towards becoming more 'upright' (as predicted by the previous model shown in Figure 9) and some of the drift is

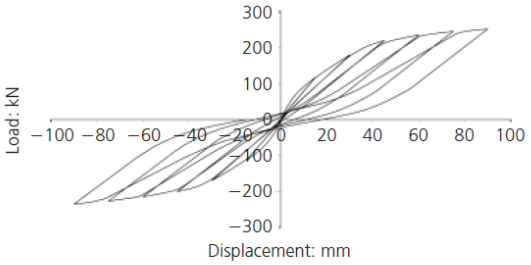

Figure 11. Modelled load displacement using 'pinching material' (OpenSees analysis)

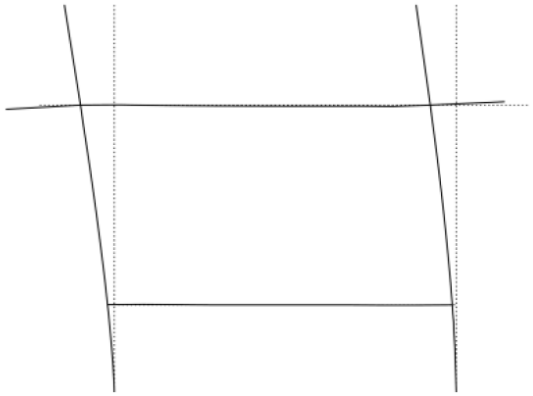

(a)

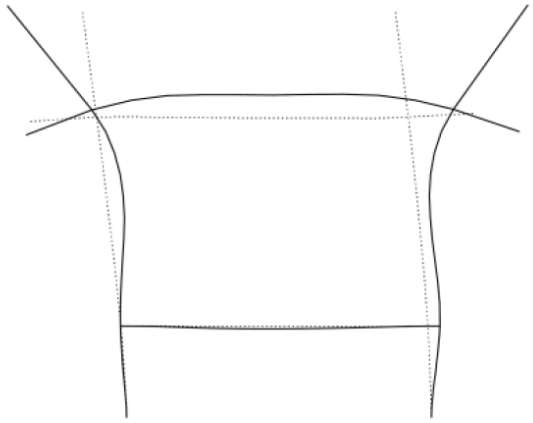

(b)

Figure 12. Frame displaced shapes (magnified 20 times): (a) at the end of the cyclic displacements; (b) at the end of fire

recovered. However, it is notable that the drift recovery is much less in this model (more consistent with the test results), suggesting that hysteretic damage has been relatively more accurately modelled by using the pinching material. Figure 12(b) also clearly shows the effect of thermal expansion. Figure 13(b) shows the lateral displacement of nodes 1 and 2 of the frame for the updated model (corresponding to Figure 9(b)). The increasing relative displacement between nodes 1 and 2 is because of thermal expansion.

Four days after the cyclic loading, the pre-damaged test frame was exposed to fire. The fire test was performed for the planned duration of 1 h. The desired temperature–time behaviour, as achieved in mock fire tests earlier (Figure 3), could be obtained precisely, and full-blown fire with flashover was attained within 8–10 min. The sound of concrete spalling off from the roof slab

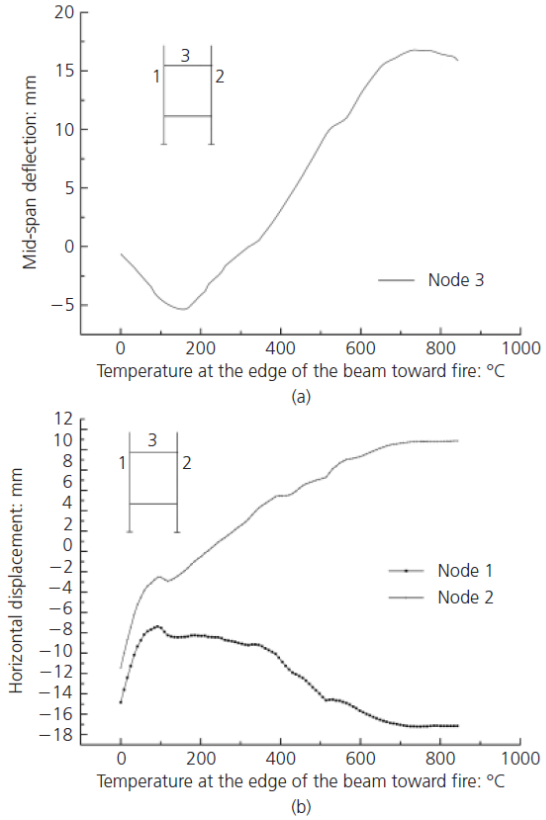

Figure 13. Displacements during the fire loading phase for the updated model: (a) node 3 at mid-span of top beam and (b) at nodes 1 and 2

could be heard clearly after 5 min from initial ignition, continuing for another 15 min. The spalling sounds corresponded to temperatures between 300 and 400°C. Later, the spalling of concrete was observed in beams and columns as well. The geo-PIV system did not perform well during the fire test owing to high temperatures and much reduced visibility because of the smoke. A detailed visual inspection of the frame was undertaken the next day after the frame had cooled down. Considerable damage was noticed in the slab in terms of spalling of concrete and resultant exposure of reinforcement. A maximum fire-induced vertical displacement of 46 mm was recorded in the roof slab. The beams and columns suffered considerable spalling on exposed surfaces, but only at a few locations; however, widespread cracks could be clearly marked in these elements. An attempt was made to drill a core for the purpose of conducting a core compression non-destructive test; this was, however, rendered impossible by disintegration of concrete all along the exposed surface. The frame was still able to withstand the 1 h fire exposure without losing structural integrity in terms of complete collapse. Temperature–time curves

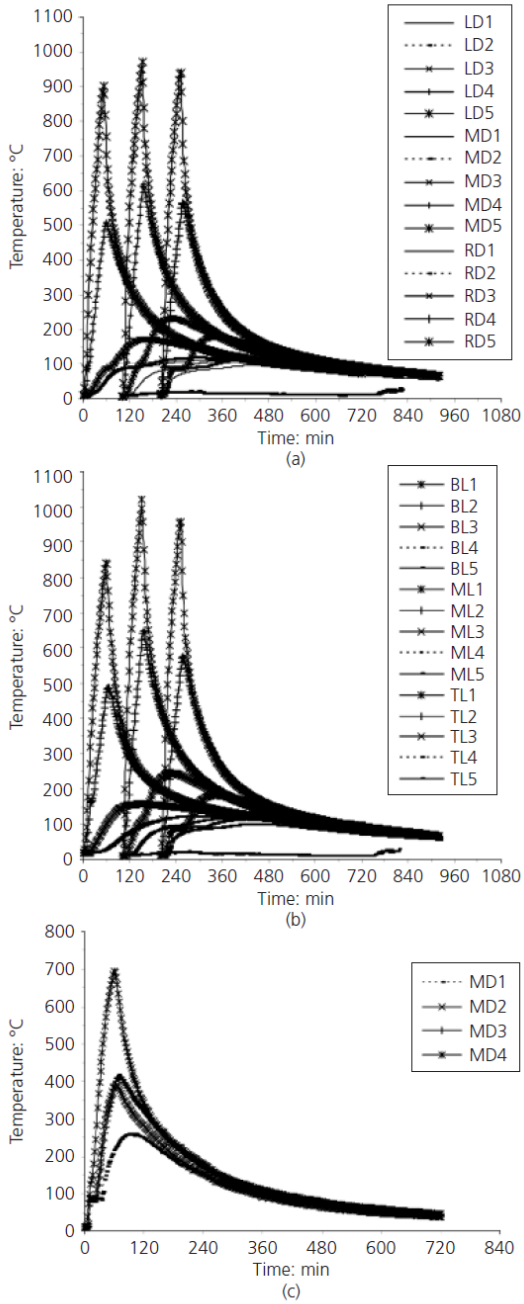

Figure 14. Temperature–time curves for: (a) typical beam (near joints and centre); (b) typical column (at ends and centre); (c) centre of slab (B – bottom of the column; T – top of the column; R – right of the beam near the joint; L – left of the beam near the joint; M – middle/centre of the beam; D1–D5 – depths at each location)

for typical members of the test frame are shown in Figures 14(a)–14(c). Maximum temperatures were recorded at the centre of the beam (972°C) and column (1002°C). Figure 14 also shows the thermal gradients existing in the beams, columns and slab by showing temperatures in deeper layers of concrete against the hottest (surface) temperature. Figure 15(a) shows the frame after pre-damage attributable to mechanical loading, and Figures 15(b) and 15(c) show the frame subjected to fire and its condition after the fire, respectively. Figure 16 and Figure 17 show typical crack patterns as noticed on columns and beams, respectively, after seven cycles of mechanical loading. Cracks were marked on the members after each cycle of displacement to highlight their initiation and propagation.

8. Conclusion

This study provides a first and early report from a novel set of tests never previously attempted. The main aim of the paper is to make the structural engineering community aware of this programme and draw their attention to this complex and potentially destructive problem. This paper presents the results of the first of the series of tests planned to be conducted under the test programme. Further tests are planned for summer and autumn of 2012. The data from all the tests will be carefully analysed, including comparisons with computational models, and will be reported in detail in reports and technical articles submitted to appropriate symposia and journals.

The results from the first test indicate that the test frame could withstand the mechanical damage and subsequent fire without collapse. As expected (based on the design modifications) the damage during initial mechanical loading phase was first noted in beams rather than in columns. The observed load–displacement response was predicted reasonably well by OpenSees and SAP computer models in terms of the peak load and the corresponding displacement for the initial cyclic loading phase. The permanent residual displacement of approximately 20 mm after the cyclic loading phase also seems to match well with the OpenSees prediction. The 'pinching' effect clearly visible in the test results was not predicted by the first OpenSees model; however, attributing OpenSees 'pinching' material to elements next to the joints produced an acceptable pinching response with the same drift at the end of the cyclic loading analysis.

One of the key lessons that has been learnt so far is perhaps typical of any large-scale testing programme, namely the unpredictability of the whole process. It is difficult to foresee all the problems that may occur in advance.

Acknowledgements

This work has been funded by the UK–India Education and Research Initiative (UKIERI). The authors would like to thank Adam Ervine and Mariyana Aida Abdel-Kadir for carrying out some of the analyses reported in this paper. The authors are also

Figure 15. (a) Pre-loaded frame before fire; (b) fire test in progress; (c) fire-damaged frame after test

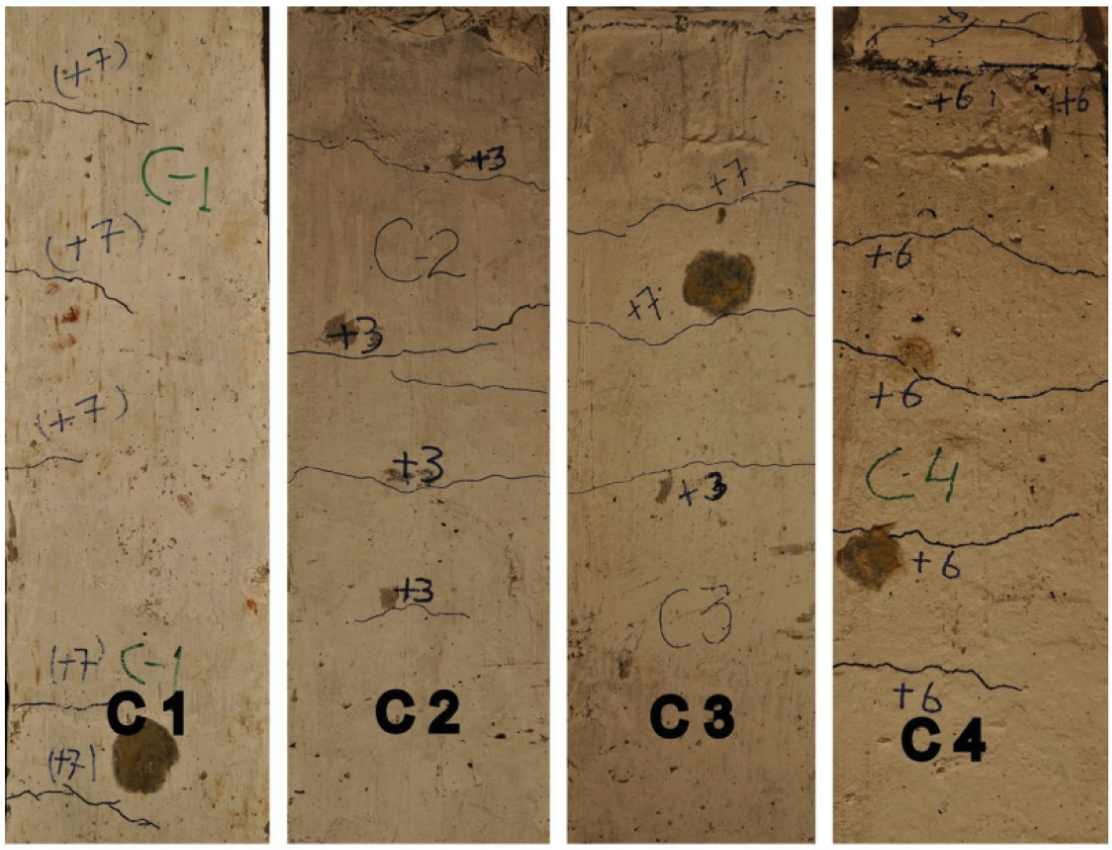

Figure 16. Crack patterns in columns attributable to pre-loading

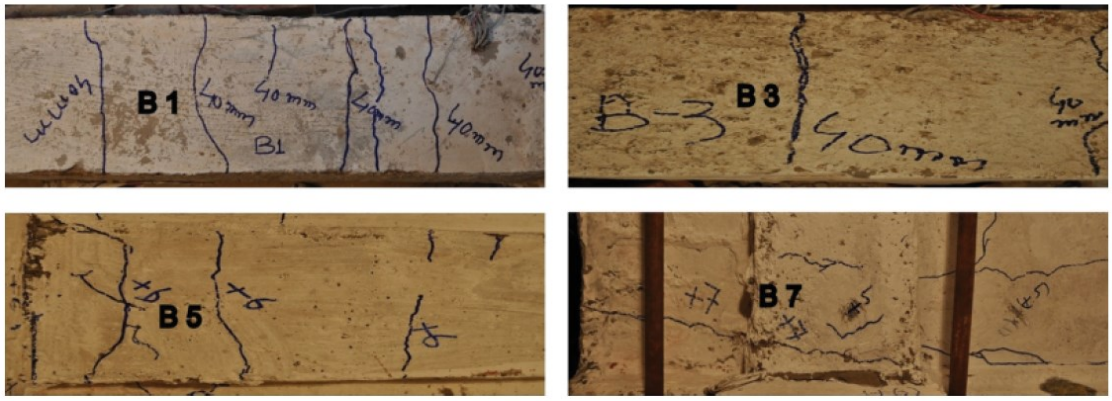

Figure 17. Crack patterns in beams attributable to pre-loading (+3, +4, +6 and +7 markings on the beams indicate cracks initiated at displacements of 30 mm, 40 mm, 60 mm and 70 mm, respectively)

grateful to the OpenSees team at UC Berkeley and PEER for maintaining OpenSees and responding helpfully to their many questions.

REFERENCES

BIS (Bureau of Indian Standards) (2002) IS 1893: Criteria for earthquake resistant design of structures, Part 1, General provisions and buildings. BIS, New Delhi, India, Figure 1, p. 5.

Botting R (1998) *The Impact of Post-Earthquake Fire of the Built-Urban Environment*. University of Canterbury, New Zealand, Fire Engineering Research Report 98/1.

British Steel (1999) *The Behaviour of Multi-Storey Steel Framed Buildings in Fire*. British Steel plc, Swinden Technology Centre, Rotherham, UK, see http://www.mace.manchester.ac.uk/project/research/structures/strucfire/DataBase/References/MultistoreySteelFramedBuildings.pdf (accessed 28/07/2011).

CEN (European Committee for Standardization) (1998) *EN 1998, Part 1.1: Design Provisions for Earthquake Resistance of Structures, Part 1.1: General rules, seismic actions and rules for buildings*. CEN, Brussels, Belgium.

Cousins WJ, Dowrick DJ and Sritharan S (1991) Fire following earthquake. *Proceedings of the Institution of Fire Engineers Conference, New Plymouth, New Zealand.*

FEMA (Federal Emergency Management Agency) (2000) Rehabilitation requirements. In *Prestandard and Commentary for the Seismic Rehabilitation of Buildings*. FEMA, US Department of Homeland Security, Washington, DC, USA, FEMA 356, Ch. 1, Table C1-3, p. 14.

Lowes L, Mitra N and Altoonash A (2004) *A Beam–Column Joint Model for Simulating the Earthquake Response of Reinforced Concrete Frames*. Pacific Earthquake Engineering Research Center (PEER), University of California, Berkeley, CA, USA, Report 2003/10.

Robertion J and Mehaffey J (2000) Accounting for fire following earthquakes in the development of performance based building codes. *Bulletin of the News Zealand Society for Earthquake Engineering*, **33(3)**.

Scawthorn C, Eidinger JM and Schiff AJ (eds) (2005) *Fire Following Earthquake*. ASCE Publications, Reston, VI, USA.

Usmani AS (2008) Research priorities for maintaining structural fire resistance after seismic damage. *Proceedings of the 14th World Conference on Earthquake Engineering, Beijing, China*, 12–17 October 2008.

Journal of Computing in Civil Engineering. Submitted October 4, 2012; accepted March 25, 2013;
posted ahead of print April 1, 2013. doi:10.1061/(ASCE)CP.1943-5487.0000305

OpenSees Software Architecture for the Analysis of Structures in Fire

Jian Jiang[1], Liming Jiang[2], Panagiotis Kotsovinos[3], Jian Zhang[4], Asif Usmani[5], Frank McKenna[6] and Guo-Qiang Li[7]

ABSTRACT

Computational modelling of structures subjected to extreme static and dynamic loads (such as snow, wind, impact, and earthquake etc.) using finite element software are part of mainstream structural engineering curricula in universities (at least at graduate level) and many experts can be found in industry who routinely undertake such analyses. However, only a handful or institutions around the world teach structural response to fire (at any level) and only a few of the top consulting engineers in the world truly specialise in this niche area. Among the reasons for this are the lack of cheap and easily accessible software to carry out such analyses and the highly tedious nature of modelling the full (often coupled) sequence of a realistic fire scenario, heat transfer to structure and structural response (currently impossible using a single software). The authors in this paper describe how finite element software can be extended to include the modelling of structures under fire load. The added advantage of extending existing finite element codes, as opposed to creating fire specific applications, is due to ability to

[1] Post doctor, College of Civil Engineering, Tongji University, Shanghai 200092, China (corresponding author). E-mail: jiangjian_0131@163.com

[2] PhD candidate, Institute for Infrastructure and Environment, University of Edinburgh, Edinburgh EH9 3JL (corresponding author). E-mail: s1134128@sms.ed.ac.uk

[3] PhD candidate, Institute for Infrastructure and Environment, University of Edinburgh, Edinburgh EH9 3JL (corresponding author). E-mail: p.kotsovinos@ed.ac.uk

[4] PhD candidate, Institute for Infrastructure and Environment, University of Edinburgh, Edinburgh EH9 3JL (corresponding author). E-mail: j.zhang@ed.ac.uk

[5] Professor, Institute for Infrastructure and Environment, University of Edinburgh, Edinburgh EH9 3JL (corresponding author). E-mail: asif.usmani@ed.ac.uk

[6] Research Engineer, Department of Civil and Environmental Engineering, University of California, Berkeley, CA 94720. E-mail: fmckenna@ce.berkeley.edu

[7] Professor, China State Key Laboratury for Disaster Reduction in Civil Enginering, Tongji University, Shanghai 200092. E-mail: gqli@tongji.edu.cn

perform multi-hazard type analysis, e.g. fire following earthquake. Due to it's open source nature and object-oriented design, the OpenSees software framework is used for this purpose. In this work the OpenSees framework, which was initially designed for the earthquake analysis of structures, is extended by the addition of new concrete classes for thermal loads, temperature distributions across element cross-sections and material laws based on Eurocodes. The paper shows through class and sequence diagrams the interaction of these classes with the existing classes in the OpenSees framework. The performance of this development is tested using benchmark solutions of a single beam with finite stiffness boundary conditions and a steel frame test. The results from OpenSees agree well with analytical solution for the benchmark problem chosen and provide reasonable agreement with the test. The experience with OpenSees so far suggests that it has excellent potential to be the basis of a unified software framework for enabling computational modelling of realistic fires, and further work is continuing towards the achievement of this goal. The extensions made to OpenSees described in this work, in keeping with the open source ideals of the framework, have been included in the current OpenSees code and are available for researchers and practicing engineers to test, develop, and use for their own purposes.

Keywords: computational modelling; OpenSees; thermomechanical analysis; software architecture; class diagram; sequence diagram.

Introduction

The traditional approach of evaluating the fire resistance of structures (based on prescriptive building codes) is by testing individual structural member under a standard fire (such as ISO-834 (ISO 1992) and ASTM-E119 (ASTM 2007)), where member capacity is associated with a limiting temperature. This approach does not consider natural fire scenarios and the enormous associated uncertainties, and furthermore the behaviour of structural members in isolation entirely ignores the structural interactions a member would experience as part of the whole structure. The unscientific nature of prescriptive approaches has led to gradual and accelerating adoption of so-called "performance-based design" or more accurately "performance-based structural engineering" (PBSE) approaches, characterised by much greater reliance on scientific understanding and numerical modelling technologies. Admirable

research advances have been made towards applying these methodologies in the field of earthquake engineering, most notably the PEER-PBEE methodology (Deierlein et al. 2003). However to enable the application of an equivalent PBSE methodology for engineering structural fire resistance considerable further development of modelling technologies is required. This is because modelling tools for simulating fire, heat transfer to structural components and structural response are typically separate and unconnected due to the significantly different physics and length & time scales, making it impossibly tedious to simulate realistic hazard scenarios and unfit to meet the challenging demand for future computational tools in this branch of science and engineering. Considerable effort has gone into the development of software for individual components of modelling structural fire resistance, e.g. computational fluid dynamics (CFD) software such as FDS (Fire Dynamics Simulator) (McGrattan 2004; McGrattan and Bouldin 2004), ANSYS Fluent (FLUENT 2003), KFX (Kameleon FireEX) (Vembe et al. 1998) and CFAST (FAST 2000). Software such as ANSYS, ABAQUS and FAHTS (1995) can be used to conduct the heat transfer analysis. Many finite element simulations of structural analysis have been published and agree well with experiments, such as the Cardington tests (Wang et al. 1995, Bailey and Moore 1999, Sanad et al. 2000 and Elghazouli and Izzuddin 2001). These have mainly used specialist programs such as VULCAN (Huang et al. 1999, 2000), ADAPTIC (Elghazouli and Izzuddin 2000; Izzuddin et al. 2004), SAFIR (Franssen 2003, Real et al. 2004), and commercial packages such as ABAQUS (Gillie et al. 2001, 2002) and ANSYS (Kodur and Dwaikat 2009; Cai et al. 2012). The computer program Vulcan has recently been extended to include a two-dimensional non-linear finite element procedure to predict the temperature distributions within the cross-sections of structural members subject to given fire time-temperature regimes (Huang 2010). SAFIR implements an uncoupled two-phase analysis to model fire-exposed structures (Quiel and Garlock 2008).

As mentioned earlier, the norm is to use separate software for fire, heat transfer and structural response, typically without considering coupling effects. (Panahshahi et al. 2006; Audebert et al. 2011; Quiel and Marjanishvili 2012). Even where the same software is used, for example in the case of a 3D thermomechanical analysis in ABAQUS, things are not easy. A heat

transfer analysis is first carried out (based on "available" heat flux boundary conditions from a separate fire model or from experimental data) on a mesh of continuum solid elements to establish the temperature evolution on sufficient points in the structure. The same solid element mesh can be used for simulating the subsequent mechanical response. This however is orders of magnitude more expensive computationally because of the much higher mesh resolution required for the same accuracy compared to using much more efficient beam-column or frame elements. This would require the modeller to "manually" assign the highly variable temperature field (based on the heat transfer output) to the structural frame model. In addition to the extraordinarily tediousness and time-consuming nature of this task, an accurate heat transfer analysis is rendered meaningless as the temperature resolution obtained is not usable in the structural frame model (currently ABAQUS only allows five temperature points over the cross-section of a 3D beam-column element).

The need for a more automated software framework is also being voiced in other quarters. The National Construction Safety Team (NCST) recommended that, based on the investigation of the collapse of the World Trade Center Towers (NIST 2005), efforts should be made to enhance the capabilities of computational methods to study the effect of realistic fire on buildings, all the way from the outbreak of fire to collapse. The FireGrid concept proposed by researchers from the University of Edinburgh (Han et al. 2010) aimed to improve the information available under emergency in a timely manner to fire-fighters. This required a platform on which the data collection and interpretation was run super-real time. The enormous disparities in spatial and temporal length scales, numerical techniques and complexity of the computer programs make the development of an efficient coupled fire-structure analysis a challenging task.

Various methodologies and tools have been developed to study the interaction between fire, thermal and structural models. Ghojel (1998) proposed a simple heat transfer model to simulate temperature profiles of steel structures under real fire condition accounting for the convective and radiative properties of the main products of combustion. It did not consider the geometrical shape of the enclosure and assumed uniform temperature distribution across or along the elements. A gap radiation model was proposed by Ali et al. (2004) to simulate

radiative heat transfer between the gas and the structure surface. It assumed the exposed portions of the structure were totally enveloped by the hot gas. Three-dimensional heat transfer analysis and subsequent two-dimensional structural analysis were performed using the ABAQUS software. Prasad and Baum (2005) proposed a FDS-interface-ANSYS analysis procedure. The interface employed a "zone model" to manage the data generated by FDS. The zone model divided the compartment into a hot upper and cool lower layer. The properties of the two layers are taken from suitably chosen temporal and spatial average of output generated by FDS. A concept of Adiabatic Surface Temperature (AST) (Wickstrom and McGrattan 2007) was introduced as an efficient interface between the fire model and structural model. The AST was calculated from the heat flux and gas temperature obtained from the fire mode and then translated back to a net heat flux in the structural model. The advantage was that only one quantity (AST) was transferred instead of heat flux and gas temperature from fire model which was computationally convenient and cost-effective. The method was tested by and FDS-AST-ANSYS simulation of series of compartment fire experiments.

Liew et al. (1998) performed a transient heat transfer analysis using FAHTS (1995) which forms a link between fire simulation model KFX and the structural analysis program USFOS. The gas temperature at each time step was prescribed in space grids that envelop the structures. The temperature distribution across the element section was calculated by subdividing line beam-column element into four node quadrilateral element which can be retrieved by structural analysis program. Shi et al. (2008) developed an integrated simulation system BFireSAS to simulate the overall fire safety performance of large buildings supported by several software tools such as AutoCAD, FDS and ANSYS. Additional model transformers were created to transfer the gas temperature from FDS to structural analysis solved by ANSYS. AutoCAD was used to construct the geometry of the structural model, FDS to simulate a fire field and ANSYS for structural analysis. A core database was developed to support the data store and exchange of integrated system and bridge the connection between the different modules. Duthinh et al. (2008) presented two interfaces in fire-thermal-structural analysis. A macroscopic finite element model was developed by Kodur et al. (2009) for

predicting the entire fire response of reinforced concrete structures from fire analysis to structural collapse analysis. Lee et al. (2011) proposed a FDS-Interface-ABAQUS analysis. A matlab subroutine was created as a tool for transferring the FDS temperatures to ABAQUS input. The transfer was conducted by tracing the same coordinate of heat transfer model with the FDS model. A novel fiber element approach was developed by Jeffers and Sotelino (2012) to evaluate the thermo-structural response of non-uniformly heated structural frames. The same fiber discretization in the structural model was used as in the heat transfer model.

Previous studies focused on the development of interfaces between specialist software or commercial packages. Although specialist programs are cost-effective to purchase and easy to use they lack generality and versatility. In addition, more tellingly continuous development, quality, robustness and long term sustainability of such research group based software must remain in perpetual doubt because of a relatively small number of users and developers. The commercial packages have a large library of finite elements and excellent GUIs to enable efficient and detailed modeling of structural responses to fire and also allow user subroutines for modeling special features of behavior. Despite obvious advantages commercial packages require substantial recurring investment for purchase and maintenance that often make them unaffordable for researchers and deter new entrants to the field. Furthermore the development of commercial codes is not in the hands of the user and users have little control over the direction the development takes. This is usually dictated by the needs of the largest commercial subscribers and rarely addresses the needs of discounted subscription paying researchers.

An alternative to commercial software is open source software, where the source code for the software is made available for anyone to download, modify, and use (mostly for free). In successful open source projects many outside developers contribute new developments and bug fixes back to the project to further its capabilities. Examples of successful open source projects include Mozilla Firefox, GNU Linux and the Apache HTTP server software. In the structural engineering field, OpenSees (McKenna 1997) is an open source object-oriented software framework developed at UC Berkeley and supported by PEER and Nees. OpenSees has so far been focussed on providing an advanced finite-element computational tool for

analysing the non-linear response of structural and geotechnical systems subjected to seismic excitations. In contrast to algorithm based programs, object-oriented programs are composed of objects, each with a number of attributes and methods, and can be viewed as the interaction between objects by the sending of messages due to the support of abstraction, encapsulation, modularity and inheritance (Booch 1994). These features of object-oriented programs make OpenSees computationally efficient, flexible, extensible and portable (McKenna 1997 and Scott et al. 2008). This means a developer can combine and reuse the existing classes in OpenSees to create an application to solve one's own specific problem. Given that OpenSees is open source and has been available for best part of this decade, it has spawned a rapidly growing community of users as well as developers who have added to its capabilities over this period. For the analysis of structural and geotechnical systems it now has capabilities developed by researchers that have yet to appear in commercial software. OpenSees offers the potential of a common community owned research program with large and growing modelling capability in many areas of structural engineering. It will enable researchers to collaborate freely across geographical boundaries with a much greater potential longevity of research and development efforts.

The research team at the University of Edinburgh has been working to add a "structures in fire" modelling capability in OpenSees. Eventually this capability will involve a heat transfer model, a structural model and an interface between them to map the temperature data automatically from the heat transfer analysis to the structural analysis, without losing the spatial and temporal resolution of the temperatures when applied to the structural elements. Further work is planned to link OpenSees to the open source CFD model OpenFOAM (capable of modelling compartment fires) leading to a fully automated software framework for modelling fire, heat transfer and structural response (as illustrated in Figure 1).

This paper presents the extensions to OpenSees to enable 2D thermomechanical analysis. This involved creating a new thermal load pattern, modifying existing material classes to include temperature dependent properties and modifying methods in element and section classes in OpenSees. The algorithm used for thermomechanical analysis of structures is given first followed by class diagrams describing the hierarchy and architecture of the development in

OpenSees. Based on the algorithm and class hierarchy, sequence diagrams are presented to illustrate the interaction between thermal load classes and material, section and element classes. The sequence diagrams provide an overview of important aspects of how to apply thermal load and obtain element forces.

Thermomechanical algorithm

In an incremental-iterative nonlinear analysis, three phases can be identified: Predictor, corrector and convergence check (Yang and Kuo 1994). The predictor needs to predict an initial out of balance force and calculate the displacement increment due to this unbalanced force given the stiffness matrix at the previous step. For thermomechanical analysis, in addition to the general external load increment, the unbalanced force should include the equivalent fixed end force due to thermal load and material softening. The corrector is concerned with the recovery of element force increment from the displacement increment obtained in the predictor phase. Equilibrium of the structure is checked at the end of each iteration to ensure that convergence is achieved in the new deformed configuration.

Predictor

The unbalanced force resulting from thermal load and material softening should be calculated in the predictor phase. The thermal load can be considered as elemental load derived from the temperature distribution along the section. In the finite element analysis, the elemental load should be transformed into equivalent nodal load. Figure 2 shows a general fibre section, which is subdivided into longitudinal fibres, with the geometric properties and temperature conditions, as defined by a uniform temperature increment, ΔT_r, and a through-depth thermal gradient, $(T_{,z})_r$, for a given fibre, r. Thermal gradient has not been implemented in OpenSees, only mean temperature is used for simplicity, however this can conceivably be implemented in future to model very steep thermal gradients with fewer fibres. If the beam that the section belongs to is fully restrained, each fibre will have a force and moment associated with it. Integrating the forces in each fibre gives section force $F_{sec} = \left[\bar{F} \quad \bar{M}\right]$, defined as (Usmani et al. 2001)

$$\bar{F} = \sum_r E_r A_r \alpha_r \Delta T_r \tag{1}$$

$$\bar{M} = \sum_r F_r \left(z_r - \bar{z}\right) + \sum_r E_r I_r \alpha_r \left(T_{,z}\right)_r \tag{2}$$

where the subscript r represents the rth fiber; E_r and A_r are the Young's modulus and area of the fiber; I_r is the second moment of area; $\bar{F}$ and $\bar{M}$ is the axial force and moment of the section; F_r is the axial force; α_r is the thermal elongation coefficient; z_r is the location of fiber r through the thickness of the section; $\bar{z}$ is the centroid of the section given by

$$\bar{z} = \frac{\sum_r A_r E_r \times z_r}{\sum_r A_r E_r} \tag{3}$$

Another source of unbalanced force is the material softening or material degradation due to the increment of the temperature. The imbalance between the applied external load and reduced resisting force leads to further deformation of the structure. Therefore, at the beginning of each thermal load step, the temperature-dependent material properties should be updated given current temperature and then the resisting force should be calculated again given the converged deformation at the previous step using the updated material properties.

The out of balance force F_u^1 at the beginning of each load step is determined by

$$F_u^1 = F_{ex} + F_{th} - F_{re} \tag{4}$$

where F_{ex} is the external load; F_{th} is the elemental thermal force by integration of section force F_{sec} along the element; F_{re} is the updated resisting force due to material softening.

Corrector

Once the initial displacement increment is obtained due to the updated out-of-balance force F_u^1, iterations are needed to determine the converged displacements for the nonlinear problem. In this case, when forming the out of balance force, there is no need to consider thermal force F_{th}, i.e.

$$F_u = F_{ex} - F_{re} \tag{5}$$

where F_u is the out-out-balance force calculated for the iterations after the first iteration (i.e. F_u^1 in Equation 4) where the temperature-induced elemental resisting force F_{th} is not considered. Remember that the stress state depends only on the mechanical strain

$$\varepsilon_{mechanical} = \varepsilon_{total} - \varepsilon_{thermal} \tag{6}$$

where $\varepsilon_{mechanical}$, ε_{total} and $\varepsilon_{thermal}$ are the mechanical strain, total and thermal strain respectively. The total strain can be obtained from the strain-displacement relation and the thermal strain can be calculated as $\varepsilon_{thermal} = \alpha \Delta T$.

With these two modifications, the corrector phase of thermomechanical analysis can follow the general procedure of mechanical analysis of structures (Spacone and Filippou 1992; Archer et al. 1999). Figure 3 shows the flowchart of element state determination for thermomechanical analysis.

Class diagrams for thermomechanical analysis in OpenSees

In order to implement the aforementioned solution algorithm in OpenSees, new subclasses were implemented and new methods were developed that derive behavior from existing components in OpenSees. These involved creating a new thermal load pattern class, and modifying existing material classes to include temperature dependent properties. Figure 4 shows the class hierarchy of new classes added in OpenSees using the graphical Unified Modeling Language notation (Booch 1998). The class ThermalLoadPattern was created to store the temperature distribution in the structure and can be used as an interface. It paralleled other load patterns such as earthquake. The temperature distribution stored can be either retrieved from the output of the heat transfer analysis or directly input by the user according to standard codes and experimental data. The data transfer between heat transfer and structural model was designed to account for the disparity in spatial and temporal scales and different element types. One of the functions of ThermalLoadPattern was to call the class Beam2dThermalAction to pass the temperature distribution across the section. It can then be retrieved by the element class such as DispBeamColumn2dThermal and be passed to

material classes (e.g. Steel01Thermal) through section classes such as FiberSection2dThermal. The material properties at elevated temperature will be updated corresponding to the temperature input. Beam2dThermalAction can also be used independently to define simple temperature profiles such as uniform and linearly distributed temperature distribution. The temperature distribution in the structural element can be considered as elemental load. Therefore the class Beam2dThermalAction defining the temperature distribution in the element was created as a subclass of ElementalLoad. The detailed attributes and implementation of these classes will be presented in the following sections.

Thermal load class

Figure 5 shows the class diagram of thermal load classes created in OpenSees and their implementations are shown in Figure 6.

Thermal load class Beam2dThermalAction was defined as a subclass of ElementalLoad ranked with point load and uniform load. Beam2dThermalAction was created to store the temperature distribution through the depth of the beam section defined by coordinate ($LocY$) and corresponding temperature (T). The temperature of each fibre located along the depth of beam section will be determined by interpolating the temperature at the nearest coordinate point according to its location. At this stage three kinds of constructors were defined in Beam2dThermalAction to deal with the input of 2, 5 and 9 temperature points through the height of beam section respectively. Uniform and linearly distributed temperatures can be defined using 2 temperature points defined at the top and bottom of the section respectively.

Thermal load pattern ThermalLoadPattern was created to define detailed and highly varying time-dependent temperature distributions in structural members. It can be used as an interface to transfer the temperature distribution from the heat transfer model to the structural model where the structural responses will be predicted. The thermal analysis and structural analysis is uncoupled in OpenSees so far which means that temperature distribution along the element should be provided as input before the structural analysis. Parallel work is under progressing on automatically generating time varying structural temperature data from a heat transfer

analysis within OpenSees (Usmani et al. 2012) however direct inputs will always be required for modelling of experiments. A series of parameters containing time points and corresponding temperature for the nine temperature points along the height of the section respectively are defined as the input of ThermalLoadPattern. The maximum temperature at each temperature point through the whole fire duration will be defined first and the temperature can then be defined as a ratio of its absolute value to the corresponding maximum temperature. This scheme can accommodate both heating and cooling scenarios.

Modified material class

There are many types of material models available in OpenSees for steel and concrete, defining their mechanical constitutive relationships, however, some of these needed to be modified to include temperature dependent properties. New temperature dependent material classes Steel01Thermal (for steel) and Concrete02Thermal (for concrete) were created by modifying the existing material class steel01 and Concrete02. These new classes while they share the same stress-strain relations in absence of thermal effects (thus our choice of names) are not to be derived from the existing classes as no re-use of any of the existing class methods was possible. The temperature dependence added in these two material classes were based on Eurocode stipulations (Eurocode 2 2004; Eurocode 3 2004). Figure 7 shows the class diagram of temperature dependent classes created in OpenSees with implementations shown in Figure 8.

Sequence diagram for thermomechanical analysis in OpenSees

The previous section presented a static view of the new classes contributed to OpenSees. To describe how these objects interoperate to conduct thermomechanical analysis, this section presents sequence diagrams (as shown in reference (Archer et al. 1999) for the existing OpenSees) showing how to apply thermal load and obtain element resisting force.

Figures 9 and 10 show the sequence diagrams for applying thermal load to beam element through thermal load classes. The thermal load is applied by invoking method *applyLoad*() in class ThermalLoadPattern. This method is primarily responsible for two operations. The

first responsibility is to retrieve temperature ratio of each temperature point according to current time point from object LinearSeries by calling method *getFactor*(). The second step is to invoke the method *addLoad*() in the associated DispBeamColumn2dThermal object to add thermal load to the beam element as shown in Figure 9. The temperatures and their distributions (dataMix) at current time are calculated and then passed to the section class by invoking the method *getTemperatureStress*() which in turn will invoke the method *getElongTangent*() in the materials. The method *getElongTangent*() has two operations. One is to update the material properties according to the current temperature. The other function is to send back the temperature dependent elastic modulus (*tangent*) and thermal elongation (*ThermalElongation*) of each fibre material to the section class. These temperature-dependent properties are then used to calculate the force of each fibre through which the section thermal force (sT) can be calculated by integration. The thermally induced resisting force of the element can be calculated by integration through sections.

Figure 11 shows the procedure for obtaining elemental resisting force. As mentioned in Section 2, the out-of-balance force of an element at the beginning of each load step comes from three sources including mechanical load, thermal load and reduced resisting force due to material degradation. In the method *getResistingForce*(), a parameter (*counterTemperature*) is set to determine whether it is the first iteration of each load step. If *counterTemperature*=0 (means first iteration), the method *update*() is invoked to update the element state due to the material degradation and the thermally induced resisting force is considered to calculate the total out-of-balance force ($s+sT$). For the next iteration, only mechanically induced out-of-balance force is considered.

Validation

In order to test the performance of the thermomechanical analysis capability in OpenSees, two benchmark cases were carried out including bending of a single beam with finite boundary conditions and a steel frame test.

Single beam benchmark

Figure 12 shows the schematic of the single beam model which is extracted from a framed structure. The beam in the middle of the frame is subjected to uniformly distributed load (UDL) and is restrained by one beam and two columns at both ends. The restraining capability offered by these surrounding elements can be represented by equivalent rotational and translational springs. Therefore the framed structure can be transformed to an equivalent single beam with finite end restraints. The dimensions of beams and columns in Cardington Restrained Beam test (Kirby 1997) are used (i.e. 305×165×40UB for beam and 254×254×89UC for column). The corresponding second moment of area of column (I_c) and beam (I_b) cross-section can be calculated as I_c=1.4×10^{-4}m^4, I_b=0.8×10^{-4}m^4. The equivalent stiffness of rotational spring (K_r) and translational spring (K_t) can be calculated as $K_r=8EI_c/l+4EI_b/l$ and $K_t=2EA_b/l+48EI_c/l^3$ with values of K_r=4.8×10^{4}kN.m/rad and K_t=3.8×10^{5}kN/m.

Based on fundamental structural mechanics, the analytical solution of the response of the beam subjected to UDL and thermal gradient $T_{,y}$ can be given as

$$\delta = \frac{5ql^4}{384EI}(1-0.8\varphi_r)+\frac{\alpha T_{,y} l^2}{8}(1-\varphi_r) \tag{7}$$

$$\theta = \left(\frac{ql^2}{12}+EI\alpha T_{,y}\right)\frac{1}{K_r+2EI/l} \tag{8}$$

$$u = \alpha\Delta T l\left(1-\varphi_t\right) \tag{9}$$

where δ, θ and u are the mid-span deflection, end rotation and horizontal displacement of the beam respectively; $\varphi_r=1/(1+2EI/K_rl)$ and $\varphi_t=1/[1+(EA/l)/K_t]$ is a factor due to the rotational and translational end restraint, respectively.

OpenSees was used to analyse the response of a 6m beam (l=3m) with finite end restraints (K_r=4.8×10^{4}kN.m/rad and K_t=3.8×10^{5}kN/m) subjected to UDL and thermal gradient. The UDL is assumed to be 30kN/m and the temperature at top of the beam was assumed to be 0°C and it varied linearly over the depth of the beam from temperatures of 100°C to 1000°C. Steel01Thermal was used to model the steel material. A finite large value was assigned to yield stress in order to make the material behaviour largely elastic. The elastic modulus at ambient temperature is 200GPa and a constant coefficient of thermal elongation α=

1.2×10^{-5}/°C was assumed. Three different analyses were conducted including materially and geometrically linear analysis, materially nonlinear but geometrically linear analysis as well as both materially and geometrically nonlinear analysis. Material nonlinearity is limited to elastic modulus being dependent on temperature. Figure 13 shows good agreement between OpenSees and analytical solutions using Equations 7-9 for the linear case.

The responses of the beam subjected to UDL and thermal load for the three analyses in OpenSees are shown in Figure 14-16. The symbol "MatL" represents materially linear analysis and "MatNL" for materially nonlinear analysis. Similarly, "GeoL" represents geometrically linear analysis and "GeoNL" for geometrically nonlinear analysis. The material nonlinearity has an obvious effect on the end rotation and horizontal movement of the beam end. In contrast, the effect of the geometrical nonlinearity is obvious on the mid-span deflection but negligible on the rotation and horizontal displacement of the beam. The mid-span deflection of the beam continued to increase and experienced a larger slope after about 600°C for nonlinear analysis. This is because the beam deflection, as temperature increases, is dominated by the thermal bowing effect and this downward bending is accelerated by material degradation at high temperature. As shown in Figure 15 and 16, the rotation and horizontal displacement of the beam increased first driven by the thermal elongation (and thermal gradient) until 500°C and then began to decrease as the decreasing of modulus of elasticity of the beam is unable to resist the stored strain energy and elastic rebound of the unheated rotational and translational spring respectively.

Three-dimensional frame models can also be transformed into an equivalent single beam model with finite end restraints as long as that the stiffness of rotational spring includes the torsional stiffness from the out-of-plane beams connected at the ends.

Steel frame test

A series of tests on plane steel frames at elevated temperatures were performed in Germany (Rubert and Schaumann 1986). A schematic diagram of two steel frames EHR3 and ZSR1 are shown in Figure 17. The braced two-bar frame (HER3) was subjected to a uniform temperature rise and only one bay of the two-portal frames (ZSR1) was uniformly heated. All

structural elements were made of IPE80 I-shaped steel. The yield stresses and modulus of elasticity are 382N/mm^2 and 210N/mm^2 at ambient temperature for EHR3 and 355N/mm^2 and 210N/mm^2 for ZSR1, respectively. Steel01 material class was used to model the properties of the Steel 37 material and nonlinear static analysis was conducted in OpenSees. Comparisons between the predicted deflections and the test results illustrated in Figure 18 show satisfactory agreement. For this steel frame example, a bilinear material was used to model the realistic steel material in the experiment and reasonable qualitative agreement was achieved. The author consider this to be adequate validation considering that actual test conditions (such as restraint, temperature distributions and material behavior at elevated temperature etc.) in large scale thermal testing (as this was) can not really be fully or accurately represented in models.

Conclusions

The open source object-oriented finite element based structural engineering framework OpenSees was extended to perform thremomechanical analysis. The class and sequence diagrams presented provide a logical overview of the hierarchy and relationship between the newly created and modified classes in OpenSees. The thermomechanical analysis capability was tested using two cases including bending of a beam and a steel frame test. Good agreements were achieved between OpenSees and analytical solutions of the beam benchmark test. Reasonable agreement was found against test data. The verification of the extended OpenSees framework is currently limited to two-dimensional cases. The classes described in this work have been added to the OpenSees framework and are available for others to review, download, and use. Further work is being done to extend OpenSees for large deflection of 3D frames including plate and shell elements in fire.

Acknowledgements

Jian Jiang and Liming Jiang were supported by China Scholarship Council and the University of Edinburgh. Jian Zhang is supported by Heriot-Watt University. The work was finalised by Jian Jiang under supervision of Professor Guo-Qiang Li with the financial support of National Natural Science Foundation of China under Grant No. 51120185001.

Reference

Ali, H. M., Senseny, P. E. and Alpert, R. L. (2004). "Lateral displacement and collapse of single-story steel frames in uncontrolled fires." Engineering Structures, 26, 593–607.

ASTM. E 119-07. (2007). "Standard test methods for fire tests of building construction and materials." ASTM International, West Conshohocken, PA.

Audebert, M., Dhima, D., Taazount, M. and Bouchair, A. (2011). "Numerical investigation on the thermo-mechanical behaviour of steel-to-timber joints exposed to fire." Engineering Structures, 33, 3257–3268.

Bailey, C. G. and Moore, D. B. (1999). "The Behaviour of Full-Scale Steel Framed Buildings Subject to Compartment Fires." The Structural Engineer, 77(8), 15–21.

Booch, G. (1994). Object-oriented analysis and design with applications, Addison-Wesley, Reading, Mass.

Booch, G., Rumbaugh, J. and Jacobson, I. (1998). "The unified modelling language user's guide." Addison-Wesley, Reading, Mass.

Cai, J. G., Feng, J. and Zhang, J. (2012). "Thermoelastic buckling of steel columns with load-dependent supports." International Journal of Non-linear Mechanics, 47, 8–15.

Chowdhury, E., Bisby, L., Green, M., Benichou, N. and Kodur, V. (2012). "Heat transfer and structural response modelling of FRP confined rectangular concrete columns in fire." Construction and Building Materials, 32, 77–89.

Deierlein, G. G., Krawinkler, H. and Cornell, C. A. (2003). "A Framework for Performance-Based Earthquake Engineering." Proceedings of Pacific Conference on Earthquake Engineering, New Zealand Society for Earthquake Engineering, 1–8.

Duthinh, D., McGrattan, K. and Khaskia, A. (2008). "Recent advances in fire-structure analysis." Fire Safety Journal, 43, 161–167.

Elghazouli, A. Y. and Izzuddin, B. A. (2000). "Response of idealised composite beam-slab systems under fire conditions." Journal of Constructional Steel Research, 56, 199–224.

Elghazouli, A. Y. and Izzuddin, B. A. (2001). "Analytical assessment of the structural performance of composite floors subject to compartment fires." Fire Safety Journal, 36, 769–793.

Eurocode 2 Design of concrete structures. (2004). Part 1.2: General rules, Structural fire design, ENV 1992-1 -2, Brussels, European Committee for Standardisation.

Eurocode 3 Design of steel structures. (2004). Part 1.2: General rules, Structural fire design, ENV 1993-1 -2, Brussels, European Committee for Standardisation.

FAHTS (1995). "Fire and heat transfer simulations of frame structures, theory and user's manual." Trondheim (Norway): SINTEF Structures and Concrete.

FAST (1997). "A User's Guide for: Engineering Tools for Estimating Fire Growth and Smoke Transport." NIST Special Publication 921.

FLUENT 6.1 (2003). "User's Guide, Fluent Inc.", Lebanon, New Hampshire.

Franssen, J. M. (2003). "SAFIR: a thermal/structural program modelling structures under fire." Proceedings of the North American Steel Construction Conference, A.I.S.C. Inc., Baltimore.

Gawin, D., Majorana, C., Pesavanto, F. and Schrefler, B. (1998). "A fully coupling multiphase

model of hydro-thermo-mechanical behavior of concrete at high temperature." In: Computational mechanics, new trends and applications. Barcelona, Spain, CIMNE, 1–19.

Ghojel, J. I. (1998). "A new approach to modelling heat transfer in compartment fires." Fire Safety Journal, 31, 227–237.

Gillie, M., Usmani, A. S., and Rotter, J. M. (2001). "Structural Analysis of the First Cardington Test." Journal of Constructional Steel Research, 57, 581–601.

Gillie, M., Usmani, A. S., and Rotter, J. M. (2002). "A Structural Analysis of the Cardington British Steel Corner Test." Journal of Constructional Steel Research, 58, 427–443.

Huang, Z., Platten, A. and Roberts, J. (1996). "Non-linear finite element model to predict temperature histories within reinforced concrete in fires." Building and Environment, 31(2), 109–18.

Han, L. X., Potter, S., Beckett, G., Pringle, G., Welch, S., Koo, S. H., Wickler, G., Usmani, A. S., Torero, J. L. and Tate, A. (2010). "FireGrid: An e-infrastructure for next-generation emergency response support." Journal of Parallel Distributed Computing, 70, 1128–1141.

Huang, Z., Burgess, I. W. and Plank, R. J. (1999). "Nonlinear analysis of reinforced concrete slabs subjected to fire." ACI Structural Journal, 96(1), 127–35.

Huang, Z., Burgess, I. W. and Plank, R. J. (2000). "Effective stiffness modelling of composite concrete slabs in fire." Engineering Structures, 22(9), 1133–1144.

Huang, Z. (2010). "The behaviour of reinforced concrete slabs in fire." Fire Safety Journal, 45, 271–282.

Huang, Z. (2010). "Modelling the bond between concrete and reinforcing steel in a fire." Engineering Structures, 32, 3660–3669.

ISO-834. (1992). Part 1: "Fire resistance tests – elements of building construction." Switzerland: International Organisation for Standardisation.

Izzuddin, B. A., Tao, X. Y. and Elghazouli, A. Y. (2004). "Realistic modelling of composite and R/C floor slabs under extreme loading-Part I : Analytical method." Journal of Structural Engineering, 130(12), 1972–1984.

Jeffers, A. E. and Sotelino, E. D. (2012). "An efficient fiber element approach for the thermo-structural simulation of non-uniformly heated frames." Fire Safety Journal, 51, 18–26.

Kirby, B. R. (1997). "British steel technical European fire test programme design, construction and results." Report of Fire, static and dynamic tests of building structures. London.

Kodur, V. and Dwaikat, M. M. S. (2009). "Response of steel beam-column exposed to fire." Engineering Structures, 31, 369–379.

Kodur, V., Dwaikat, M. and Raut, N. (2009). "Macroscopic FE model for tracing the fire response of reinforced concrete structures." Engineering Structures, 31, 2368–2379.

Lee, C. H., Chiou, Y. J., Chung, H. Y. and Chen, C. J. (2011). "Numerical modelling of the fire-structure behaviour of steel beam-to-column connections." Journal of Constructional Steel Research, 67, 1386–1400.

Liew, J. Y. R., Tang, L.K., Holmaas, T. and Choo, Y. S. (1998). "Advanced analysis for the assessment of steel frames in fire." Journal of Constructional Steel Research, 47, 19–45.

McGrattan, K.B. (2004). "Fire Dynamics Simulator (Version 4), Technical Reference Guide."

NIST Special Publication 1018, National Institute of Standards and Technology, Gaithersburg, MD.

McGrattan, K.B. and Bouldin, C. (2004). "Simulating the fires in the World Trade Center." Proceedings of the Tenth International Conference, Interscience, London.

McKenna, F. T. (1997). "Object-Oriented Finite Element Programming: Frameworks for Analysis, Algorithms and Parallel Computing." PhD thesis, University of California, Berkeley.

McKenna, F., Scott, M. H. and Fenves, G. L. (2010). "Nonlinear finite-element analysis software architecture using object composition." Journal of Computing in Civil Engineering, 24(1), 95–107.

Mounajed, G. and Obeid, W. (2004). "A new coupling F.E. model for the simulation of thermal hydro-mechanical behavior of concrete at high temperatures." Materials and Structures, 37, 422–432.

NIST NCSTAR. (2005). "Final report on the collapse of the World Trade Center Towers." National Institute of Standards and Technology, Gaithersburg, MD.

Panahshahi, N., Molki, M., Rossow, M., Rabiei, K. and Gharib, K. (2006). "The response of framed steel structures to fire." Structures Congress.

Prasad, K. and Baum, H. (2005). "Coupled fire dynamics and thermal response of complex building structures." Proceedings of the Combustion Institute, 30, 2255–2262.

Quiel, S. E. and Garlock, M. E. M. (2008). "A closed-form analysis of perimeter member behaviour in a steel building frame subject to fire." Engineering Structures, 30, 3276–3284.

Quiel, S. E. and Marjanishvili, S. M. (2012). "Fire resistance of a damaged steel building frame designed to resist progressive collapse." Journal of Performance of Constructed Facilities, 26(4), 402–409.

Rubert, A. and Schaumann, P. (1986). "Structural steel and plane frame assemblies under fire action." Fire Safety Journal, 10, 173–184, 1986.

Sanad, A. M., Rotter, J. M., Usmani, A. S. and O'Connor, M. A. "Composite beams in large buildings under fire - numerical modelling and structural behaviour", Fire Safety Journal, 35, 165–188, 2000.

Scott, M. H., Fenves, G. L., McKenna, F. and Filippou, F. C. (2008). "Software patterns for nonlinear beam-column models." Journal of Structural Engineering, 134(4), 562–571.

Spacone, E. and Filippou, F. C. (1992). "A beam element for seismic damage analysis." Report of University of California, Berkeley.

Usmani, A. S., Rotter, J. M., Lamont, S., Sanad, A. M. and Gillie, M. (2001). "Fundamental principles of structural behavior under thermal effects." Fire Safety Journal, 36(8), 721–744.

Usmani, A. S., Zhang, J., Jiang, J., Jiang, Y. Q. and May, I. (2012). "Using OpenSees for structures in fire." Journal of Structural Fire Engineering, 3(1), 57–70.

Vila Real P. M. M., Lopes, N., Silva, L. S., Piloto, P. and Franssen, F. M. (2004). "Numerical modelling of steel beam-column in case of fire-comparisons with Eurocode 3." Fire Safety Journal, 39(1), 23–39.

Vembe, B. E., Lilleheie, N. I., Holen, J. K. and Magnussen, B. F. (1998). "Kameleon FireEX, A simulator for gas dispersion and fires." International Gas Research Conference.

Wang, Y. C., Lennon, T. and Moore, D. B. (1995). "The behaviour of steel frames subject to fire." Journal of Constructional Steel Research, 35, 291–322.

Wickstrom, U., Duthinh, D. and McGrattan, K. (2007). "Adiabatic surface temperature for calculating heat transfer to fire exposed structures." Proceedings of 11th International Conference on Fire Science and Engineering Interflam.

Yang, Y. B. and Kuo, S. R. (1994). "Theory & Analysis of Nonlinear Framed Structures." Prentice Hall, Singapore.

List of figures

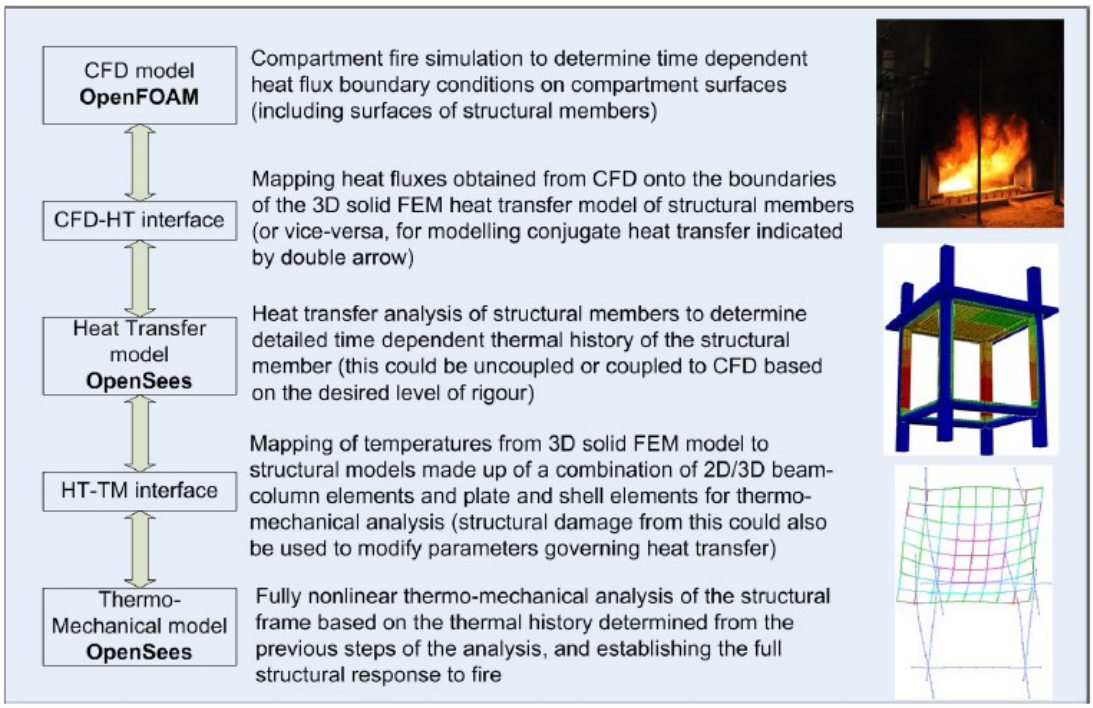

Figure 1: An open software framework for modelling structures in fire

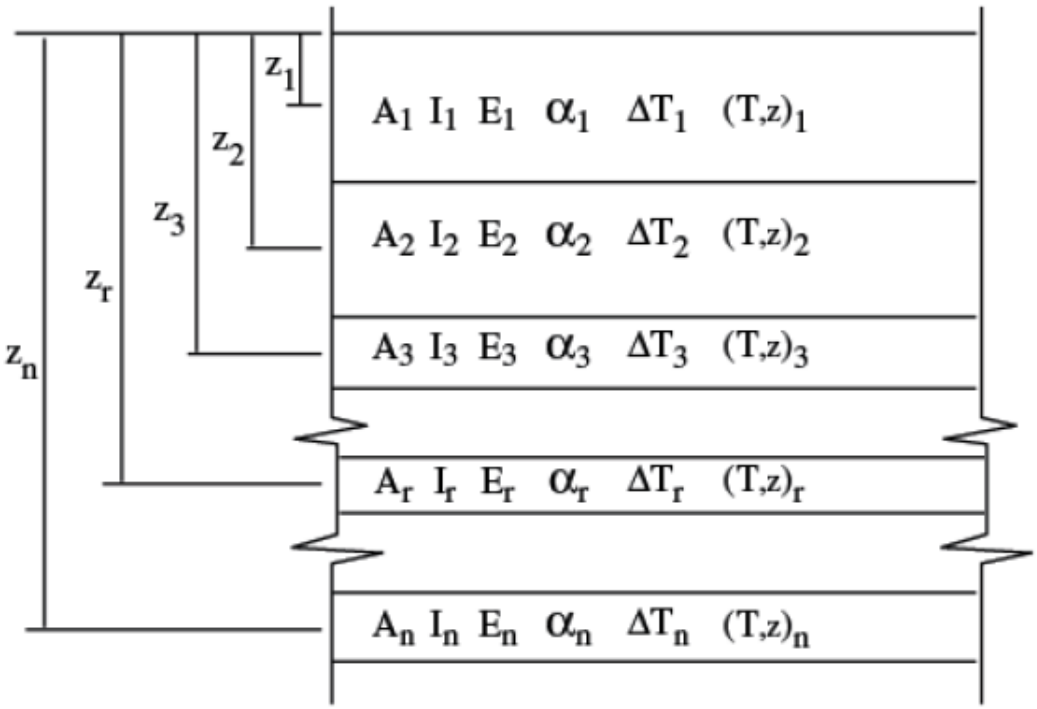

Figure 2: A general section divided into n fibres

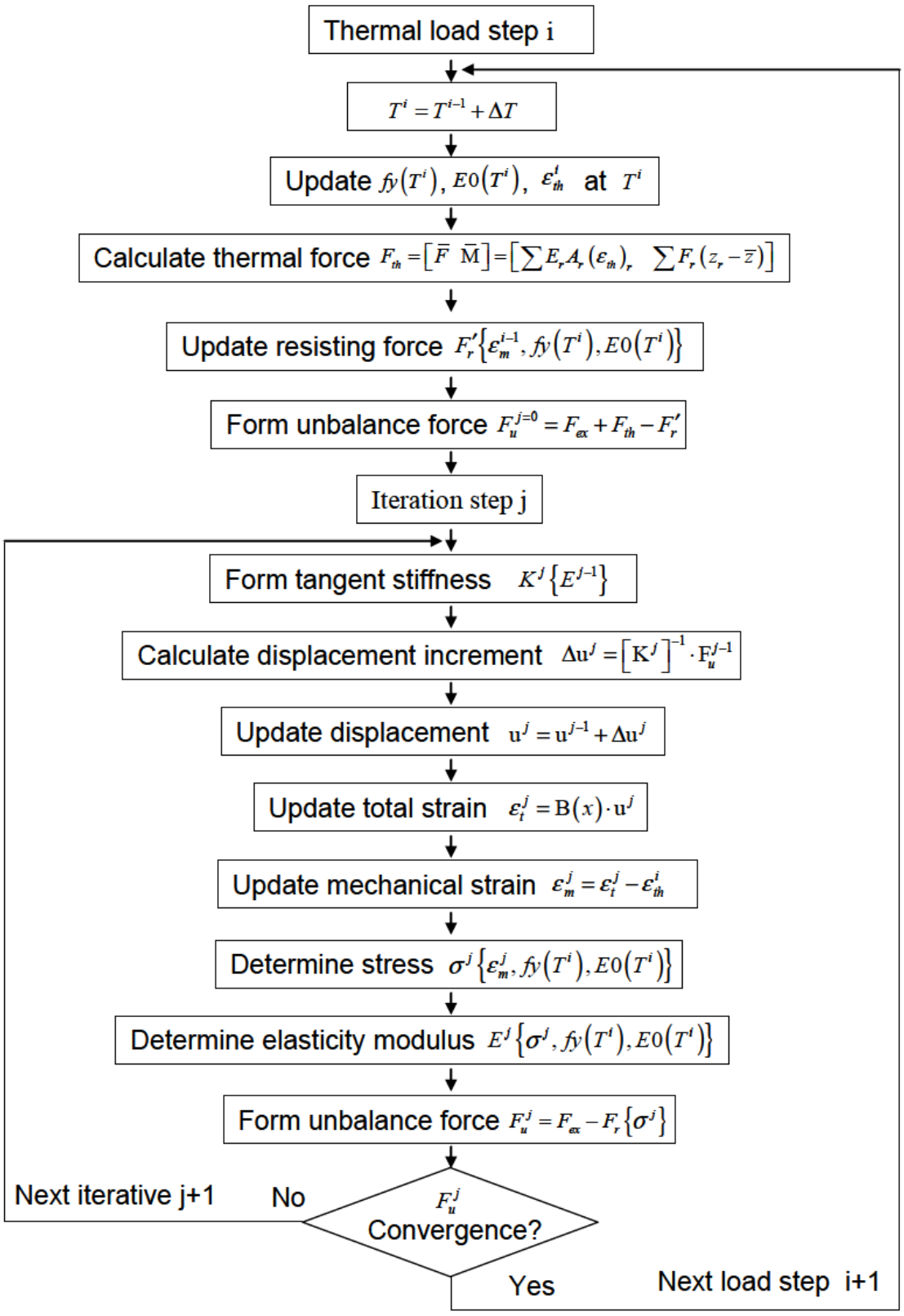

Figure 3: Flowchart for thermal-mechanical analysis

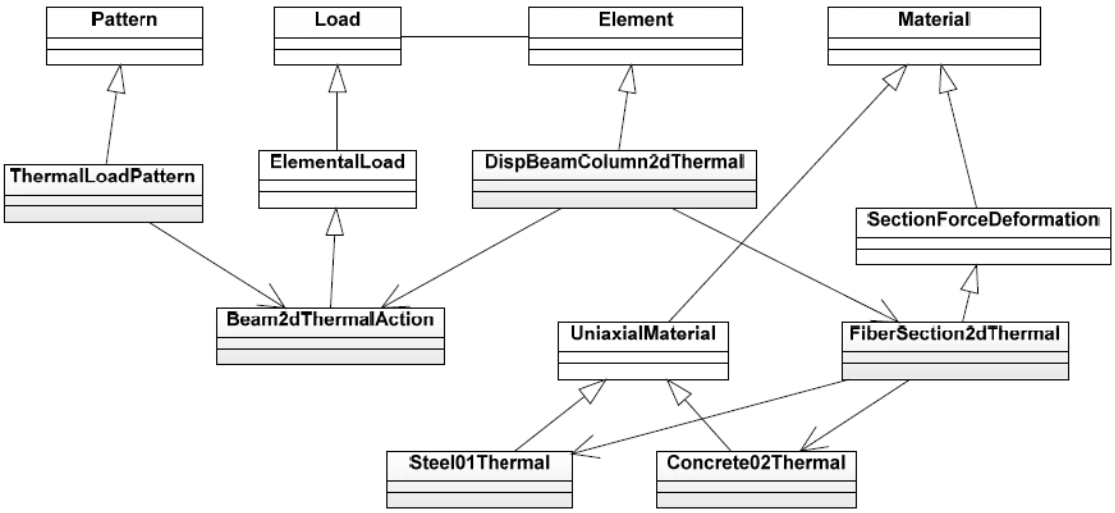

Figure 4: Class diagram for thermomechanical analysis in OpenSees

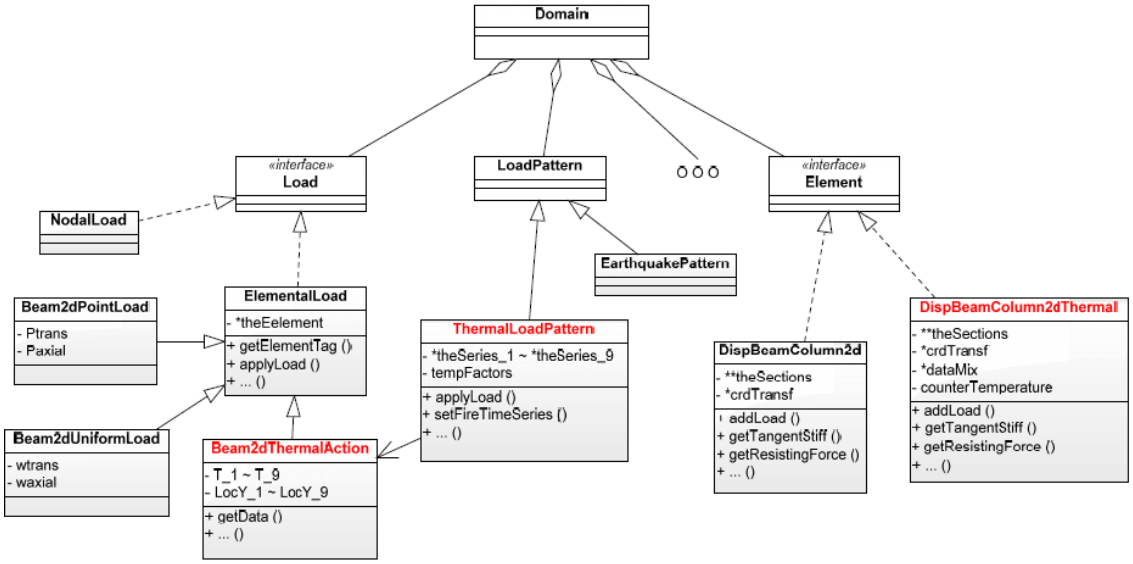

Figure 5: Class diagram of thermal load classes in OpenSees

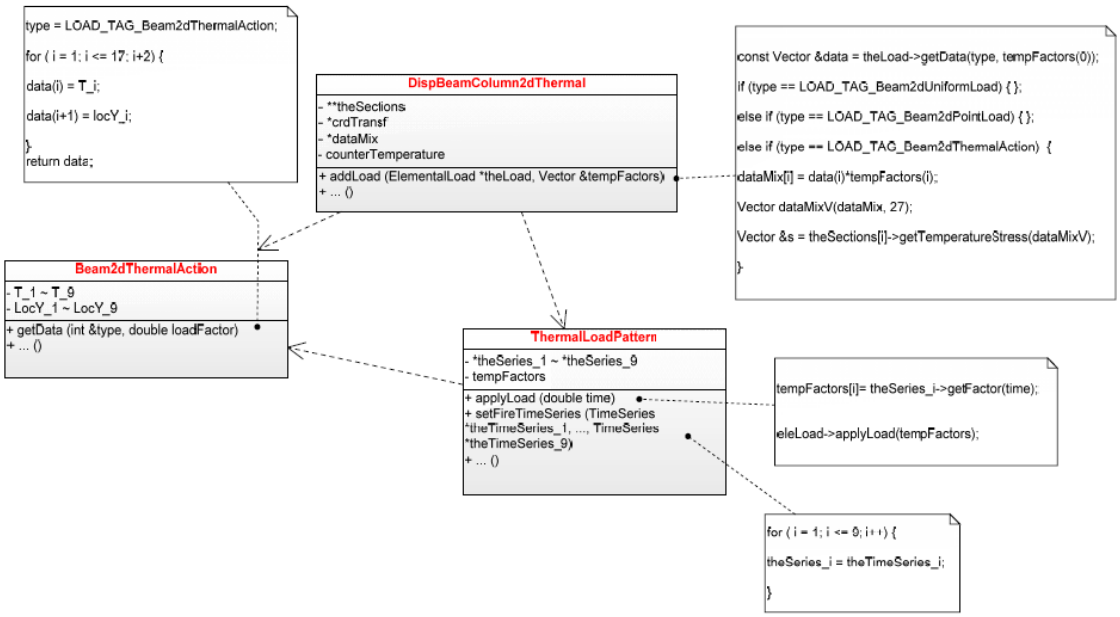

Figure 6: Implementation of functions defined in thermal load classes in OpenSees

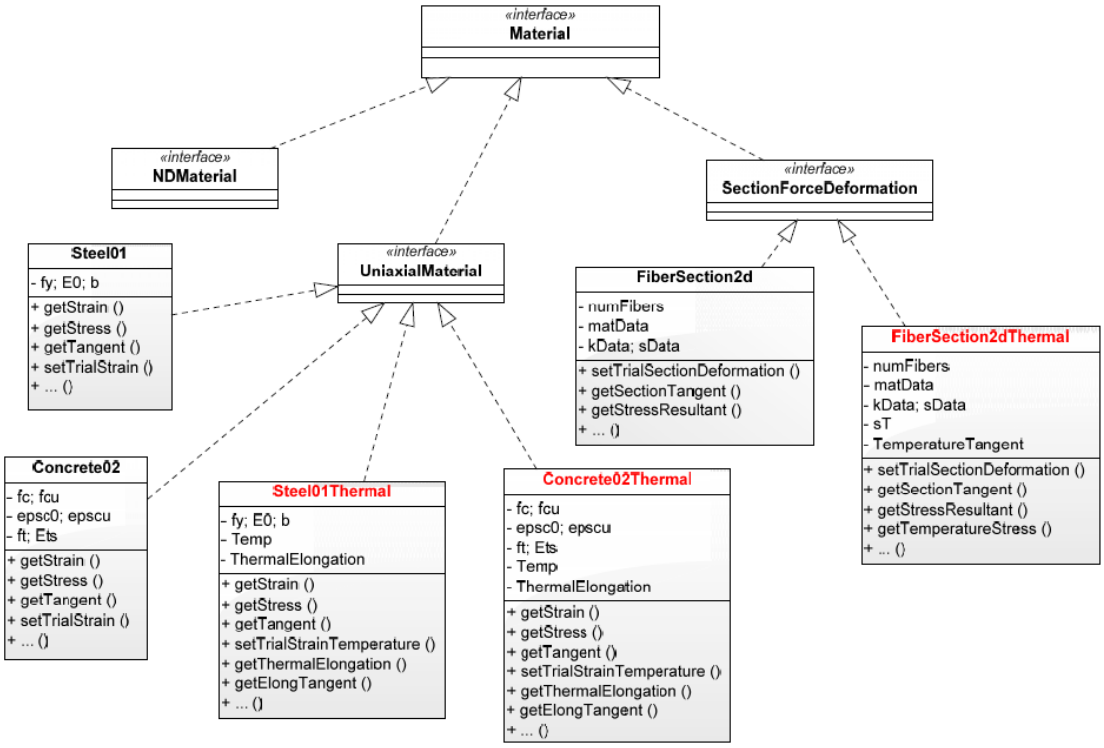

Figure 7: Class diagram of temperature-dependent material classes in OpenSees

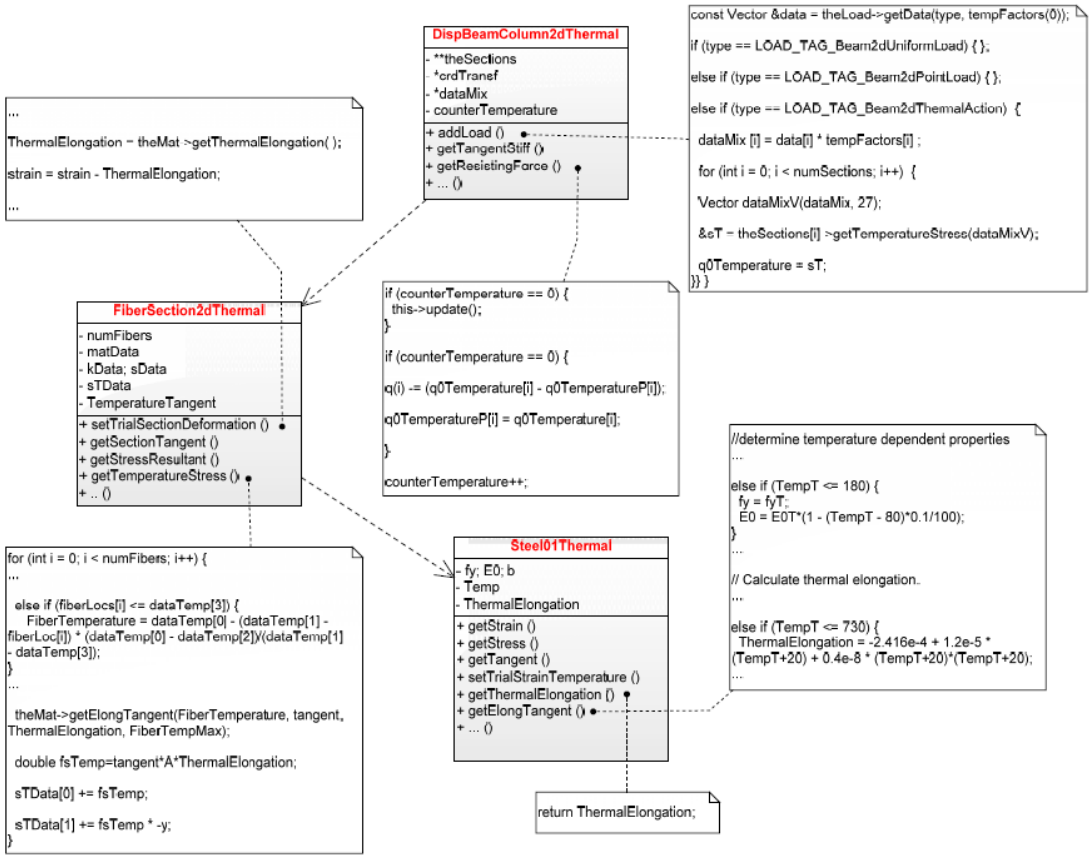

Figure 8: Implementation of functions defined in temperature-dependent material classes in OpenSees

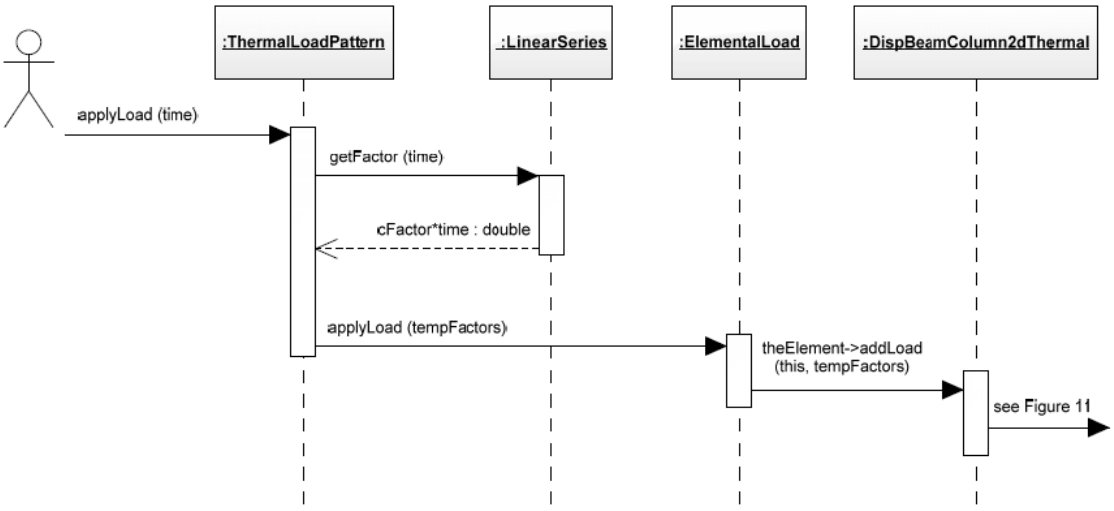

Figure 9: Sequence diagram for applying thermal load in thermal load classes

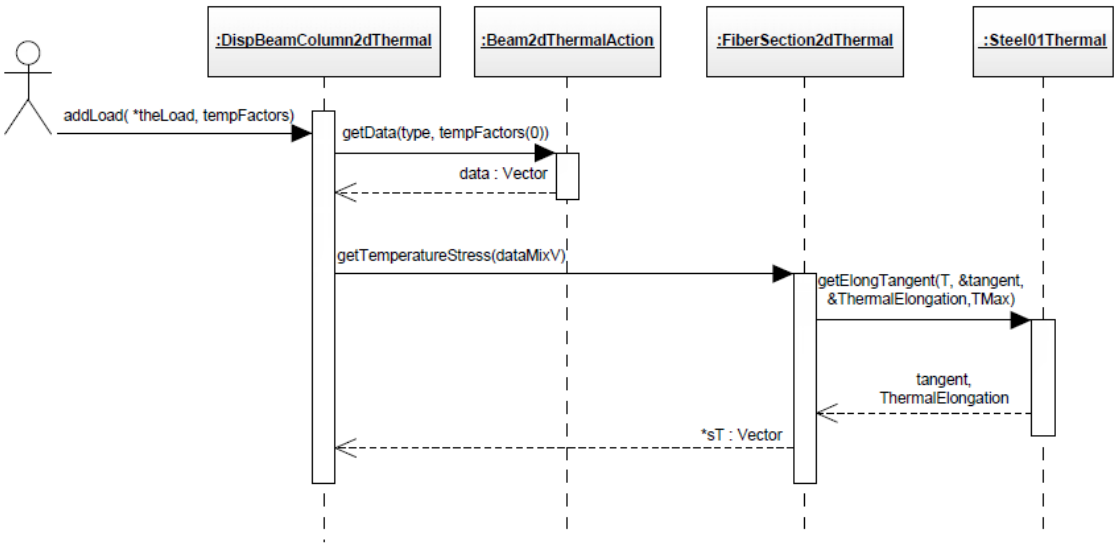

Figure 10: Sequence diagram for adding thermal load in beam element

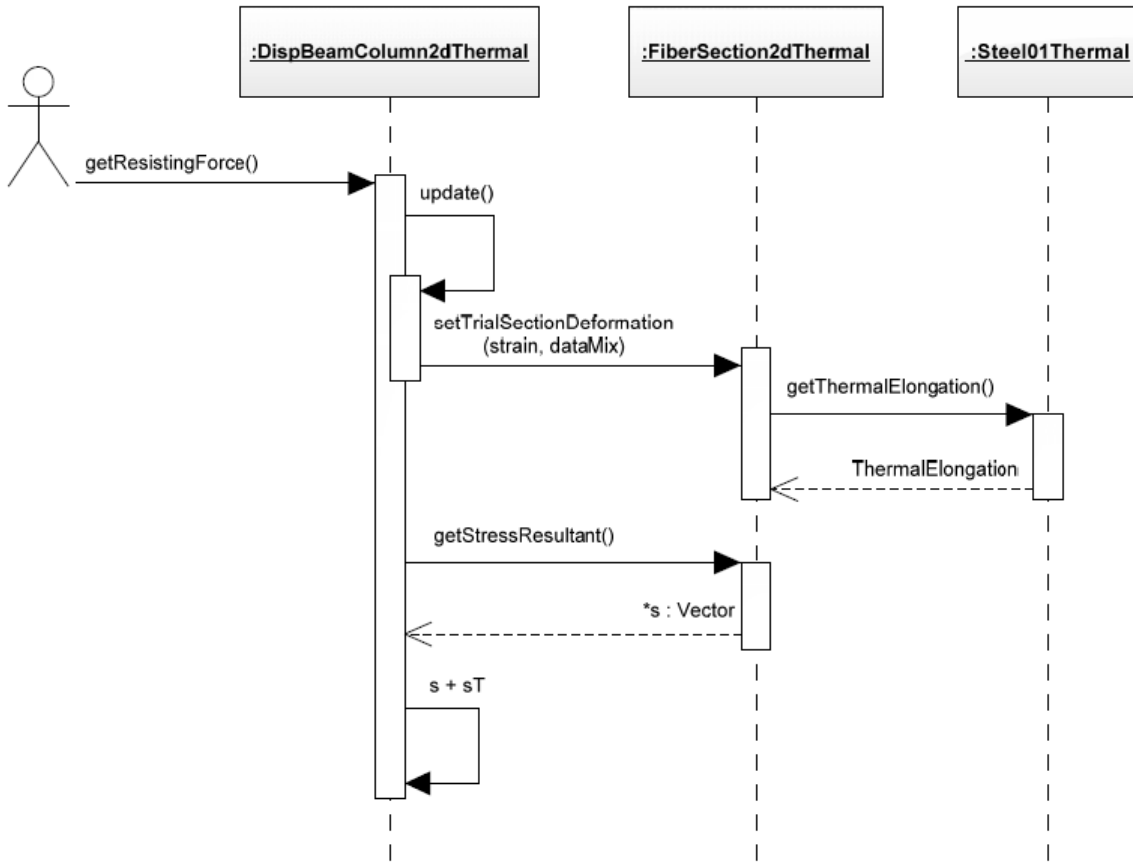

Figure 11: Sequence diagram for obtaining element resisting force

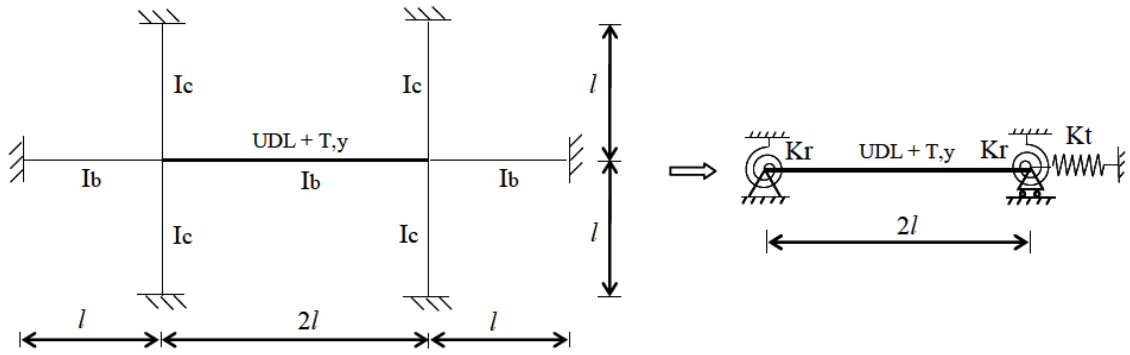

Figure 12: Beam with translational and rotational springs at the ends

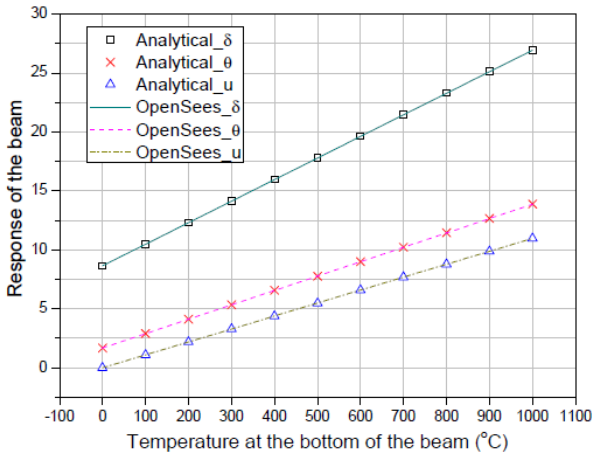

Figure 13: Responses of the beam from OpenSees compared with analytical solutions (δ, u: mm; θ: 10^{-3}rad)

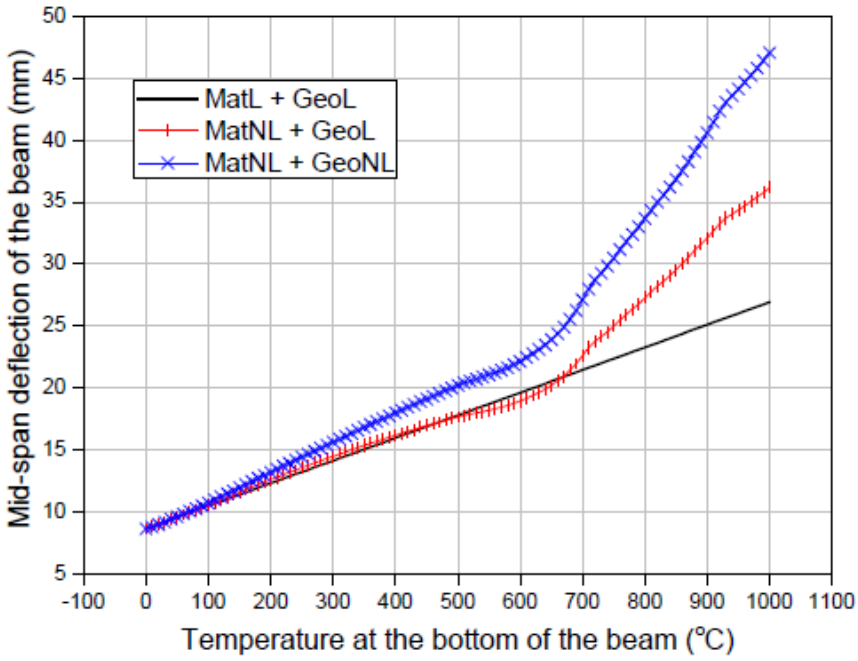

Figure 14: Mid-span deflection of the beam against temperature

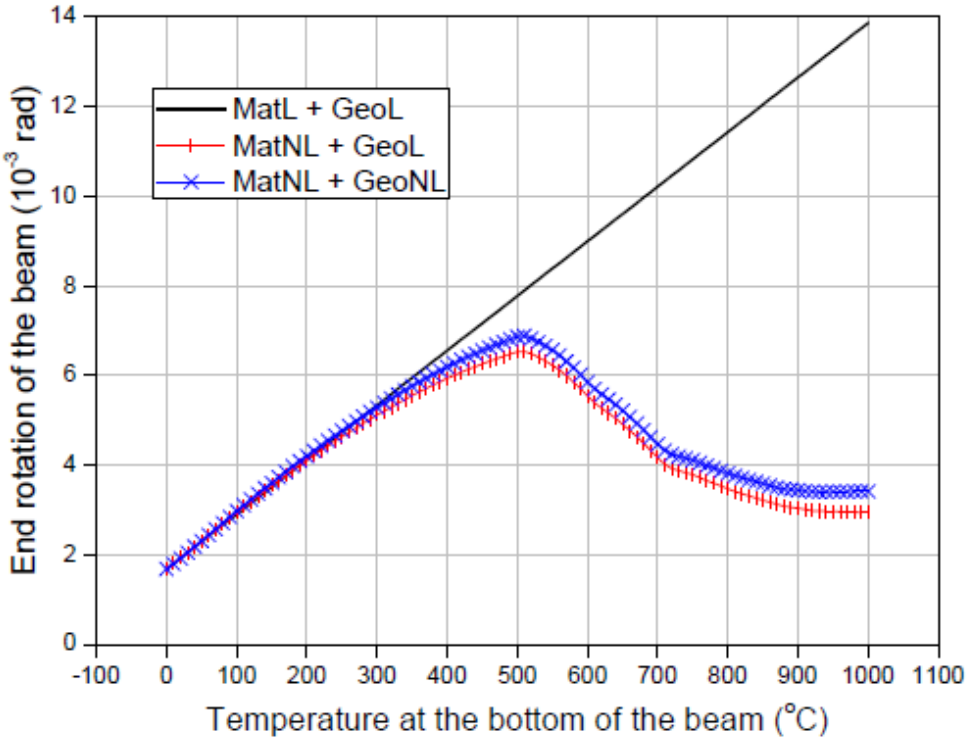

Figure 15: End rotation of the beam against temperature

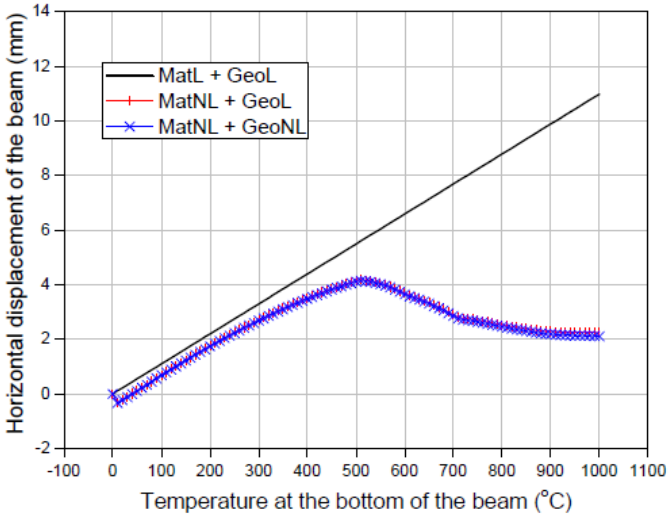

Figure 16: Horizontal displacement of movable end of the beam against temperature

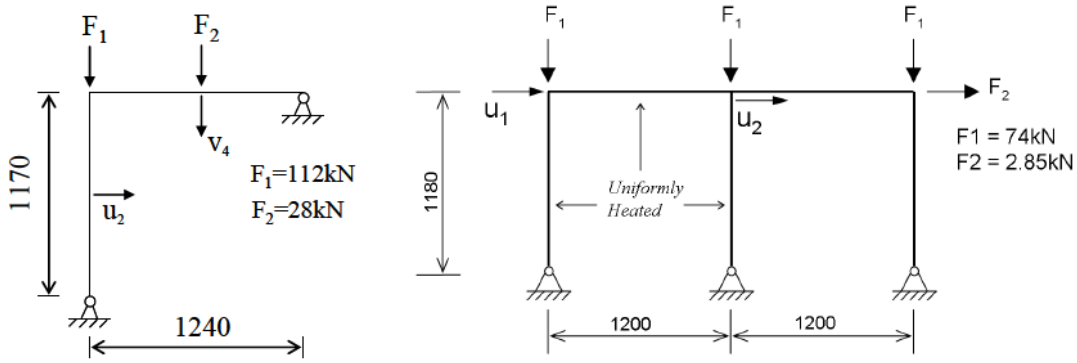

(a) (b)

Figure 17: Schematic of the tested steel frames (mm): (a) frame EHR3; (b) frame ZSR1

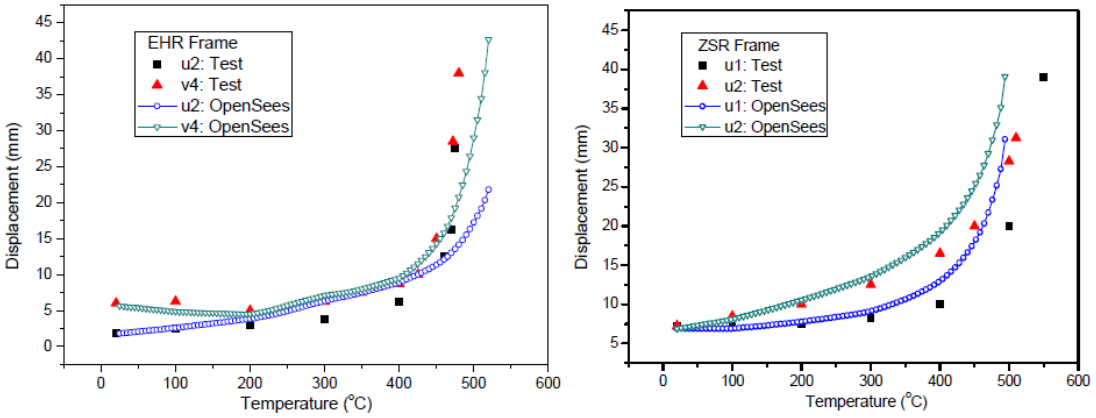

(a) (b)

Figure 18: Comparison between predicted and test deflection results: (a) frame EHR3; (b) frame ZSR1

References

1. Bažant, Z.P. and M.F. Kaplan, *Concrete at high temperatures: material properties and mathematical models*. 1996: Longman, Harlow.
2. Khoury, G.A., *Effect of fire on concrete and concrete structures.* Progress in Structural Engineering and Materials, 2000. **2**(4): p. 429-447.
3. Lindblad, Å., et al., *Fire in storehouse 6 in the free port of Stockholm.* Väg- och vattenbyggaren, 1966. **12**.
4. Jansson, R., *Fire spalling of concrete: Theoretical and Experimental Studies*. 2013, KTH Royal Institute of Technology.
5. Tenchev, R. and P. Purnell, *An application of a damage constitutive model to concrete at high temperature and prediction of spalling.* International Journal of Solids and Structures, 2005. **42**(26): p. 6550-6565.
6. Both, C., et al., *Evaluation of passive fire protection measures for concrete tunnel linings.* 1999.
7. Wetzig, V. *Destruction mechanisms in concrete material in case of fire, and protection systems*. 2001.
8. Georgali, B. and P.E. Tsakiridis, *Microstructure of fire-damaged concrete. A case study.* Cement and Concrete Composites, 2005. **27**(2): p. 255-259.
9. Abbasi, A. and P.J. Hogg, *Fire testing of concrete beams with fibre reinforced plastic rebar.* Composites Part A: Applied Science and Manufacturing, 2006. **37**(8): p. 1142-1150.
10. Williams, B., et al., *Fire insulation schemes for FRP-strengthened concrete slabs.* Composites Part A: Applied Science and Manufacturing, 2006. **37**(8): p. 1151-1160.
11. Abbasi, A. and P.J. Hogg, *A model for predicting the properties of the constituents of a glass fibre rebar reinforced concrete beam at elevated temperatures simulating a fire test.* Composites Part B: Engineering, 2005. **36**(5): p. 384-393.
12. Wang, Y.C. and V. Kodur, *Variation of strength and stiffness of fibre reinforced polymer reinforcing bars with temperature.* Cement and Concrete Composites, 2005. **27**(9-10): p. 864-874.
13. Anderberg, Y., *Mechanical Behaviour at Fire of Concrete and Hyperstatic Concrete Structures*. 1976, Bulletin of Division of Structural Mechanics and Concrete Construction.
14. Beitel, J. and N. Iwankiw, *Analysis of Needs and Existing Capabilities for Full-Scale Fire Resistance Testing.* National Institute of Standards and Technology, 2002. **NIST GCR 02-843**.
15. Mostafaei, H., M.A. Sultan, and N. Bénichou, *Recent developments on structural fire performance engineering - a state-of-the-art report.* NRC-CNRC, 2009.
16. Harrit, N., *The seventh tower.* 911truth.dk Articles, 2006. http://www.911truth.dk/first/en/art_Harrit.htm.
17. NIST, *Final Report on the Collapse of World Trade Center Building 7.* National Institute of Standards and Technology, 2008. www.nist.gov.
18. Lane, B., *The Response of Steel Framed Structures under Fire Conditions.* PhD thesis, 1997. University of Edinburgh.

19. Anderberg, Y., *Fire engineering design of structures based on design guides*, in *2nd International Conference on Performance-Based Codes and Fire Safety Design Methods*. 1998: Maui, USA.
20. Jeffers, A., D. Lange, and A. Usmani, *Performance-based Fire Safety Engineering of Structures*, in *The 1st International Conference on Performance Based and Life Cycle Structural Engineering*. 2012: Hong Kong.
21. Gewain, R.G., et al., *Facts for Steel Buildings.* Canadian Institute of Steel Construction, 2006.
22. EN, *Eurocode 3: Design of steel structures* in *Part 1-2: General rules — Structural fire design*. 1993.
23. EN, *Eurocode 2: Design of concrete structures: Part 1.2.* General rules, Structural fire design, 1992.
24. EN, *Eurocode 4 Design of composite steel and concrete structures: Part 1.2* General rules, 1994.
25. BS, *BS 5950 Structural use of steelwork in buildings: Part 8: Code of practice for fire resistant design.* 1990.
26. BS, *BS 476: Parts 20-23: 1987 Fire tests on building materials and structures.* 1987.
27. Kodur V.K.R., D.M., *Performace-Based Fire Safety Design of Reinforced Concrete Beams.* Journal of Fire Protection Engineering, 2007. **17**: p. 293-320.
28. Bailey, C., *Holistic behaviour of concrete buildings in fire.* Proceedings of the ICE - Structures and Buildings, 2002. **152**(3): p. 199-212.
29. Usmani, A.S., et al., *Fundamental principles of structural behaviour under thermal effects.* Fire Safety Journal, 2001. **36**(8): p. 721-744.
30. Ellingwood, B. and T. Lin, *Flexure and Shear Behavior of Concrete Beams during Fires.* Journal of Structural Engineering, 1991. **117**(2): p. 440-458.
31. Kodur, V. and M. Dwaikat, *A numerical model for predicting the fire resistance of reinforced concrete beams.* Cement and Concrete Composites, 2008. **30**(5): p. 431-443.
32. Bratina, S., M. Saje, and I. Planinc, *The effects of different strain contributions on the response of RC beams in fire.* Engineering Structures, 2007. **29**(3): p. 418-430.
33. Wu, B. and J.Z. Lu, *A numerical study of the behaviour of restrained RC beams at elevated temperatures.* Fire Safety Journal, 2009. **44**(4): p. 522-531.
34. Dotreppe, J.C. and J.M. Franssen, *The use of numerical models for the fire analysis of reinforced concrete and composite structures.* Engineering Analysis, 1985. **2**(2): p. 67-74.
35. Huang, Z., I.W. Burgess, and R.J. Plank. *Behaviour of reinforced concrete structures in fire*. in *Structures in Fire Workshop, Aveiro, Portugal*. 2006.
36. Kelly, F. and J. Purkiss, *Reinforced concrete structures in fire: a review of current rules.* The Structural Engineer, 2008. **86**(19): p. 33-39.
37. Plank, R., *The fire resistance of reinforced concrete structures.* Proc. Concrete 07, the 23rd Biennial Conf. of the Conc. Inst. of Australia, 2007.
38. Cvetkovska, M., *Nonlinear stress–strain behaviour of RC elements and RC frames exposed to fire.* MASE Award, 10th International Symposium of Macedonian Association of Structural Engineers – MASE, Ohrid, Macedonia, 2003.
39. Lennon, T., et al., *Concrete structures in fire.* Performance design and analysis, BR490, BRE, 2007.
40. Li, L.-y. and J. Purkiss, *Stress-strain constitutive equations of concrete material at elevated temperatures.* Fire Safety J., 2005. **40**: p. 669-686.

41. Wu, B. and G. Tang, *State-of-the-art of fire-resistance study on concrete structures in recent years.* Jianzhu Jiegou Xuebao(Journal of Building Structures), 2010. **31**(6): p. 110-121.
42. McGuire, W., R.D. Ziemian, and R.H. Gallagher, *Matrix structural analysis*. 2nd ed. 1999, New York: John Wiley & Sons.
43. Argyris, J.H., S. Kelsey, and H. Kamel, eds. *Matrix methods of structural analysis: a precis of recent developments*. 1964, Pergamon Press: Oxford.
44. Connor, J.J., R.D. Logchter, and S.C. Chan, *Nonlinear analysis of elastic framed structures.* Journal of Structural Division, 1968. **94**(ST6): p. 1525-1548.
45. Korn, A. and T.V. Galambos, *Behavior of elastic-plastic frames.* journal of the Structural Division, ASCE, 1968. **94**: p. 1119-1142.
46. Alvarez, R. and C. Birnstiel, *Inelastic analysis of multistory multibay frames.* J. Struct. Div., ASCE, 1969. **95**(11): p. 2477-2503.
47. Hajjar, J.F. and B.C. Gourley, *A cyclic nonlinear model for concrete-filled tubes. I: Formulation.* Journal of Structural Engineering, 1997. **123**(6): p. 736-744.
48. Spacone, E., F.C. Filippou, and F.F. Taucer, *Fibre beam-column model for non-linear analysis of R/C frames: part I. Formulation.* Earthquake Engineering and Structural Dynamics, 1996. **25**(7): p. 711-726.
49. Spacone, E., F.C. Filippou, and F.F. Taucer, *Fibre beam-column model for non-linear analysis of R/C frames: part II. Applications.* Earthquake Engineering and Structural Dynamics, 1996. **25**(7): p. 727-742.
50. El-Tawil, S. and G.G. Deierlein, *Nonlinear analysis of mixed steel-concrete frames. I: element formulation.* Journal of Structural Engineering, 2001. **127**(6): p. 647-655.
51. El-Tawil, S. and G.G. Deierlein, *Nonlinear analysis of mixed steel-concrete frames. II: Implementation and verification.* Journal of Structural Engineering, 2001. **127**(6): p. 656-665.
52. Sfakianakis, M.G., *RC column model for inelastic seismic response analysis in 3D.* Journal of engineering mechanics, 1991. **117**: p. 2770.
53. Coleman, J. and E. Spacone, *Localization issues in force-based frame elements.* Journal of Structural Engineering, 1999. **127**(11): p. 1257.
54. Kent, D.C. and R. Park, *Flexural members with confined concrete.* Journal of the Structural Division, 1971. **97**(7): p. 1969-1990.
55. Scott, B., R. Park, and M. Priestley. *Stress-strain behavior of concrete confined by overlapping hoops at low and high strain rates*. 1982: ACI.
56. El-Tawil, S., C.F. Sanz-Picón, and G.G. Deierlein, *Evaluation of ACI 318 and AISC (LRFD) strength provisions for composite beam-columns.* Journal of Constructional Steel Research, 1995. **34**(1): p. 103-123.
57. Hajjar, J.F. and B.C. Gourley, *Representation of concrete-filled steel tube cross-section strength.* Journal of Structural Engineering, 1996. **122**(11): p. 1327-1336.
58. Bursi, O. and M. Ballerini. *Behavior of a steel-concrete composite substructure with full and partial shear connection*. 1996.
59. Salari, M.R., et al., *Nonlinear analysis of composite beams with deformable shear connectors.* Journal of Structural Engineering, 1998. **124**(10): p. 1148-1158.
60. Ramberg, W., W.R. Osgood, and NACA, *Description of stress-strain curves by three parameters*. 1943: National Advisory Committee for Aeronautics Washington, DC.
61. Menegotto, M. and P.E. Pinto. *Method of Analysis for Cyclically Loaded RC Plane Frames, Including Changes in Geometry and Non-Elastic Behavior of Elements Under Combined Normal Force and Bending*. in *International Association for Bridge and Structural Engineering*. 1973. Zurich, Switzerland.

62. Hajjar, J.F., A. Molodan, and P.H. Schiller, *A distributed plasticity model for cyclic analysis of concrete-filled steel tube beam-columns and composite frames.* Engineering Structures, 1998. **20**(4-6): p. 398-412.
63. Shen, C., et al., *Cyclic behavior of structural steels. II: Theory.* Journal of engineering mechanics, 1995. **121**: p. 1165.
64. Franssen, J.M., *SAFIR A Thermal/Structural Program Modelling Structures under Fire.* Engineering Journal, A.I.S.C., 2005. **42**(3): p. 143-158.
65. P. J. E. SULLIVAN, M. J. TERRO, and W.A. MORRIS, *Critical Review of Fire-Dedicated Thermal And Structurual Computer Pregrams.* Journal of Applied Fire Science, 1993. **3**(2): p. 113-135.
66. R. Iding, B. Bresler, and Z. Nizamuddin, *FIRES-T3: A computer program for the fire response of structures -- thermal (three dimensional version)*, in *Fire Research Group Report* 1996, National Institute of Standards and Technology: No. NIST GCR 95-682.
67. Sterner, E. and U. Wickstrom, *TASEF – Temperature Analysis of Structures Exposed to Fire- User's manual*, in *SP Report 1990:05*. 2001, Swedish National Testing and Research Institute (SP): Boras.
68. Anderberg, Y., *SUPER-TEMPCALC. A commercial and user friendly computer program with automatic FEM-generation for temperature analysis of structures exposed to heat*. 1991, Fire Safety Design: Lund.
69. Rudolph, K., et al. *Principles for calculation of load-bearing and deformation behaviour of composite structural elements under fire action (STABA-F)*. in *Proceedings of te First International Symposium on Fire Safety Science*. 1986. Gaithburg, USA.
70. Franssen, J.M., *A study of the behaviour of composite steel-concrete structures in fire*. 1987, University of Liege: Belgium.
71. Jeanes, D.C., *Application of computer in modelling fire endurance of structural steel floor systems.* Fire Safety Journal, 1985. **9**(1): p. 119-135.
72. Forsen, *A theoretical study on the fire resistance of concrete structures - CONFIRE*, in *SINTEF Report*. 1982, The Norwegian Institute of Technology: No. STF65 A82062.
73. Towler, K., G. Khoury, and P. Sullivan, *Computer modelling of effect of of fire on large panel structures*, in *Final Report Submitted to the Department of Environment by Fire Safety Design Consultants*. 1989, UK.
74. Newman, G.M., *Fire resistance of slim floor beams.* Journal of Constructional Steel Research, 1995. **33**: p. 87-100.
75. Wang, Y.C., *Steel and composite structures: Behaviour and design for fire safety*. 2004: Taylor & Francis.
76. Becker, J., H. BiZri, and B. Bresler, *Fires-T. A computer program for the fire response of structures - reinforced concrete*, in *Report No. UCB FRG 74-3*. 1974: University of California, Berkeley.
77. Becker, J., H. BiZri, and B. Bresler, *Fires-R.C. A computer program for the fire response of structures - thermal*, in *Report No. UCB FRG 74-1*. 1974, University of California, Berkeley.
78. Iding, R., B. Bresler, and Z. Nizamuddin, *FIRES-RC II. Computer Program for the Fire Response of Structures--Reinforced Concrete Frames. Second Revised Version*. 1977, University of California, Berkeley: NBS-G7-9006.
79. Liu, T.C.H., *Theoretical modelling of steel portal frame behabiour*, in *Department of Civil Engineering*. 1988, the University of Manchster.
80. Liu, T.C.H., *Finite element modelling of behaviour of steel beams and connections in fire.* Journal of Constructional Steel Research, 1996. **36**(2): p. 181-199.

81. Liu, T.C.H., *Three-dimensional Modelling of Steel/Concrete Composite Connection Behaviour in Fire.* Journal of Constructional Steel Research, 1998. **46**(1): p. 319-320.
82. Liu, T.C.H., *Moment-rotation-temperature characteristic of steel/composite connections.* Journal of Structural Engineering-Asce, 1999. **125**(10): p. 1188-1197.
83. Lim, L., et al., *Numerical modelling of two-way reinforced concrete slabs in fire.* Engineering Structures, 2004. **26**(8): p. 1081-1091.
84. El-Zanaty, M.H., D.W. Murray, and R. Bjorhovde, *Inelastic behaviour of multistorey steel frames.* Structural Engineering Report No. 83, 1980.
85. El-Zanaty, M.H. and D.W. Murray, *Finite element programs for frame analysis*, in *Structural Engineering Report No. 84*. 1980: Department of Civil Engineering University of Alberta.
86. El-Zanaty, M.H. and D.W. Murray, *Non-linear element analysis of steel frames.* ASCE Jouranal of Structural Division, 1983. **109**(ST2): p. 353-368.
87. Saab, H.A., *Non-linear element analysis of steel frames in fire conditions*. 1990, Univerisity of Sheffiedl.
88. Saab, H.A. and D.A. Nethercot, *Modelling steel frame behaviour under fire conditions.* Engineering Structures, 1991. **13**: p. 371-382.
89. Najjar, S.R., *Three-dimensional analysis of steel frames and subframes in fire*, in *Department of Civil and Structural Engineering*. 1994, the University of Sheffield.
90. Najjar, S.R. and I.W. Burgess, *A nonlinear analysis for three-dimensional steel frames in fire conditions.* Engineering Structures, 1996. **18**(1): p. 77-89.
91. Bailey, C.G., *Simulation of the struactural behavour of steel-framed building in fire*, in *Department of Civil and Structural Engineering*. 1995, the University of Sheffield.
92. Bailey, C.G., *Development of computer software to simulate the structural behaviour of steel-framed buildings in fire.* Computers & Structures, 1998. **67**(6): p. 421-438.
93. Bailey, C.G., I.W. Burgess, and R.J. Plank, *Computer Simulation of a Full-Scale Structural Fire Test.* The Structural Engineering, 1996. **74**(6): p. 93-100.
94. Huang, Z.H., *Nonlinear analysis of reinforced concrete slabs subjected to fire.* ACI Structural Journal, 1999. **96**(1): p. 127-135.
95. Huang, Z.H., I.W. Burgess, and R.J. Plank, *Three-dimensional analysis of composite steel-framed buildings in fire.* Journal of Structural Engineering-Asce, 2000. **126**(3): p. 389-397.
96. Huang, Z., I.W. Burgess, and R. J. Plank, *Effective stiffness modelling of composite concrete slabs in fire.* Engineering Structures, 2000. **22**(9): p. 1133-1144.
97. Yu, X. and Z. Huang, *An embedded FE model for modelling reinforced concrete slabs in fire.* Engineering Structures, 2008. **30**(11): p. 3228-3238.
98. Yu, X., et al., *Nonlinear analysis of orthotropic composite slabs in fire.* Engineering Structures, 2008. **30**(1): p. 67-80.
99. Huang, Z.H., I. Burgess, and R. Plank, *Modeling Membrane Action of Concrete Slabs in Composite Buildings in Fire. I: Theoretical Development* Journal of Structural Engineering, 2003. **129**(8): p. 1093-1102.
100. Huang, Z.H., I. Burgess, and R. Plank, *Modeling Membrane Action of Concrete Slabs in Composite Buildings in Fire. II: Validations.* Journal of Structural Engineering, 2003. **129**(8): p. 1103-1112.
101. Huang, Z., *Modelling the bond between concrete and reinforcing steel in a fire.* Engineering Structures, 2010. **32**(11): p. 3660-3669.

102. Huang, Z., *The behaviour of reinforced concrete slabs in fire.* Fire Safety Journal, 2010. **45**(5): p. 271-282.
103. Abaqus, *Abaqus Analysis User's Manual*. 2010, Dassault Systemes Simulia Corp: Providence.
104. Palm, J., *Temperature analysis using ABAQUS.* Fire Technology, 1994. **30**(3): p. 291-303.
105. Sanad, A.M., et al., *Composite beams in large buildings under fire -- numerical modelling and structural behaviour.* Fire Safety Journal, 2000. **35**(3): p. 165-188.
106. Gillie, M., A.S. Usmani, and J.M. Rotter, *A structural analysis of the Cardington British Steel Corner Test.* Journal of Constructional Steel Research, 2002. **58**(4): p. 427-442.
107. Sanad, A.M., et al., *Structural behaviour in fire compartment under different heating regimes -- Part 1 (slab thermal gradients).* Fire Safety Journal, 2000. **35**(2): p. 99-116.
108. Sanad, A.M., et al., *Structural behaviour in fire compartment under different heating regimes -- part 2: (slab mean temperatures).* Fire Safety Journal, 2000. **35**(2): p. 117-130.
109. O'Callaghan, D. and M. O'Connor. *Comparison of finite element models of composite steel framed buildings behaviour in fire*. in *Procedings of the First International Workshop on Structures in Fire*. 2000. Copenhagen, Danmark.
110. O'Connor, M.A. and D.M. Martin, *Behaviour of a multi-storey steel framed building subjected to fire attack.* Journal of Constructional Steel Research, 1998. **46**(1-3): p. 295-295.
111. Gillie, M., *The behaviour of steel-framed composite structures in fire conditions*. 2000, the University of Edinburgh.
112. Feng, M., Y.C. Wang, and J.M. Davies, *Axial strength of cold-formed thin-walled steel channels under non-uniform temperatures in fire.* Fire Safety Journal, 2003. **38**(8): p. 679-707.
113. Feng, M., Y.C. Wang, and J.M. Davies, *Thermal performance of cold-formed thin-walled steel panel systems in fire.* Fire Safety Journal, 2003. **38**(4): p. 365-394.
114. Wang, Y.C. and J.M. Davies, *An experimental study of the fire performance of non-sway loaded concrete-filled steel tubular column assemblies with extended end plate connections.* Journal of Constructional Steel Research, 2003. **59**(7): p. 819-838.
115. Al-Jabri, K.S., A. Seibi, and A. Karrech, *Modelling of unstiffened flush end-plate bolted connections in fire.* Journal of Constructional Steel Research, 2006. **62**(1-2): p. 151-159.
116. Dai, X.H., Y.C. Wang, and C.G. Bailey, *Numerical modelling of structural fire behaviour of restrained steel beam-column assemblies using typical joint types.* Engineering Structures, 2010. **32**(8): p. 2337-2351.
117. Hu, Y., et al. *Modelling of flexible end plate connections in fire using cohesive elements*. in *Fifth International Workshop (Structures in Fire)*. 2008. Singapore.
118. Yu, H., et al., *Numerical simulation of bolted steel connections in fire using explicit dynamic analysis.* Journal of Constructional Steel Research, 2008. **64**(5): p. 515-525.
119. Dwaikat, M.B. and V.K.R. Kodur, *Hydrothermal model for predicting fire-induced spalling in concrete structural systems.* Fire Safety Journal, 2009. **44**(3): p. 425-434.
120. Trahair, N.S., *The behaviour and design of steel structures to EC3*. 2008: Taylor & Francis Group.

121. Qiang, X., F. Bijlaard, and H. Kolstein, *Dependence of mechanical properties of high strength steel S690 on elevated temperatures.* Construction and Building Materials, 2012. **30**(0): p. 73-79.
122. Cooke, G.M.E., *An introduction to the mechanical properties of structural steel at elevated temperatures.* Fire Safety Journal, 1988. **13**(1): p. 45-54.
123. Zhao, J.-C., *Application of the direct iteration method for non-linear analysis of steel frames in fire.* Fire Safety Journal, 2000. **35**(3): p. 241-255.
124. Anderberg, Y., *Modelling steel behaviour.* Fire Safety Journal, 1988. **13**(1): p. 17-26.
125. Cervenka, V. and J. Cervenka, *COMPUTER SIMULATION AS A DESIGN TOOL FOR CONCRETE STRUCTURES*, in *The Second International Conference in Civil Engineering on Computer Applications, Research and Practice*. 1996: Bahrain.
126. Castillo, C. and A.J. Durani, *Effect of transient high temperature on high-strength concrete.* ACI Materials Journal, 1990. **87**(1): p. 47-53.
127. Khoury, G.A. and P.J.E. Sullivan, *Resear at Imperial College on the effect of elevated temperatures on concrete.* Fire Safety Journal, 1988. **13**(1): p. 69-72.
128. ISO-834, *Part 1: Fire resistance tests – elements of building construction*. 1992: Switzerland: International Organisation for Standardisation.
129. NCSTAR, N., *Final report on the collapse of the World Trade Center Towers, National Construction Safety Team for the Federal Building and Fire Safety Investigation of the World Trade Center Disaster, National Institute of Standards and Technology, Gaithersburg, MD.* 2005.
130. Deierlein, G.G., H. Krawinkler, and C.A. Cornell, *A Framework for Performance-Based Earthquake Engineering*, in *2003 Pacific Conference on Earthquake Engineering*. 2003: New Zealand Society for Earthquake Engineering. p. 1-8.
131. McGrattan, K.B., ed. *Fire Dynamics Simulator (Version 4), Technical Reference Guide. NIST Special Publication 1018*. 2004, National Institute of Standards and Technology: Gaithersburg, MD.
132. McGrattan, K.B. and C. Bouldin. *Simulating the fires in the World Trade Center*. in *Proceedings of the Tenth International Conference*. 2004. London: Interscience.
133. FLUENT, *User's Guide, Fluent Inc*. 2003, Lebanon: New Hampshire.
134. Vembe, B.E., et al., *Kameleon FireEX, A simulator for gas dispersion and fires.* International Gas Research Conference, 1998.
135. Peacock, R.D., et al., *User's Guide for FAST: Engineering Tools for Estimating Fire Growth and Smoke Transport.* NIST Special Publication 921, 1997.
136. FAHTS, *Fire and heat transfer simulations of frame structures, theory and user's manual.* Trondheim (Norway): SINTEF Structures and Concrete, 1995.
137. Wang, Y.C., T. Lennon, and D.B. Moore, *The behaviour of steel frames subject to fire.* Journal of Constructional Steel Research, 1995. **35**: p. 291–322.
138. Bailey, C.G. and D.B. Moore, *The Behaviour of Full-Scale Steel Framed Buildings Subject to Compartment Fires.* The Structural Engineer, 1999. **77**(8): p. 15–21.
139. Sanad, A.M., et al., *Composite beams in large buildings under fire - numerical modelling and structural behaviour.* Fire Safety Journal, 2000. **35**: p. 165–188.
140. Elghazouli, A.Y. and B.A. Izzuddin, *Analytical assessment of the structural performance of composite floors subject to compartment fires.* Fire Safety Journal, 2001. **36**(769–793).
141. Huang, Z., I.W. Burgess, and R.J. Plank, *Nonlinear analysis of reinforced concrete slabs subjected to fire.* ACI Structural Journal, 1999. **96**(1): p. 127–35.

142. Huang, Z., I.W. Burgess, and R.J. Plank, *Effective stiffness modelling of composite concrete slabs in fire.* Engineering Structures, 2000. **22**(9): p. 1133–1144.
143. Elghazouli, A.Y. and B.A. Izzuddin, *Response of idealised composite beam-slab systems under fire conditions.* Journal of Constructional Steel Research, 2000. **56**: p. 199–224.
144. Izzuddin, B.A., X.Y. Tao, and A.Y. Elghazouli, *Realistic modelling of composite and R/C floor slabs under extreme loading-Part I : Analytical method." Journal of Structural Engineering.* Journal of Structural Engineering Structures, 2004. **130**(12): p. 1972–1984.
145. Franssen, J.M., *SAFIR: a thermal/structural program modelling structures under fire*, in *Proceedings of the North American Steel Construction Conference*. 2003, A.I.S.C. Inc.: Baltimore.
146. Vila Real P. M. M., et al., *Numerical modelling of steel beam-column in case of fire-comparisons with Eurocode 3.* Fire Safety Journal, 2004. **39**(1): p. 23–39.
147. Gillie, M., A.S. Usmani, and J.M. Rotter, *Structural Analysis of the First Cardington Test.* Journal of Constructional Steel Research, 2001. **57**: p. 581–601.
148. Gillie, M., A.S. Usmani, and J.M. Rotter, *A Structural Analysis of the Cardington British Steel Corner Test.* Journal of Constructional Steel Research, 2002. **58**: p. 427–443.
149. Kodur, V. and M.M.S. Dwaikat, *Response of steel beam-column exposed to fire.* Engineering Structures, 2009. **31**: p. 369–379.
150. Cai, J.G., J. Feng, and J. Zhang, *Thermoelastic buckling of steel columns with load-dependent supports.* International Journal of Non-linear Mechanics, 2012. **47**: p. 8–15.
151. Huang, Z., *The behaviour of reinforced concrete slabs in fire.* Fire Safety Journal, 2010. **45**: p. 271–282.
152. Huang, Z., *Modelling the bond between concrete and reinforcing steel in a fire.* Engineering Structures, 2010. **32**: p. 3660–3669.
153. Quiel, S.E. and M.E.M. Garlock, *A closed-form analysis of perimeter member behaviour in a steel building frame subject to fire.* Engineering Structures, 2008. **30**: p. 3276–3284.
154. Panahshahi, N., et al., *The response of framed steel structures to fire.* Structures Congress, 2006.
155. Audebert, M., et al., *Numerical investigation on the thermo-mechanical behaviour of steel-to-timber joints exposed to fire.* Engineering Structures, 2011. **33**: p. 3257–3268.
156. Quiel, S.E. and S.M. Marjanishvili, *Fire resistance of a damaged steel building frame designed to resist progressive collapse.* Journal of Performance of Constructed Facilities, 2012. **26**(4): p. 402–409.
157. NCSTAR, N., *Final report on the collapse of the World Trade Center Towers.* National Institute of Standards and Technology, Gaithersburg, MD, 2005.
158. Han, L.X., et al., *FireGrid: An e-infrastructure for next-generation emergency response support.* Journal of Parallel Distributed Computing, 2010. **70**: p. 1128–1141.
159. Ghojel, J.I., *A new approach to modelling heat transfer in compartment fires.* Fire Safety Journal, 1998. **31**: p. 227–237.
160. Ali, H.M., P.E. Senseny, and R.L. Alpert, *Lateral displacement and collapse of single-story steel frames in uncontrolled fires.* Engineering Structures, 2004. **26**: p. 593–607.

161. Prasad, K. and H. Baum, *Coupled fire dynamics and thermal response of complex building structures.* Proceedings of the Combustion Institute, 2005. **30**: p. 2255–2262.
162. Wickstrom, U., D. Duthinh, and K. McGrattan, *Adiabatic surface temperature for calculating heat transfer to fire exposed structures.* Proceedings of 11th International Conference on Fire Science and Engineering Interflam, 2007.
163. Liew, J.Y.R., et al., *Advanced analysis for the assessment of steel frames in fire.* Journal of Constructional Steel Research, 1998. **47**: p. 19–45.
164. Shi Jian-yong, R. Ai-zhu, and C. Chi, *Application of the BFIRESAS system on fire safety evaluation.* Fire Science and Technology, 2007. **2007-5**.
165. Duthinh, D., K. McGrattan, and A. Khaskia, *Recent advances in fire-structure analysis.* Fire Safety Journal, 2008. **43**: p. 161–167.
166. Kodur, V., M. Dwaikat, and N. Raut, *Macroscopic FE model for tracing the fire response of reinforced concrete structures.* Engineering Structures, 2009. **31**: p. 2368–2379.
167. Lee, C.H., et al., *Numerical modelling of the fire-structure behaviour of steel beam-to-column connections.* Journal of Constructional Steel Research, 2011. **67**: p. 1386–1400.
168. Jeffers, A.E. and E.D. Sotelino, *An efficient fiber element approach for the thermo-structural simulation of non-uniformly heated frames.* Fire Safety Journal, 2012. **51**: p. 18–26.
169. McKenna, F.T., *Object-Oriented Finite Element Programming: Frameworks for Analysis, Algorithms and Parallel Computing.* PhD thesis, University of California, Berkeley, 1997.
170. Booch, G., *Object-oriented analysis and design with applications.* Addison-Wesley, Reading, Mass., 1994.
171. Scott, M.H., et al., *Software patterns for nonlinear beam-column models.* Journal of Structural Engineering Structures, 2008. **134**(4): p. 562–571.
172. Yang, Y.B. and S.R. Kuo, *Theory & Analysis of Nonlinear Framed Structures.* Prentice Hall, Singapore, 1994.
173. Usmani, A.S., et al., *Fundamental principles of structural behavior under thermal effects.* Fire Safety Journal,, 2001. **36**(8): p. 721–744.
174. Spacone, E. and F.C. Filippou, *A beam element for seismic damage analysis.* Report of University of California, Berkeley, 1992.
175. Booch, G., J. Rumbaugh, and I. Jacobson, *The unified modelling language user's guide.* Addison-Wesley, Reading, Mass, 1998.
176. Usmani, A.S., et al., *Using OpenSees for structures in fire." Journal of Structural Fire Engineering.* Journal of Structural Fire Engineering, 2012. **3**(1): p. 57–70.
177. Eurocode 2 Design of steel structures, E.D.o.s., *Part 1.2: General rules, Structural fire design, ENV 1992-1 -2, Brussels, European Committee for Standardisation.* Brussels, European Committee for Standardisation, 2004.
178. Eurocode 3 Design of steel structures, E.D.o.s., *Part 1.2: General rules, Structural fire design, ENV 1993-1 -2.* Brussels, European Committee for Standardisation, 2004.
179. Lippman, S.B., *C++ Primer (4th Edition)*. 2005: Addison-Wesley.
180. Jones, K. and J. Hobbs, *Practical Programming in Tcl and Tk (4th Edition)*. 2003: Brent Welch.
181. McKenna, F.T., *Object-Oriented Finite Element Programming: Frameworks for Analysis, Algorithms and Parallel Computing*. 1997, University of California, Berkeley
182. *http://www.mace.manchester.ac.uk/project/research/structures/strucfire/.*

183. *http://wtc.nist.gov/.*
184. Jowsey, A., *Fire Imposed Heat Fluxes for Structural Analysis*. 2006, University of Edinburgh
185. Masters, I., et al., *Finite element analysis of solidification using object-oriented and parallel techniques*, in *International Journal for Numerical Methods in Engineering*. 1997. p. 2891- 2909
186. Welch, S., et al., *"FIRESTRUC - Integrating advanced three-dimensional modelling methodologies for predicting thermo-mechanical behaviour of steel and composite structures subjected to natural fires"* Fire Safety Science 9: p. 1315-1326.
187. Gawin, D., F. Pesavento, and B.A. Schrefler, *Modelling of hygro-thermal behaviour of concrete at high temperature with thermo-chemical and mechanical material degradation, .* Comput. Methods Appl. Mech. Engrg., 2003. **192**: p. 1731-1771
188. Ervine, A.A., *The effect of tensile cracking on thermal diffusivity, internal communication*. 2009, University of Edinburgh
189. Khoury G. A., G.B. N., and S.P.J. E., *Strain of concrete during first heating to 600oC under load.* Magazine of Concrete Research, 1985. **37**: p. 195–215
190. Neilsen, C.V., C.J. Pearce, and N. Bicanic, *Theoretical model of high temperature effects on uniaxial concrete member under elastic restraint.* Magazine of Concrete Research, 2002. **54**: p. 239–249
191. Spacone, E., V. Ciampi, and F.C. Filippou, *Mixed formulation of nonlinear beam finite element.* Computers & Structures, 1996. **58**(1): p. 71-83.
192. McKenna, F., *Object-Oriented Finite Element Programming: Frameworks for Analysis, Algorithms and Parallel Computing*. 1997, University of California, Berkeley.
193. Usmani, A.S., *Understanding the Response of Composite Structures to Fire.* Engineering Journal, 2005. **42**: p. 83-98.
194. Rubert, A. and P. Schaumann, *Structural steel and plane frame assemblies under fire action.* Fire Safety Journal, 1986. **10**: p. 173-184.
195. O'Connor, M.A. and D.M. Martin, *Behaviour of a multi-storey steel framed building subjected to fire attack.* Journal of Constructional Steel Research, 1998. **46**: p. 1-3.
196. Sanad, A.M., et al., *Composite beams in large buildings under fire numerical modelling and structural behaviour.* Fire Safety Journal, 2000. **35**: p. 165-88
197. Botting, R., *The Impact of Post-Earthquake Fire of the Built-Urban Environment*. 1998, University of Canterbury.
198. BOTTING, R. and A. BUCHANAN. *Building design for fire after earthquake*. 2000.
199. Buchanan, A.H., *Structural design for fire safety*. 2001: Wiley.
200. Usmani, A.S. *RESEARCH PRIORITIES FOR MAINTAINING STRUCTURAL FIRE RESISTANCE AFTER SEISMIC DAMAGE*. 2008: International Association for Earthquake Engineering.
201. Cousins, W.J., D.J. Dowrick, and S. Sritharan. *Fire following earthquake*. 1991.
202. Robertson, J.N. and J. Mehaffey, *Accounting for Fire Following Earthquakes in the Development of Performance Based Building Codes*. 1998, University of British Columbia.
203. Scawthorn, C., J.M. Eidinger, and A.J. Schiff, *Fire following earthquake*. 2005: Amer Society of Civil Engineers.
204. Steel, B., *The behaviour of multi-storey steel framed buildings in fire.* Swinden Technology Centre, Rotherham, UK, 1999.
205. EN, *Eurocode 2, Design of Concrete Structures.* 1992.

206. Umesh Kumar Sharma, et al., *Full Scale Testing of A Damaged RC Frame in Fire.* Structures and Buildings, 2012. **165**(7): p. 335-346.
207. Lowes, L.N., N. Mitra, and A. Altoontash, *A beam-column joint model for simulating the earthquake response of reinforced concrete frames*. 2003: Pacific Earthquake Engineering Research Center, College of Engineering, University of California.
208. Mazzoni, S., F. McKenna, and G.L. Fenves, *OpenSees command language manual.* Pacific Earthquake Engineering Research (PEER) Center, 2007.
209. Jiang, J., Jiang, L., Kotsovinos, P., Zhang, J., Usmani, A., McKenna, F., and Li, G. *OpenSees Software Architecture for the Analysis of Structures in Fire.*Journal of Computing in Civil Engineering, 10.1061/(ASCE)CP.1943-5487.0000305 (Apr. 1, 2013)
210. Huang, H. and Usmani, A. S., *Finite Element Analysis for Heat Transfer*. 1993: Springer-Verlag.
210. Qiang, X., *Behaviour of High Strength Steel Endplate Connectionsin Fire and after Fire*. 2013: Delft Academic Press.
211. Jiang, Y., *Development and application of a thermal analysis framework in OpenSees for structures in fire.* PhD thesis, 2013. University of Edinburgh.
212. Gere, J. M., and Timoshenko, S. P., *Mechanics of materials,* 3rd Ed.. 1993: PWS-KENT Publishing Company, Boston.